University of Southampton
Faculty of Medicine, Health and Life sciences
School of Medicine

Investigating the proteolytic function of A Disintegrin And Metalloproteinase 33 (ADAM33) and its role in asthma pathogenesis

by

Yun Yun Pang

Thesis for the degree of Doctor of Philosophy

July 2007

UNIVERSITY OF SOUTHAMPTON

ABSTRACT

FACULTY OF MEDICINE, HEALTH AND LIFE SCIENCES

Doctor of Philosophy

INVESTIGATING THE PROTEOLYTIC FUNCTION OF A DISINTEGRIN AND METALLOPROTEINASE 33 (ADAM33) AND ITS ROLE IN ASTHMA PATHOGENESIS

by Yun Yun Pang

Rationale: Positional cloning identified the A Disintegrin And Metalloproteinase 33 (*ADAM33*) gene as an asthma susceptibility gene. It was shown to be associated with bronchial hyperresponsiveness rather than atopy, leading to the hypothesis that ADAM33 plays a role in airway remodelling. The ADAM33 protein has multiple domains, but its exact function is yet to be established. ADAM33 possesses a conserved metalloproteinase domain, with an active site that resembles that of the matrix metalloproteinases that are involved in the modelling of the extracellular matrix. The evolutionary conservation of its proteolytic capability signifies functional importance, although the identity of its relevant substrate is unknown. The discovery of a biologically important substrate for ADAM33 will advance the understanding of its function. Uncovering the function of ADAM33 may clarify why and how it is implicated in airway remodelling and asthma susceptibility.

Aims: The aims of this study were to characterise the proteolytic activity of ADAM33 and to establish a role for ADAM33 mediated proteolysis that may be relevant to the development of asthma.

Methods: The pro and metalloproteinase domains of ADAM33 and a proteolytically inactive mutant form were expressed as secreted recombinant proteins in insect cells. A purification strategy using a series of chromatographic steps was devised to recover ADAM33 proteins from the culture medium. The activity of purified ADAM33 proteins was assessed using the α2-Macroglobulin protease binding assay and a FRET peptide cleavage assay. The sensitivity of the ADAM33 activity to various biochemical parameters and inhibitors were evaluated. The functional relevance of the proteolytic activity of ADAM33 was investigated by treating primary epithelial and endothelial cells with ADAM33. To search for a substrate for ADAM33 a novel PNA-FRET peptide library was screened for cleaved sequences. These were used to identify potentially relevant substrates.

Results: *ADAM33* transfected insect cells secreted high levels of ADAM33 proteins. A 5-step purification procedure involving, Con A affinity chromatography followed by IMAC, then cation exchange chromatography, then IMAC concentration of the sample, and lastly gel filtration produced highly pure ADAM33 protein preparations. The purified wild type ADAM33 protein was shown to be catalytically active and as expected the mutant exhibited no activity. ADAM33 was sensitive to inhibition by a hydroxamate compound (3R)-(+)-[2-(4-methoxybenzenesulfonyl)-1,2,3,4-tetrahydroisoquinoline-3-hydroxymate and also to the MMP activity regulator TIMP-3. ADAM33 was found to induce endothelial cell differentiation *in vitro*. The screening of the PNA-FRET peptide library highlighted a number of potential substrates for ADAM33. Further validation studies are required to establish whether these are genuine substrates for ADAM33.

Conclusion: Recombinant ADAM33 enzyme produced in insect cells was proteolytically active. A new synthetic inhibitor for ADAM33 was identified, and the inhibitory effect of TIMP-3 was confirmed. The ability of ADAM33 to induce endothelial cell differentiation, suggests that ADAM33 cleaves a substrate that has an important role in angiogenesis and airway remodelling.

Contents

List of Figures

List of Tables

Acknowledgements

First and foremost I would like to express my gratitude to my supervisors Prof. Donna Davies and Dr Ben Nicholas. Donna and Ben have guided and supported me throughout my postgraduate studies and have been endless sources of encouragement and expertise. I truly appreciate the time they have taken to teach and mentor me. I am also grateful to Dr Sarah Puddicombe for her supervision in the early months of my studies, and to Prof. Stephen Holgate for his optimism and eagerness in my work.

Thanks must be given to the ever enthusiastic Dr Ilaria Puxeddu with whom it has been a real pleasure to work. Her expertise in angiogenesis has been invaluable to this project and she has been a great inspiration. In addition I would like to thank Dr Juanjo Diaz-Mochon for being interested in my work and for giving me access to the PNA-FRET peptide microarray platform that he designed. I thank Dr. Rob Powell, Dr Hajime Yoshisue and Dr Hans-Michael Haitchi for their assistance in the cloning and microscopy work carried out in this study.

I would like to acknowledge all the past and present members of the Brooke Lab that I have worked with, for making the PhD experience an unforgettable and rewarding journey. Dr Sarah Field deserves a special mention for sharing the ups and downs of research with me and, in addition to Dr Chrissy Boxall, Rona Haynes and Anna Harvey have been there for much valued friendship and support. As the Newby, I would like to thank Dr James Wicks and Dr James Hughes for hours of amusement and their encouragement. I give thanks to Sue Martin and Richard Mould for their technical assistance. I would really like to thank to Phil Sanders and Jody Kirkham-Brown for sharing the PhD milestones with me. I also thank David Chau for being available to bounce ideas around.

I am forever indebted to the MRC and AAIR charity whose funding has given me this opportunity to study in Southampton.

Lastly but not leastly, a sincere thank you to my family, Mum, Dad, John and Anna for their motivating encouragement and unfaltering support.

Abbreviations

1D	One dimension
2D	Two dimension
α2-M	Alpha 2 Macroglobulin
α-SMA	Alpha- Smooth Muscle Actin
ADAM	A Disintegrin and Metalloproteinase
ADAM-TS	A Disintegrin and Metalloproteinase-with Thrombospondin motifs
ALI	Air Liquid Interface
APP	Amyloid Precursor Protein
BAL	Broncho-alveolar Lavage Fluid
bFGF-2	Basic Fibroblast Growth Factor
BHR	Bronchial hyperresponsiveness
BSA	Bovine Serum Albumin
COPD	Chronic Obstructive Pulmonary Disease
Con A	Concanavalin A
Dis	Disintegrin
DNA	Deoxyribonucleic Acid
dNTP	Deoxyribonucleotide Triphosphate
DPP10	Dipeptidyl peptidase 10
ECD	Extracellular Domain
ECM	Extra Cellular Matrix
ECP	Eosinophil Catatonic Protein
EDTA	Ethylenediaminetetraacetic acid
EGTA	Ethyleneglycol (aminoethylether) tetraacetic acid
EGF	Epidermal Growth Factor
EGFR	Epidermal Growth Factor Receptor
ELISA	Enzyme Linked Immunosorbent Assay
EMTU	Epithelial Mesenchymal Trophic Unit
EPO	Eosinophil Peroxidase
ET-1	Endothelin 1
Fc	Fragment Crystallisable (fragment of an immunoglobulin)
FcεRI	High Affinity IgE Receptor
FCS	Foetal Calf Serum
FEV_1	Forced Expiratory Volume in one second
FGF	Fibroblast Growth Factor
FGFR	Fibroblast Growth Factor Receptor
FPLC	Fast Performance Liquid Chromatography

FRET	Fluorescence Resonance Energy Transfer
FVC	Forced Vital Capacity
GCH	Goblet Cell Hyperplasia
CACL1	Calcium Activated Chloride Channel 1
CHO	Chinese Hamster Ovary Cells
GMCSF	Granulocyte Macrophage Colony Stimulating Factor
GPCR	G Protein Coupled Receptor
HB-EGF	Heparin Binding EGF like Growth Factor
HBSS	Hank's Balanced Salt Solution
HEPES	4- (2-hydroxyethyl)-1- piperazineethanesulphonic acid)
His	Histidine
HLA	Human Leukocyte Antigen
HRP	Horse Radish Peroxidase
HUVEC	Human Vascular Endothelial Cells
ICS	Inhaled Glucocorticosteroids
IFN	Interferon
IgE	Immunoglobulin E
IgG	Immunoglobulin G
IgM	Immunoglobulin M
IGF	Insulin-like Growth Factor
IGFBP	Insulin-like Growth Factor Binding Protein
IMAC	Immobilised Metal Affinity Chromatography
IL	Interleukin
IPG	Immobilised pH Gradient
kDa	KiloDalton
KL-1	Kit Ligand-1
MBP	Major Basic Protein
MCF	Monocyte Cytotoxicity Inducing Factor
MHC	Major Histocompatibility Complex
MIF	Macrophage Migration Inhibitory Factor
MIP-1α	Macrophage Inflammatory Protein-1 alpha
MMP	Matrix Metalloproteinase
MP	Metalloproteinase
mRNA	Messenger Ribonucleic Acid
M_w	Molecular weight
MWCO	Molecular Weight Cut Off
NP-40	Nonidet P40

NF-κβ	Nuclear Factor kappa-beta
N-TIMP	N terminal Domain of Tissue Inhibitor of Metalloproteinase
PC_{20}	Provocating concentration producing a 20% decrease in FEV_1.
PBS	Phosphate Buffered Saline
PCR	Polymerase Chain Reaction
PDGF	Platelet Derived Growth Factor
PI3-K	Phosphatidylinsitol-3 Kinase
PMA	Phorbol 12-Myristate 13-Acetate
PMSF	Phenylmethylsulphonyl Fluoride
PNA	Peptide Nucleic Acid
PVDF	Polyvinylidene Fluoride
qPCR	Quantitative Polymerase Chain Reaction
RGD	Arginine Glycine Aspartic acid
RNA	Ribonucleic Acid
RT-PCR	Reverse Transcription Polymerase Chain Reaction
SDS	Sodium Dodecyl Sulphate
SDS PAGE	Sodium Dodecyl Sulphate Polyacrylamide Gel Electrophoresis
SELDI	Surface Enhanced Laser Desorption Ionization
SNP	Single Nucleotide Polymorphism
ssDNA	Single Stranded Deoxyribonucleic Acid
STAT	Signal Transducer and Activator of Transcription
SVMP	Snake Venom Metalloproteinase
TGF-α	Transforming Growth Factor-alpha
TGF-β	Transforming Growth Factor-beta
T_H1	T helper type I
T_H2	T helper type II
TER	Trans-epithelial Resistance
TGF	Transforming Growth Factor-alpha
TIMP	Tissue Inhibitor of Matrix Metalloproteinase
TOF	Time of Flight
TNF-α	Tumour Necrosis Factor-alpha
TRANCE	Tumour Necrosis Activation Induced Cytokine
Tris-HCl	Tris (hydroxymethyl) aminomethane hydrochloride
VEGF	Vascular Endothelial Growth Factor
VEGFR	Vascular Endothelial Growth Factor Receptor

Chapter 1 Introduction

1.1 The asthma problem

The United Kingdom has a population of 60 million, of which over 5 million are currently receiving treatment for asthma. One tenth of those receiving treatment are children. Asthma is a respiratory disease which not only compromises the quality of life of the individual sufferers; it also poses a heavy socio-economic burden. Asthma costs the UK an estimated £2.3 billion per year, half of which is attributed to costs incurred to the NHS for treatment and in security and benefits, the other half is accounted for by a loss in productivity. With an average of one asthma related death every seven hours in the UK, and epidemiological studies showing rising trends in the prevalence of asthma globally, it is a serious problem[1;2]. The need to understand the mechanisms underlying the development of asthma and its progression is therefore both urgent and crucial if advances are to be made in terms of prevention, diagnosis, and treatment.

1.2 What is asthma?

Asthma manifests itself as recurrent episodes of wheezing, shortness of breath and airflow restriction[3]. These symptoms result from the narrowing of the lumen of the airways by bronchial constriction, and blockage by excessive production and secretion of mucus. These changes are marked during exacerbations but are reversible. Exacerbations are often temporally linked, with the most severe occurring in the early morning and/or at night[4]. In the absence of timely treatment, the most severe exacerbations can result in the complete occlusion of the bronchial tract and can be fatal. The age of onset of the disease is variable, but half the cases manifest before the age of 10 years[5].

To diagnose asthma, an individual's lung function, the ability to move air in and out of the lungs is assessed using spirometry. The forced vital capacity (FVC) and the forced expiratory volume over one second (FEV_1)[2] are measured. The FVC is the maximum volume of air that can be forcibly exhaled. The FVC is similar in asthmatic and non-asthmatic individuals, but asthmatics have a marked decrease in their FEV_1 relative to their non asthmatic counterparts. This indicates that the reduction in lung function for an asthmatic is a result of airflow restriction rather than altered lung capacity. Bronchial hyperresponsiveness is also a feature of asthma. The asthmatic

airway can be over-reactive to environmental antigens, cold air and exercise, and will constrict if stimulated with even low doses of the antigen. In the clinic, BHR can be assessed using the PC_{20} index, which is a measurement of the dose of agonist required to induce a drop of 20% in FEV_1. Histamine and methacholine are commonly used agonists for this test[6]. Administration of bronchial dilators such as a beta agonist which relaxes the smooth muscle of the airway can restore an asthmatic FEV_1 to normal.

1.3. Immunological features of asthma

Much of the current understanding of asthma has come from studies examining post mortem tissue from fatal asthma cases and bronchial biopsies, brushings, bronchial lavage or sputum taken from asthmatic subjects. From these tissues, comparisons have been made with non-asthmatic individuals and striking differences have been observed at both the histological and cellular level. The most heavily studied until recently are the immunological differences associated with the diseased airway.

There are relatively few immunological features in the normal airway. Typically there are resident macrophages and a few leukocytes that survey the tissue for the entry of foreign antigens. In contrast, a massive infiltration of leukocytes is observed in the asthmatic airway. Activated neutrophils, basophils, eosinophils, mast cells, macrophages and T cells are represented in a greater number[7-10], indicating the presence of persistent inflammation even in the absence of infection. This curious observation has encouraged the theory that asthma is a disease that has a chronic inflammatory and allergic basis, and that persistence of an inappropriate immune response contributes to its progression. The observation that asthma exacerbations correlate with exposure to otherwise relatively harmless aero-allergens[11-13] has strengthened this hypothesis.

1.3.1 Allergic asthma

Typically, when a normal individual is exposed to an environmental antigen, an IgM or an IgG response will be mediated against the foreign particle. IgE responses are more commonly observed in parasitic worm infections[14]. Some individuals differ and are prone to eliciting allergic responses to environmental antigens. These individuals are described as being atopic. Atopic individuals have an increased propensity towards developing IgE mediated responses, and this can be assessed by a skin

prick test or measuring serum IgE titre[15]. Atopy is not a pre-requisite for asthma, indeed there are many asthmatics who are non-atopic, and not all atopic individuals are asthmatic. However, atopy has been shown to be a prominent risk factor for disease. It is estimated that just under half of all cases of asthma can be attributed to atopy[16]. In these individuals, asthma exacerbations often immediately follow exposure to allergen.

The dynamics of asthma exacerbations can be correlated directly with immunological events *in vivo.* Asthmatic episodes are frequently biphasic. Spirometry data show that FEV_1 decreases immediately after allergen exposure in the early response, and again at 4-6 hours later in the late response. During both phases patients will experience difficulty in breathing, and experience symptoms such as chest tightness.

The Early Response

Mast cells are the key players in mediating the early response. Derived from bone marrow stem cells, they migrate and distribute throughout the airway, in the epithelium[17], mucosal glands[18] and smooth muscle bundles of asthmatics. The infiltration of activated mast cells into the smooth muscle is a hallmark of asthma which is not seen in other related lung diseases such as eosinophilic bronchitis, where eosinophilia is not accompanied by BHR. This difference was shown by quantifying tryptase positive cells in bronchial biopsies taken from both patient groups to identify mast cells[19]. Recently electron microscopy has shown that mast cells in the bronchial smooth muscle bundles of atopic asthmatics are partially or totally degranulated unlike those observed in control subjects[20]. This suggests that mast cells have an active role in asthma.

Individuals are sensitised to an antigen through a primary challenge or encounter, after which IgE against the antigen is produced by the humoral arm of the immune system. The circulating IgE can be captured by mast cells which express the high affinity FcεRI receptors on their cell surface. The interaction with the receptor stabilises the IgE and allows it to persist in the body. Subsequent exposure to the same allergen results in the cross linking of the FcεRI receptors and induces rapid mast cell degranulation. Potent immuno-regulatory mediators such as histamine, leukotrienes[21] and prostaglandins are released into the immediate environment[22]. These mediators initiate a cascade of events which lead to the broncho-constriction recognised as an asthmatic exacerbation. Allergen induced asthma studies *in vivo* have shown that increased levels of histamine, prostaglandin D_2, thromboxane B_2,

leukotriene C_4 can be found in the BAL fluid of asthmatics immediately after allergen exposure[23;24]. Reduction in airflow through smooth muscle contraction, edema resulting from increased vascular permeability, increased mucus secretion and plugging contribute to the narrowing of the airway lumen[25].

The Late Response

Activated mast cells can also express pro-inflammatory cytokines such as IL-4, IL-5, IL-6, IL-8, IL-13 and TNFα[26]. These cytokines recruit neutrophils and eosinophils to the respiratory tract to drive the late response. An increase in eosinophil and neutrophil numbers in BAL fluid has been demonstrated in asthmatic subjects who undergo a late response after bronchoprovocation when compared with those who do not[27;28]. This suggests that inflammatory cell infiltration is implicated in the late response. In addition to neutrophils and eosinophils, macrophages, basophils and lymphocytes are also recruited to the airway. Both neutrophils and eosinophils express cell surface Fc receptors which enable the cells to capture antibody-allergen complexes. Successful capture of these complexes causes these cells to degranulate[29;30]. Like in the early response, the release of histamine, leukotrienes, and free radicals may serve to increase vascular permeability, mucus secretion and promote smooth muscle contraction resulting in bronchoconstriction.

1.3.2 Ongoing inflammation and tissue damage

During any inflammatory process, a balance exists between the beneficial and adverse outcomes, usually the former outweighs the latter. However, in the absence of infection, the release of copious amounts of Major Basic Protein (MBP), Eosinophil Cationic Protein (ECP), and Eosinophil Peroxidase (EPO) from eosinophils serves minimal purpose. On the contrary these mediators can be highly cytotoxic to host cells[31;32]. High levels of MBP have been found adjacent to areas of epithelial damage in post mortem lung tissue from asthmatics but not non asthmatics[33]. The continual release of these mediators causes significant damage to the airway tissues and promotes airflow restriction. Activated eosinophils can also escalate the allergic response by releasing MIP1-α, a chemokine for monocytes and neutrophils, recruiting them to the airway. Activated eosinophils also secrete a number of cytokines such as IL-3, IL-5 and GM-CSF[34;35] which participate in a positive feedback loop, recruiting and activating further eosinophils. In addition, secretion of IL-4 and IL-13 by eosinophils stimulates and promotes T cells to develop towards a T_H2 like phenotype. Thus eosinophil activation promotes the persistent inflammatory response that is the feature of chronic asthma[36].

Antigen specific T cells and macrophages also play a role in airway inflammation. Activation of antigen specific T cells can cause their migration into the airway. These T cells can secrete cytokines such as MCF, IFNγ and MIF which promote macrophage infiltration and activation. Activated macrophages release an array of proteases[37;38], which in the absence of pathogens, may cause added insult to airway tissue. Macrophages are also capable of secreting multiple pro-inflammatory cytokines such as IL-1β, IL-8, MIP-1α, GMC-SF and IFNγ. Primary alveolar macrophages activated *in vitro* from asthmatics produce less anti-inflammatory cytokines such as IL-10, but produce elevated levels of IL-8, GM-CSF and TNFα relative to those from non asthmatics[39;40]. This suggests that they maybe important in mediating airway inflammation.

T lymphocytes found in the airway of asthmatics are predominantly of the T_H2 phenotype. This has been confirmed in characterisation studies of T cells present in the bronchial biopsies and BAL fluid from asthmatic subjects using *in situ* hybridisation techniques[41;42]. T_H2 cells can secrete cytokines such as IL-4, IL-5, IL-6, IL-10 and IL-13. T_H2 cytokines and most notably IL-4 and IL-13 can promote further B cell activation and promote isotype switching of antibodies from IgM to IgE[43] which is a key event in driving the allergic response.

1.4 Structural differences in the asthmatic airway

In addition to the inflammation seen in the asthmatic airways, structural differences in the airway architecture are also apparent. Until recently, it was believed that these structural changes or remodelling events were a consequence of chronic inflammation. The view that remodelling is a relatively passive process has changed with the emergence of evidence to suggest that remodelling occurs much earlier than previously thought. Furthermore, there is a component of bronchoconstriction which does not respond to steroid treatment despite the reduction in the airway inflammation[10].

1.4.1 Normal airway architecture

Asthma is typically perceived to be a disease of the large and medium airways. On the luminal surface of the airway is the epithelial cell barrier. This is comprised of

several distinct epithelial cell types with varying functions, including columnar ciliated epithelial cells, basal cells, goblet cells and clara cells[44-47]. Tight junctions between the cells create a physical barrier restricting the access of foreign material, and preventing the penetration of antigens further into the tissue[48]. Goblet cells are specialised in mucus production. The mucus is secreted out into the luminal surface and lubricates the epithelium and traps inhaled particulates. The ciliated cells have beating cilia on the cell surface which ensure that the mucus is gradually transported together with aero-allergens up and out of the airway. The cells of the mucosa are anchored to the basement membrane. Electron microscopy used to study the ultrastucture of the epithelium has revealed the presence of fibroblasts directly below the basement membrane[49]. There are few studies to determine the spatial organisation of these fibroblasts in human airway epithelium, but in one study of rat epithelium, it was shown that cells of the fibroblast sheath of the trachea form a mesh and lie flat against the *lamina reticularis* covering about 70% of the its surface[50]. The localisation of these fibroblasts in close proximity to the basement membrane has fuelled speculation that these cells may be important for cross talk between with the epithelial cells and the mesenchymal tissues. The *lamina propria* below the basement membrane consists of connective tissue, elastic fibres, capillaries, nerves and fibroblasts. The submucosa under the *lamina propria* contains cartilage, glands supported by connective tissue[49] and also smooth muscle bundles. A schematic of the airway is shown in **Fig. 1.1(a).**

1.4.2 The remodelled airway

Distinct structural abnormalities are observed in specimens of the asthmatic airway. The changes to the airway architecture are thought to be regulated by the cross talk between the epithelial and mesenchymal layers of the epithelium, reminiscent of that which occurs during embryonic modelling of the airways. During embryonic modelling, autocrine and paracrine signals within the Epithelial Mesenchymal Trophic Unit (EMTU) control the differentiation of the unit into a specialised bronchial tree[51]. Thus the processes involved in the development of abnormal structural changes to the asthmatic airway are described as remodelling. A schematic and histological section of the remodelled airway are shown in **Fig.1.1(b)and (c)**. Descriptions of the remodelling processes are detailed in this section, and the mechanisms which drive the remodelling processes are discussed in **section 1.5**.

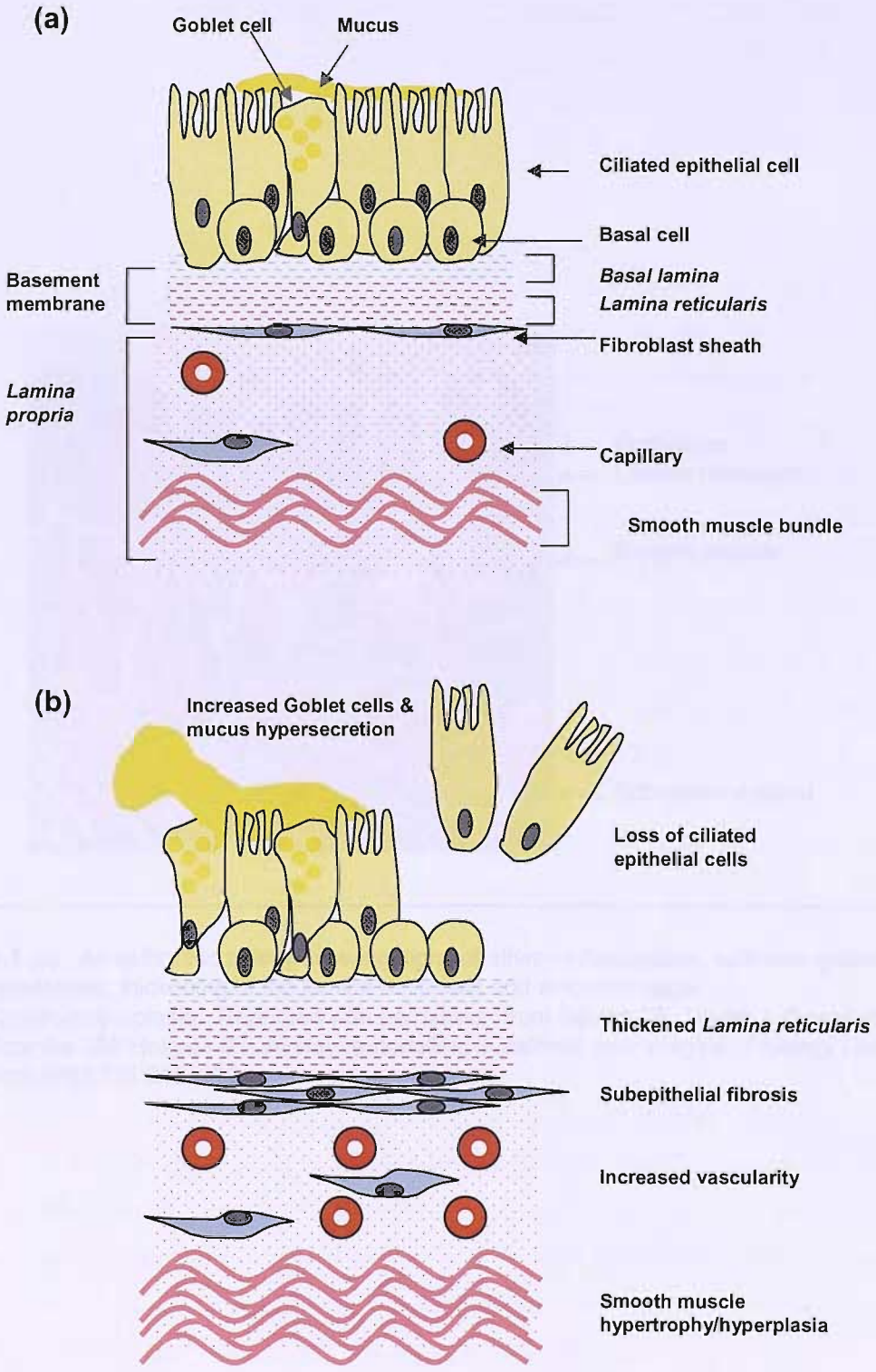

Fig. 1.1 The normal and remodelled airway. A pictorial representation of the normal central airway (a), and the changes observed in the remodelled airway in asthma (b). A histological section from the airway of an asthmatic subject showing some aspects of remodelling (c) see next page.

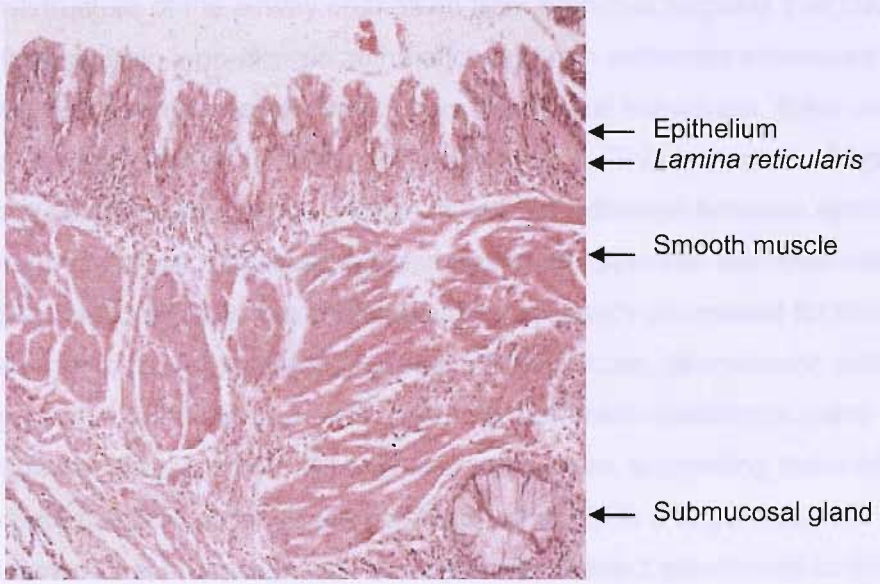

Fig. 1.1 (c). An asthmatic airway showing signs of airway inflammation, epithelial goblet cell hyperplasia, thickening of the *lamina reticularis* and smooth muscle hypertrophy/hyperplasia. Reprinted with permission from Davies DE, Wicks J, Powell RM, Puddicombe SM, Holgate ST. Airway remodelling in asthma: new insights. *J Allergy Clin Immunol* 2003;111:215–225

1.4.3 Altered epithelial barrier

The epithelial cell layer from asthmatic airway epithelium is noticeably more fragile when compared with normal specimens. The loss of ciliated cells is reported from an early age. Ciliated cells can be seen as sloughed clusters known as *Creola bodies* in sputum[52]. Ciliated epithelial cells also frequently appear in the lumen of specimens from cases of fatal asthma. The lack of epithelial detachment in samples from normal individuals clearly indicates that the integrity of the epithelium of asthmatic airways is altered, although there has been some controversy as to whether the epithelium is actually shed, or if it is an artifact of tissue sampling and processing. Recent studies have used scanning and transmission electron microscopy to study the ultrastructure of the airway epithelium from bronchial biopsies that have been taken from allergic, non-allergic asthmatics and non-asthmatic individuals. Whilst the epithelial cell layers remained in-tact from the normal individuals, there was a loss of ciliated epithelial cells in both the asthmatic groups. This increase in fragility was shown to be associated with a change in cell-cell adhesion between epithelial cells. The length of the desmosomes, adhesive junctions between epithelial cells (cuboidal-cuboidal, cuboidal-basal, basal-basal) was significantly decreased for the columnar and basal cells for both asthmatic groups. Furthermore, desmosome plaques are usually seen in both adjacent cells, but in the asthmatic specimens many hemi-desmisomes (plaque in one cell only) were observed, suggesting reduced attachment between cells. Since columnar cells rely to a large extent on hemidesmosomal interaction with basal cells for indirect attachment to the *basal lamina*, this may explain the increased susceptibility of asthmatic epithelium to damage[53;54].

In addition to increased fragility, the epithelial cells themselves exhibit altered behaviour, in particular increased susceptibility to oxidative stresses. Bucchierri and colleagues showed that cultured human epithelial cells from bronchial brushings have a much stronger apoptotic response to exposure to oxidant stress if they were from asthmatics, in comparison to those from normal subjects. Here apoptosis was detected using an early apoptotic marker p85 PARP by flow cytometry[55]. In another study, confluent epithelial cell cultures derived from bronchial biopsies were exposed to ozone or nitrogen dioxide and changes to the permeability of the epithelial monolayer were assessed by measuring electrical resistance and passage of ^{14}C-BSA across the cells. The study showed that whilst asthmatic and non asthmatic cultures behaved similarly when exposed to air, they showed marked differences in sensitivity to the oxidants. Whilst no significant effects were observed at exposure to

low concentrations of ozone and nitrogen dioxide on non-asthmatic cultures, the permeability of asthmatic cultures were significantly increased[56].

In combination the sloughing off of epithelial cells and the increased sensitivity of the cells to environmental insults reduce the efficacy of the epithelial barrier function, and prevent normal mucus and inhaled particle clearance. This may facilitate the penetration of aero-allergens deeper into the epithelium where it has ample opportunity to elicit an immune response. These may in part explain the increased airway hyperresponsiveness of the asthmatic airway.

1.4.4 Increased number of goblet cells and mucus production

Flakes of mucus coating the luminal surface of the airways is normal and functions to facilitate the removal of inhaled particulates. In asthmatics the amounts of mucus found in the airways increases and can form plugs which can completely or partially block the airways. In a relaxed state, a slight increase in the mucus which reduces the lumen of the airway may barely impact airflow, but when coupled with airway constriction this increase in mucus can contribute to the occlusion of the airway preventing airflow. This exaggerated narrowing of the airway can contribute to airway hyperresponsiveness and is frequently associated with cases of fatal asthma[57].

Mucus is produced by goblet cells and mucous cells in the submucousal glands. It is a mixture of heavily glycosylated proteins called mucins, plasma derived proteins such as albumin and inorganic salts. The mucus produced in asthmatics is highly viscous and difficult to dislodge. Electron microscopy of mucus plugs from cases of fatal asthma highlights differences in the cross-linking and size of the mucus when compared with control mucus, and this difference in assembly is speculated be implicated in the difference in mucin viscosity[58]. Quantitative PCR analyses of mucin gene expression in homogenised bronchial biopsies show a 60% higher expression of *MUC5AC* in asthmatics when compared with non asthmatics, although the increase was not significant it did correlate with increased MUC5AC staining observed in biopsies from the same subjects[59].

Goblet cell metaplasia or hyperplasia has been consistently found in cases of fatal asthma, and it is thought to contribute to the increased levels of mucus in the asthmatic airway. Although the underlying basis of the increase in goblet cells is

complex, there is evidence to link its development to the inflammatory processes in asthma.

1.4.5 Basement membrane thickening

The basement membrane is the structure on which the basal surfaces of airway epithelial cells sit. When examined by electron microscopy, the basement membrane can be seen as two distinct structures[60]. The *basal lamina* is the layer which epithelial cells attach to via hemidesmosomes and immediately below this is the *lamina reticularis*. These extracellular matrix rich structures are thought to originate from different cell populations. The *basal lamina* is thought to be produced predominantly by epithelial cells and the *lamina reticularis* by cells of mesenchymal origin.

The *basal lamina* is thought to be composed of collagen IV, laminin, entactin, and heparin sulfate proteoglycans. The *lamina reticularis* is composed of fibronectin, collagen I, III (predominantly), V, VI, tenascin, elastin, elastin associated fibrils and proteoglycans. Collagen VII is thought to loop from the *basal lamina*, through the *lamina reticularis* and back into the *basal lamina* [61;62]. The thickening of the basement membrane has been widely reported to be associated with asthma but is not a marked feature in other chronic inflammatory diseases such as COPD[63]. Thickening of the basement membrane is attributed to the increase in the *lamina reticularis*. Different groups of asthmatics, including children and adults, mild, moderate and severe asthmatics have been shown to have basement membrane thickening relative to non asthmatic controls[63-67]. The correlation with disease severity or symptoms is more controversial, with some studies showing basement membrane thickening to be correlated to decreased airway distensibility[66], decreased lung function (FEV_1)[63;67] and increased airway hyperresponsiveness (PC_{20})[68], whilst others show no correlation with lung function[63;64]. Heterogeneity in the manifestation of disease, treatment regimes and sampled populations may account for some of the differences observed and highlights difficulty in directly comparing such studies.

1.4.6 Increase in fibroblasts and smooth muscle

Fibroblasts are mesenchymal in origin. Typically they are spindle shaped cells which reside in most tissues and have a role in maintaining the extracellular matrix. There is a degree of plasticity in the phenotype of the fibroblast, ranging from a highly synthetic cell to a highly contractile phenotype which is sometimes known as the

myofibroblast. Myofibroblasts are important in wound closure and healing. The plasticity in the fibroblast phenotype and its reversibility has given rise to inconsistent and sometimes confusing usage of the terms in the literature, especially in cases where the cells have not been well characterised. The expression of α-smooth muscle actin (α-SMA) is the most common marker that is used to distinguish between fibroblasts and myofibroblasts. However, this can also cause confusion since both myofibroblasts and smooth muscle cells express α-SMA. As yet, there is no known cytoskeletal protein that conclusively distinguishes myofibroblasts and smooth muscle cells apart. For a review on myofibroblasts see Hinz 2007[69].

Increased numbers of fibroblasts or myofibroblasts in the submucosa of the asthmatic airway has been a long established feature of airway remodelling. This increase in fibroblasts is thought to account to some extent for the increased collagen deposition below the basement membrane[70;71]. Another hallmark of remodelling is the obvious increase in the size and number of smooth muscle cells in the airway[72]. This smooth muscle cell hyperplasia and hypertrophy has been associated with increased disease severity, and smooth muscle cell thickness can be increased up to 3 fold when compared to non asthmatic controls[71]. A review of numerous studies which evaluate smooth muscle mass in the asthmatic airways by James and Carroll has shown, that despite the differences in subject selection, sampling techniques and quantification (and therefore the inability to make direct comparisons between studies), there was consistent reporting of increased smooth muscle in the samples from asthmatic airways relative to non asthmatic controls. The greatest differences were observed in cases of severe asthma[73].

It can be speculated that contraction of an increased smooth muscle mass in asthmatic may be mechanically associated with increased airway hyperresponsiveness and airflow restriction, since airway smooth muscle is largely responsible for regulating airway calibre. In one recent study by Masumoto, smooth muscle cells from 5 asthmatic and 6 non-asthmatic subjects were cultured in collagen gels. These gels were treated with histamine to stimulate contraction. The maximal contraction achieved was significantly higher for the asthmatic smooth muscle cells when compared with the non asthmatic cells[74]. Although the study was limited by its size and its choice of non asthmatic subjects which suffered from other diseases, it does suggest that the smooth muscle cells of asthmatics could be more contractile. This is in agreement with another study in which smooth muscle shortening induced by electrical stimulation was assessed in smooth muscle cells derived from bronchial

biopsies from asthmatic and non asthmatic individuals[75]. Increased muscle mass which is more contractile is clearly an attractive explanation for bronchoconstriction associated with asthma but its relevance remains to be verified *in vivo.*

1.4.7 Increased vascularity

Capillaries in the submucosa are necessary to ensure adequate nourishment of the epithelium and are required for the removal of waste products. Typically, vessels are tube like structures, with a single layer of endothelial cells lining the lumen of the vessel. These cells sit on a basement membrane made up of collagen type IV, laminin, entactin and heparan sulphate proteoglycans. Pericytes are in close proximity to the basement membrane and endothelial cells and have a stabilising effect on the vessels[76].

Increased vascularisation of the airways was first described in patients with fatal asthma. It has since become a recognised and confirmed feature of the remodelled airway of living asthmatics. Kuwano and colleagues analysed lung specimens from 15 asthmatics (8 cases of fatal asthma, 3 asthmatics who did not die from asthma and 4 asthmatics who had undergone lung resection for tumours) and 15 non asthmatics (also undergoing resection for peripheral tumours) and 15 COPD patients. They found that asthmatics had marked increase in the proportion of the submucosa which occupied by blood vessels[77]. In a separate study of fatal asthma, an increase in the number of large vessels and vascular area was observed in the large cartilaginous airways[78].

Bronchial biopsy studies have consistently shown increased vascularity in asthmatic airways when compared with non asthmatic individuals. A study in 2000 by Vrugt and colleagues, took bronchial biopsies from 15 atopic severe asthmatics, 15 mild atopic asthmatics and 8 non atopic individuals. Bronchial biopsies were sectioned and stained with an antibody against the endothelial cell marker CD31, and the vessels in two areas of the section were counted. The number of vessels was found to be significantly increased per unit area in severe asthmatics in comparison to mild asthmatics and control subjects[79]. In a study by Hoshino and colleagues bronchial biopsies from 16 atopic asthmatics and 9 non asthmatic individuals were taken and sections were taken for immunohistochemistry and stained with an antibody again collagen IV to identify vessels by the presence of the vessel basement membrane. It was found that both the number of vessels per section area and the percentage of vessel per section area were significantly increased in the asthmatic subjects,

although there was no difference in the actual size of the vessels. The lung function of the asthmatics defined by FEV_1 was found to negatively correlate with increased vascular area[80].

Although the increase in vascularity may not increase the thickening of the airway epithelium, it can be speculated that enhanced blood supply can provide nourishment for thickened tissue, and provide increased entry points for inflammatory cells migrating into the epithelium. In addition, stimulation by histamine may render the vessels leaky and increase the exudate into the airway and also contribute to the increase in the viscosity of secreted mucus, which may explain its association with more severe disease symptoms.

1.4.8 Evidence for airway remodelling early in life

Historically there has been more emphasis on studies focused on the inflammatory processes associated with asthma. Remodelling of the airways was perceived to be secondary and a result of the damage inflicted by the chronic inflammation. In more recent years the importance of airway remodelling in the development of asthma has been realised.

It is evident from bronchial biopsies taken from children with moderate asthma that the remodelling events begin early in disease development. In a retrospective study Pohunek *et al.* demonstrated that the airways of children who develop asthma show basement membrane thickening and inflammatory cell infiltration of the airway even prior to the clinical diagnosis of asthma. Children between the age of 1.3 and 11.7 years old underwent bronchial biopsies after showing respiratory symptoms such as chronic cough and mild wheezing in most cases, but not clinical asthma. These children were followed up between 22 to 80 months after the bronchoscopy to assess whether they had developed asthma. Comparing the bronchial biopsies taken prior to disease development, it was shown that eosinophilic inflammation and increased *lamina reticularis* thickening was increased significantly in the children who developed asthma in comparison to those who did not[81]. This observation of early remodelling events suggested that remodelling may start at the same time as airway inflammation or could even precede it and may not necessarily follow chronic inflammation. This view was further supported by a subsequent study by Cokugras *et al.*, which showed that 9 out of the 10 bronchial biopsy samples from children aged between 5-14 years old with moderate asthma showed increased thickening of the basement membrane. In a few cases goblet cell hyperplasia and loss of cilia from epithelial cells were also seen. In three cases, the fibroblasts appeared to be

activated and showed deposition of collagen. However out of these ten samples, although infiltrating lymphocytes, and degranulating mast cells were observed, only one sample showed the traditional hallmark of asthma, eosinophilia[82].

1.5. Mechanisms regulating the remodelling processes

Although the underlying mechanisms that lead to asthma remodelling of the airway is still an area of intense research, data is already emerging to suggest that asthmatics have an impaired epithelium which makes them more susceptible to damage. Once damaged, the repair and inflammatory processes orchestrate the remodelling of the airway and result in the progression of disease, **Fig. 1.2**.

1.5.1 Defective epithelial cell barrier

In asthma, the epithelium can be considered as a chronic wound. The damage to the epithelium is evident from the sloughing of epithelial cells into the airway lumen, and the functionally impaired irregular epithelial cell layer left behind. Bronchial biopsies from asthmatic patients have shown that the epithelial cells are actively mediating a repair response. In the repair process, epithelial cells are required to migrate to the wound sites, proliferate and differentiate to repopulate the damaged areas. Growth factors of the epithelial growth factor (EGF) superfamily are able to simulate these processes. These growth factors mediate their responses through the family of EGF tyrosine kinase receptors. *In vitro,* damaged (16HBE) epithelial cell monolayers can accelerate the rate of wound closure if they are stimulated with exogenous EGF. Bronchial biopsies from the asthmatic airway have elevated expression of EGFR in the epithelial cell layer. Its expression extends through the epithelial layers right through to the apical surface of the cells in both mild and severe asthmatics, unlike the limited expression to the basal cell and their connections with cuboidal cells in non asthmatic controls[83]. New data coming from the studies of bronchial biopsies and primary bronchial epithelial cells grown as differentiated cultures *in vitro,* suggest that tight junction formation between epithelial cells is impaired in asthmatics. This could therefore increase an individual's susceptibility to insults from the environment such as pollutants, biologics and allergens as a result of reduced barrier function[84]. This may explain the increased bronchial hyperresponsiveness seen in asthmatics. Many allergens such as pollen[85], house dust mite allergen Der p1[86] and cat allergen Fel-d1[87] have proteolytic activity which may promote epithelial cell damage and allergic sensitisation if allowed to pass through the physical barrier. If this is the

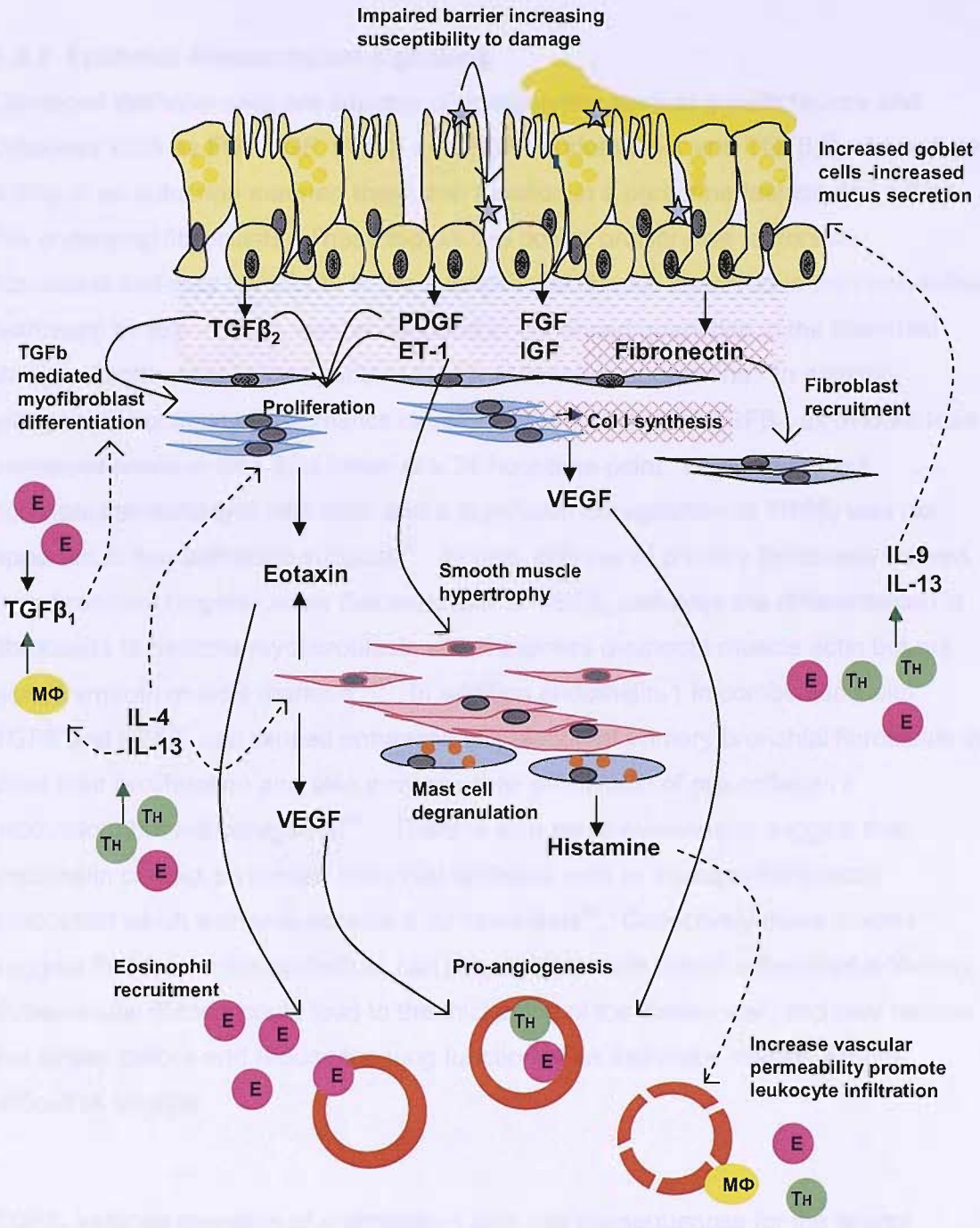

Fig. 1.2 Airway remodelling orchestrated by EMTU signalling and its interaction with inflammatory cells and mediators. Schematic highlighting the mechanisms involved in the airway remodelling in asthma. Mediators that are released by resident airway cells can participate in EMTU signalling. Mediators released from inflammatory cells (green arrows) are also able to modulate the process are also shown. T_H, E, MΦ, and stars represent T_H2 cells, eosinophils and macrophages, and air-bourne allergens/pollutants /pathogenic agents respectively. The curved arrows highlight the target cell type of the EMTU released (solid) and inflammatory mediators (dotted), and the processes in which they are involved in.

case, then it is worth speculating whether defective epithelial function could be the basis for the initiation of remodelling and asthma.

1.5.2 Epithelial-Mesenchymal signalling

Damaged epithelial cells are capable of upregulating several growth factors and cytokines such as FGF, IGF, PDGF and EGF , endothelin-1 and $TGF\beta_2$[88]. As well as acting in an autocrine manner, these can function in a paracrine fashion and act on the underlying fibroblasts. These factors are potent proliferative factors for fibroblasts and may contribute to the subepithelial fibrosis observed in the remodelled asthmatic airway. $TGF\beta_1$ can be detected in enhanced quantities in the bronchial lavage of asthmatics in comparison to non asthmatics at baseline. In addition, allergen provocation of asthmatics causes an upregulation of $TGF\beta_1$, as evident from increased levels in BAL fluid taken at a 24 hour time point. Levels were not correlated to leukocyte infiltration and a significant upregulation of $TGF\beta_1$ was not apparent in non asthmatic subjects[89]. *In vitro,* cultures of primary fibroblasts derived from bronchial biopsies show that exposure to $TGF\beta_2$ can drive the differentiation of fibroblasts to become myofibroblasts which express α-smooth muscle actin but not typical smooth muscle markers[90;91]. In addition endothelin-1 in combination with TGFβ and PDGF can caused enhanced stimulation of primary bronchial fibroblasts to drive their proliferation and also increase their production of pro-collagen I production, but not collagen III[92]. There is also some evidence to suggest that endothelin can act on human bronchial epithelial cells to increase fibronectin production which a chemo-attractant for fibroblasts[93]. Collectively these studies suggest that *in vivo* the epithelium can play an extensive role in subepithelial fibrosis. Subepithelial fibrosis could lead to the thickening of the airway wall, and may reduce the airway calibre and reduce the lung function of an asthmatic making it more difficult to breathe.

$TGF\beta_2$ induced secretion of endothelin-1 also has consequences for the airway smooth muscle[90]. Endothelin is an extremely potent smooth muscle contractant and has been shown to induce broncho-constriction in several animals. *In vitro*, its potential role in asthma is further highlighted by the ability to induce smooth muscle cell hypertrophy and reduce apoptosis in response to stress[94]. This gives rise to the possibility of that damaged epithelial cells can signal to the smooth muscle below and be involved in mediating smooth muscle cell hypertrophy and hyperresponsiveness.

In addition, TGFβ_2 also increases the expression of VEGF in primary bronchial fibroblasts *in vitro.* VEGF is a potent pro-angiogenic agent which may be implicated in the increased vascularity in the bronchial airway. In addition, VEGF can increase the permeability of existing vessels; this may increase vascular leakage and impact the viscosity of the secreted mucus.

1.5.3 Interaction with the immune system

The impaired barrier function of the epithelium increases the likelihood of bacteria, viruses, environmental pollutants and allergens to penetrate further into the epithelium than normal. This may increase the ability of noxious agents and allergens to damage the epithelium further and/or interact with the immune system leading to inflammation. In the majority of cases the inflammation tends towards a T_H2 mediated response, and eosinophilia representing the allergic element of the disease.

T_H2 cells release cytokines capable of interacting with several targets to enhance remodelling processes. In guinea pig epithelial cells cultures treated with IL-13 cells can be driven to differentiate into goblet cells, but subsequent withdrawal of IL-13 can reduce the expression of the mucin gene *MUC5AC* and goblet cell numbers[95;96]. A murine model demonstrated that intra-tracheal injection of IL-9 into mice could rapidly induce the upregulation of *MUC5AC* gene expression and the appearance of goblet cells in the large airways. These differences were observed as early as 24 hours after the initial injection before the development of inflammation, but were not observed in mice injected with BSA saline as a control. Repeated exposure to daily IL-9 doses led to increased inflammation, the upregulation of IL-13 and also further increases in goblet cell number[97]. Similarly treatment of differentiated human epithelial cells grown as air-liquid interface cultures treated with IL-13 and IL-4 between 7-14 days increases the goblet cell density in the cultures and drives the cells into a hypersecretory phenotype[98].

In normal and asthmatic individuals IL-9 is found at undetectable or low levels in BAL fluid. However, significantly elevated IL-9 levels have been found in the BAL fluid of mild atopic asthmatics 24 hours after bronchoprovocation with allergen compared with saline controls. This was found to be a result of increased *IL-9* gene expression in lymphocytes[99]. Similarly, IL-13 levels are also increased in BAL fluid of atopic

asthmatics at 48 hours post bronchoprovocation[100]. The increased levels of these cytokines in the airway make it plausible that these may influence airway mucus production and obstruction of the airway, leading to coughing and difficulty in breathing. Whether the upregulation of these T_H2 cytokines is characteristic of allergic asthmatics or just allergy remains to be confirmed.

In vitro, differentiated epithelial cells derived from human trachea that are grown as air liquid interface cultures, show that IL-9 treatment does not affect the organisation of the differentiated epithelium. However, it could do so if the epithelium was damaged. Fluorescence microscopy and scanning and transmission electron microscopy showed that exposure of the damaged epithelium to IL-9 increased the goblet cell to ciliated cell ratio. IL-9 also increased mucus secretion onto the apical surface in comparison with control cultures. The damage was speculated to be a secondary signal required by the epithelium before it could gain responsiveness to the IL-9 [101;102]. Similarly, IL-13 has been shown to be able to alter epithelial cell differentiation in cultures of primary human nasal epithelial cells in culture. Epithelial cells grown in suspension as spheroids typically undergo mucocillary differentiation into ciliated cells, however under influence IL-13 cells can be directed to differentiate into non ciliated MUC5AC positive cells[103]. Although further *in vivo* evidence in cases of asthma is required to confirm that these processes occur in disease, it can be conceived how an impaired and damaged epithelium may respond to these cytokines which would in turn contribute to remodelling.

IL-4 and IL-13 produced by T_H2 cells and eosinophils can stimulate primary bronchial fibroblasts to increase collagen synthesis and also increase fibroblast proliferation [90]. IL-4 can be upregulated in allergic asthmatics in response to bronchoprovocation, and the increased levels can be detected in BAL fluid[104]. In mice the overexpression of IL-13 can result in elevated $TGF\beta_1$ levels in epithelial cells and macrophages[105]. As discussed previously, TGFβ is a potent inducer of myofibroblast differentiation. It therefore opens up the possibility that IL-4 and IL-13 may increase the extent of subepithelial fibrosis through a TGFβ mediated mechanism in the asthmatic airway.

Both human airway fibroblasts and smooth muscle cells respond to IL-4 and IL-13 by producing eotaxin, a potent eosinophil chemo-attractant. There is also some evidence to suggest that the induction is increased when IL-13 works synergistically

with TGFβ[106-108]. Eosinophils can be recruited by this surge of eotaxin and eosinophilia has been associated with remodelling events in murine models [109]. Furthermore in a study in which eosinophilia was reduced in atopic asthmatic patients by the administration of anti-IL-5 antibody (mepolizumab) a reduction of extracellular matrix proteins collagen III, lumican, tenascin was observed in the basement membrane relative to the patients treated with the placebo, and this was speculated to be a consequence of a reduction of eosinophil derived $TGF\beta_1$[110]. This suggests that eosinophilia can also influence the remodelling processes that occur in the asthmatic airway.

1.5.4 Mediating increased blood vessel growth

The mechanisms which underlie the increased vascularity are believed to arise through the process of angiogenesis. Angiogenesis is the process in which new blood vessels form from pre-existing ones and it is the predominant method in which blood vessels form in post-natal life. This process is tightly regulated by both pro-angiogenic and angiostatic mediators in the tissue. A stimulus such as hypoxia can cause perturbation in the balance of these mediators and result in increased vessel formation. In support of this imbalance in the setting of asthma, a recent study into the angiogenic potential of bronchial lavage fluid taken from asthmatic and non asthmatics has shown that asthmatic BAL fluid can promote angiogenesis *in vitro*. In this study co-cultures of endothelial cells (HUVECs) and dermal fibroblasts were stimulated with BAL fluid from asthmatic and non asthmatic individuals, the cells' ability to organise into tube like structures which bear similarities to vessels was assessed. This process is considered to be an important step in angiogenesis. A brief schematic of the events that occur during angiogenesis is shown in **Fig. 1.3**. The pro-angiogenic factors VEGF and angiogenin were found to be increased in BAL fluid from asthmatics relative to angiostatic mediators endostatin and angiopoietin-2 which remained similar in asthmatic and control subjects. Depletion of VEGF from the asthmatic BAL fluid abrogated its angiogenic effects [111]. Increased immuno-reactivity against the angiogenic mediators VEGF, bFGF and angiogenin has been observed in asthmatic airway biopsies when compared with those from normal individuals. The number of positively stained cells for each of the angiogenic mediators also correlates to increased vessel area in the airway. The immuno-reactivity predominantly localised to cells of the immune system, especially eosinophils, mast cells, T cells, macrophages, and $CD34^+$ (a haemopoietic stem cell marker) cells[80].

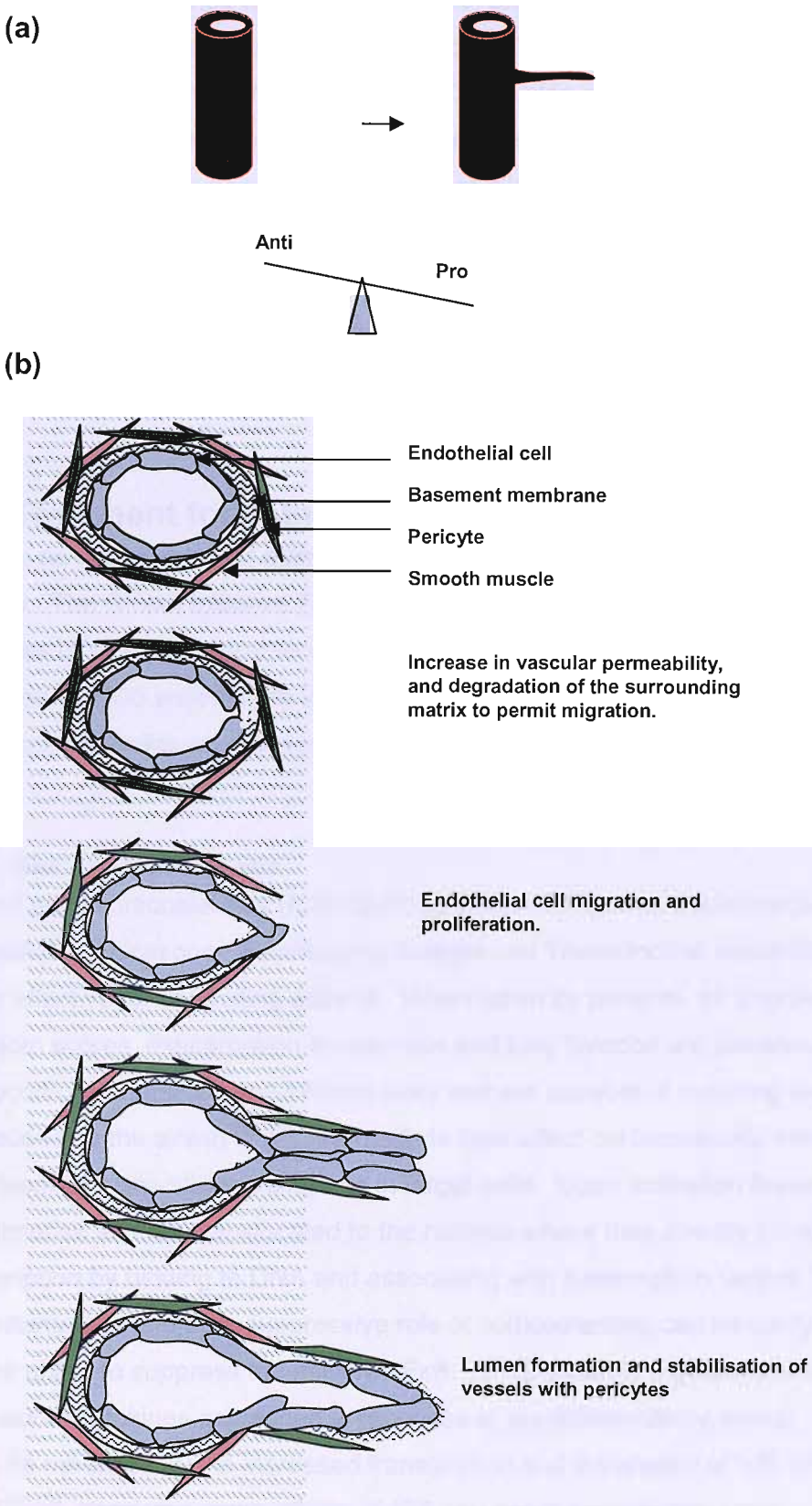

Fig. 1.3. Schematic of angiogenesis. The perturbation of the pro- and anti-angiogeneic mediator in tissues can lead to angiogenesis. New capillaries sprout from existing vessels (a) and is regulated by many different types. This schematic (b) shows some of the main processes involved in angiogenesis and sprouting.

There is further evidence to show that *in vitro*, pro-inflammatory cytokines such as TNFα and IL-1β can stimulate smooth muscle cells to release VEGF by 2-3 fold over basal levels[112]. T_H2 cytokines IL-4 and IL-13 can also stimulate increased VEGF release from human tracheal smooth muscle cells, but the magnitude of the effect can be affected by the possession of different alleles of the *VEGF* gene. This upregulation appears to result from the stabilisation of *VEGF* mRNA[113]. The ability of the immune cells to secrete and influence angiogenic mediators in the airway again re-emphasises the importance of the interaction between the resident cells in the airway and inflammatory cells in orchestrating aspects of airway remodelling.

1.6. Treatment for asthma

There is no known cure for asthma, only treatments to target the symptoms of disease. The Global Initiative For Asthma (GINA) program initiated in 1993 continues to provide recommendations for asthma management. The revised report published in 2005 outlines the treatments available for dealing with asthma. Glucocorticosteroids and β2 agonists are the most widely used to control asthma[2].

1.6.1 Glucocorticosteroids

Inhaled glucocorticosteroids (ICS) (such as Beclomethasone, Budenoside, Flunisolide, Fluticasone, Memetasone fluorate and Triamcinoline acetonide) are highly effective for controlling asthma. When taken by patients, an improvement in symptom scores, exacerbation frequencies and lung function are observed[114;115]. Glucocorticosteroids are anti-inflammatory and are capable of reducing leukocyte infiltration into the airway[115;116]. To mediate their effect corticosteroids interact with cytoplasmic glucocorticoid receptors in target cells. Upon activation these receptors can dimerise and are translocated to the nucleus where they directly modulate gene transcription by binding to DNA and associating with transcription factors [117-119]. The anti-inflammatory/immunosuppressive role of corticosteroids can be partly attributed to their ability to suppress the activity NFκB. NFκB which is a potent transcriptional regulator of cytokines expressed in response to pro-inflammatory stimuli. This effect could be mediated by the increased transcription and translation of IκB, an inhibitor of NFκB[120;121]. However, some effects of ICS can occur immediately upon administration and can not be attributed to a change in gene expression patterns which takes place over hours. It is now recognised that ICS have non genomic effects which may contribute to its efficacy as an asthma treatment. Non genomic

effects can result in decreased blood flow to the airway which may reduce airway obstruction, and slow down the clearance of other treatments such as β2 agonists[122].

1.6.2 β2-agonists

The dose response to glucocorticosteroids is relatively flat. So for the treatment of moderate and severe asthma, add on therapies used in combination to ICS can be a more effective treatment than increasing the dose of ICS[123;124]. Inhaled long acting β2-agonists (such as Formoterol and Salmeterol) can act over 12 hours, short acting β2 agonists (such as Salbutamol) provide shorter relief. The primary roles of these drugs are to relax the airway smooth muscle to achieve bronchodilation and reduce bronchial hyperresponsiveness. These drugs mediate their effects by stimulating the β2 adrenergic receptor, a G protein coupled receptor which can be found on the surface of smooth muscle cells[125]. The downstream signalling from this receptor results in muscle relaxation and bronchodilation. In addition there are some non bronchodilatory effects of β2 agonists that maybe relevant to asthma treatment. Bronchoconstriction induced by AMP is significantly reduced after β2 agonist treatment in comparison with methacholine induced bronchoconstriction[126]. AMP causes bronchoconstriction indirectly through mast cell activation, unlike methacholine which acts directly on smooth muscle cells. Since antihistamine can also reduce AMP induced bronchoconstriction in asthmatics,[127] it has been postulated that β2 agonists may also target mast cell function. There is also evidence to show that the downstream effects of β2 agonists and ICS may interact and complement each other, for example ICS may cause the upregulation of the β2 adrenergic receptor[128].

1.6.3 Add-on treatments

There are also other several add on treatments that are sometimes used in addition to ICS and β2 agonist treatments[2]. They are usually used if ICS and β2 agonists alone provide insufficient control of asthma in a patient. These include leukotriene modifiers such as Montelukast, Pranlukast and Zafirlukast. These are antagonists of the leukotriene receptor CysLT1, and therefore reduce the effect of the leukotrienes released from mast cells and basophils. Chromones (such as sodium chromoglycate) are used as non steroid anti-inflammatory drugs. Theophylline is used as both an anti-inflammatory and a bronchodilator, but side effects occur more commonly[2;129].

1.6.4 Anti-IgE therapy

In recent years, there have been several studies looking at the effect of using neutralising antibodies in asthma treatment. In particular anti-IgE therapy (Omalizumab) has been promising. Anti-IgE therapy is targeted at reducing the inflammation in the airway of allergic asthmatics. It removes IgE from the circulation, reducing its availability for binding onto mast cells, and it also decreases the expression of the high affinity IgE receptor on mast cells, basophils and dendritic cells. This results in decreased mast cell activation and airway inflammation, in particular a reduction in airway eosinophilia. This leads to a reduction in the frequency of exacerbations, hospitalisation and an increased quality of life for patients. It has been shown to be an effective add on therapy for treating moderate to severe asthmatics with poorly controlled asthma[130-133]. However, ~35% of allergic asthmatics do not respond to anti-IgE therapy, although why this should be so is still to be explained[134].

1.6.5 Anti-TNFα therapy

It is being increasingly recognised that there are cases of severe difficult to treat asthma in which the inflammatory profile of the airway deviates from the typical allergic asthma and T_H2 response. The inflammation in these cases have resemblance to a T_H1 response, with neutrophilia[10;135-137] and elevated levels of TNFα[138] in the airway. Anti-TNFα therapy is already being successfully used to treat other chronic inflammatory diseases such as rheumatoid arthritis[139]. Recently anti-TNFα therapy in the form of a soluble TNF receptor fusion protein (Etanercept) has been trialled as treatment in severe asthma. Initial studies have shown that anti-TNFα therapy improved asthma symptoms, lung function and airway-hyperresponsiveness in patients with severe asthma[138;140]. Further clinical trials using both Etanercept and blocking antibodies against TNFα are being undertaken.

1.6.6 Treatment and airway remodelling

Treatments for asthma are predominantly aimed at reducing the inflammation in the airway and are effective for controlling mild and moderate disease. Whether these drugs are capable of reversing remodelling is still somewhat controversial. Several studies have investigated the effect of ICS treatment on the subepithelial thickening in the airways of mild to moderate asthmatics. These subjects were not on ICS treatment prior to participation in the study. Treatment with Beclomethasone for 4 or 6 months significantly reduced the thickness of the *lamina reticularis* and collagen III deposition relative to subjects treated with a placebo[141;141-143]. In other studies

treatment with ICS have not been reported to reduce these parameters[144;145]. These differences may reflect differences in the duration and dosing of ICS treatment, with the studies using higher doses of ICS and longer treatment periods showing a more significant effect.

In another study, asthmatics on ICS treatment have been reported to have reduced airway vascularity relative to those not on ICS treatment[146]. These findings are in agreement with another study in which treatment with inhaled fluticasone for 3 months lead to a reduction in airway vascularity in mild to moderate asthmatics (not on ICS prior to participation)[147]. However, in a study of severe glucocorticoid dependent asthmatics (on ICS and oral corticosteroids medication) a marked increase in vascularity was still observed in comparison to mild and non-asthmatics not on ICS[79]. This suggests that while ICS may be able to reverse some of the remodelling processes in mild disease, doing so in severe disease maybe more difficult. Whether ICS treatment can influence other aspects of remodelling remains to be elucidated. Despite the evidence suggesting that ICS may influence some of the remodelling processes, prolonged ICS treatment does not necessarily return airway hyperresponsiveness to within the normal range[148].

1.6.7 Treatment and the natural history of asthma

Although ICS are effective in controlling asthma, a recent clinical trial has demonstrated that ICS treatment does not alter the natural history of the disease. The Prevention of Early Asthma in Kids (PEAK) study tested whether giving ICS treatment to young children (2-3 years of age) who were in high risk of developing asthma could prevent the development of disease. In the PEAK study, 285 children were recruited and split into two groups. One group received inhaled Fluticasone propionate (44µg) twice a day, the other received a placebo. ICS and placebo were given for 2 years after which they were withdrawn. The children were monitored throughout the treatment period and for a year after treatment withdrawal. The study showed that ICS treated children had an increased number of episode free days in which no asthma-like symptoms were reported, supplementary asthma medications were not used and there were no medical visits for respiratory symptoms, relative to placebo taking group. However, during the post-treatment observation year the clinical improvement in the children treated with ICS disappeared, and the two groups of children did not significantly differ in the development of asthma symptoms or lung function. Therefore, ICS treatment was shown to have little therapeutic effect on the processes that determine the progression of asthma[149].

1.6.8 An unmet clinical need

Corticosteroid resistance in a subgroup of asthmatics has been well documented[150;151]. Asthmatics and in particular severe asthmatics who are refractory to corticosteroid treatment and remain symptomatic with frequent exacerbations represent an unmet clinical need. With airway remodelling implicated in the underlying basis for asthma, the development of new therapeutics targeted directly at the remodelling processes and not at inflammation maybe of clinical benefit. Perhaps these could be used as alternatives or add on treatments alongside current therapies. In the most optimistic scenario, drugs which prevent or effectively reverse airway remodelling may serve to alter the progression of asthma and may be suitable for use as a prophylactic..

1.7. Genetic predisposition to asthma

Asthma does not occur randomly within the population. It tends to run in families indicating a genetic component to susceptibility. The risk of a child developing asthma is increased if one or both of the child's parents are asthmatic. It has been estimated that the risk factor is 3 times for a child developing asthma if one parent is asthmatic. This figure doubles if both parents are asthmatic. Interesting, maternal asthma has been demonstrated in several studies to be a greater risk factor than paternal asthma, leading to the speculation that maternal conditioning of the developing foetus in utero maybe an attributing factor[152;153]. Further support for a genetic susceptibility for asthma comes from twin studies, in which the concordance for asthma was shown to be greater in genetically identical monozygotic twins relative to dizygotic twins[154].

Genetic studies into asthma susceptibility have demonstrated that simple Mendelian genetics are insufficient to explain the complex inheritance patterns seen in asthma. It appears that asthma susceptibility is not conferred by one single genetic factor alone, but may result from a sum of multiple susceptibility genes which exert a mild to moderate influence on lung function and the asthma phenotype. It also appears that the combination of the genes which cause asthma is variable with different combinations of asthma susceptibility genes able to result in increased disease susceptibility. To complicate the genetics further, there is the added concept of gene-environment interactions which can influence the development of disease. It is accepted that environmental exposure to airbourne antigens can influence lung and asthma development, and how an individual responds to the exposure can be

dependent on their genetic make up. Therefore a genetically susceptible individual may not necessarily develop clinical asthma due to the lack of exposure of a potentiating environmental stimulus, and this can add to the difficulty and confusion in studying into the genetic component of asthma in different populations.

1.7.1 Identifying genes and loci associated with increased asthma susceptibility

A combination of positional cloning and candidate gene approaches have been used to identify asthma susceptibility genes. In both approaches, it is advantageous to choose subjects in which there is a strong hereditary component conferring susceptibility as indicated by familial clustering of disease. The candidate gene approach involves focusing efforts on genes which can be intuitively linked to asthma and the mechanisms underlying the disease process. For example, genes encoding cytokines found in elevated levels in the asthmatic airway or genes which could modify lung function may be candidates. The polymorphisms in the candidate gene and their influence on disease are then subsequently studied by comparison between asthmatic and non asthmatics individuals. The positional scanning approach has a wider scope and is used to scan initially for broad regions of the genome that are associated with disease. The completion of the human genome project in (working draft 2001, and complete sequencing in 2003)[155;156] has accelerated the positional cloning efforts. It has reduced the need to sequence regions of chromosomes found to be linked to asthma, in order to determine which genes are found in the region. The DNA markers that are frequently used for positional scanning studies are microsatellites and more recently single nucleotide polymorphisms (SNPs). SNPs occur at high frequency and are relatively evenly distributed throughout the genome; this allows fine mapping of the DNA region associated with disease[157]. The distribution of SNPs in a linked region are analysed to find those with distinct patterns or alterations which are more commonly associated with asthmatic individuals relative to non-asthmatic individuals. Once identified, chromosomal regions which confer susceptibility are examined more closely to establish which gene(s) is responsible for the linkage, and it is at this point where the positional cloning and candidate gene approaches come together. Genes in the linked region which have roles which are known or suspected to be factors that modulate the development or manifestation of asthma are usually the first to be investigated. Using the candidate gene strategy, further population genetic studies, *in vivo* and *in vitro* studies can be

used to establish the risk associated with the specific loci, and explore possible mechanisms underlying the susceptibility.

1.7.2 Susceptibility genes

To date, numerous loci and genes have been reported to be associated with asthma. Since asthma is intricately associated with atopy, many are key players in the immune system. Their gene products could potentially have modulatory effects on allergic responses, and therefore also on asthma. Others that have been identified appear to modulate normal airway function. The sheer number of asthma associated genes highlights the genetic complexity of the disease. The discrepancies in the associations shown between different studies could be due to differences in the ethnic group, environmental exposure and variation in the asthma phenotypes studied. Some of the identified loci and the candidate genes in the region are outlined below[158].

Chromosome 5q31-33

This region on chromosome 5 harbors the T_H2 cytokine cluster containing the *IL-3, IL-4, IL-5, IL-9 and IL-13* genes. These cytokines as discussed before, are important in both regulating the chronic inflammation and the remodelling processes involved in asthma. Polymorphisms in the *IL-4* promoter have been associated with asthma and its severity. There have been studies to indicate the polymorphisms in the promoter are associated with airway hyperresponsiveness in Taiwanese populations[159] and differential serum IgE levels in asthmatics[160], although this does not appear to be reflected in all studies[161]. The *IL-13* gene has been extensively studied. A polymorphism in the *IL-13* promoter at position -1111 shows linkage with both allergic asthma and the BHR phenotype in Dutch populations[162]. A coding change at position 110 of IL-13, substitutes glutamine for arginine in the protein and has also been linked to asthma rather than serum IgE levels in British and Japanese populations[163].

Chromosome 6pq21

The susceptibility region on chromosome 6 harbours the *MHC* gene cluster. Different MHC haplotypes, will cause changes in the way antigens are presented to T cells. T cells play a role in coordinating the innate and adaptive immune responses, and therefore can affect disease development and progression. A non classical MHC class I molecule found in this region is *HLA-G*. *HLA-G* is selectively expressed

by the foetus in trophoblast tissue at the mother-foetus interface and is thought to protect the foetus from maternal rejection by promoting a T_H2 milieu. The possession of certain *HLA-G* haplotypes confers susceptibility of the fetus to asthma, and the precise haplotype is dependent on whether the mother has bronchial hyperresponsiveness. The dependency on maternal phenotype with foetal genotype supports the theory that foetal-maternal interaction during gestation is important in asthma development[164;165].

Chromosome 7p14 and 7q32-7

The G protein coupled receptor for asthma susceptibility (GPR154, also *GPRA*) gene resides on chromosome 7. The receptor has been found to be associated with asthma in Finnish, Canadian, German and Italian populations with some of the studies also showing association with elevated serum IgE levels and atopy or bronchial hyperresponsiveness. Neuropeptide S has been identified as its ligand. Both *GPR154* and Neuropeptide S are expressed in bronchial epithelial cells and smooth muscle of the epithelium, therefore localising them to an area where they could potentially modulate the immune response and the airway remodelling processes in asthma. However the functional significance of GPR154 and its ligand are yet to be determined[166-170].

The calcium activated chloride channel gene 1 (*CLCA1*) also found here appears to have a role in increased mucus secretion. Different haplotypes of this gene are associated with low and high risk of asthma in the Japanese population[171]. *CLCA1* is the human homologue to the mouse *Gob-5* gene, which encodes a chloride channel involved in regulating mucus secretion and hypersecretion in response to allergen challenge. There is some evidence to suggest that *CLCA1* expression is regulated by the T_H2 cytokines IL-9 and IL-13. *CLCA1* may therefore be a target through which inflammatory cytokines influence the airway remodelling processes[172;173]

Chromosome 11q13-21

Clara Cell Secretory gene (*CC16*) is found on chromosome 11. Different haplotypes of the gene show association with asthma in children[174] and adults[175]. The level of this protein has also been reported to be lower in asthmatic children[176]. Clara cells are non ciliated cells that are found among the epithelial layer of the airway and are thought to be pluripotent cells which are important in the regeneration of the epithelium after injury. Clara cells secrete CC16, an anti-inflammatory mediator that has a protective role against oxidative stresses. It can be envisaged that defects in

the function or expression of the CC16 protein could have an effect on the restoration of the damaged epithelium and therefore affecting its integrity and barrier function.

Also in this chromosome region is the gene encoding the FcεRI β chain. This receptor as mentioned previously is important for mast cell activation. It plays a major role in mast cell degranulation when receptors come in to contact with aero-allergens. Genetic variants of this gene have been associated with asthma and atopy[177;178]. Studies in different populations do not necessarily show the same association and again highlight the difficulty in genetic studies in asthma. Linkage to this gene may indicate an association with atopy rather than asthma *per se*.

Another asthma susceptibility gene on chromosome 11 the Glutathione S transferase P1 (*GSTP1*) gene, encodes an enzyme that is highly expressed in the lung and is thought to have a protective role against oxidative stress from aero-pollutants. Interestingly the polymorphism giving rise to a codon change at position 105 changes the efficiency of this enzyme. Isoleucine at this position decreases enzyme activity seven fold compared to the enzyme with valine at this position. Although some studies have not shown an association with this polymorphism with asthma or bronchial hyperresponsiveness[179], other studies have showed that it poses significant increased risk when children living in areas polluted areas are considered. Thus, indicating the importance of gene- environment interactions in determining risk and manifestation of asthma[180].

Chromosome 20p13

In 2002, a collaborative study between the University of Southampton and research groups in the United States identified *ADAM33* as a novel asthma susceptibility gene. In the initial study 460 asthmatic Caucasian Sib-pairs in the UK and the US were used to pinpoint a 2.5Mbp region on chromosome 20 that showed linkage with the asthmatic phenotype, with a LOD score of 2.94. The LOD score is a mathematical calculation of the likelihood of real linkage between a DNA region and a defined phenotype. When the studied population was then further analysed with regards to atopy and bronchial hyper responsiveness (BHR), the resulting LOD scores were 2.3 and 3.93 respectively, suggesting that the presence of polymorphism(s) in this region of DNA are likely to be more important in the development of asthma associated with bronchial hyperresponsiveness rather than the atopic phenotype[181]. Genes in the highlighted region were characterised. Using case controlled studies, a total of 135

SNPs were typed within 23 genes to provide allele and genotype frequencies. A significant cluster of these SNPs lay within the *ADAM33* gene. SNPs identified in the *ADAM33* gene from that study are shown in **Fig 1.4**. This initial finding was exciting and identified a gene that was suspected to play a role in airway remodelling rather than atopy and inflammation. Subsequent genetic studies have found *ADAM33* to be associated with asthma in different populations such as the Japanese, Dutch, German, Australian, African-American and Hispanic populations[182-184], but not some others such as the Puerto-Rican, Mexican and some Chinese populations[184-187]. A Korean study showed that *ADAM33* was associated with BHR but not asthma *per se*[188]. The SNPs that have been found to be associated with asthma in the different studies have been variable. A meta-analysis study was carried out in 2005, analyses of the published *ADAM33* association studies in addition to two extra patient cohorts from the UK and Iceland confirmed the significant association between *ADAM33* and asthma[189]. However, it is noted that linkage disequilibrium of the SNPs extends upstream and downstream of the *ADAM33* loci into other genes[190].

Genetic studies have also extended the *ADAM33* association beyond asthma, to include association with lung function. In a Dutch cohort of 200 asthma patients, significant association was found between the *ADAM33* S2 SNP and the accelerated decline in FEV_1 over a 23 year period[191]. This accelerated decline was found to extend to the general population, with the S1, S2 and Q-1 SNPs being attributed to the association[192]. In addition to accelerated decline in lung function in adulthood, specific SNP genotypes in *ADAM33* can predict impaired lung function in early life. A study carried out in a birth cohort in the UK evaluated the lung function of children at 3 years of age, and at 5 years of age. It showed that the A allele of the F+1 SNP in *ADAM33* was significantly associated with poorer lung function at 3 years of age. Similarly 4 SNPs in *ADAM33* could predict lung function at 5 years of age. Furthermore no association was found between *ADAM33* and atopy in the study[193].

There is also interest in the role of *ADAM33* in COPD. COPD is a disease which is characterised by airflow restriction which unlike asthma is not fully reversible. The airways of COPD patients also show changes in their airway architecture in the small and large airways, such as goblet cell and smooth muscle hyperplasia together with inflammation[194;195]. In a study of Dutch individuals, the F+1,S1, S2 and T2 SNPs were found more frequently in individuals with COPD[192]. The association between

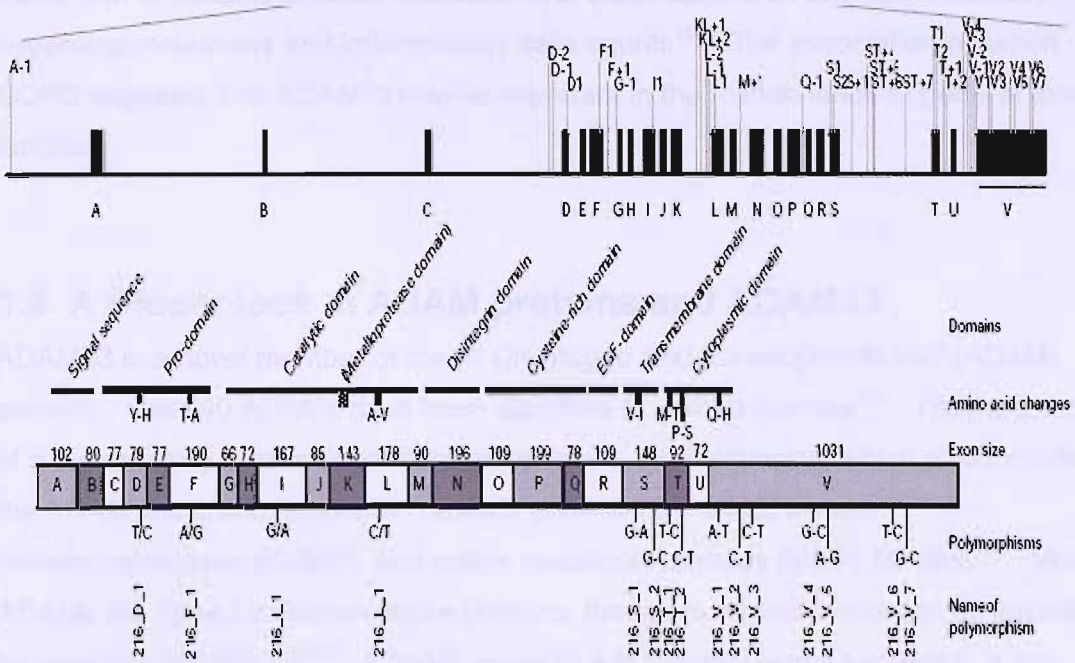

Fig. 1.4 Orignial SNPs that are found in *ADAM33* gene. SNPs typed in the ADAM33 gene (exons A-V). SNPs found to be associated with asthma in the UK population were F+1,Q-1,S1,S2,ST+4,V-1,V4; in the US population these were I1,L-1,M+1,T1,T2, T+1, in the combined UK and US population these were Q-1,S1,ST+4,ST+7, V-1,V4.

Figure adapted from Van Eerdewegh P,et al., Association of the *ADAM33* gene with asthma and bronchial hyperresponsiveness. Nature. 2002 Jul 25;418(6896):426-30.

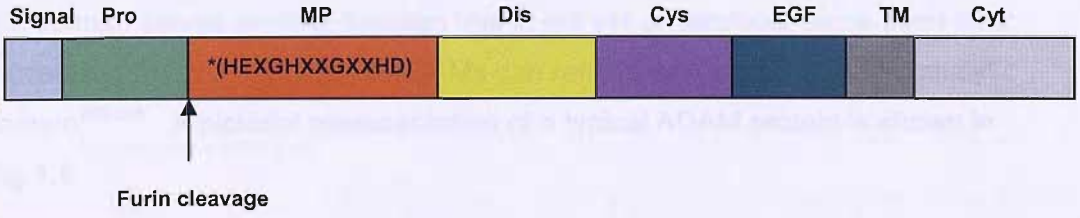

Fig. 1.5. Basic Structure of A Disintegrin And Metalloproteinase. Protein is made up of 8 domains, the signal, pro, metalloproteinase,disintegrin, cysteine rich, EGF like, transmembrane domains and cytoplasmic tail. Most ADAMs are expressed on the cell surface. ADAMs which contain the conserved zinc binding consensus sequence * are predicted or have demonstrated proteolytic activity.

ADAM33 and COPD has since been confirmed in a small study of COPD patients. In these COPD patients different *ADAM33* SNPs also appeared to influence airway hyperresponsiveness and inflammatory cells counts[196]. The association between COPD suggests that *ADAM33* maybe important in the maintenance of general airway function.

1.8 A Closer look at ADAM proteins and ADAM33

ADAM33 is a novel member of the "A Disintegrin And Metalloproteinase" (ADAM) proteins. Over 30 ADAMs have been identified in various species[197]. They are a part of a super-family of zinc dependent proteinases, the metzincins, which also include the ADAM with thrombospondin repeats (ADAM-TS), snake venom metalloproteinases (SVMP), and matrix metalloproteinases (MMP) families[198]. Most ADAMs are Type I transmembrane proteins, though truncated forms can be secreted for example ADAM12-S[199]. ADAMs possess a N terminal signal sequence, a pro, metalloprotease, disintegrin, cysteine rich and EGF like domain followed by a transmembrane tail. The signal sequence targets the protein to the cell surface.

The N terminal pro-domain has multiple functions in ADAMs. It can regulate the proteolytic activity of the metalloproteinase domain. After an ADAM is synthesised, the pro-domain acts as an inhibitor of the protease through a cysteine switch mechanism[200]. It occupies the active site of the metalloproteinase domain, preferentially coordinating the zinc ion in the active site. The proteinase remains latent until the enzymatic removal or displacement of the pro-domain. The pro-domain also acts as a tag to direct the protein into the secretory pathway in a cell and ensures its proper folding[201;202]. To remove the pro-domain an ADAM is processed by furin or furin like enzymes[203;204] to activate protease activity. It is possible that the pro-domain serves another function that is not yet understood, since even after processing the pro-domains of ADAMs can remain associated with the catalytic domain[205;206]. A pictorial representation of a typical ADAM protein is shown in **Fig.1.5**.

1.8.1 Cell-ECM interaction

ADAMs are proteins which potentially have multiple functions. They are known to play roles in cell-cell and cell-extracellular matrix adhesion and migration. The disintegrin and cysteine rich domains are of particular interest when considering these functions. The disintegrin domain has the ability to bind integrins[198], which are

important adhesion molecules found on the surface of cells. The disintegrin domain of different ADAMs can have selective but sometimes overlapping integrin binding profiles. ADAM33 has been shown to bind to integrin $\alpha_9\beta_1$, but not leukocyte integrins $\alpha_4\beta_1$ or $\alpha_4\beta_7$, whereas ADAM7 and ADAM28 could bind all three integrins[207]. Despite this, the transfection of ADAM33, has been reported to disrupt the migration of CHO cells expressing integrins $\alpha_4\beta_1$ and $a_5\beta_1$, which suggests that other domains besides the disintegrin domain influences ADAM33 adhesion[208]. Cell surface integrins usually bind extracellular matrix components such as fibronectin which have the RGD consensus sequence required for integrin recognition. Disruption of integrin-ECM binding by the disintegrin domain of an ADAM protein has the potential to change cell adhesion and migratory behaviour which is dependent on interactions with the ECM. This concept is clearly demonstrated by the SVMP jararhagin. Its disintegrin domain interacts with the platelet integrin $\alpha_2\beta_1$ preventing collagen induced platelet activation, which results in the failure of the normal blood clotting response[209]. However most ADAMs unlike SVMPs lack the RGD sequence, ADAM15 (Metargidin) being an exception, and are capable of binding to integrins using other sites on the disintegrin domain[207].

The protease domain of ADAMs has also been shown to have an effect on cell attachment and migration on extracellular matrix. Over-expression (by transfection) of proteolytically inactive *Xenopus* ADAM-13, (the most similar ADAM to ADAM33) acts as a dominant negative mutant which disrupts the normal migration patterns of neural crest cells during development. The ability of the ADAM13 to cleave extracellular components such as fibronectin has led Alfandari *et al.* to speculate that ADAM13 loosens neural crest cells by remodelling the extracellular matrix around them, in doing so loosening their attachment and allowing them to migrate[210]. This is similarly reported for ADAM-9, in which its proteolytic activity is thought to aid the migration of tumour cells into the liver[211].

1.8.2 Cell-cell adhesion

ADAMs can mediate cell-cell adhesion through both the disintegrin and cysteine rich domains. The cysteine rich domain of an ADAM mediates interactions with syndecans expressed on the surface of cells. Syndecans are heparin sulphate proteoglycans expressed on the cell membrane of most cells, although members of this family may show tissue specific expression. They mediate a diverse range of functions from ECM interaction, growth factor signaling, cell migration to cell spreading[212]. Synthetic peptides of the ADAM12 cysteine rich domain can mediate

tumour cell adhesion through interaction with heparin sulphate proteoglycans[213]. Furthermore, mesenchymal cells including lung fibroblast cell lines (MRC-5, WI-38) can also adhere to recombinant ADAM12 in a dose dependent manner, and go on to undergo integrin dependent cell spreading[214]. In humans, ADAM2 also mediates sperm and cell attachment before fusion. ADAM2 lacks a functional proteinase domain and it is its domain which has been implicated in the adhesion and fusion process between egg and sperm cells during fertilisation[215].

1.8.3 Sheddase Activity - Immune response modulation

Despite their name, not all ADAMs are proteinases. Those that are proteolytically active possess the conserved HEXGHXXGXXHD sequence in the active site of the metalloprotease domain, allowing them to coordinate zinc ions. The best characterised sheddase to date is ADAM17 (TACE). ADAM17 was shown to be responsible for cleaving pro TNFα from the cell membrane, enabling its mobilisation to become an active soluble form. In 1997, Black *et al.* showed that ADAM17 was localised on the cell surface of neutrophils, monocytes, PBMCs, T cells, endothelial cells and smooth muscle cells using cell surface biotinylation experiments. In the same study ADAM17 knock out mice were shown to have an 80-90% reduction in TNFα release in comparison to wild type mice. Cleavage of recombinant TNFα was also confirmed using recombinant ADAM17[216]. TNFα is an important inflammatory cytokine with multiple functions and has been implicated in many diseases including asthma. Marked increase in the level of TNFα has been observed in the BAL fluid of severe asthmatics in comparison with mild asthmatics and healthy subjects[138]. This may be correlated with the increased cell surface levels of ADAM17 seen in the peripheral blood monocytes of severe asthmatics[140].

1.8.4 Sheddase Activity - Growth factor signalling

Members of the Epidermal Growth Factor (EGF) superfamily are important signalling molecules which are involved in regulating the growth, differentiation and survival processes. EGF ligands are cell surface proteins which need to be released or shed from the membrane before they are capable of interacting with their receptor, the EGFR. The importance of EGFR ligand shedding is demonstrated *in vivo* where changes to EGFR signalling between cells are implicated in normal development and disease. For example increased growth factor release and the upregulation of EGFR are implicated in cancers, for a review see Salomon *et al.*[217].

Analyses of EGF ligand shedding in embryonic mouse fibroblasts lacking endogenous ADAM17 showed a major reduction in the shedding of epiregulin, TGFα, amphiregulin and HB-EGF when stimulated with PMA relative to wild type fibroblasts. Thus demonstrating that ADAM17 is also the major sheddase for these proteins[218]. *In vivo* data also supports this, with *Adam17* knock-out mice showing some similar heart and skin developmental defects as *Egfr*$^{-/-}$, *Hb-egf*$^{-/-}$, and *Tgfα*$^{-/-}$ mice[219-221]. Furthermore, mouse embryonic lung explants treated with an ADAM17 inhibitor (TAPI) or anti-sense oligonucleotides to ADAM17 show decreased branching morphogenesis of the lungs. This phenotypic could be rescued by the administration of exogenous TGFα[222]. Unlike ADAM17, mouse cells which are deficient in ADAM10 do not show a reduction in PMA induced shedding of epiregulin, TGFα, amphiregulin and HB-EGF, but instead show a reduction in the constitutive shedding of EGF and betacellulin[218]. Interestingly, in another model of murine cardiac hypertrophy, administration of inhibitor of ADAM12 (KB-R7785) could attenuate signs of hypertrophy[223]. Together this demonstrates the importance of ADAMs and EGF superfamily shedding in regulating development and tissue modelling.

The shedding of EGF superfamily ligands has also been implicated in G protein coupled receptor (GPCR) transactivation of the EGFR. Typically, stimulation of cells using GPCR ligands such as lysophosphatidic acid and angiotensin II leads to transactivated EGFR signalling which can promote cell proliferation and survival. However, treatment of human bladder and kidney cancer cell lines with metalloproteinase inhibitors prior to stimulation abolishes this effect, without affecting direct EGFR stimulation. The transfection of the dominant negative mutant of ADAM10, ADAM15 or ADAM17 could abolish the transactivation effect in a cell line specific manner. The shedding of HB-EGF, amphiregulin and TGFα were also shown to be implicated, showing that ADAMs could be important mediators in GPCR signalling in cancer[224;225].

1.9 A role for ADAM33 in the development of asthma

In addition to the human genetics studies, *Adam33* in mice has been shown to be implicated in the development of respiratory symptoms. The F_1 progeny of A/J mice crossed with C57BL/6J mice develop a bronchial hyperresponsiveness. A genetic study of these mice identified a locus on chromosome 2 that shows linkage to the BHR like phenotype with a LOD score of 3.0 [226]. This region spans the region in which the mouse *Adam33* gene is located. Mouse *Adam33* shares ~70% homology

with human *ADAM33*. Therefore, this further supports the importance of *ADAM33* in the development of an abnormal airway that results in the twitchy airways seen in asthmatic patients.

Several studies have investigated the expression of *ADAM33* in cells and tissues. A northern blotting study showed that *ADAM33* is expressed in a diverse range of tissues such as the urethra, bladder, vasculature, and bronchus. In particular, organs containing a large smooth muscle component expressed *ADAM33* but not haemopoietic cells or epithelial cells[227]. A study by Powell *et al.* showed that many splice variants are expressed in primary human airway fibroblasts[228]. This is in agreement with multiple ADAM33 protein isoforms that can be detected in airway fibroblasts and bronchial biopsies[228;229]. Quantification of *ADAM33* gene expression in bronchial biopsies from asthmatics and healthy subjects have showed contrasting results. One study showed no significant differences between asthmatics and healthy subjects[229], and two studies showed that moderate and severe asthmatics express higher levels of *ADAM33* relative to mild asthmatics or healthy subjects[230;231]. An *in situ* hybridisation study also showed that asthmatics had an increased number of *ADAM33* positive smooth muscle cells in bronchial biopsies[231]. These differences may have been attributed to differences in subject selection criteria and is an area which is currently undergoing further research.

Four studies into the relationship between the levels of ADAM33 protein expression in bronchial biopsies have reported contrasting results. These differences again highlight the difficulty in direct comparisons between asthma studies which sample different ethnic populations (British, Canadian and Korean) exposed to different environmental stimuli, the inclusion of varying asthma phenotypes, and contrasting experimental protocols. In one study, using a commercial antibody against the cytoplasmic tail of ADAM33, no reported differences were observed in staining patterns between asthmatic and normal biopsies, and this was verified by qPCR[229]. In two similar studies increased ADAM33 expression was reported in asthmatics[230;231]; in one of those the ADAM33 level correlated to disease severity and the differences were supported by matching qPCR data[230]. In the third study the staining of bronchial biopsies using the anti-ADAM33 metalloproteinase antibody a difference between asthmatic and normal biopsies was again observed, with slightly different staining patterns and the data was not further confirmed using a second technique[232]. However using the same anti-metalloproteinase antibody, Lee and colleagues reported a correlation between the protein levels of ADAM33 in BAL fluid

with asthma severity. The ADAM33 in BAL fluid was identified as a soluble form of ADAM33 which lacked the cytoplasmic tail. It could be detected in bronchial lavage fluid of both asthmatic and non asthmatic individuals but ADAM33 was found at consistently higher levels in the asthmatic subjects, and the level found was negatively correlated with the lung function (FEV_1)[232].

An *Adam33* knockout mouse model has been established, but it has not yielded many clues regarding the function of ADAM33. These mice are developmentally normal and exhibit no obvious abnormal phenotypes. The histology of the mice tissues, inflammatory response to antigen challenge, IgE levels and mucus production and fertility resemble that of wild type mice[233]. However, this study is a loss of function study, and it is unclear whether ADAM33 is implicated in asthma as a result of 'loss of function' or a 'gain of function'. Furthermore, murine asthma models are predominantly models of allergic asthma and not intrinsic remodelling. It has already been shown that ADAM33 is associated with bronchial hyperresponsiveness rather than the allergic phenotype[181].

1.10 A functional role for the metalloproteinase domain of ADAM33

ADAM33 has retained the conserved zinc binding motif HEXGHXXGXXHD in its metalloproteinase domain which is necessary to maintain the proteolytic function. In 2004 the crystal structure of the catalytic domain was solved by Orth *et al.* and confirmed that the catalytic domain does bind zinc[234]. In ADAMs which function predominantly through a domain other than the metalloproteinase domain, this conserved sequence has been lost. This strongly suggests that evolutionary constraints have preserved the proteolytic activity of ADAM33 and that it has functional significance. In recent years, the demonstration of ADAM33 mediated proteolysis of peptide substrates *in vitro*[205;235] has been confirmation of its potential to act as a sheddase, or perhaps like its close relations *Xenopus* ADAM13 and ADAM9 it may play a role in cell migration by proteolysis of extracellular matrix components[210;211].

In vitro, when cells transfected with *ADAM33* were biotinylated and subsequently immunoprecipitated, about 10% of ADAM33 was shown to be expressed on the cell surface[236]. Its localisation suggests that ADAM33 has the potential to act as an extracellular proteinase, shedding potent growth factors, cytokines or extracellular

matrix proteins which may modulate inflammation and airway remodelling in asthma. *ADAM33* is expressed in the trachea and the bronchus[227], and is detectable in lung fibroblasts[236]. Several immunohistochemical studies have showed that ADAM33 protein co-localises with smooth muscle bundles in adult bronchial biopsies[229;230;232]. In the developing human lung, abundant ADAM33 is expressed in bronchial tubes and some of the mesenchymal tissue[229]. However its absence from immune tissues[227] suggest a role for ADAM33 in airway remodelling as opposed to direct immune response modulation.

ADAM33 mRNA expression studies show that transcripts containing the MP domain is low, at around 5% of the total *ADAM33* transcripts in human airway fibroblasts. However, the selective transport of the transcripts encoding the MP domain from the nucleus to the cytoplasm suggests that it is translated into protein[228]. It can be envisaged that this low expression reflects a need for its proteolytic activity to be tightly regulated and therefore it may be biologically potent and important. The low expression of the MP domain is not a reason to doubt the role of the MP domain in asthma development, since enzymes are catalysts, and even small amounts of enzyme can have a profound effect on substrate turnover, and lead to relevant downstream effects.

In vitro, ADAM33 is able to cleave purified α2-Macroglobulin (α2-M)[236]. α2-M is an abundant proteinase inhibitor found in serum. Cleavage of α2-M results in the covalent linkage between α2-M and ADAM33 which inactivates ADAM33. Therefore α2-M may have a role in regulating ADAM33 activity *in vivo*. Recently ADAM33 has been reported to cleave CD23, the low affinity IgE receptor. When ADAM33 is transfected into immortalised mouse fibroblasts or human epithelial cell lines expressing CD23, the level of CD23 on the cell surface is decreased and the level in the medium is increased[237]. However, the same study confirmed that ADAM33 is not expressed in B cells and that constitutive shedding of CD23 from primary cells could be blocked by inhibiting ADAM10 without inhibiting ADAM33. This strongly suggests that CD23 is not shed by ADAM33 *in vivo*. Since the association between ADAM33 and the asthma phenotype decreases if atopic phenotype is considered[181], it is unlikely that the shedding of CD23 by ADAM33 is responsible for the association.

The substrates that have been identified to date in cell free systems are peptides derived from proteins that are candidate substrates for sheddases. These were Kit Ligand-1 (KL-1), β-ameyloid protein (APP), Tumour necrosis factor activation induced cytokine (TRANCE), and Insulin B chain. Kinetic data has been obtained for KL-1 and APP. The kinetic constant kcat/km for KL-1 was found to be (2.6 ± 0.5) x 10^2 $M^{-1}s^{-1}$, and for APP (1.6.±0.3) x 10^2 $M^{-1}s^{-1}$ [205]. Compared to the calculated kinetics for ADAMs with well defined biological substrates such as ADAM17 and pro-TNFα, these values are approximately 3 orders of magnitude smaller. This suggests that these are not optimal substrate for ADAM33 and therefore may not be biologically relevant. Therefore the identity of the physiological substrate for ADAM33 is still to be discovered.

1.11 Hypothesis

There is strong evidence to suggest that ADAM33 is implicated in asthma pathogenesis. It is hypothesised that the proteolytic activity of ADAM33 plays a central role in disease development. The potential for ADAM33 to shed cytokines, inflammatory mediators and growth factors or to cleave extracellular matrix proteins, puts it in a position to mediate the underlying airway remodelling associated with asthma. Identification of the relevant substrate for ADAM33, and insight into how and why it is implicated in asthma susceptibility will lead to a greater understanding of the disease process. It may also identify an alternative avenue for therapeutic intervention in the future, which will be of particular importance in cases of asthma refractory to currently available treatments.

1.12 Aims

The aim of this project is to establish a biologically relevant function for ADAM33. The core focus will be directed towards its proteolytic activity, since the MP domain of ADAM33 is believed to be central to its activity. Purified recombinant ADAM33 will be generated and characterised. Then it will be used *in vitro* to answer the following questions: What is the target cell for ADAM33? What effect does its proteolytic activity mediate? What are its substrates? How can the findings help to explain the involvement of ADAM33 in asthma?

Chapter 2 Materials And Methods

2.1. Materials and suppliers

The Tissue Inhibitor of Metalloproteases (TIMPs) and the DNA vectors pcPPP and pcEcto were gifts from my collaborator Prof. G Murphy at the University of Cambridge. The PNA-FRET peptide library and DNA microarrays were supplied by my collaborator Dr J. Diaz-Mochon at the University of Edinburgh. All other reagents were purchased from suppliers as detailed below.

Cell culture

BD Biosciences, Oxford, UK Growth factor reduced matrigel

Fisher Scientific Leicester, UK Nunc tissue culture plastics

Invitrogen, Paisley UK Bovine serum albumin (BSA) fraction V, *Drosophila* Serum Free medium, Dulbecco's Modified Eagle's Medium (DMEM), Foetal bovine serum, Hank's buffered saline solution (HBSS), Hygromycin B, L-glutamine, M199 medium, Non-essential amino acids, Penicillin, RPMI-1640, Schneider's medium, Sodium heparin, Sodium pyruvate, Streptomycin, Trypsin-EDTA

Lonza, Wokingham, UK UltraCulture medium

Merck Chemicals Ltd. Nottingham, UK G418 antibiotic

R&D Systems, Abingdon, UK Basic fibroblast growth factor 2 (bFGF2)

Sigma, Dorset, UK Collagenase, Gelatin, Endothelial cell growth supplement, Newborn calf serum, Trypan blue, Copper sulphate

Plasmid DNA preparation and mutagenesis

Qiagen, West Sussex, UK Effectene transfection kit , Endo-Free plasmid maxi kit

Invitrogen, Paisley UK DH5α-T1 *E. coli.* competent cells, *Drosophila* expression system (DES) with vectors: pMT/Bip-V5-His, pMT/Bip-V5-His-GFP, pCoHygro, SOC medium

Sigma, Dorset, UK Ampicillin, Isopropyl β-D-galactoside (IPTG), Luria Bertani (LB) broth, LB agar, X-Gal

Stratagene Europe, Amsterdam, The Netherlands Quick change multi-site directed mutagenesis kit

Immunoglobulin reagents

Bethyl Laboratories, Texas, USA Human IgG-Fc

Dako, Cambridgeshire, UK Sheep anti-rabbit-HRP antibody

Jackson ImmunoResearch Europe Ltd, Suffolk, UK Goat anti-rabbit-HRP antibody

Sigma, Dorset, UK Mouse IgG, Protein A, Sheep anti-human IgG Fc,

Triplepoint Biologics, Oregon, USA Rabbit anti-ADAM33 Pro domain antibody (RP1), Rabbit anti-ADAM33 MP domain antibody (RP2)

Protein analysis and purification

Autogen Bioclear, Calne, UK Protein A-agarose

Amersham Biosciences - GE Healthcare, Buckinghamshire, UK 2D-SDS-PAGE standards, CHAPS, Dithiothreitol (DTT), Cobalt chloride, ECL plus, Glycine, HisTrap column (1ml) (IMAC), Hyper ECL film, Imidazole, IPG buffer 3-10, IPG strips, Nickel sulphate, Pre-cast SDS PAGE gels (Criterion), Wide range rainbow protein markers, SP Sepharose fast flow column (1ml), Superose 12 column (24cm), SyproRuby blot stain, Urea

Bio-Rad, Hertfordshire, UK 30% Acrylamide/ Bis Acrylamide (37:1), Filter paper, Iodoacetamide, Kaleidoscope precision plus protein markers, Polyvinylidine fluoride (PVDF) membrane

Ciphergen Biosystems Ltd, Surrey, UK IMAC 30 SELDI chip, Sinapinic acid

Fotospeed, Corsham, UK Photographic fixative and developer solutions

Genetix, Hampshire, UK GenHyb buffer

Invitrogen, Paisley UK DQ Collagen type IV

Merck Chemicals Ltd. Nottingham, UK Active human MMP-2

New England Biolabs, Hertfordshire, UK N-glycosidase F (PNGase F)

Promega, Southampton, UK Low melting point agarose

Roche Applied Science, Burgess Hill, UK Complete protease inhibitor cocktail tablets

Sigma, Dorset, UK 1,10 Phenanthroline monohydrate, Ammonium persulphate, Ammonium sulphate, Blue dextran, Bovine Serum albumin fraction V, β-mercaptoethanol, Bromophenol blue, Carbonic anhydrase, Casein, Concanavalin A sepharose-4B, Coomassie blue stain, Cytochrome C, Dialysis tubing, Ethylenediaminetetraacetic acid (EDTA), Ethylene glycol-(aminoethyl ether) tetra-acetic acid (EGTA), EZ blue staining reagent, Gelatin, Glacial acetic acid, Hydrochloric acid, Glycine, Isopropanol, Magnesium chloride, Manganese chloride, Methanol, Methyl α-D mannopyranoside, N,N,N',N'-tetramethylethylenediamine (TEMED), Phenylmethanesulphonyl fluoride (PMSF), Protein A, Proteosilver plus gel staining kit, Sodium fluoride, Sodium orthovandate, Sulphuric acid, Tetramethylbenzidine, Triton-X100, Tween-20, Vitamin B12

VWR International Ltd, Leicestershire, UK BDH Analar glycerol

***In vitro* ADAM33 activity and inhibition assays**

Merck Chemicals Ltd. Nottingham, UK Calbiochem Inhibitor set I ((2R)-2-[4(-Biphenylylsulfonyl)amino]-3-phenyl propionic acid, N-Isobutyl-N-(4-methoxyphenylsulfonyl)-glycylhydroxamic acid, (3R)-(+)-[2-(4-methoxybenzenesulfonyl)-1,2,3,4-tetrahydroisoquinoline-3-hydroxymate and GM6001)

Severn Biotech Ltd, Worcestershire, UK FRET peptides (collagen type IV and ADAM15)

Sigma, Dorset, UK Brij-35, Human α2-Macroglobulin, Dimethyl sulphoxide (DMSO)

General Buffer reagents

Sigma, Dorset, UK Calcium chloride, Disodium hygrogen phosphate, HEPES, MES, Potassium chloride, Potassium dihydrogen phosphate, Sodium acetate, Sodium azide, Sodium carbonate, Sodium chloride, Sodium dodecyl sulphate (SDS),Sodium hydrogen carbonate, Tris-HCl, Zinc chloride,

2.2 Routine cell culture

2.2.1 Materials and growth conditions

Mammalian cells were cultured on Nunc tissue culture plastic, and were kept in Heraeus humidified incubators set at 37°C, 5% CO_2. Cells were taken to class II biological safety laminar flow cabinets for passaging and treatments. COS-7 cells were maintained in RPMI-1640, supplemented with 10% FBS, 2mM L- glutamine, 1x non- essential amino acids, 10U/ml Penicillin, 10µg/ml Streptomycin and 1mM sodium pyruvate. CHO cells were grown in DMEM, 10% FBS, 2mM L- glutamine, 1x non- essential amino acids, 10U/ml Penicillin, 10µg/ml Streptomycin and 1mM sodium pyruvate. A549 human lung carcinoma cells were typically grown on in DMEM supplemented with 10% FBS, 2mM L- glutamine, 1x non- essential amino acids, 10U/ml Penicillin, 10µg/ml Streptomycin and 1mM sodium pyruvate. *Drosophila* S2 cells (Invitrogen, Paisley, UK) were maintained in Schneider's medium supplemented with 10% FBS, 10U/ml penicillin and 10µg/ml streptomycin, or *Drosophila* Serum Free medium supplemented with 10U/ml penicillin and 10µg/ml streptomycin. Cells were cultured at 27°C.

Human vascular endothelial cells (HUVECs) were isolated from human umbilical cord soon after birth. Umbilical cord was collected after ethical approval from the Southampton and South West Hampshire Research Ethics Committee and informed consent from the donor. To isolate HUVEC cells, the umbilical vein was cannulated at both ends with syringe fittings and secured with surgical thread. The vein was flushed with PBS to remove residual blood and then the PBS was discarded. Collagenase in M199 medium was pre-warmed to 37°C and infused into the vein. This was left in the vein for 10 minutes, after which it was used to flush out detached HUVECs. The cell suspension was collected in a sterile 30ml polystyrene container. Cells were collected by centrifugation at 150g for 5 minutes. HUVECs were grown on tissue culture plastic coated in 1% gelatin and maintained in M199 medium supplemented with 10%FBS, 10% new born calf serum, 1mM L-glutamine, 10U/ml

Penicillin, 10µg/ml Streptomycin, 100µg/ml sodium heparin and 30µg/ml endothelial cell growth supplement.

2.2.2 Passaging cells

Cells were grown on tissue culture plastic. Adherent cells were grown until they reached 90-100% confluence and subsequently passaged. To passage cells, the culture medium was removed without disturbing the cell monolayer. The monolayer was gently washed with calcium and magnesium free Hank's Buffered Saline Solution (HBSS) to remove residual medium. 1x trypsin-EDTA solution (1.5ml per $75cm^2$ flask) was added to the culture vessel and the vessel tilted to evenly distribute the trypsin-EDTA solution over the monolayer. The cells were incubated at 37°C until they had detached from the culture vessel, detachment was verified by observing the cells under a phase contrast microscope. Trypsin activity was neutralised by the addition of growth medium containing 10% FBS. A viable cell count (see below) was taken and cells were resuspended into fresh medium, before being seeded into new culture vessel at the appropriate density.

Semi adherent *Drosophila* S2 cells were passaged when they reached a density of 6-$10x10^6$ cells per ml. To passage cells, the culture vessel was tapped to dislodge the loosely attached cells. The cell suspension was centrifuged at 100g for 10 minutes to pellet cells. The pellet was resuspended into fresh medium, and a viable cell count performed. Cells were seeded at $5x10^5$ cells per ml into fresh medium, and seeded into new flasks.

2.2.3 Cell counting

Viable cell counts were carried out in 0.2% trypan blue solution (final concentration). Trypan blue is impermeable to the intact cell membrane of live cells. However, dead or dying cells with a damaged membrane take up the dye. Therefore blue stained cells were excluded from the counting in order to produce a viable cell count. Cell suspension was mixed with an equal volume of 0.4% trypan blue solution. This was drawn into the space between a hemocytometer slide and its coverslip by capillary action. Under the light microscope the number of viable cells was counted in the main 5x5 squares grid ($1mm^2$). The number counted was multiplied by two to take into account of the dilution factor, and then multiplied by 10^4 to give cells per ml (since the depth of the chamber is 0.1mm, and $1000mm^3$ is equivalent to 1 ml).

2.3 Preparation of DNA for transfections

2.3.1 Details of plasmids

The plasmids used for mammalian cell transfections were pcPPP and pcEcto, see **Fig. 2.1**. These plasmids consist of a pCDNA3.1 vector backbone with inserts encoding ADAM33-Fc fusion proteins. The pcPPP insert encodes the ADAM33 signal, Pro, and MP domains fused to a C-terminal Fc tag. The pcEcto insert encodes the full extracellular domain of ADAM33 fused to a C-terminal Fc tag. Both constructs were kind gifts from Prof. G. Murphy, University of Cambridge.

The plasmids used for S2 insect cell transfections were:
(i) pMT-Bip-V5-His
(ii) pMT-Bip-V5-His-GFP
(iii) pCoHygro
(iv) pMT-Bip-V5-His ADAM33 Pro-MP-Fc
(v) pMT-Bip-V5-His ADAM33 ECD-Fc,
(vi) pMT-Bip-V5-His ADAM33 Pro-MP-His
(vii) pMT-Bip-V5-His ADAM33 Pro-MP(E346A)-His

Plasmids (i),(ii) and (iii) were commercial vectors from Invitrogen (Paisley, UK). Plasmids (i) and (ii) were used for mock and control transfections. Plasmid (iii) was co-transfected into S2 cells simultaneously with another vector to generate stable cell lines. The plasmids (iv) to (vii) consist of a pMT-Bip-V5-His vector backbone, with *ADAM33* domains inserted into the cloning site. Plasmid (iv) encodes the ADAM33 Pro and MP domains fused to a C-terminal Fc tag. Plasmid (v) encodes the full extracellular domains of ADAM33 fused to a C-terminal Fc tag. Plasmid (vi) encodes the ADAM33 Pro and MP domains fused to a C-terminal V5 and 6x histidine tag. Plasmid (vii) is the same as plasmid (vi) except that adenine has been substituted for cytosine at position 1124 of the *ADAM33* gene. This results in a glutamic acid to alanine substitution in ADAM33 at position 346. The *ADAM33* inserts for (i) to (iv) were cloned into the pMT-Bip-V5-His vector by Dr. H. Yoshisue. For more details about the vectors see **Fig. 2.2-2.4,** and for cloning see **section 2.4**. To obtain sufficient quantities of plasmid DNA to use in cell transfections, the plasmids were

(a) **pcPPP** ADAM33-Pro-MP Fc in mammalian expression vector

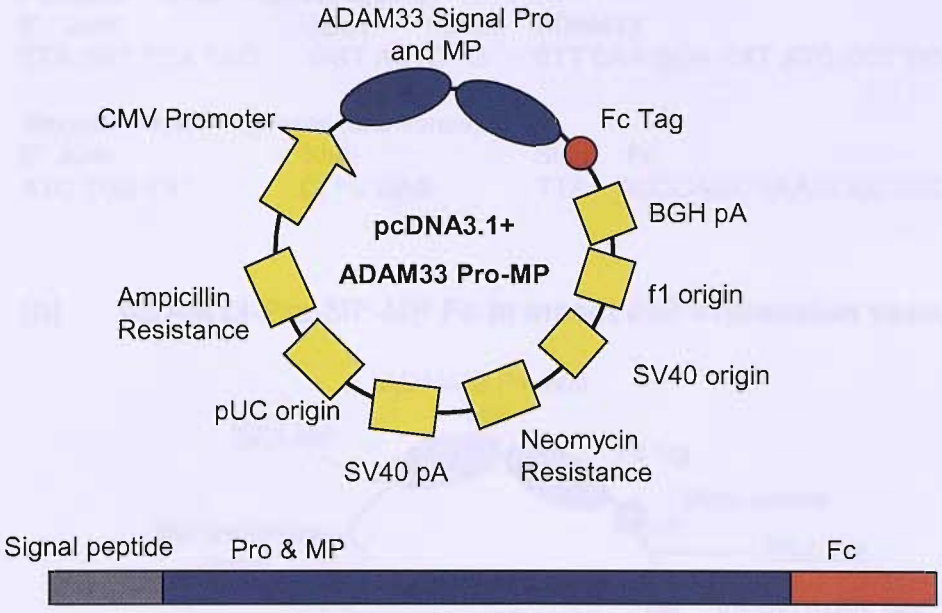

(b) **pCEcto** ADAM33-ECD Fc in mammalian expression vector

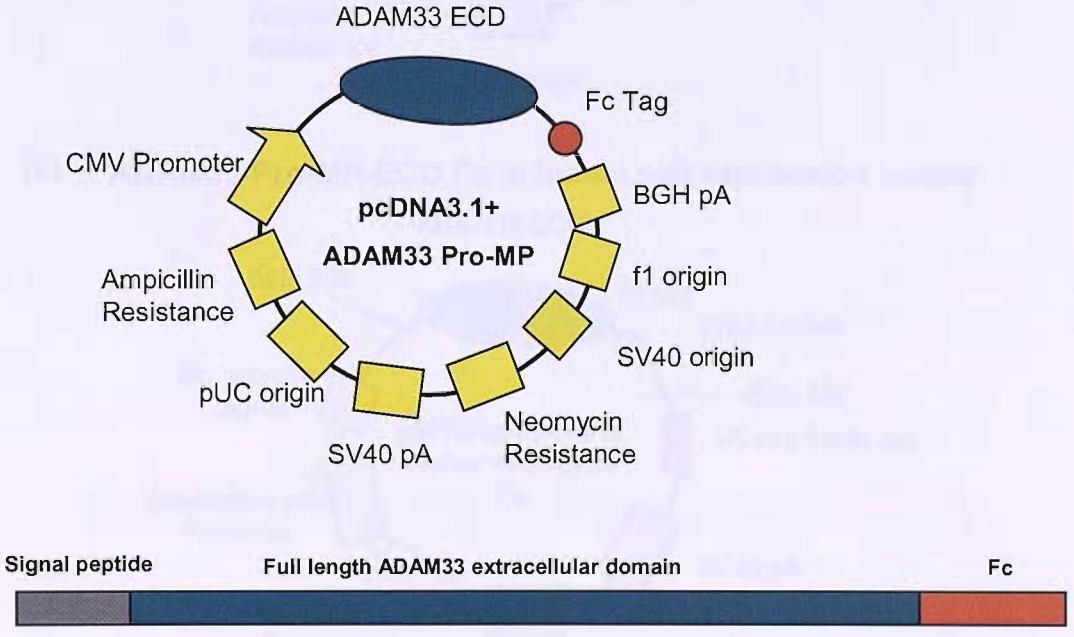

Fig. 2.1. Mammalian expression vectors encoding ADAM33-Fc fusion proteins. The two plasmids used to transfect COS-7 and CHO cells were gifts from Prof. G Murphy at the University of Cambridge. (a) The pcPPP construct consists of the mammalian vector pCDNA3.1 with the sequences encoding the ADAM33 Signal, Pro and MP (amino acid residues 1-419) fused to a Fc tag inserted into its cloning site. (b) The pcEcto construct consists of the mammalian vector pCDNA3.1 with the sequences encoding the ADAM33 extracellular domain (amino acid residues 1-701) fused to a Fc tag. BGH pA and SV40 pA are polyadenylation signals which ensures the addition of a polyadenine tail to the mRNA transcript of the adjacent genes and thereby improving stability.

(a) Primer sequences used for cloning ADAM33-Fc

Forward Primer 43bases (sense)

5' Junk	kpn1	Extra	ADAM33	3'
TTA GAT TCA TAG	GGT AC↓C	G	CTT CAA GGA CAT ATC CCT GGG CAG	

Reverse Primer 35bases (anti-sense)

5' Junk	XhoI	Stop	Fc	3'
ATC TGA TAT	C↓TC GAG	TTA	ACCCAGGGAAGCCCTCC	

(b) ADAM33-Pro-MP-MP Fc in insect cell expression vector

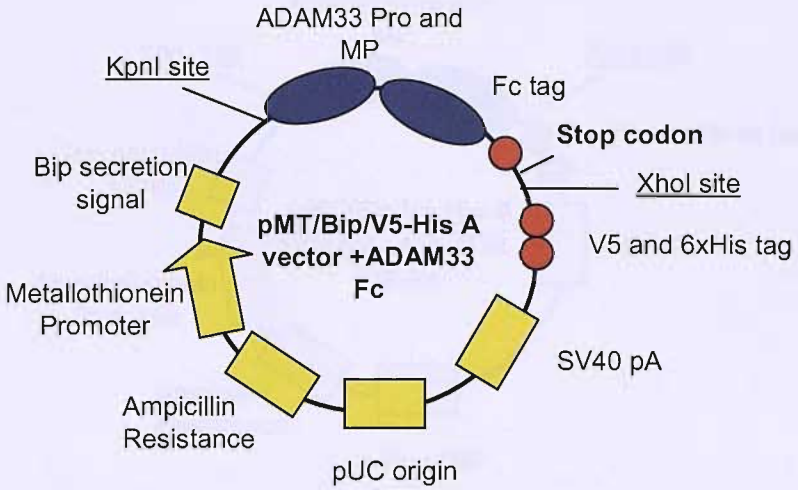

(c) ADAM33-Pro-MP-ECD Fc in insect cell expression vector

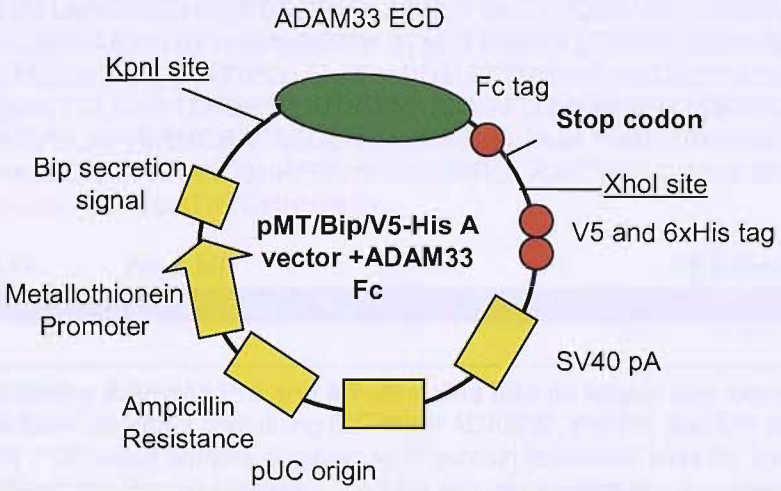

Fig. 2.2 Cloning ADAM33-Fc into an insect cell expression vector. (a) The pcPPP and pcEcto constructs were used as templates from which ADAM33-Pro-MP-Fc and ADAM33 ECD-Fc sequences were amplified by PCR using primers engineered to contain restriction sites for kpn I and xho I which facilitated the cloning process. A stop codon was engineered after the Fc tag to prevent the expression of the V5 and 6xHis tag. (b)(c) Pictorials of the insect expression construct with ADAM33 Pro-MP-Fc or ADAM33 ECD-Fc sequence cloned in. PCR products were digested with kpn I and xho I to produce overhangs, and ligated into pMT/Bip.V5-His A vector (Invitrogen) that had been digested using the same enzymes. The ADAM33 sequence was ligated in frame with the 5' Bip secretion signal. The cloning was carried out by Dr H. Yoshisue.

(a) Primer sequences used for cloning ADAM33 Pro-MP

Forward Primer 43bases (sense)

5' Junk	kpnI	Extra	ADAM33	3'
TTA GAT TCA TAG	GGT AC↓C	G	CTT CAA GGA CAT ATC CCT GGG CAG	

Reverse Primer 38bases (anti sense strand)

5' Junk	XhoI	ADAM33	3'
ATC TGA TAT	C↓TC GAG	CGG GGC ATT GGA GAG GCA AGC GC	

(b) ADAM33-Pro-MP-His construct

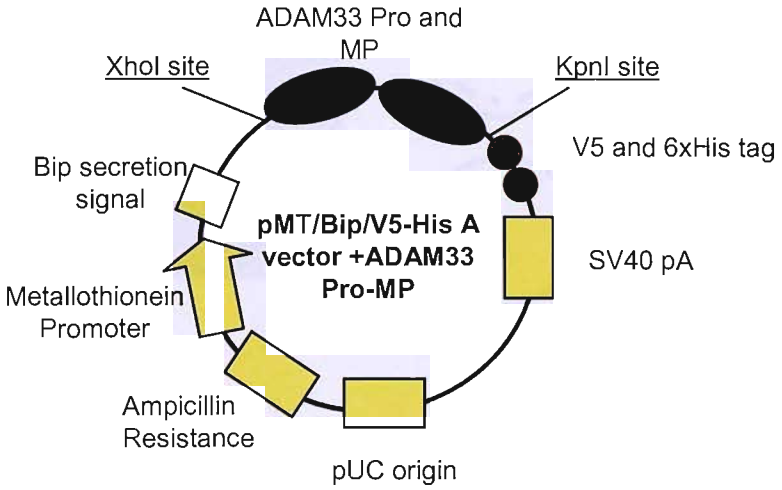

(c) Amino acid sequence of the recombinant ADAM33 Pro-MP-His

RSPWPGVPLQGHIPGQPVTPHWVLDGQPWRTVSLEEPVSKPDMGLVALEAEGQEL
LLELEKNHRLLAPGYIETHYGPDGQPVVLAPNHTDHCHYQGRVRGFPDSWVVLCTC
SGMSGLITLSRNASYYLRPWPPRGSKDFSTHEIFRMEQLLTWKGTCGHRDPGNKAG
MTSLPGGPQSRGRREARRTRKYLELYIVADHTLFLTRHRNLNHTKQRLLEVANYVDQ
LLRTLDIQVALTGLEVWTERDRSRVTQDANATLWAFLQWRRGLWAQRPHDSAQLLT
GRAFQGATVGLAPVEGMCRAESSGGVSTDHSELPIGAAATMAHEIGHSLGLSHDPD
GCCVEAAAESGGCVMAAATGHPFPRVFSACSRRQLRAFFRKGGGACLSNAPLESR
GPFE GKPIPN PLLGLDSTRTGHHHHHH

Fig. 2.3. Cloning ADAM33 Pro and MP domains into an insect cell expression vector. (a) From a DNA construct containing full length ADAM33, the Pro and MP domains were amplified by PCR using primers engineered to contain restriction sites for kpn I and xho I which facilitated the cloning process. The junk sequence overhang improved restriction digestion of the amplified product. (b) Pictorial of the insect expression construct with ADAM33 sequence cloned in. PCR products were digested with kpnI and xhoI to produce overhangs, and ligated into pMT/Bip.V5-His A vector (Invitrogen) that had been digested using the same enzymes. The ADAM33 sequence was ligated in frame with the 5' Bip secretion signal and 3' V5 and 6xHis tag in the vector. (c) The amino acid sequence of the ADAM33 recombinant protein after Bip signal sequence cleavage. ADAM33 Pro domain amino acid residues 31-203, and MP domain residues 204-409 (residue 204 underlined) sequence in blue, and V5 and 6XHis tag in red, spacer sequences in grey. The cloning was carried out by Dr. H. Yoshisue.

(a)

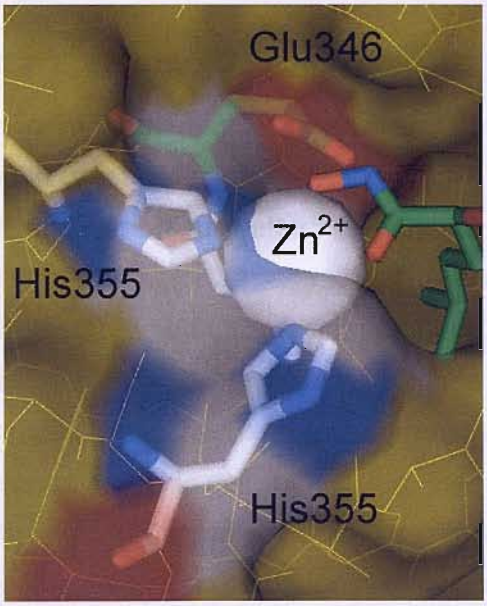

(b)

Methylated pMT/Bip/V5-His A + ADAM33 Pro-MP construct used as the mutagenesis template.

↓

Thermal cycling with primer containing a single base substitution that encoded the E346A mutation.

↓

Digested wild type template using Dpn I. This selectively digested methylated DNA, and not the newly synthesised unmethylated strand.

↓

Transform *E.coli* with ssDNA that had the base change. Amplified colonies and identified clones containing the successfully mutated construct by sequencing.

(c) Protein Sequence Data: ADAM33 Pro-MP (E346A)-His

RSPWPGVPLQGHIPGQPVTPHWVLDGQPWRTVSLEEPVSKPDMGLVALEAEGQELLLE
LEKNHRLLAPGYIETHYGPDGQPVVLAPNHTDHCHYQGRVRGFPDSWVVLCTCSGMSG
LITLSRNASYYLRPWPPRGSKDFSTHEIFRMEQLLTWKGTCGHRDPGNKAGMTSLPGGP
QSRGRREARRTRKYLELYIVADHTLFLTRHRNLNHTKQRLLEVANYVDQLLRTLDIQVALT
GLEVWTERDRSRVTQDANATLWAFLQWRRGLWAQRPHDSAQLLTGRAFQGATVGLAP
VEGMCRAESSGGVSTDHSELPIGAAATMAH**A**IGHSLGLSHDPDGCCVEAAAESGGCVM
AAATGHP FPRVFSACSRRQLRAFFRKGGGACLSNAPLESRGPFE GKPIPN
PLLGLDSTRTGHHHHHH

Fig. 2.4. Mutagenesis of ADAM33 Pro-MP-His to produce the inactive mutant. (a) The glutamic residue at position 346, is situated in the catalytic site, near to the zinc binding site as shown in this space filled model. The charged residue is critical for catalysing the proteolytic cleavage of substrates. A substitution for alanine at this position abolishes proteolytic activity. (b) To make this mutant, a single base change was made in the codon; GAG-> GCG. The Stratagene Quick Change mutagenesis kit was used to make this base change encoding the amino acid substitution and a main steps of the procedure are outlined above. (c) The sequence of the expressed protein after Bip signal sequence cleavage is shown below. ADAM33 Pro domain amino acid residues 31-203, and MP residues 204-409(residue 204 underlined) sequence in blue, and V5 and 6XHis tag in red, spacer sequences in grey. The mutation at position 346; a glutamic acid (E) to alanine (A) substitution has been highlighted in bold and black.

transformed into *E.coli.* and amplified before being purified using the Endo-free plasmid maxi kit.

2.3.2 *E. coli.* transformation

DH5α-T1 competent *E.coli.* cells (50µl) were thawed on ice. 1-5ng of plasmid or 3µl from a cloning ligation reaction from Dr. H Yoshisue was pipetted into the competent cell suspension, and left for 30 minutes on ice. The cells were heat shocked at 42°C in a waterbath, for 30 seconds. These were placed immediately back onto ice for 2 minutes. Sterile SOC medium (250µl) (2% Tryptone, 0.5% yeast extract, 0.05% NaCl, 2.5mM KCl, 10mM $MgCl_2$, 20mM glucose) supplemented with 100µg/ml of ampicillin which had been pre-warmed to 37°C was pipetted into the competent cell suspension. This cell suspension (50-100µl) was spread onto a LB agar plate containing 100µg/ml of ampicillin. The ampicillin selected for bacteria that had become ampicillin resistant by taking up plasmid DNA. Plates were left for 16 hours in an oven set at 37°C to allow bacteria which had taken up the plasmid to grow into colonies.

2.3.3 Culturing *E. coli.*

After transformation, one ampicillin resistant colony was picked from the bacterial plate and used to innoculate 5ml of sterile LB broth containing 100µg/ml of ampicillin. This was placed in an orbital shaker at 37°C, 250rpm for 7 hours to expand the culture. 330µl of this culture was used to innoculate 160ml of sterile LB broth Fig.2.2 containing 100µg/ml of ampicillin. This was placed an orbital shaker at 37°C, 250rpm for 16 hours.

2.3.4 Purifying plasmid DNA from *E. coli.* culture

The overnight *E.coli.* culture was taken and divided into sterile 50ml polystyrene tubes. These were centrifuged at 6000g for 15 minutes at 4°C, to pellet the bacterial cells and the supernatant was discarded. The Endo-free plasmid maxi kit was used to extract the plasmid DNA from the bacterial cells. The bacterial cell pellets were resuspended into 10ml of buffer P1 (50mM Tris-HCl pH8.0, 10mM EDTA, 100µg/ml RNAse). The lysis buffer P2 (200mM NaOH, 1% SDS (w/v)) was added to the resuspended cells. The cell lysate was neutralised by adding 10ml of pre-chilled buffer P3 (2M potassium acetate pH5.5) and mixed. The sample was immediately transferred into a capped QIAfilter cartridge and left at room temperature for 10

minutes. Then the plunger was inserted into the cartridge and the cartridge cap was removed. The sample was filtered into a sterile 50ml polystyrene tube. Endotoxin removal buffer (2.5ml) was added to the filtered sample before it was incubated on ice for 30 minutes. This prevented endotoxin binding to the QIAGEN-tip in the next steps. A QIAGEN-tip-500 was equilibrated with 10ml of buffer QBT (750mM NaCl, 50mM MOPS pH7.0, 15% isopropanol (v/v), 0.15% Triton X-100 (v/v)). The filtered cell lysate was then loaded into the QIAGEN-tip and allowed to flow through by gravity flow. The DNA was captured by the QIAGEN-tip. The QIAGEN-tip was subsequently washed twice with 30ml of buffer QC (1M NaCl, 50mM MOPS pH7.0, 15%isopropanol (v/v)) which removed contaminants. The DNA was eluted from the QIAGEN-tip with 15ml of buffer QN (1.6M NaCl, MOPS pH7.0, 15% isopropanol). The DNA was precipitated by adding 10.7ml of isopropanol. To pellet the precipitated DNA, the sample was centrifuged at 5000g for 1 hour at 4°C. The pellet was washed with 70% ethanol which removed salt. The pellet was air-dried and resuspended in 100-300µl of endotoxin free dH_2O.

2.4. Cloning *ADAM33* into an insect vector

The primers used in this section were designed with the help of Dr. R. Powell. The cloning of the inserts into the pMT/Bip/V5-His A vector was carried out by Dr. H. Yoshisue. The cloning procedure is briefly described below.

2.4.1 Amplification of insert by PCR

From a DNA construct containing full length *ADAM33*, the Pro and MP domains were amplified by the polymerase chain reaction (PCR) to produce the insert to be cloned into the vector. Similarly the *ADAM33* signal, Pro-MP-Fc and *ADAM33* ECD-Fc inserts were amplified from the pcPPP and pcEcto vectors.

The primer sequences that were used for *ADAM33* Pro and MP amplification were:
forward 5'-TTAGATTCATAGGGTACCGTTCAAGGACATATCCCTGGGCAG-3',
reverse 5'-ATCTGATATCTCGAGCGGGGCATTGGAGAGGCAAGCGC-3'.
The primer sequences that were used for *ADAM33* Pro-MP-Fc and *ADAM33* ECD-Fc amplification were:
forward 5'-TTAGATTCATAGGGTACCGCTTCAAGGACATATCCCTGGGCAG-3'
reverse 5'-ATCTGATATCTCGAGTTAACCCAGGGAAGCCCTCC-3'.
Restriction sites (kpnI and xhoI) were engineered into the primers to facilitate the cloning process. A junk sequence overhang was added to improve the efficiency of restriction digestion of the amplified product.

Each PCR reaction had ~37ng of DNA template, 2.5µl of 10x for poly Pfu polymerase, 0.5µl PfuTurbo DNA polymerase (Stratagene, Amsterdam, NL), 0.2µM of forward and reverse primer mix, 250µM dNTPs, and 1.25µl DMSO. PCR cycling conditions were step (i) 95°C for 2 minutes (ii) 95°C for 2 minutes followed by 60°C for 1 minute and then 72°C for 3 minutes. Step (ii) was repeated for 25 cycles, (iii) 72°C for 10 minutes.

2.4.2 Digestion and ligation of inserts and the pMT/Bip-V5-His vector

The amplified PCR products were purified using QIAquick PCR purification kit (Qiagen, West Sussex, UK) The pMT/Bip-V5-His A vector and the PCR products were separately digested with kpnI 7 hours at 37°C. The digested products were precipitated with 6 volumes of ethanol and 1/5 volume of 5M NaCl at -80°C in the presence of 15µg of glycogen. The DNA was pelleted by centrifugation, and washed with 70% ethanol before being air-dried. The recovered DNA pellets were resuspended in dH_2O and then digested with xhoI for 7 hours at 37°C. This was again precipitated, air-dried and resuspended. The inserts were ligated into the vector using T4 DNA ligase (NEB, Hertfordshire, UK) over 5 hours at 37°C. The ligated products were used to transform DH5α-T1 *E.coli.* competent cells.

2.5 Generation of proteolytically inactive ADAM33

2.5.1 Site directed mutagenesis

To generate a proteolytically inactive ADAM33, site directed mutagenesis was carried out on the pMT/Bip/V5-His A -ADAM33 Pro-MP DNA construct using the Stratagene Quick change multi-site directed mutagenesis kit (#200514), **Fig. 2.4**. A coding change was introduced to mutate the triplet encoding glutamic acid at position 346 to an alanine. This glutamic acid is essential in the catalysis mechanism of metallproteinases, mutating this residue abolishes proteolytic capability. The steps of the procedure are outlined below.

(i). Thermocycling with a mutant primer

Mutant Primer : gcc acc atg gcc cat gCg atc ggc cac agc (base change capitalised). Thermocycling carried out in an iCycler (Bio-Rad, Hertfordshire, UK) using the following protocol:

Step 1: Denature DNA 95°C ,1 minute

Step 2: (i) 95°C, 1 minute, denature DNA

Step 2: (ii) 55°C, 1minute- anneal primer

Step 2: (iii) 65°C, 10 minutes – extension

Repeat step 2 for a total of 30 cycles.

Step 3: Reaction is cooled to 4°C, then brought up to 37°C.

(ii). Digest wild type parental strand

The wild type plasmid was generated in a methylation competent strain of *E.coli.* 1µl of Dpn I (10units) was added to the 25µl reaction from step 1 to digest away the wild type parental strand, to leave single stranded mutant DNA. Digestion was carried out at 37°C for 1 hour.

(iii). Transforming competent cells

45µl of XL-10 Gold competent cells (Stratagene) were aliquoted into a pre-chilled 14ml round bottomed tube. 2µl of β-mercaptoethanol was added to the cells which were swirled gently every 2 minutes to mix over 10 minutes. 1.5µl of the single stranded mutant DNA reaction from the previous step was added to the cells, and left to stand on ice for 30 minutes. Cells were heat shocked at 42°C for 30 seconds, then incubated on ice for 2 minutes. 0.5ml of pre-warmed SOC medium was added to cells, and subsequently incubated at 37°C for 1 hour on an orbital shaker set at 250rpm.

2.5.2 Screening for mutants

LB agar plates containing 100µg/ml ampicillin were coated with X-gal (5-bromo-4-chloro-3-indolyl-bD-galactoside) and IPTG (Isopropyl-ß-D-thiogalactopyranoside). 40µl of X-gal (40mg/ml in dimethyl formamide), and 40µl of 100mM IPTG (dissolved in dH_2O) were used per plate and allowed to dry. 100µl of SOC medium (2% Tryptone, 0.5% yeast extract, 0.05% NaCl, 2.5mM KCl, 10mM $MgCl_2$, 20mM glucose) was spread with 1µl,10µl or 100µl of transformed competent cells onto each of the coated agar plates. Plates were incubated at 37°C for 18 hours.

Colonies were selected and sent as agar stabs for DNA sequencing at Bath Genomics Centre (University of Bath, UK) using *ADAM33* FGHI forward primer 5'-GATCCTGGGAACAAAGCGGG-3'. DNA was isolated from 100ml of *E. coli* culture innoculated using a colony shown to contain the desired mutation using the Endotoxin Free DNA plasmid Maxi-Prep kit, see **section 2.34**. A sample of this DNA was sent to Macrogen (Korea) for complete sequencing using the vector primers

pMT (forward) 5'-TCATCTCAGTGCAACTAA-3', and BGH-rev 5'-TAGAAGGCACAGTCGAGG-3'.

2.6 Transfection of *ADAM33* constructs into cell lines

2.6.1 COS-7 and CHO cells

Cells were seeded in 6 well dishes at 9 x 10^4 cells/well one day prior to transfection in serum containing growth medium. Next day cells at 40-80% confluency were washed with HBSS, then re-fed with 1.6ml of UltraCulture serum free medium. A transfection mixture was made using the Effectene kit. 99.7µl of EC buffer, 8.5µl DNA, (0.8µg of pcEcto or pcPPP), and 3.2µl of Enhancer were mixed and incubated at room temperature for 5 minutes. Then 10µl of Effectene reagent was added to this and mixed by pipetting. The transfection mixture was added dropwise to the cells with constant swirling of the culture vessel. The transfection reagent complexes were removed after 4 hours and 2ml of fresh UltraCulture medium was added to each well. 48 hours post transfection G418 selection at 400µg/ml was applied and subsequently maintained. Transfections carried out in larger vessels were scaled according to increase to vessel surface area.

2.6.2 *Drosophila* S2 cells

Transient and stable S2 transfectants, were generated using reagents provided in the *Drosophila* Expression kit. The plasmids used in the transfections were detailed previously in **section 2.3.1**. S2 Cells were seeded at 2-2.5x10^6 cells per well (1x10^6/ml) in 6 well dishes one day prior to transfection. The following day, a transfection mixture was prepared as follows, 36ul of 2M $CaCl_2$ was mixed with the plasmid DNA and made up to 300µl with dH_2O. This was added dropwise to 300µl of 2x HEPES buffered saline whilst gently vortexing. The DNA quantities used for each transfection were as follows: 19µg for ECD-Fc, Pro-MP-His, Pro-MP(E346A)-His, empty vector and GFP control, 10µg for Pro-MP-Fc. The transfection reagent complexes were then left to stand at room temperature for 30-45 minutes being added dropwise to S2 cells in suspension. To generate stable transfectants, in addition to the vector DNA 1µg of pCoHygro plasmid DNA was co-transfected into cells simultaneously. Stable transfectants were selected and maintained in selective medium containing Hygromycin B (300µg/ml).

When inducing protein expression for recombinant protein purification, cells were pelleted at 100g for 10 minutes, washed once with PBS, pelleted and resuspended to $4x10^6$ cells/ml in *Drosophila* Serum free medium supplemented with copper sulphate (500μM).

2.7 Endothelial cell differentiation assay

Growth factor reduced matrigel was aliquoted at 50μl/well and allowed to polymerise at 37°C for 1 hour, in 96 well plates. Confluent human vascular endothelial cells (HUVECs) were trypsinised from $25cm^2$ flasks, washed with complete medium, and seeded at a density of $2\text{-}4x10^4$ cells/well in serum reduced complete growth medium (1% serum or 1% BSA) in a final volume of 200μl with or without treatment. For further details of exact treatments refer to **chapter 5**. Typically treatments were added at the time of cell seeding. Treatments included bFGF-2 used at 30ng/ml, ADAM33 Pro-MP-His or ADAM33 Pro-MP(E346A)-His used at 50ng/ml, 100ng/ml, 150ng/ml together with 20μM $ZnCl_2$ to enhance enzyme activity. In experiments involving carboxylate and hydroxamate compounds 5μM of the compound was pre-mixed with ADAM33 Pro-MP-His or control treatments 5-10 minutes prior to treating the cells. Images were taken of the cells after 18-21 hours using phase contrast on a Leica inverted microscope and a Nikon digital camera. The number of complete meshes in the images was calculated using Leica Qwin V3 software with macroroutines developed by Guidolin and colleagues at the University of Padua Medical School, Italy. In some cases the experiment was followed by time lapse microscopy using the Olympus IX81 microscope with a motorised stage and ORCA-AG firewire digital camera, where one image was taken every five minutes.

2.8 Treatment of epithelial cells with exogenous ADAM33

For growth on non-coated tissue culture plastic: a confluent flask of A549 cells was trypsinised and resuspended into 30ml of complete DMEM medium. 0.5ml of this cell suspension was seeded per well of a 12 well plate. The cells were allowed to adhere overnight into a confluent monolayer. These were subsequently serum starved in UltraCulture for 24 hours. Cells were then treated with either buffer, ADAM33 Pro-MP-His (150ng/ml) or ADAM33 Pro-MP-His (150ng/ml) in UltraCulture. The treatments were supplemented with 20μM $ZnCl_2$ to enhance enzyme activity. The cells were re-treated with buffer and enzyme daily.

For growth grown on matrigel, growth factor reduced matrigel was allowed to polymerise at 37°C for 1 hour in each well of a 96 well plate (30-50µl/well). A549 cells were seeded at $2x10^4$ cells per matrigel coated well in complete DMEM containing only 1% serum. Cells were treated with 20µM $ZnCl_2$ and either buffer, ADAM33 Pro-MP-His (150ng/ml) or ADAM33 Pro-MP-His (150ng/ml) in a total volume of 200µl at the time of seeding. The second day post initial treatment, half the medium from each well was removed and replenished with fresh medium containing fresh treatments.

Primary bronchial epithelial cells were a kind gift from Synairgen Research Ltd, (Southampton, UK). Primary epithelial cells derived from a bronchial biopsy of a healthy individual were grown as air-liquid interface cultures in collagen coated transwells (24 well plate). The cells were received as differentiated cultures with visible cilia on the apical surfaces. The details of the establishment and culture of an ALI culture have been documented by Yoshisue *et al.* [238]. The cells were treated apically and basally with 20µM $ZnCl_2$ and either buffer, ADAM33 Pro-MP-His (150ng/ml) or ADAM33 Pro-MP-His (150ng/ml) in ALI culture medium. The volume of medium added to the apical and basal surfaces were 100µl and 300µl respectively. The medium was removed daily from each transwell with a thin tipped pasteur pipette and replenished with fresh medium and treatments. Trans-epithelial resistance (TER) measurements were taken using an epithelial voltohmmeter (World Precision Instruments Inc, Hertfordshire, UK), in which two electrode probes were placed into the transwell. One probe is placed in the apical medium and the other in the basal medium. A current is passed through the culture to measure TER. All the images of A549 and primary bronchial epithelial cells were taken under phase contrast using an inverted Leica microscope.

2.9 Detection and quantification of ADAM33-Fc proteins by ELISA

To enable rapid quantitative screening of transfectants for ADAM33-Fc a sandwich ELISA was devised. Protein A was selected for capturing the recombinant protein due to its high affinity for IgG Fc binding. After capture, free Protein A sites were blocked using mouse IgG. This ensured that the detecting antibody was not captured by the Protein A via its own Fc domain. Horse radish peroxidase (HRP) conjugated to sheep anti-human IgG Fc was used to detect recombinant protein. The layers of this ELISA are summarised in the **Fig. 2.5**, and the protocol is outlined in the following pages.

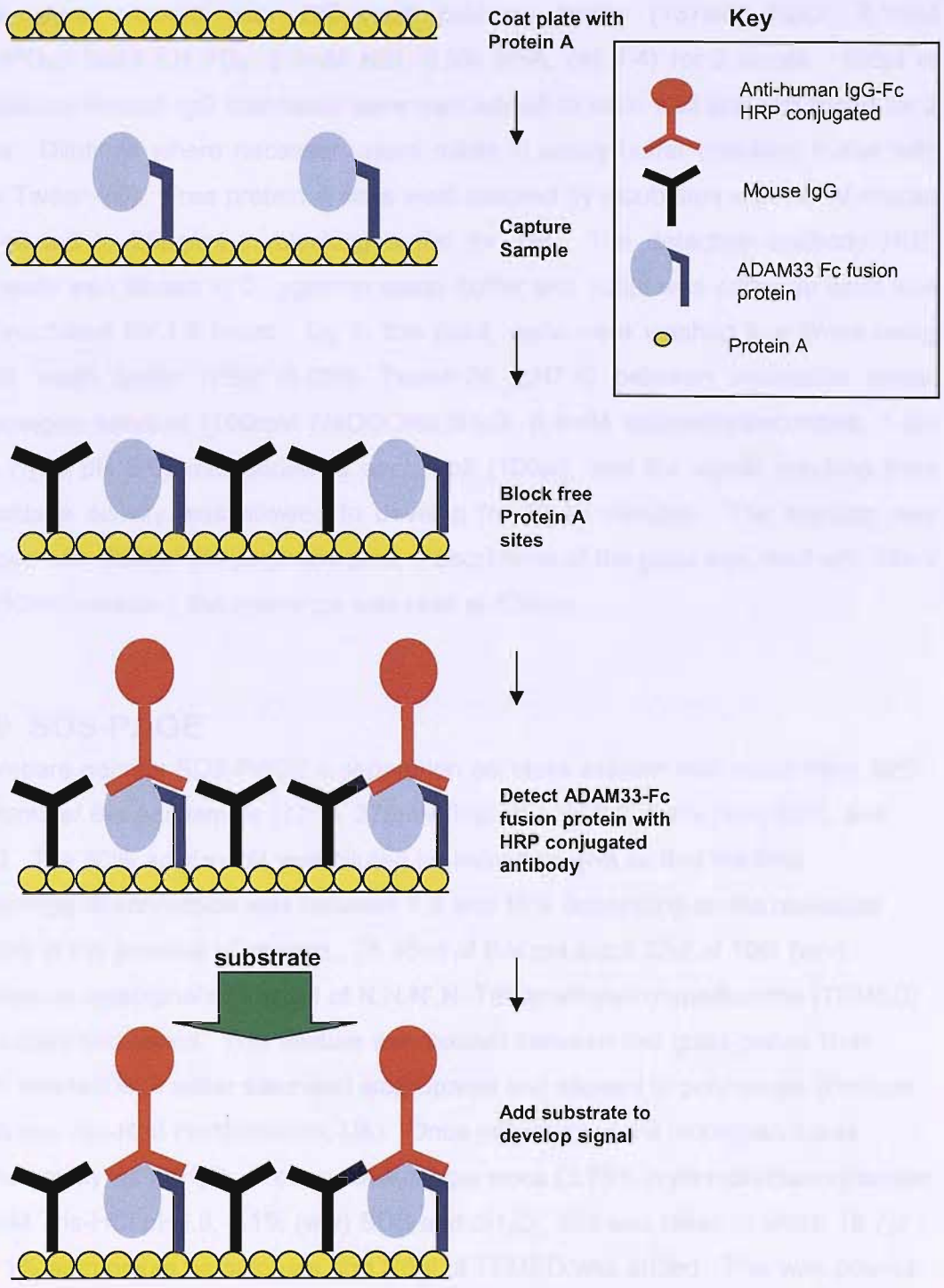

Fig. 2.5. Detection of ADAM33-Fc recombinant protein. In order to quantify the ADAM33-Fc fusion protein present in conditioned medium, an ELISA was developed. Recombinant protein was captured using protein A. Free protein A sites are blocked with mouse IgG. Recombinant protein was then detected using an anti-human IgG Fc HRP conjugated antibody. Signal was given on addition of TMP substrate, and absorbance was read on a microplate reader at 450nm.

96 well plates (Nunc Maxisorp) were pre-coated overnight at 4°C with 100µl of Protein A diluted to 25µg/ml in coupling buffer (15mM Na_2CO_3, 35mM $NaHCO_3$, 0.02% NaN_3, pH9.6). All subsequent steps were carried out at room temperature. Wells were blocked with 250µl/well blocking buffer (137mM NaCl, 8.1mM Na_2HPO_4,1.5mM KH_2PO_4, 2.7mM KCl, 0.5% BSA, pH 7.4) for 2 hours. 100µl of samples or human IgG standards were then added to each well and incubated for 2 hours. Dilutions where necessary were made in assay buffer (blocking buffer with 0.1% Tween-20). Free protein A sites were blocked by incubation with 250µl mouse IgG diluted to 25µg/ml in blocking buffer for 1hr. The detection antibody HRP conjugate was diluted to 0.1µg/ml in assay buffer and 100µl was added to each well and incubated for 1.5 hours. Up to this point, wells were washed four times using ELISA wash buffer (PBS, 0.05% Tween-20, pH7.4) between incubation steps. Chromagen solution (100mM NaCOONa.$3H_2O$, 0.4mM tetamethylbenzidine, 1.2µl 30% H_2O_2, pH 6.0) was added to each well (100µl), and the signal resulting from peroxidase activity was allowed to develop for 10-15 minutes. The reaction was stopped with 50µl of 2M sulphuric acid. Absorbance of the plate was read with filters for 450nm emission, the reference was read at 630nm.

2.10 SDS-PAGE

To prepare gels for SDS-PAGE a separation gel stock solution was made from 30% Acrylamide/ Bis Acrylamide (37:1), 375mM Tris-HCl pH 8.8, 0.1% (w/v) SDS, and dH_2O. The 30% acrylamide was diluted for individual gels so that the final percentage of acrylamide was between 7.5 and 15% depending on the molecular weights of the proteins of interest. To 10ml of this gel stock 33µl of 10% (w/v) ammonium persulphate, and 5µl of N,N,N',N'-Tetramethylethylenediamine (TEMED) was added and mixed. This mixture was poured between two glass plates 1mm apart, overlaid with water saturated isopropanol and allowed to polymerise (Protean III system, Bio-Rad Hertfordshire, UK). Once polymerised the isopropanol was washed away with dH_2O. From a stacking gel stock (3.75% crylamide/Bisacrylamide, 125mM Tris-HCl pH6.8, 0.1% (w/v) SDS and dH_2O), 5ml was taken to which 16.7µl of 0.1% ammonium persulphate and 3.6µl of TEMED was added. This was poured over the separation gel. A plastic comb was inserted into the stacking gel to create wells and this was left to polymerise. When the gel was set the comb was removed.

Samples were denatured by the addition of 5x sample buffer (313mM Tris-HCl pH6.8, 50% (v/v) glycerol, 25% (v/v) β-mercaptoethanol, 10% (w/v) SDS, 0.01% (w/v) bromophenol blue) and were heated to 95°C for 5 minutes before being loaded onto

a SDS-PAGE gel. Wide range rainbow markers or Kaleidoscope precision plus markers were used to estimate the molecular weight of sample proteins. Gels were run at 160V for 1 hour in running buffer (25mM Tris-HCl pH8.3, 192mM glycine, 0.1% SDS). Proteins were visualized either by staining the gel with Coomassie Brilliant Blue, or Colloidal Coomassie for 1 hour-overnight at room temp, and de-stained overnight (25%(v/v) methanol and 10%(v/v) glacial acetic acid or dH_2O respectively. For western blotting, proteins were transferred from the gels onto PVDF membranes at 90V on ice for 1.5 hours. Membranes were stored at 4°C or taken immediately for blotting.

2.11 Western blotting

2.11.1 ADAM33 recombinant protein detection

Before use, PVDF membranes were rinsed with methanol for 3 minutes, rehydrated in water for 3 minutes, then equilibrated in wash buffer (PBS, 0.1% Tween-20) for 10 minutes and finally blocked in 5% skimmed milk powder in wash buffer at room temperature for 1 hour. Membranes were then incubated with primary antibody, ADAM33 Pro or MP antibody (RP1, and RP2,) 0.2µg/ml, in blocking buffer at room temperature for 1.5 hours. Membranes were subsequently washed 3 times in high salt wash solution (0.4M NaCl in wash buffer). After washing, membranes were incubated with detection antibody HRP conjugated anti-rabbit antibody (either 1.3µg/ml DAKO or 0.04µg/ml Jackson laboratory) in wash buffer. Membranes were washed using wash buffer and peroxidase activity was visualized using an ECL plus detection kit according to the manufacturer's instructions. Briefly, 2ml of solution A was mixed with 50µl of solution B. This was used to cover the surface of each membrane (mini gel size), and left for 5 minutes, after which the membrane was wrapped in cling film and the luminescence was detected by exposing light sensitive Hyper ECL film (Amersham) to the sealed membrane. The film was developed by rocking the film in 1 minute of photographic film developer, followed by 1 minute in fixative, and finally rinsed in tap water and air dried. The primary antibodies RP1 and RP2 detected ADAM33 Pro-MP-His and ADAM33 Pro-MP(E346A)-His produced in insect cells specifically. No specific staining was detected when an irrelevant rabbit IgG antibody was used as an isotype control.

2.11.2 Fc detection

For anti-human IgG Fc blots, the blotting protocol was similar to above except different antibodies were used. HRP conjugated goat anti-human IgG-Fc 0.05µg/ml

was used as the primary antibody with an incubation time of 1.5 hours at room temperature. A secondary antibody was not required.

2.11.3 Stripping and re-probing Membranes

Membranes to be probed more than once were incubated in stripping buffer (62.5mM Tris-HCl pH6.8, 100mM β-mercaptoethanol, 2% w/v SDS) at 50°C for 30 minutes, after being probed once. These were then washed with PBS/Tween (0.1%) and blocked and re-probed using the standard western blotting protocols outlined above.

2.12 Protein A pull down

Samples were buffered in 1x triton buffer (10mM Tris-HCl pH 7.4, 150mM NaCl, 5mM EDTA, 5mM EGTA, 1mM PMSF, 1mM Na_3VO_4, 50mM NaF, 1% (v/v) Triton X-100, 0.5% (v/v) NP-40, 0.5X Complete inhibitor Cocktail (Roche)). Protein A agarose beads were incubated with samples at 4°C overnight on a rotary mixer. Beads were pelleted at 1400g at 4°C for 15 minutes, and then washed four times with 1x triton buffer without protease inhibitors. Bound protein was eluted with 3M glycine pH 3.0, and neutralized immediately with 1M Tris-HCl pH 7.5.

2.13 Alpha-2 Macroglobulin binding assay

Principle: Human α-2 Macroglobulin is a protease inhibitor capable of inactivating many different classes of proteases[239;240]. It forms a tetrameric protein, containing a pair of dimers. Each subunit is 185kDa, and each possesses a bait region which is rich in proteolytic cleavage sites. If a protease attacks this bait region, the subunit will be split into a 100KDa and 85 kDa unit that remain linked via disulfide bonds. A highly reactive thioester group is thought to be exposed on the 100kDa portion, which undergoes attack from an amine group from the protease which is in close proximity, forming a covalent complex. This complex can be visualized by staining for the appearance of a band corresponding to 100kDa and the added molecular weight of the active protease, on a denaturing SDS PAGE gel, **Fig.2.6**.

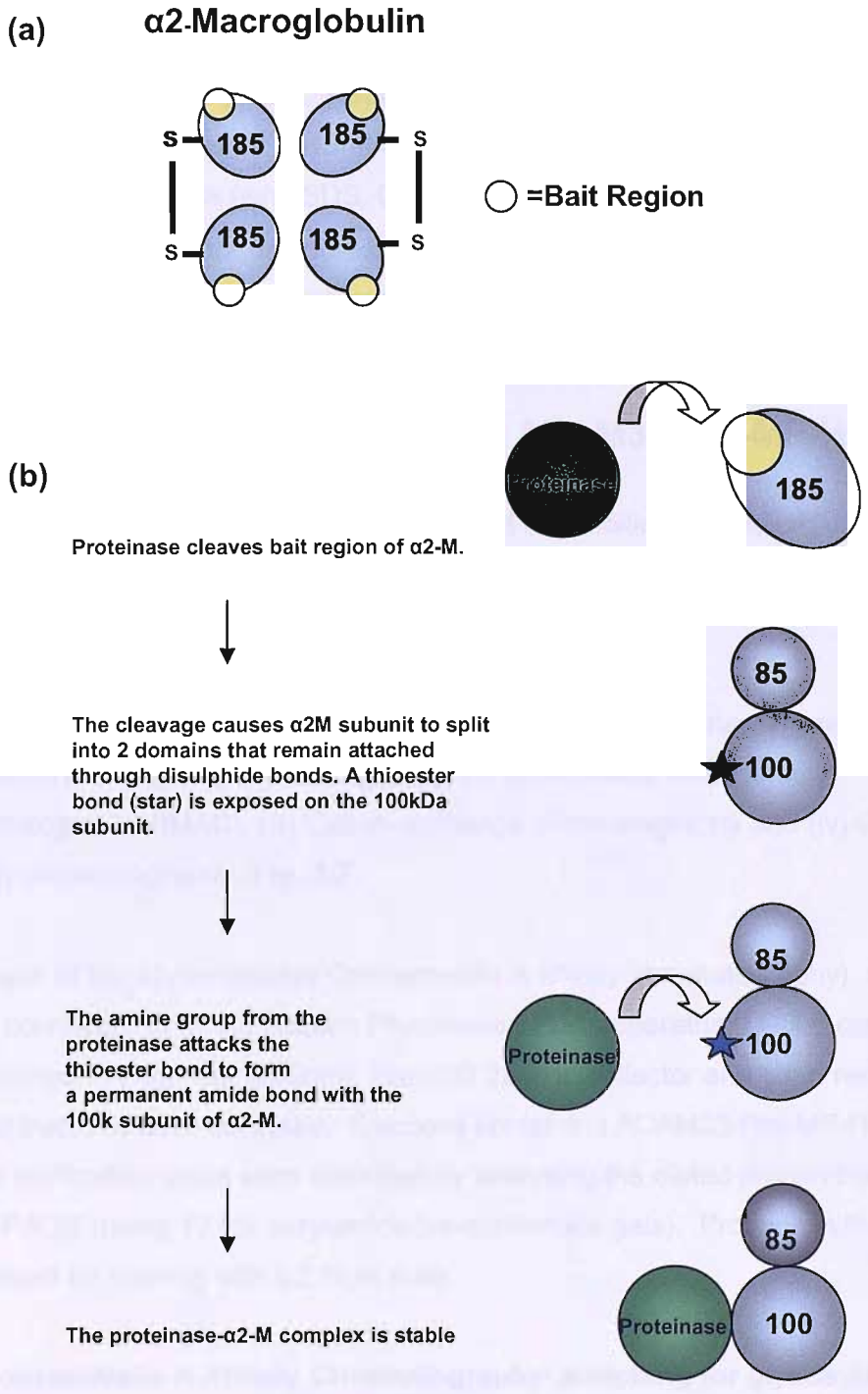

Fig. 2.6. α2-Macroglobulin proteinase binding assay. (a) Pictorial of the domains of tetrameric α2-Macroglobulin (α2-M). (b) Schematic of the events that occur during the α2-M proteinase trapping assay. Only one α2-M domain is shown, but all four domains are identical. Numbers represent Molecular weight in kDa. Active proteinases of cleaving α2-M become covalently bound and trapped in a high molecular weight complex.

Assay Conditions

ADAM33 Pro-MP-His and ADAM33 Pro-MP(E346A)-His (working concentration ~645μM) were incubated overnight at 25°C with α-2 Macroglobulin (175μg/ml) in assay buffer (50mM Tris-HCl pH7.4, 0.1M NaCl, 10mM $CaCl_2$, 0.2% (v/v) NaN_3), in the presence or absence of 10mM of the metalloproteinase inhibitor 1,10 phenanthroline monohydrate. Reactions were stopped with the addition of 5μl of 5X SDS-PAGE sample buffer (313mM Tris-HCl pH6.8, 50% (v/v) glycerol, 25% (v/v) β-mercaptoethanol, 10% (w/v) SDS, 0.01% (w/v) bromophenol blue) followed by denaturation at 95°C for 5 minutes. Samples were analysed by SDS-PAGE and proteins were visualized by western blotting.

2.14 Purification of recombinant ADAM33 Pro-MP-His and ADAM33 Pro-MP(E346A)-His protein

ADAM33 Pro-MP-His protein was purified out of conditioned medium using the purification scheme detailed below. The ADAM33 Pro-MP(E346A)-His protein was also purified using the same scheme.

Four different chemistries were used in the purification scheme. These were (i) Concanavalin A affinity chromatography, (ii) Immobilised metal affinity chromatography (IMAC), (iii) Cation-exchange chromatography and (iv) Gel filtration affinity chromatography, **Fig. 2.7**.

For each of the above (except Concanavalin A affinity chromatography), columns were connected to an Amersham Pharmacia FPLC apparatus (LC500 controller, P-500 pumps, UV monitor (280nm), Frac100 fraction collector and chart recorder), and eluted fractions were collected. Fractions containing ADAM33-Pro-MP-His from each of the purification steps were identified by analysing the eluted protein fractions using SDS-PAGE (using 12.5% acrylamide/bis-acrylamide gels). Proteins in the gels were visualised by staining with EZ Blue stain.

(i) Concanavalin A Affinity Chromatography- enriching for glycosylated proteins

20ml of Concanavalin A conjugated Sepharose was packed into a glass column by mixing it with equilibration buffer (20mM Tris-HCl pH7.4, 0.5M NaCl) and allowing it to settle. The matrix was subjected to a high salt wash (20mM Tris-HCl pH7.4, 1.0M NaCl, 5mM $MnCl_2$, 5mM $MgCl_2$, 5mM $CaCl_2$) of 5 column volumes, before being

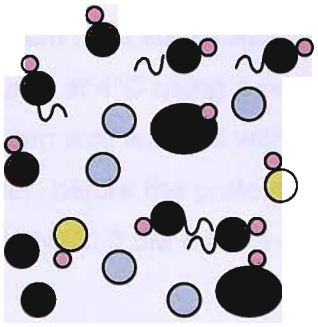

Complex protein mixture. 6xHis tagged ADAM33 shown in lime green and glycosylation shown in pink.

Step 1.

Concanvalin A Afiinity Chromatography.

Selected glycosylated proteins, including ADAM33. have high affinity for the lectin Concanvalin A.

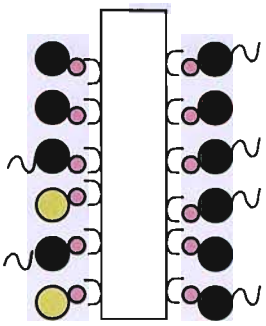

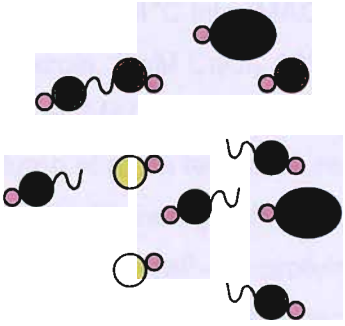

Step 2.

Immobilised Metal Affinity Chromatography.

Selected histidine rich proteins, including the 6xHis tagged ADAM33 using immobilised nickel ions.

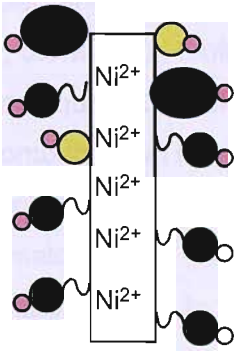

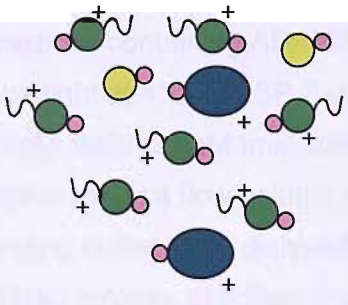

Step 3.

Cation Exchange Chromatography

Selected positively charged proteins at pH7.0 using a negatively charged column.

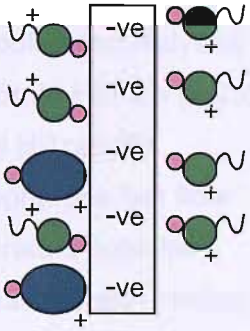

Step 4.

IMAC Used step 2 again, to concentrate up sample for loading on to gel filtration column

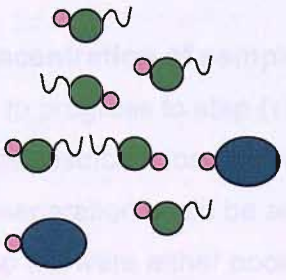

Step 5.

Gel Filtration

Separated proteins on the basis of molecular weight. Larger proteins travelled down the column faster and eluted in an earlier fraction than smaller ones.

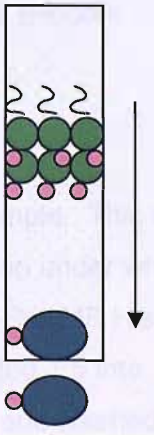

Fig. 2.7. ADAM33 purification scheme outline. This schematic shows the steps involved in the purification of ADAM33 from conditioned medium from transfected cells to a pure preparation.

equilibrated with 10 column volumes of equilibration buffer. 500ml of conditioned medium from stable *ADAM33* transfectants was degassed, and loaded onto the column at 4°C using a peristaltic pump operating at a flow rate 0.5ml/minute. The column was washed with 10 column volumes of equilibration buffer, before the protein was eluted in 140ml elution buffer (20mM Tris-HCl pH7.4, 0.5M NaCl 0.5M methyl α-D mannopyranoside).

(ii) Immobilised Metal Affinity Chromatography (IMAC) –enrichment of histidine rich proteins

Fractions containing ADAM33-Pro-MP-His from step 1 were pooled and dialysed overnight at 4°C into IMAC binding buffer (25mM HEPES pH7.9, 0.5M NaCl, 5mM Imidazole, 5mM $CaCl_2$, 10% glycerol). A 1ml HisTrap column was equilibrated with 10ml of IMAC binding buffer. The dialysed sample was loaded onto the HisTrap column at room temperature, at a flow rate of 1ml/minute. The column was washed with IMAC binding buffer until baseline was reached on the chromatogram. ADAM33-Pro-MP-His protein was eluted using a gradient of imidazole from 5 to 250mM over 50 minutes (increase in gradient 5mM/minute).

(iii) SP Sepharose Fast Flow – enrichment of proteins with ~PI≥8

Fractions containing ADAM33-Pro-MP-His from step (ii) were pooled and dialysed overnight at 4°C into SP Sepharose Fast Flow binding buffer (25mM HEPES pH7.0, 50mM NaCl, 20mM Imidazole, 5mM$CaCl_2$, 10% glycerol). A 1ml HiTrap SP sepharose fast flow column was equilibrated with 10ml of SP sepharose fast flow binding buffer. The dialysed sample was loaded at room temperature onto the HiTrap column, at a flow rate of 1ml/minute. The column was washed with binding buffer until baseline was reached on the chromatogram. ADAM33-Pro-MP-His protein was eluted using a gradient of NaCl from 50 to 500mM over 20 minutes (increase in gradient 25mM/minute).

(iv) Concentration of sample using IMAC

In order to progress to step (v) it was necessary to concentrate the sample. This was due to the restricted loading volume imposed by the gel filtration column under which optimal separation could be achieved. Fractions containing ADAM33-Pro-MP His from step (iii) were either pooled and dialysed overnight at 4°C or diluted 1:5 into IMAC binding buffer. Samples were loaded onto the HisTrap column and washed as outlined in step (ii). ADAM33-Pro-MP-His protein was eluted using a step of either 250mM or 500mM imidazole in IMAC binding buffer.

(v) Gel filtration using Superose 12

A 24cm Tricorn Superose 12 column was equilibrated at room temperature using 50ml of Superose12 equilibration buffer (25mM HEPES pH7.5, 150mM NaCl, 50mM Imidazole, 5mM $CaCl_2$, 10%glycerol) at a flow rate of 0.5ml/minute. 200µl samples of fractions containing ADAM33 Pro-MP-His from step (iv) were loaded onto the Superose 12 column via a sample loop. Equilibration buffer was pumped through the column at 0.5ml/minute for 50 minutes, until the ADAM33 protein was eluted.

2.15 Calibrating Superose 12 column

A 24cm Tricorn Superose 12 column was equilibrated using 50ml of buffer (25mM HEPES pH7.5, 150mM NaCl, 50mM Imidazole) at a flow rate of 0.5ml/minute. 200µl of 0.22µm sterile filtered protein calibrator mixture (240µg Blue dextran, 240µg BSA, 100µg Carbonic anhydrase, 200µg Cytochrome c, and 240µg Vitamin B_{12}) was loaded onto the column via the sample loop. The absorbance at 280nm of the column flow through was monitored using an in-line UV monitor. A typical elution profile and calibration curve is shown in, **Fig 2.8**.

2.16 Ammonium sulphate precipitation

Principle: Ammonium sulphate precipitation is a method used to crudely separate proteins of different molecular weights. The addition of salt stabilises the charges on the surface of proteins, and also forms hydrogen bonds to water molecules, diminishing the bonding between water and protein. This causes proteins to precipitate out, or 'salt out'. This method was carried out in an attempt to reduce the complexity of the conditioned medium prior to affinity chromatography. The protocol used is outlined below.

95ml of harvested conditioned medium from S2 transfectants expressing ADAM33 Pro-MP-His was adjusted to pH7.4 by the addition of 5ml of 1M Tris-HCl pH 7.4. The sample was stirred slowly in an ice water bath. To achieve 25% ammonium sulphate saturation, 14.4g of the salt was added slowly. The pH was monitored and kept constant by the addition of 1M HCl when necessary. After the crystals had dissolved, the sample was centrifuged at 4369g at 4°C for 30 minutes. The pellets were kept and resuspended in ~800µl into buffer (25mM HEPES, 150mM NaCl, 50mM imidazole pH7.0).

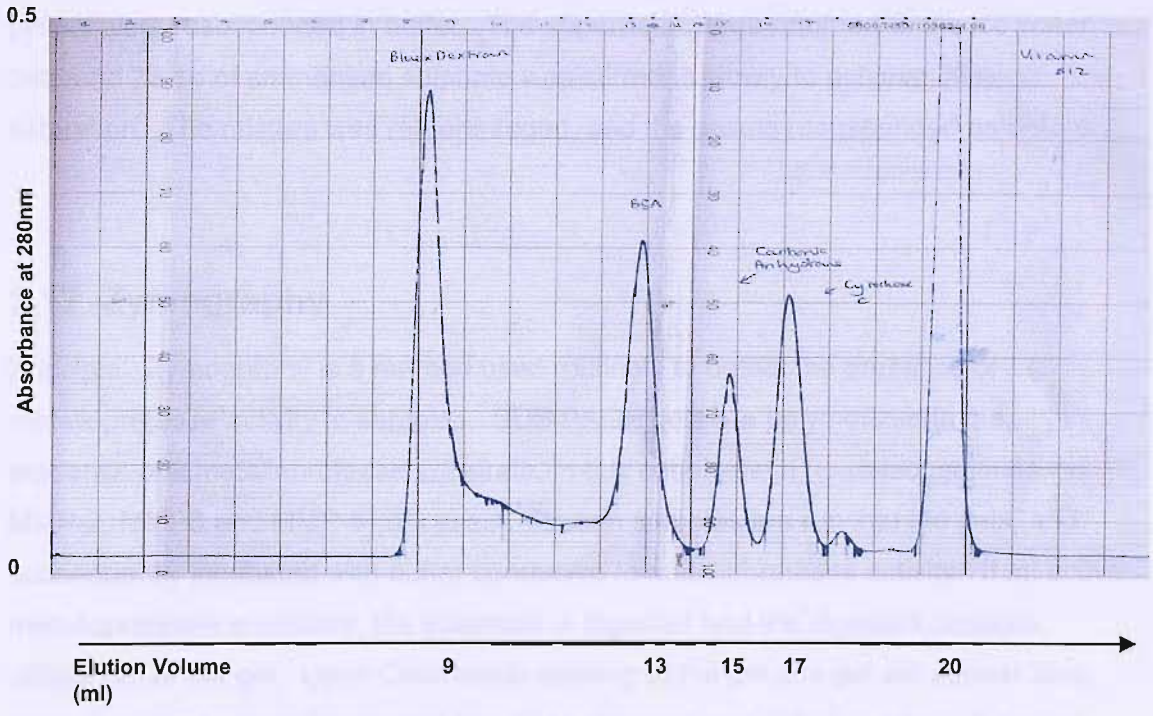

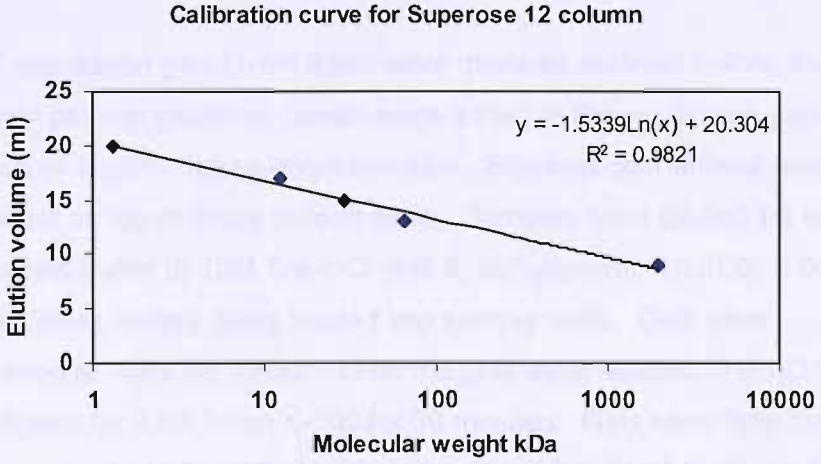

Fig. 2.8. Calibration of the 24cm Superose 12 column. A typical elution profile for a 200µl sample of mixed protein standards run in 25mM HEPES pH7.5, 50mM Imidazole, 150mM NaCl buffer at a flow rate of 0.5ml/minute. The molecular weight of the protein standards and the peak elution volume was as follows: Blue dextran, 2000 kDa, 9ml; Bovine serum albumin, 66kDa, 13ml; Carbonic Anhydrase 29.1 kDa, 15ml; Cytochrome C, 12.4 kDa,17ml; Vitamin B12, 1.3kDa, 20ml. The relationship between the molecular weight of the protein standards and their peak elution volume is shown in the graph.

The supernatant was returned to the beaker in the ice water bath. A further 15.8g of ammonium sulphate crystals were stirred in slowly, to achieve 50% saturation. After which the precipitated proteins were recovered by centrifugation as before. The pellets were resuspended in buffer. The supernatant was returned to the ice water bath and 23.1g of ammonium sulphate was stirred in slowly to achieve 80% saturation. The mixture was re-centrifuged, and the pellets resuspended as before.

2.17 Zymography

Principle: Zymography is a method used routinely to detect the presence of metalloprotease activity in samples. SDS PAGE gels are polymerized in the presence of a metalloprotease substrate, in this case gelatin (to detect gelatinases MMP-2, MMP8 and MMP-9) or casein. Protein samples are run into the gels, and subsequently incubated with buffer conducive to metalloprotease activity. If an active metalloprotease is present, the substrate is digested and the digested peptides diffuse out of the gel. Upon Coomassie staining of the gel, the gel will appear blue, except in areas where the protein has been digested and diffused away. A typical protocol that was used is outlined below.

SDS PAGE separation gels (1mm thick) were made as outlined before, but in addition either porcine gelatin or casein were added to the separation gels to a final concentration of 1mg/ml before polymerisation. Stacking gels without gelatin and casein were set on top of these to form wells. Samples were diluted 1:2 with non reducing sample buffer (0.13M Tris-HCl pH6.8, 20%glycerol, 4%SDS, 0.004% bromophenol blue), before being loaded into sample wells. Gels were electrophoresed at 160V for 1 hour. Then the gels were washed in dH_2O for 10 minutes, followed by 2.5%Triton X-100 for 30 minutes. Gels were then incubated in 100ml of zymography buffer (50mM Tris-HCl HCl pH 7.5, 5mM $CaCl_2$, 1µM $ZnCl_2$, 0.02% NaN_3) at 37°C overnight. Gels were stained in Coomassie Brilliant Blue stain at room temperature for 1 hour, before being de-stained (25%(v/v) methanol, 10%(v/v) glacial acetic acid). Gels were imaged using the GS-800 gel scanner (Bio-Rad, Hertfordshire, UK).

2.18 2D Gel Electrophoresis analysis of ADAM33 Pro-MP –V5-6xHis

Purified ADAM33 Pro-MP-His and ADAM33 Pro-MP(E346A)-His preparations were analysed by 2D gel electrophoresis. 4-8µg pf purified protein was precipitated in ice cold acetone at -20°C over 5 hours. The precipitated protein was recovered by centrifugation at 16000g for 5 minutes, and was washed twice with ice cold acetone before being air-dried. Pellets were resuspended in rehydration buffer (8M Urea, 2% (w/v) CHAPS, IPG buffer 3-10, 18.2mM DTT, 0.002%bromophenol blue) to give a concentration of 10µg/ml. 200µl of each sample (with or without 5µl of 2D-SDS PAGE standards) was pipetted into a loading tray. An 11cm non linear pH 3-10 IPG strip was put gel side down on top of the sample. Coverstrip fluid was put on top of the IPG strip and the tray lid sealed. IPG strips were rehydrated at 20°C for a minimum of 12 hours. After hydration, IPG strips were transferred to a cup loading rehydration tray and isoelectric focused using the following program on the IPGphor (Amersham Biosciences-GE Healthcare, Buckinghamshire, UK):

Step 1: 500V 1 hour
Step 2: 1000V 1 hour
Step 3: 8000V 1 hour 50 minutes
Temperature help at 20°Cfor steps 1-3.

The IPG strips were incubated with 5ml of equilibration buffer (50mM Tris-HCl pH 6.8, 6M Urea,30% of 87% glycerol, 2% (w/v) SDS, 0.002% bromophenol blue) containing 50mg of dithiothreitol (DTT) to reduce proteins, for 15 minutes on a shaker. The strips were then incubated with 5ml of equilibration buffer containing 125mg of Iodoacetamide, for 15 minutes. Iodoactemide inhibits the re-oxidation of the proteins by acetylating free –SH groups. Excess fluid was drained away. IPG strips were then sealed onto the top of 12.5% pre-cast Criterion SDS PAGE separation gels (Bio-Rad, Hertfordshire, UK) using 0.5% low melting point agarose in running buffer. The second dimension was run at 200V for 60 minutes. Gels were either stained for proteins or the proteins were transferred onto PVDF membranes. To stain gels, they were fixed in 10%methanol with 7% acetic acid for 1 hour prior to being stained with SyproRuby gel stain for 16 hours. The stain was washed off in fixative (3 times for 10 minutes) before being imaged. To transfer proteins onto PVDF membranes, semi dry transfer was achieved using the Trans Blot SD Semi-Dry Transfer cell (Bio-Rad, Hertfordshire, UK). For this, filter paper and PVDF membrane were pre-wetted and assembled as follows: 1 sheet of extra thick filter paper was placed onto the platinum anode, on top of which a PVDF membrane was placed,

followed by the SDS PAGE gel, then another sheet of extra thick filter paper, and lastly the cathode. Proteins were transferred from the gel to the membrane using 22V for 25 minutes (for two membranes). The proteins were fixed onto the membranes by floating membranes protein side down in fixative for 15 minutes. After fixation the membranes were washed four times with dH_2O for 5 minutes, before being stained for 15 minutes in SyproRuby blot stain. Excess stain was removed by rinsing membranes 2-3 times in dH_2O before being air-dried. Gels and blots were imaged using the Versa-Doc imager (Bio-Rad, Hertfordshire, UK).

2.19 Deglycosylation of ADAM33 Pro-MP-His and ADAM33 Pro-MP(E346A)-His proteins

Proteins were deglycosylated using the N-glycosidase F (PNGase F) **Fig. 2.9**. A 1:10 volume of 10x denaturing sample buffer (0.5% SDS, 1% β-mercaptoethanol) was added to the sample to be deglycosylated. This was heated to 100°C for 10 minutes. The sample was allowed to cool to room temperature, then 1:10 volume of 10x G7 buffer (50mM Sodium Phosphate, pH7.5), and 1:10 volume of 10% NP-40 was added to the reaction. This was then incubated at 37°C for 2 hours. Samples were then either lysed in 5x sample buffer for SDS-PAGE, or precipitated for later analysis by mass spectroscopy (Ciphergen Biosystems). The protein precipitation procedure involved adding 4 volumes of ice cold acetone to the sample and allowing the proteins to precipitate at -20°C overnight. The protein pellet was washed 3 times using ice cold acetone (500µl/wash) and then air-dried and resuspended in a volume of denaturing buffer (2% CHAPS, 9M Urea) that was sufficient to re-solubilise the protein pellet.

2.20 Mass spectroscopy analysis of ADAM33 Pro-MP-His and Pro-MP(E346A)-His

IMAC30 chips were selected for recombinant protein capture (8 spots per chip). Like the IMAC column, the chip has Nitrilotriacetic acid (NTA) groups on the surface which can chelate Nickel ions. The His tag of the recombinant proteins has a high affinity for the nickel ions and could be captured by the nickel ions on the IMAC30 chip's surface. Once the proteins were bound to the chip, the protein was mixed with a matrix (Sinapinic acid) and subjected to time of flight (TOF) mass spectroscopy analysis (Ciphergen Biosystems, Sussex, UK).

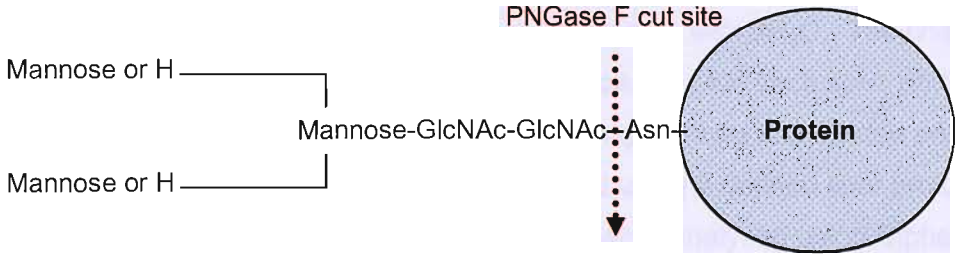

Fig. 2.9. Deglycosylation of Proteins using PNGase F. PNGase F is a deglycosylse isolated from *Chryseobacterium [Flavobacterium] menigosepticum.* It removes N-linked carbohydrate chains from proteins by hydrolysing the bond between N-Acetyl glucosamine, and the asparagine of the protein of interest.

Preparing the IMAC30 chip

The chip was loaded into a chip holder, and then attached to a bioprocessor , that allowed larger volumes of liquid to be incubated with each spot. First 50µl of 0.1M nickel sulphate was loaded onto each spot and incubated at room temperature for 10 minutes with vigorous shaking. This was washed off with 200µl of dH_2O, followed by two washes in 200µl of PBS with vigorous shaking for 5 minutes. The PBS from the wash step was tipped away and diluted sample was applied to each spot on the chip. 225µl of PBS together with 25µl of sample was loaded onto each spot on the chip, and incubated for 1hour at room temperature with vigorous shaking. The chip was then washed three times using PBS, followed by twice with dH_2O. The chip was air dried for 15 minutes. 1µl of Sinapinic acid was loaded onto each spot, and air dried for 5 minutes. After 5 minutes another 1µl of Sinapinic acid was loaded onto each spot and allowed to dry. The chip was then read using a defined spot protocol in the Ciphergen Mass Spectrophotometer. The data were analysed using Ciphergen Protein Chip Software 3.2.1.

2.21 Fluorescence Resonance Energy Transfer (FRET) peptide cleavage assay

Principle: A FRET peptide cleavage assay is an assay used to assess enzyme activity. A short peptide known to be cleaved by a proteinase is modified so that one terminus is linked to a fluorescent reporter dye and the other terminus is labelled with a quencher dye. When the peptide is intact the quencher absorbs the fluorescence emitted by the reporter dye, so minimal reporter fluorescence is detectable. When the peptide is incubated with the proteinase and is cleaved, the peptide is split into two allowing the reporter and quencher dyes to diffuse away from each other. The spatial separation of the two dyes prevents the quencher from absorbing energy from the reporter, allowing the reporter dye's fluorescence to be detected. A FRET peptide cleavage assay based on the study by Zou *et al.*[235] was used to assess the activity of purified ADAM33 Pro-MP-His, **Fig. 2.10**. All FRET peptide assay measurements were made in real time using the iCycler (Bio-Rad, Hertfordshire, UK), using the FAM filter (490nm). Typically 20µl reactions containing 4.4µM FRET peptide (DABCYL-YRVAFQKLAE(FAM)K-NH_2), were incubated with ADAM33 Pro-MP-His or ADAM33 Pro-MP(E346A)-His, at 37°C in assay buffer containing 20mM HEPES pH7.0, 0.5M NaCl, 10mM $CaCl_2$, 10µM $ZnCl_2$, and 0.2mg/ml BSA unless otherwise stated below or detailed in the results chapters. This FRET peptide was synthesised and supplied by Dr. J Diaz-Mochon, University of Edinburgh.

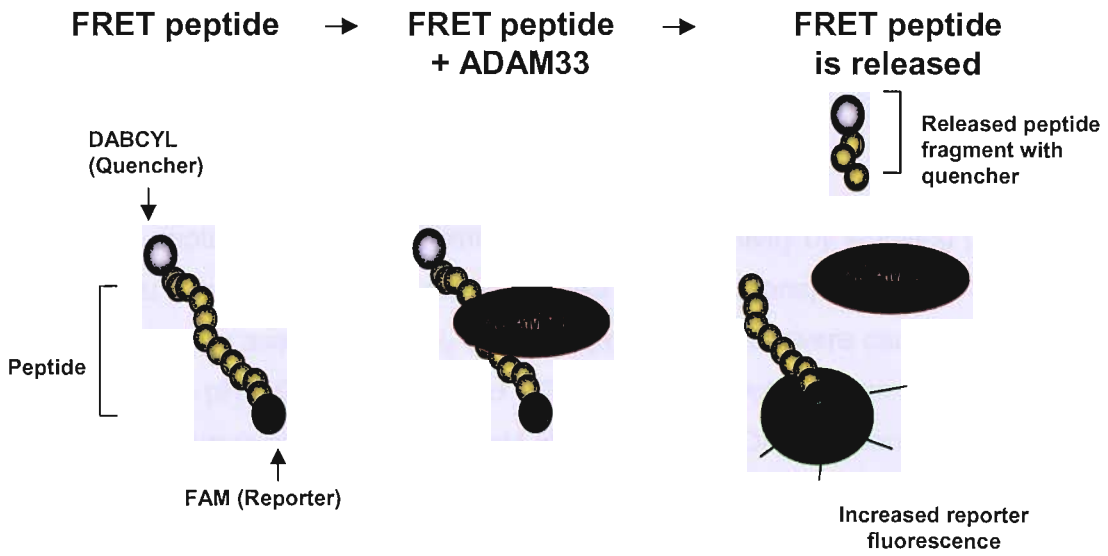

Fig. 2.10. FRET peptide cleavage assay. Schematic showing the principle of the FRET peptide cleavage assay. The detected fluorescence from the reporter dye of intact FRET peptide is minimal due to the reporter's close proximity with the quencher. If the peptide is incubated with a proteinase such as ADAM33 and is subsequently cleaved the peptide is released as two fragments. The spatial separation of the quencher from the reporter abolishes the quenching effect, and the fluorescence of the reporter increases.

Reactions were carried out in typical polystyrene PCR plates used for qPCR (Abgene, Hampshire, UK), sealed with transparent plate seals. The enzyme activity was determined by plotting the background subtracted relative fluorescence units (RFU) against time and calculating the rate at which RFU changes from a line of best fit. Rates were determined in the initial linear phase of the assay.

2.21.1 Optimisation of the FRET peptide assay

The FRET peptide assay was optimised for ADAM33 activity by studying proteolytic activity over a range of $ZnCl_2$, $CaCl_2$ and NaCl concentrations, and also a range of pH. Optimisation assays for $ZnCl_2$ and $CaCl_2$ concentration were carried out in 20mM HEPES pH 7.0, 0.5M NaCl and 0.2mg/ml BSA. Optimisation assays for NaCl concentration were carried out in 20mM HEPES pH7.0. Optimisation assays to study pH were carried out in 0.5M NaCl, 10mM $CaCl_2$, 10µM $ZnCl_2$, 0.2mg/ml BSA with one of the following buffers, sodium acetate pH 4.0 , pH 5.0, MES pH 6.0, HEPES pH 7.0, pH 7.5, HEPES pH 8.0 or Tris-HCl pH 9.0. To read the fluorescence of the reactions carried out at different pH, the reactions were first quenched and neutralised with equal volume of 2M HEPES pH 7.0, 150mM EDTA. The average fluorescence of reactions quenched and neutralised at time=0 was subtracted from the end point readings then divided by the duration of the assay in minutes to calculate the rate of enzymic activity.

2.21.2 Kinetic studies

To calculate the kinetic parameters, it was necessary to convert the activity typically measured in RFU/minute into nM/minute. To do this a calibration curve was constructed by measuring the RFU of known concentrations of FRET peptide digested to completion with trypsin. Using this curve a linear relationship between measured RFU and concentration of peptide was observed.

2.21.3 Inhibition studies

The sensitivity of purified ADAM33 Pro-MP-His (130nM) to four synthetic inhibitors of MMPs was tested in a typical FRET assay. The four inhibitors were (i) (2R)-2-[4(-Biphenylylsulfonyl)amino]-3-phenyl propionic acid, the zinc binding group of this compound is the carboxylate ion, (ii) N-Isobutyl-N-(4-methoxyphenylsulfonyl)-glycylhydroxamic acid, (iii) (3R)-(+)-[2-(4-methoxybenzenesulfonyl)-1,2,3,4-tetrahydroisoquinoline-3-hydroxymate and (iv) GM6001. Inhibitors were tested at 5µM, 1µM, 0.2µM, 40nM, 8nM, and 1.6nM. The sensitivity of purified ADAM33 Pro-

MP-His to TIMPs was also tested by pre-incubating TIMP-1, N-TIMP-2 and N-TIMP-3 at varying concentrations with the enzyme for 1 hour at 37°C, before the standard FRET peptide assay was carried out. The TIMPs were gifts from Prof. G Murphy, University of Cambridge.

2.22 Peptide PNA-DNA Microarrays

The microarray work was carried out in collaboration with Prof. Mark Bradley's research group based at the University of Edinburgh, in particular Dr J. Díaz-Mochón who designed, synthesised and supplied the PNA-peptide library[241;242].

Principle: The PNA-FRET-peptide library is a 10,000 member peptide library. Like the FRET peptide described previously, each member of the library is tagged with a quencher and a reporter dye. In this case, the quencher was TAMRA, and the reporter was FAM. Unlike DABCYL, TAMRA is not a dark quencher, and emits at~580nm. In addition, each member of the library is labelled with a unique peptide nucleic acid (PNA) molecule. PNA has a pseudo peptide backbone unlike the phospho backbone of DNA. However this does not affect its ability to hybridise to complementary nucleic acids, and in fact does so with higher affinity than DNA-DNA interactions. The library was designed so that each amino acid in the peptide sequence corresponds to a particular PNA triplet. Therefore the peptide sequence was used to dictate the exact PNA triplet code sequence of the associated PNA tag. The unique tag on member of the library acts as an identifier from which the peptide sequence can be deduced. This PNA-FRET-peptide library can be incubated with a proteinase in a FRET peptide cleavage assay similar to that described in **section 2.21**. To distinguish the peptides that are cleaved from those that are not, the library is pulled down onto a 2 dimensional platform which in this case is a customised DNA microarray. The DNA spots on the microarray are complementary to the PNA tag, therefore each spot corresponds to one library member. When the microarray is scanned the fluorescence emitted from both the reporter and the quencher dyes are recorded for every peptide, **Fig.2.11**.

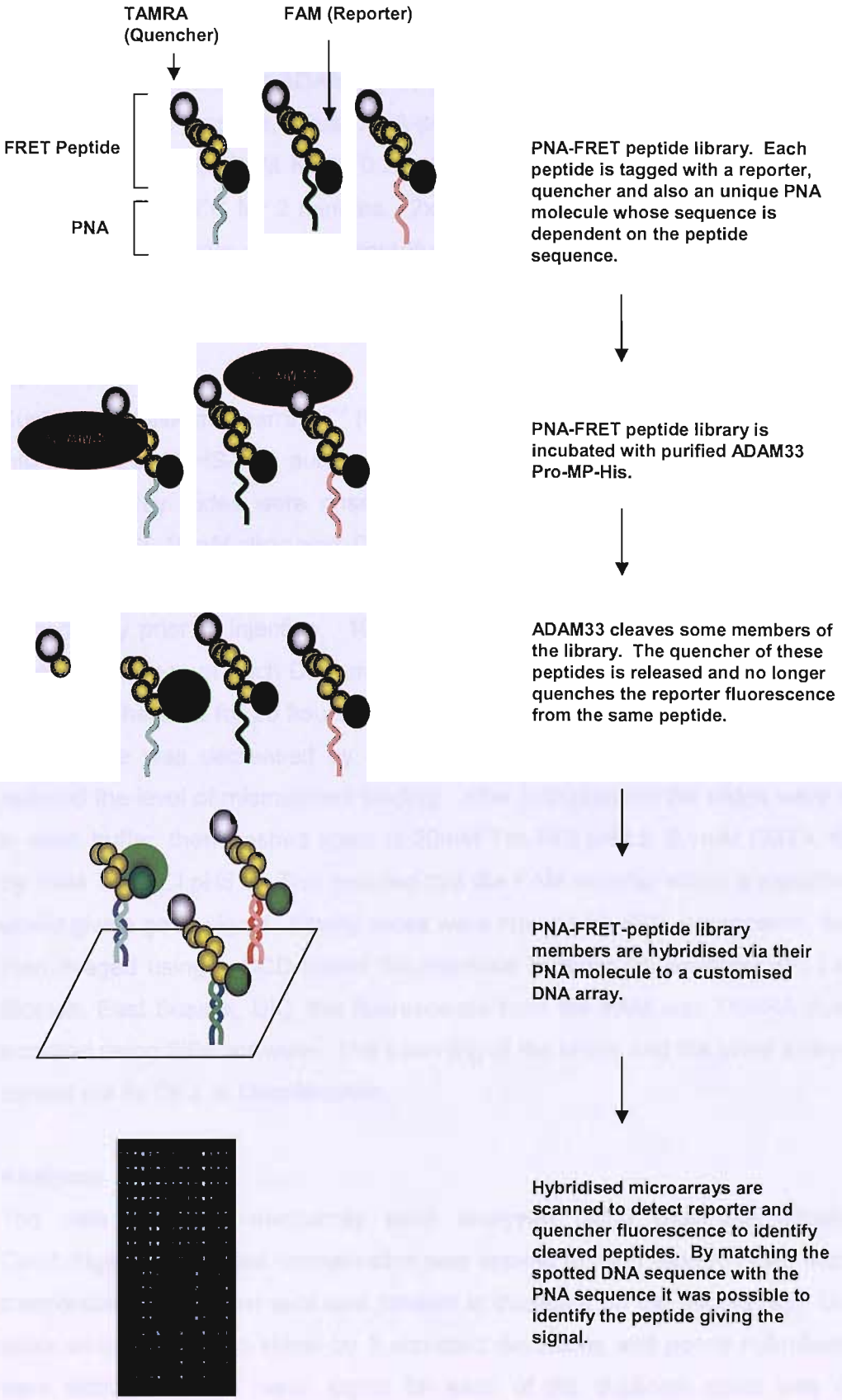

Fig. 2.11. PNA-FRET-peptide microarray. Schematic showing the novel PNA-FRET peptide microarray approach used to identify ADAM33 peptide substrates. This powerful technology allowed the simultaneous screening of 10,000 peptides. Figure adapted from :Diaz-Mochon JJ *et al. 2005 Chem. Commun. 1384-1386.*

Sample preparation

For this study the 10,000 member PNA encoded peptide library was incubated with ADAM33 Pro-MP-His, or ADAM33 Pro-MP(E346A)-His in assay buffer for 1 hour at 37°C (160nM of enzyme, 35μM PNA-peptide library, 20mM HEPES pH 7.0, 10mM $CaCl_2$, 10μM $ZnCl_2$, 0.5M NaCl, 0.2mg/ml BSA). The reactions were quenched by denaturation at 95°C for 2 minutes. 2x GenHyb buffer (71.4μl) was added to each sample. The sample was then centrifuged at 16000g for 5 minutes to remove any insoluble particles.

Hybridisation

Customised DNA microarrays[242] (Oxford Gene Technology, Oxford, UK) were placed into the TECAN HS-400 automated hybridisation station (TECAN, Reading, UK). The microarray slides were rinsed with dH_2O and then cleaned with wash buffer (100mM NaCl, 10mM citric acid, 0.1mM EGTA, 0.7% N-lauroylsarcosine, pH7.4), and rinsed again with dH_2O. The slides were warmed to 50°C and the samples to 65°C immediately prior to injection. 100μl of sample was injected into each chamber to cover the surface of each DNA microarray slide. The sample was agitated over the surface of the slide for 20 hours. The initial hybridisation temperature was 50°C, the temperature was decreased by 2°C every 2 hours until 33°C was reached; this reduced the level of mismatched binding. After hybridisation the slides were washed in wash buffer, then washed again in 20mM Tris-HCl pH8.5, 0.1mM EGTA, followed by 1mM Tris-HCl pH8.5. This ensured that the FAM reporter which is sensitive to pH would give a good signal. Finally slides were rinsed with 90% isopropanol, dried and then imaged using a CCD based fluorescence scanner (Bioanalyser 4F, La Vision Biotech, East Sussex, UK), the fluorescence from the FAM and TAMRA dyes were acquired using FIPs software. The scanning of the slides and the initial analysis was carried out by Dr J. J. Díaz-Mochón.

Analyses

The data from the microarray were analysed using BlueFuse (BlueGnome, Cambridge, UK). Global normalisation was applied to each slide to make them more comparable. Every test spot was present in duplicate on the microarray. Duplicate spots which differed in signal by 3 standard deviations and poorly hybridised spots were excluded. The mean signal for each of the duplicate spots was used to calculate an average. The ratio of FAM toTAMRA (F/T) fluorescence for each spot sequence was calculated for each slide. A spot which had cleaved substrate hybridised to it was expected to have a higher F/T ratio than one hybridised to in tact

peptide. The differences between the ADAM33 Pro-MP-His and ADAM33 Pro-MP(E346A)-His slides were visualised by plotting the F/T ratio from the wild type treated slide with the F/T ratio of the mutant treated slide. In cases where a peptide was not cleaved, the plotted values were predicted to lie close to the hypothetical identity line on which wild type F/T=mutant F/T.

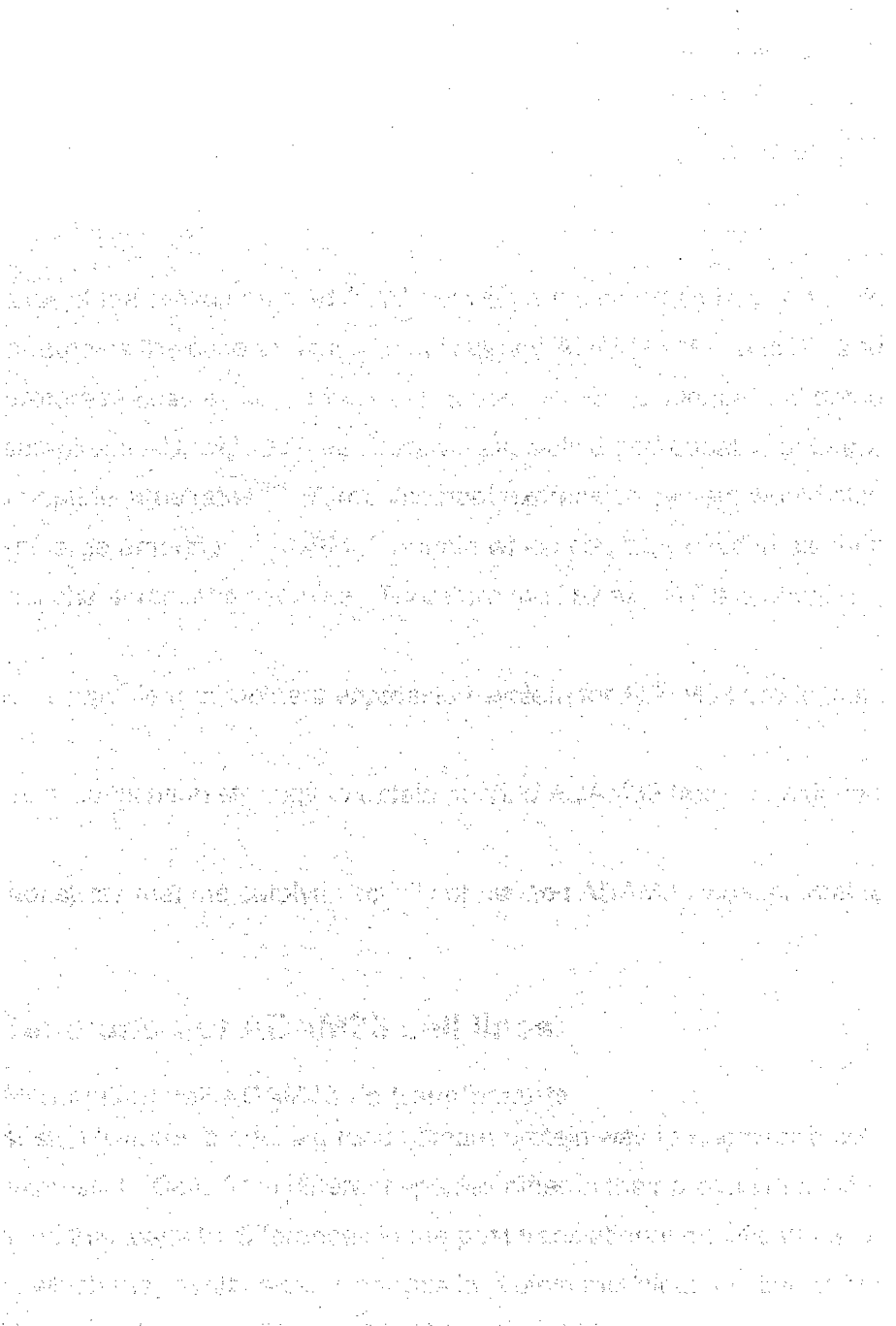

Chapter 3 Recombinant Protein Expression and Purification

The ADAM family of proteins is responsible for shedding growth factors and cytokines from the cell surface. This activity is mediated by their metalloproteinase (MP) domain. Although the biological function of ADAM33 is yet to be established, it is likely that the MP domain will play a fundamental role similar to that seen in its sheddase relatives. This is supported by the evolutionary conservation of the zinc binding motif in ADAM33. The motif is characteristic of catalytically active ADAMs. Furthermore, the selective transport of mRNA transcripts encoding the ADAM33 MP domain from the nucleus to the cytoplasm of human bronchial fibroblasts[228] suggests functional significance.

At the start of the project purified ADAM33 was not a commercially available reagent, and this remains the case to date. To investigate ADAM33 MP function and activity it was therefore necessary to produce it in house. *In vitro* evidence had demonstrated that recombinant ADAM33 MP was catalytically active and capable of degrading several peptide substrates[205]. A recombinant expression system would also be a source of large amounts of ADAM33 protein which could be used in biochemical and functional characterisation studies. Therefore the key aims of this chapter were to

(i) select a suitable recombinant expression system for ADAM33 production.

(ii) derive a purification strategy to obtain purified ADAM33 from conditioned medium.

(iii) demonstrate that the catalytic activity of purified ADAM33 was maintained.

3.1 Generation of ADAM33 cell lines

3.1.1 Mammalian cell ADAM33-Fc transfectants

The first step towards producing recombinant protein was to engineer a cell line that would express it. Cells from different species differ in their protein modification machinery, this leads to differences in the post translational modifications on the proteins which they synthesise. Changes in protein modifications can at times alter or inhibit protein function. Since ADAM33 is thought to be important in mammals, it was appropriate that mammalian cell lines were chosen for recombinant protein expression. Initially, cell lines derived from the African green monkey (COS-7) and

Chinese hamster (CHO) were transfected with a construct containing either the whole extracellular domain (ECD) of ADAM33 or a construct containing the Pro and MP domains. The recombinant ADAM33 constructs were designed to encode fusion proteins, ADAM33-ECD or ADAM33 Pro-MP linked to a C-terminal IgG Fc tag. The IgG Fc tag has previously been used successfully with other recombinant ADAMs[243;244] and allows the protein to be targeted into the secretory pathway. In addition, IgG Fc has a high affinity for Protein A. This property could be exploited for affinity chromatography to simplify the purification of the recombinant protein.

Having transfected COS-7 and CHO cells with ADAM33 constructs as described in materials and methods **section 2.6,** the conditioned media from the cell lines were assayed for the level of recombinant protein secreted over a period of 7 days. The serum free conditioned medium was harvested from 6 well plates, and replenished with fresh medium daily. A sandwich ELISA using Protein A as the capturing reagent and an anti-IgG Fc-HRP as the detection antibody was used to quantify the level of ADAM33-Fc in the medium. Both the COS-7 and CHO cell transfectants secreted ADAM33 Pro-MP-Fc, leading to its accumulation in the surrounding medium. The COS-7 cells showed a higher level of expression of recombinant protein with ADAM33 Pro-MP-Fc levels reaching ~20ng/ml over 7 days, which was approximately five times more than that seen in the CHO cells. The expression levels of the ADAM33 ECD-Fc from transfectants were considerably lower than that of the Pro and MP domain, reaching ~2ng/ml for the COS-7 cells, and being undetectable in the medium from the CHO cells, **Fig. 3.1**.

Since the expression of ADAM33 was found to be higher in the COS-7 transfectants, these were taken for further analysis by SDS PAGE and western blotting to further confirm the presence of ADAM33. ADAM33-Fc proteins in the conditioned medium were concentrated by precipitation using Protein A-agarose beads before analysis. Cell lysates prepared by solubilisation in hot sample buffer were also analysed, **Fig.3.2**. In the western blots probed with anti-ADAM33 Pro domain (RP1) with or without pre-incubation with a ten fold molar excess of blocking peptide as a control, a specific signal can be observed at ~150kDa and ~85kDa for ADAM33 ECD-Fc and ADAM33 Pro-MP-Fc respectively. In a complimentary western blot probed with anti-Fc-HRP, bands of the same molecular weight were detected, confirming the identity of the fusion proteins as unprocessed ADAM33-Fc. In addition, the anti-IgG Fc blots

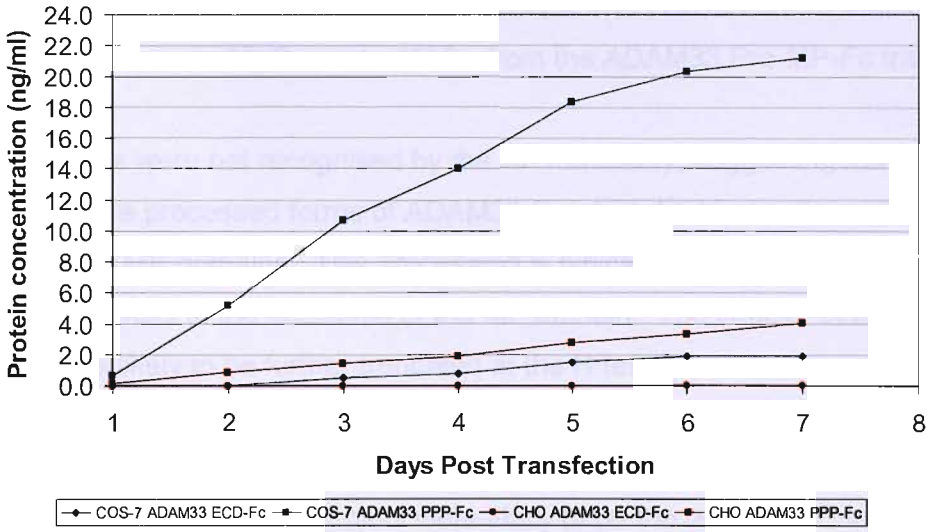

Fig. 3.1. Quantification of ADAM33-Fc secreted by transfected mammalian cell lines. COS-7 and CHO cells were seeded in 6 well dishes, and transfected with either the pcEcto or the pcPPP plasmid which encode ADAM33-Fc proteins. Serum free media was replaced daily and the recombinant protein expression levels were quantified using an anti-human IgG Fc ELISA. The titre of recombinant protein expressed has been plotted as cumulative concentration over time.

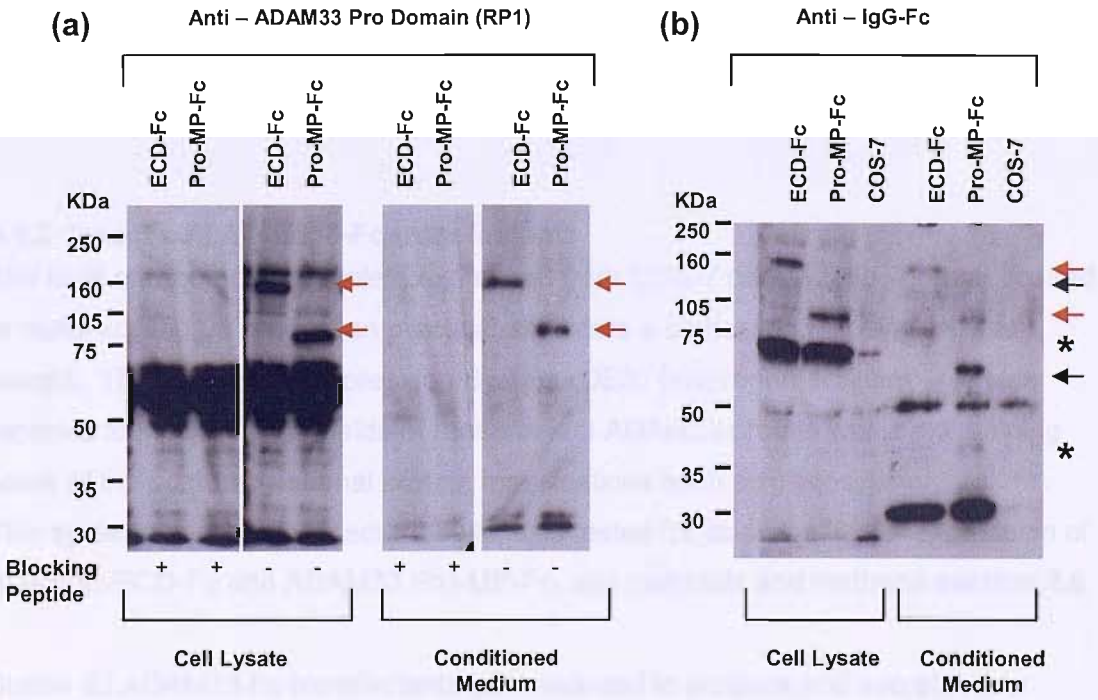

Fig. 3.2. Western blot analysis of COS-7 ADAM33ECD-Fc and ADAM33 Pro-MP-Fc transient transfectants. Transfectants were solubilised in sample buffer, and conditioned medium was concentrated onto Protein A agarose beads before being solubilised in sample buffer. These were analysed by SDS PAGE (7.5%acrylamide gels) before being transferred onto PVDF and further analysed by western blotting. Separate membranes were probed with (a)anti-ADAM33 Pro domain antibody (RP1) with and without pre-incubation with blocking peptide, or (b) anti IgG-Fc. Unprocessed (red) and processed (black) ADAM33-Fc fusion proteins are represented using arrows. * denotes truncated forms of the fusion proteins.

also identified fusion protein bands at ~120kDa and 70kDa from ADAM33 ECD-Fc transfectants, and ~60kDa and ~40kDa from the ADAM33 Pro-MP-Fc transfectants.

These forms were not recognised by the RP1 antibody, suggesting that these smaller species were processed forms of ADAM33-Fc which had been cleaved between the Pro and the MP domains. This processing is typical for MMPs and ADAMs and generally results in the activation of the MP domain. The smaller of the processed forms were likely to be further truncated at the N termini, and were perhaps degradation products. It was also apparent that the recombinant protein concentrated from the culture medium lacked stability, the strong bands at ~30kDa observed in the anti-Fc-HRP blots were likely to be the degraded C termini that resulted from the break down of the ADAM33 ECD-Fc and ADAM33 Pro-MP-Fc proteins.

The molecular weights of the intact and processed ADAM-Fc fusion proteins described above were greater than the predicted mass of the recombinant proteins based on their primary sequence, however this is not unusual for proteins which undergo extensive post translational modifications which can alter their mass or change their mobility through an SDS-PAGE gel.

3.1.2 Insect cell ADAM33-Fc transfectants

The level of recombinant protein expressed from COS-7 cells was lower than desired to make scaling up production practical, therefore a higher yielding system was sought. The *Drosophila* Expression System (DES) (Invitrogen, Paisley, UK) was reported to produce high yields of recombinant ADAM33 protein whilst maintaining some of the post-translational protein modifications such as glycosylation[205;234;245]. This system which uses insect S2 cells, was tested for its suitability for expression of ADAM33-ECD-Fc and ADAM33 Pro-MP-Fc, see materials and methods **section 2.6**.

Stable S2 ADAM33-Fc transfectants were induced to produce and secrete recombinant protein into the culture medium. Cell lysates and conditioned medium samples from these cells were analysed by SDS PAGE, followed by western blotting with an anti-ADAM33 MP domain antibody (RP2), **Fig.3.3**. Fusion protein bands were identified in the cell lysates at ~150kDa and ~85kDa for ADAM33 ECD-Fc and ADAM33 Pro-MP-Fc respectively, these were absent from the GFP transfectant control sample. This resembled the protein banding profile seen in the mammalian cells, and again indicated a considerable level of intracellular protein accumulation.

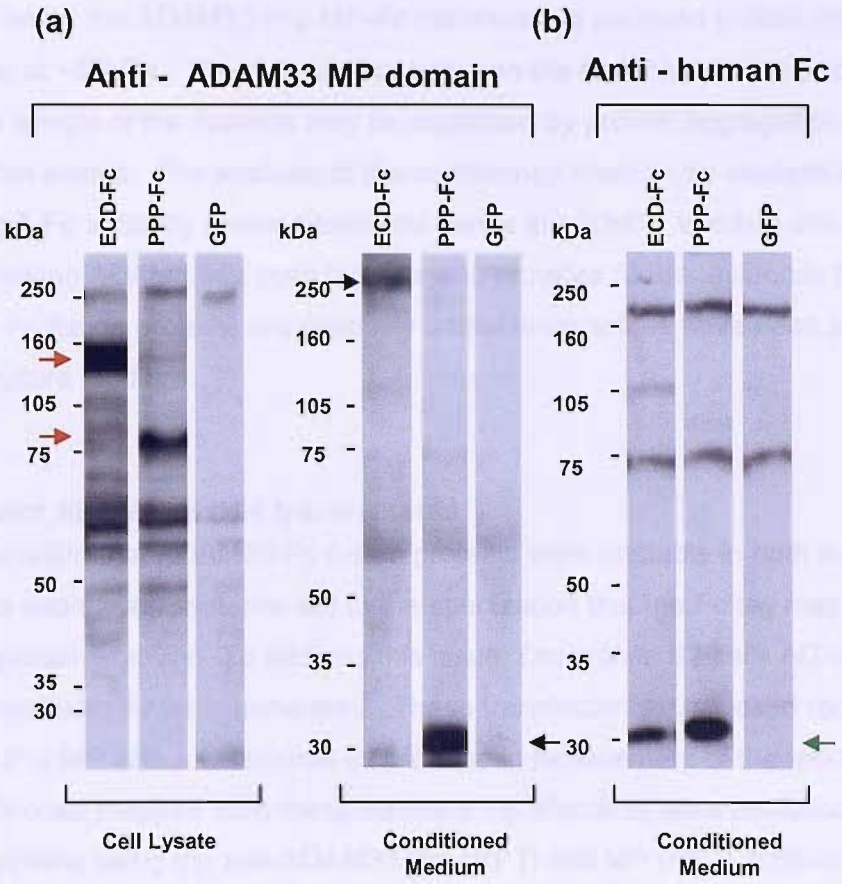

Fig. 3.3. Western blot analysis of S2 ADAM33ECD-Fc and ADAM33 Pro-MP-Fc stable transfectants. Transfectants were seeded at 4.5million cells/well in a 6 well plate. Four days post recombinant protein induction, the conditioned medium was solubilised in sample buffer. Cells were solubilised into 200µl of sample buffer. 20ul of each sample was analysed by SDS PAGE (7.5%acrylamide gels) before being transferred onto PVDF and further analysed by western blotting. Separate membranes were probed with (a) anti-ADAM33 MP domain antibody (RP2) or (b) anti IgG-Fc. Intracellular (red), secreted (black) ADAM33-Fc fusion proteins, and free IgG Fc tag (green) are represented using arrows.

Specific immuno-reactivity was also detectable in the conditioned medium from the transfectants, but not at the expected molecular weight. The ADAM33 ECD-Fc transfectants secreted recombinant protein, the majority of which was detected at >250kDa whilst the ADAM33 Pro-MP-Fc transfectants secreted protein that was detectable at ~30kDa. The discrepancy between the observed and expected molecular weight of the proteins may be explained by protein aggregation or degradation events. The analysis of the conditioned medium by western blotting with the anti-IgG-Fc antibody shows prominent bands at ~30kDa, which is consistent with the mammalian ADAM33-Fc transfectants and provides further evidence that ADAM33-Fc fusion proteins are relatively unstable once they have been secreted into the culture medium.

3.1.3 Insect ADAM33-6xHis transfectants

The observation that ADAM33-Fc fusion proteins were unstable in both mammalian and insect expression systems, led to the speculation that the Fc tag may be affecting protein stability. To address this issue, *Drosophila* S2 cells ADAM33 Pro-MP-His transfectants were generated. These transfectants expressed recombinant ADAM33 Pro-MP with a C-terminal 6x histidine in replacement of the IgG Fc tag. The conditioned medium from these transient transfectants were analysed by western blotting using the anti-ADAM33 Pro (RP1) and MP (RP2) antibodies, **Fig.3.4**. The ADAM33 Pro domain could be detected at ~25kDa in the sample from the ADAM33 transfectants but not in that from the empty vector mock transfectants. An intense signal from secreted ADAM33 Pro-MP-His was detected in the conditioned medium at ~33kDa. This suggested that ADAM33 was being secreted at high levels into the culture medium by the transfectants. Importantly, the Pro and MP domains migrated separately when analysed by SDS-PAGE which showed that the secreted species had been processed, therefore the MP domain may be active. In addition, a high molecular weight species >250kDa was also detected in the conditioned medium from ADAM33 transfectants. This may be aggregated protein and appears as a major band at the top of the blot.

The levels of recombinant protein secreted from the ADAM33 Pro-MP-His transfected cells were sufficient to make scaling up recombinant protein expression feasible. To establish the kinetics of recombinant expression and its accumulation in the culture medium, protein production was induced in the transfected cells and the conditioned medium was sampled daily and analysed by western blotting. The transfectants were typically grown in serum containing medium, but serum free

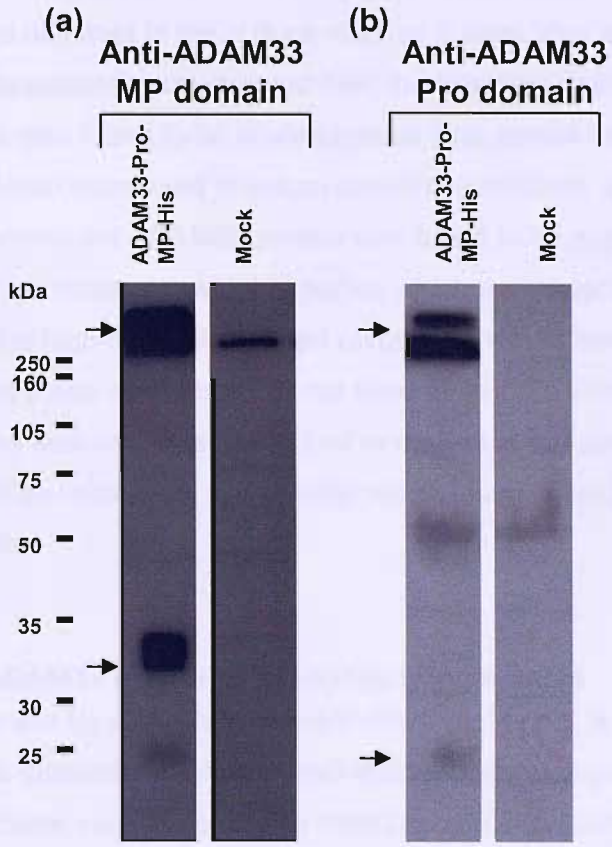

Fig. 3.4 Western blot analysis of S2 ADAM33 Pro-MP-His transient transfectants. S2 cells were transfected with ADAM33 Pro-MP-His or empty vector (mock). The following day recombinant protein expression was induced. Conditioned medium was collected and denatured in sample buffer 4 days post induction. 20µl of each sample was analysed by SDS PAGE (12.5%acrylamide gels) before being transferred onto PVDF and further analysed by western blotting. The membrane was first probed with (a) anti-ADAM33 MP domain antibody (RP2) then subsequently stripped and re-probed using (b) anti-ADAM33 Pro domain antibody (RP1). Specific bands are indicated by the arrows.

medium being less complex was more suitable for downstream protein purification. So in addition to inducing cells in serum containing medium, serum free medium was also tested, **Fig. 3.5**. The time course showed that the ADAM33 Pro and MP domains could be detected in the culture medium 2 days after expression was induced, and subsequently accumulated over the following days. The use of serum free medium was also found to be advantageous over serum containing medium in terms of yield. When expressed in serum containing medium, a considerable proportion of recombinant ADAM33 protein was found to be aggregated or complexed into high molecular weight species which was detected at >250kDa. ADAM33 within the high molecular weight complexes would have been difficult to purify. In contrast these complexes did not form when cells were induced in serum free medium. The time course showed that to maximise the amount of recombinant protein that could be recovered, the conditioned medium should be collected at 5-7 days post induction.

3.1.4 Inactive ADAM33 Pro-MP (E346A)-His transfectants

In addition to the wild type ADAM33 Pro-MP-His transfectant, a proteolytically inactive form was generated. Site directed mutagenesis was used to engineer an adenosine to cytosine substitution in the insect construct encoding the wild type ADAM33 Pro-MP-His, see materials and methods **section 2.5**. This single base change resulted in a coding change in the protein at position 346, replacing the essential glutamic acid residue in the active site for an alanine. The mutated construct was used to transform *E.coli*, and mini-preps were prepared from different clones. These were sent for sequencing at Bath Genomics (University of Bath, UK) and Macrogen, (Korea). **Fig. 3.6.** shows the sequencing data for a successfully mutated clone. The mutated construct was subsequently transfected into S2 cells, and stable S2 ADAM33 Pro-MP(E346A)-His transfectants were established by antibiotic selection.

3.2 Purification of ADAM33 Pro-MP-His and ADAM33 Pro(E346A)-His proteins

The cultures of stable S2 ADAM33 Pro-MP-His and ADAM33 Pro-MP(E346A)-His transfectants were scaled up. Cells were taken from culture, washed with PBS before being transferred into serum free culture medium containing copper sulphate to induce recombinant protein expression. The conditioned medium was harvested 5

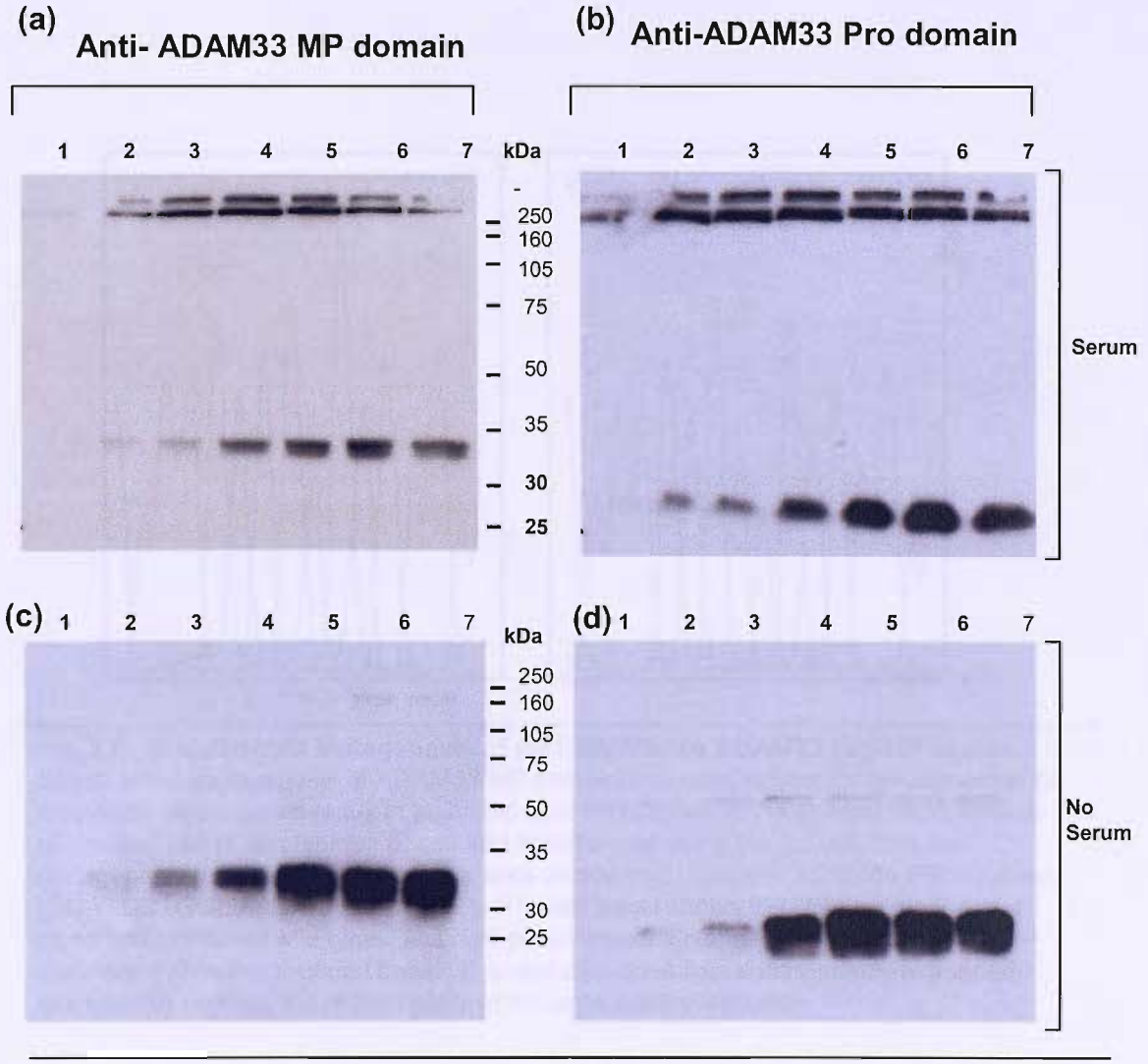

Fig. 3.5. ADAM33 Pro-MP His expression over time. Stable S2 PPP-His transfectants were plated at $4x10^6$ cells/well in a 6 well plate in either serum containing (a) (b) or serum free medium (c) (d). 200µl of cell suspension was sampled daily on days 1-7 (lanes 1-7) after induction of recombinant protein expression. The cells were removed by centrifugation and the medium was solubilised in sample buffer. 20µl of each sample was analysed by SDS PAGE (12.5%acrylamide gels) before being transferred onto PVDF and further analysed by western blotting using RP2 (a) (c). Membranes were subsequently stripped and re-probed using RP1 (b) (d).

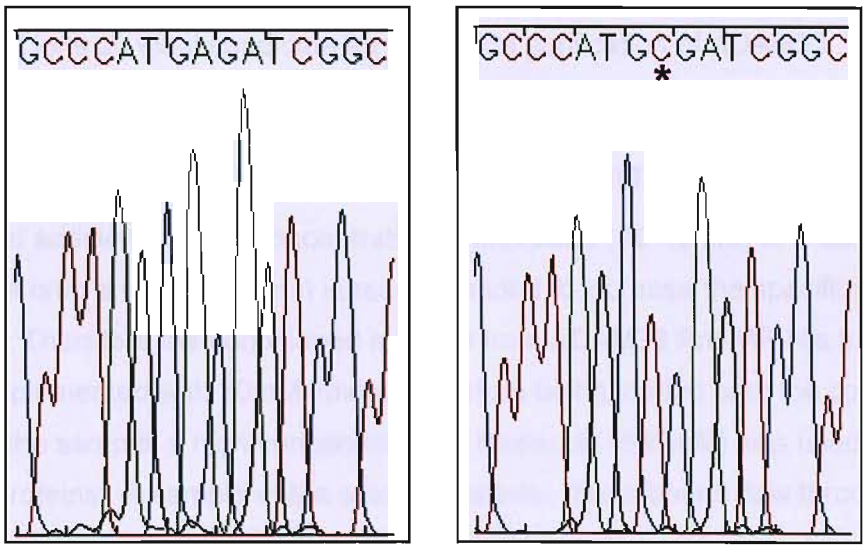

Fig. 3.6. Site directed mutagenesis of pMT/Bip/V5-His ADAM33 Pro-MP vector. Site directed mutagenesis of ADAM33 MP domain was used to change an adenosine to a cytosine which would result in an amino acid substitution of the glutamic acid residue at position 346 to an alanine. *E. coli was* transformed using the ssDNA from the mutagenesis reaction. Several clones were sequenced using the ADAM33 FGHI primer (5'GATCCTGGGAACAAAGCGGG3'). The left panel shows the DNA sequence of a clone that remained wild type. The right panel shows a clone that was successfully mutated. * Denotes mutated base. This mutated clone was subsequently expanded and used to express the mutant plasmid for large scale purification.

days after induction. Since the collected medium was a complex sample containing many insect derived proteins including proteases, it was necessary to devise a purification scheme that would remove these contaminants and enrich for ADAM33. Protein purification strategies are designed around the biochemical properties of the protein of interest. In this case, the recombinant ADAM33 proteins have a 6xHis C-terminal tag which enables them to bind to divalent cations such as Ni^{2+} and Co^{2+} with high affinity. This made an immobilised metal affinity chromatography column loaded with such ions an ideal candidate for use in the purification of ADAM33.

3.2.1 Immobilised metal affinity chromatography (IMAC) using Ni^{2+} ions

Often the addition of a low concentration of imidazole (20-40mM) to a sample prior to loading it onto an IMAC column is recommended to increase the specificity of protein binding. Therefore the conditioned medium from ADAM33 Pro-MP-His transfectants was supplemented with 30mM imidazole before being loaded onto the column. After loading the sample, a high concentration of imidazole (500mM) was used to elute the bound proteins. A sample of the starting material, the unbound flow through from the sample loading step, and the eluted fractions were collected and analysed by western blotting using the RP2 antibody, **Fig.3.7**. In the western blot, ADAM33 is clearly detectable in the starting sample, and in the unbound fraction, but is not detectable in the eluted fractions. This demonstrated that the addition of 30mM imidazole into the starting sample was sufficient to inhibit any ADAM33 protein from binding to the column. To confirm this, a second IMAC run was performed using conditioned medium that had not been supplemented with imidazole. Western blot analysis showed that ADAM33 was no longer found in the flow through sample, but did appear in the eluted fractions.

In a separate run where the imidazole was again omitted from the starting sample, the eluted fractions were analysed by SDS PAGE. The gels were stained with Coomassie brilliant blue, a protein stain. This allowed the proteins in the eluted fraction to be visualised, and the complexity of the sample to be determined, **Fig.3.8**. The stained gel showed that ADAM33 was the most abundant protein species eluted, with the ADAM33 Pro and MP bands appearing at the molecular weights seen previously in western blots, 25kDa and 33kDa respectively. It was also clear that many contaminating proteins of varying molecular weights were present in the eluate, the majority being 40kDa and above. A sample of the eluted fraction was also analysed by casein zymography. Casein is a good metalloproteinase substrate and was used for detecting residual insect proteases in the eluted fraction, **Fig. 3.9**.

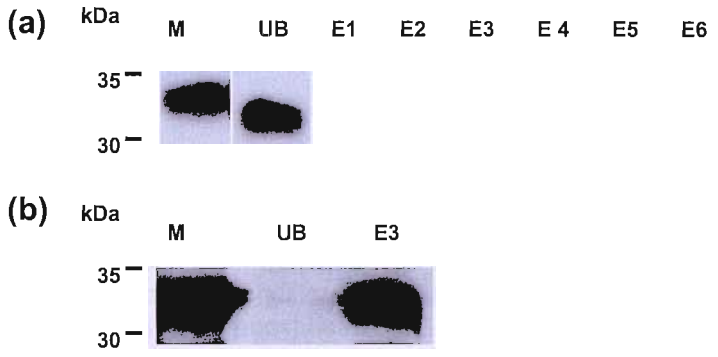

Fig. 3.7. Western blot analysis of samples from IMAC column loaded with conditioned medium from ADAM33 Pro-MP-His transfectants. Conditioned medium was loaded onto a 1ml IMAC column pre-equilibrated with 20mM sodium phosphate and 0.5M NaCl. The column was washed until a steady base line was reached at A280nm using equilibration buffer, and eluted using imidazole. Samples from the media (M), unbound fraction (UB) and eluted fractions (E), were solubilised in sample buffer and separated on by SDS PAGE (12.5% gel). Proteins were transferred to PVDF, and western blotted using the RP-2 antibody. (a) 10ml of conditioned medium was adjusted to 20mM sodium phosphate, 0.5M sodium chloride and 30mM imidazole and loaded onto the column. Elution was carried out in equilibration buffer with progressive 50mM increments of imidazole. (b) 50ml of conditioned medium was adjusted to 20mM sodium phosphate, 0.5M sodium chloride without any imidazole and loaded on to the column. Bound proteins were eluted with binding buffer containing 500mM of imidazole.

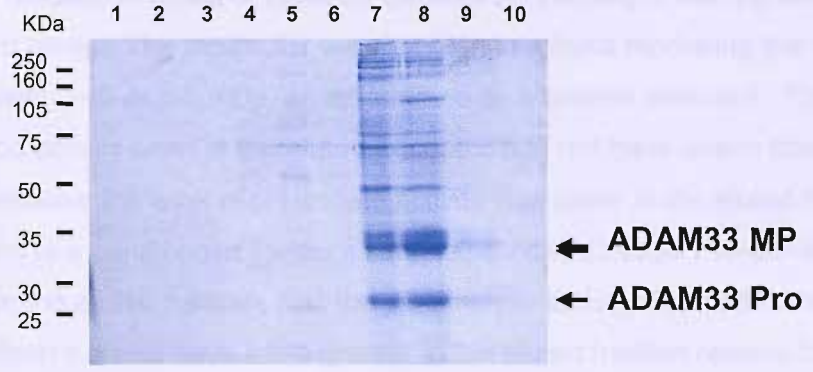

Fig. 3.8. Protein stain of eluted fractions from an IMAC column loaded with conditioned medium from S2 ADAM33 Pro-MP-His transfectants. ADAM33 pro-MP-His was purified from conditioned medium. 200ml of conditioned medium was adjusted to 20mM sodium phosphate, 0.5M sodium chloride without any imidazole, then loaded onto an IMAC column. The column was washed until A280nm base line was reached, and eluted with a step of 500mM imidazole. Samples of eluted 1ml fractions (1-10) were solubilised and separated on a 12.5% SDS-PAGE gel, and subsequently stained with Coomassie brilliant blue. ADAM33 bands are indicated by arrows.

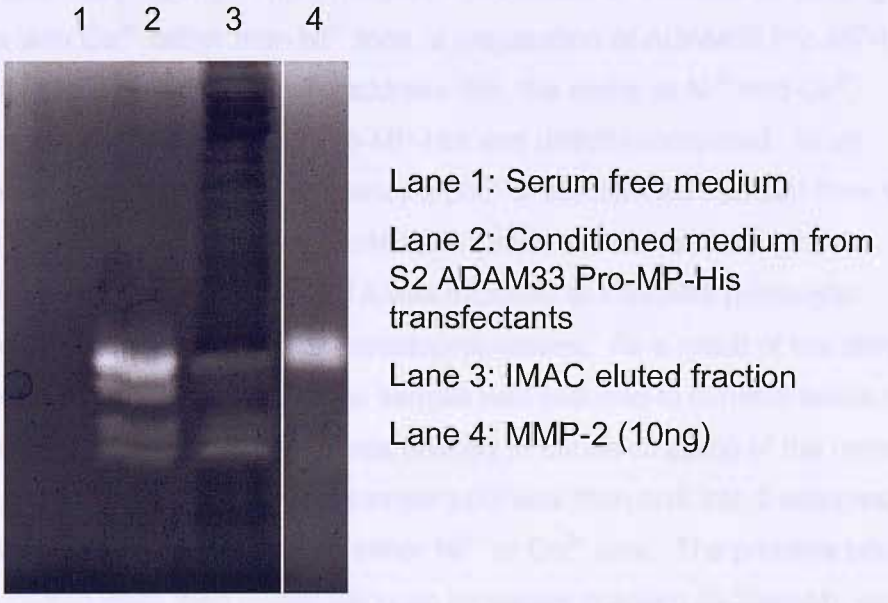

Fig. 3.9. Casein zymogram of partially purified ADAM33 Pro-MP-His. A sample of serum free medium, conditioned medium from ADAM33 Pro-MP-His transfectants, a fraction eluted from the IMAC column loaded with conditioned medium and MMP-2 were solubilised in non denaturing sample buffer, and subjected to SDS-PAGE. After an overnight incubation in assay buffer, the gels were visualised with Coomassie brilliant blue staining, and imaged using the Bio-Rad GS-800 scanner.

The zymogram showed multiple protein species that were able to digest the casein. Digestion resulted in areas of reduced Coomassie staining in comparison with undigested areas. The molecular weights of the proteins mediating the degradation were between ~40 and 70kDa, as determined by a protein standard. The caseinolytic activity seen in the eluted fraction could not have arisen from ADAM33 activity, because the level of proteolytic activity was lower in the eluted fraction in comparison to a conditioned medium sample. Since ADAM33 Pro-MP-His was enriched in the eluted fraction, had the caseinolytic activity been attributed to ADAM33 then it would have been greater in the eluted fraction relative to that seen in the conditioned medium sample.

3.2.2 Immobilised metal affinity chromatography (IMAC) using Co^{2+} ions

It has been reported in the literature that loading an IMAC column with Co^{2+} rather than Ni^{2+} can improve the efficiency of an IMAC column for 6x histidine tagged proteins[246]. This is because Co^{2+} but not Ni^{2+} shows a greater specificity towards capturing tracts of adjacent histidines relative to histidine rich proteins that do not necessarily have this property. This prompted speculation of whether by loading the IMAC column with Co^{2+} rather than Ni^{2+} ions, a preparation of ADAM33 Pro-MP-His of higher purity could be achieved. To address this, the ability of Ni^{2+} and Co^{2+} loaded columns to capture ADAM33 Pro-MP-His was directly compared. In an attempt to improve protein binding efficiency a pool of conditioned medium from the transfectants was supplemented with 1mM EDTA and then dialysed into IMAC binding buffer prior to loading. The EDTA was included to minimise proteolytic degradation of the sample proteins by metalloproteinases. As a result of the dialysis procedure the EDTA concentration in the sample was reduced to minimal levels by the end of the process and therefore it was unlikely to cause stripping of the metal ions present in the IMAC column. The sample pool was then split into 2 samples, and loaded onto columns chelated with either Ni^{2+} or Co^{2+} ions. The proteins bound to the IMAC column were then eluted using an imidazole gradient (5-250mM); when the concentration of imidazole reached 50mM it was held constant to allow the major peak to elute fully, before allowing the gradient to continue. The eluted fractions were analysed by SDS-PAGE, **Fig.3.10**. The gels were stained with EZ Blue, a sensitive colloidal Coomassie blue stain. As expected the ADAM33 Pro and MP domains were seen to elute as the concentration of imidazole was increased, and their molecular weights were found to be 25kDa and 33kDa respectively. From the numerous other protein bands in the eluted fractions, it can be concluded that the Co^{2+} column was not markedly more specific for ADAM33-Pro-MP-His than the Ni^{2+}

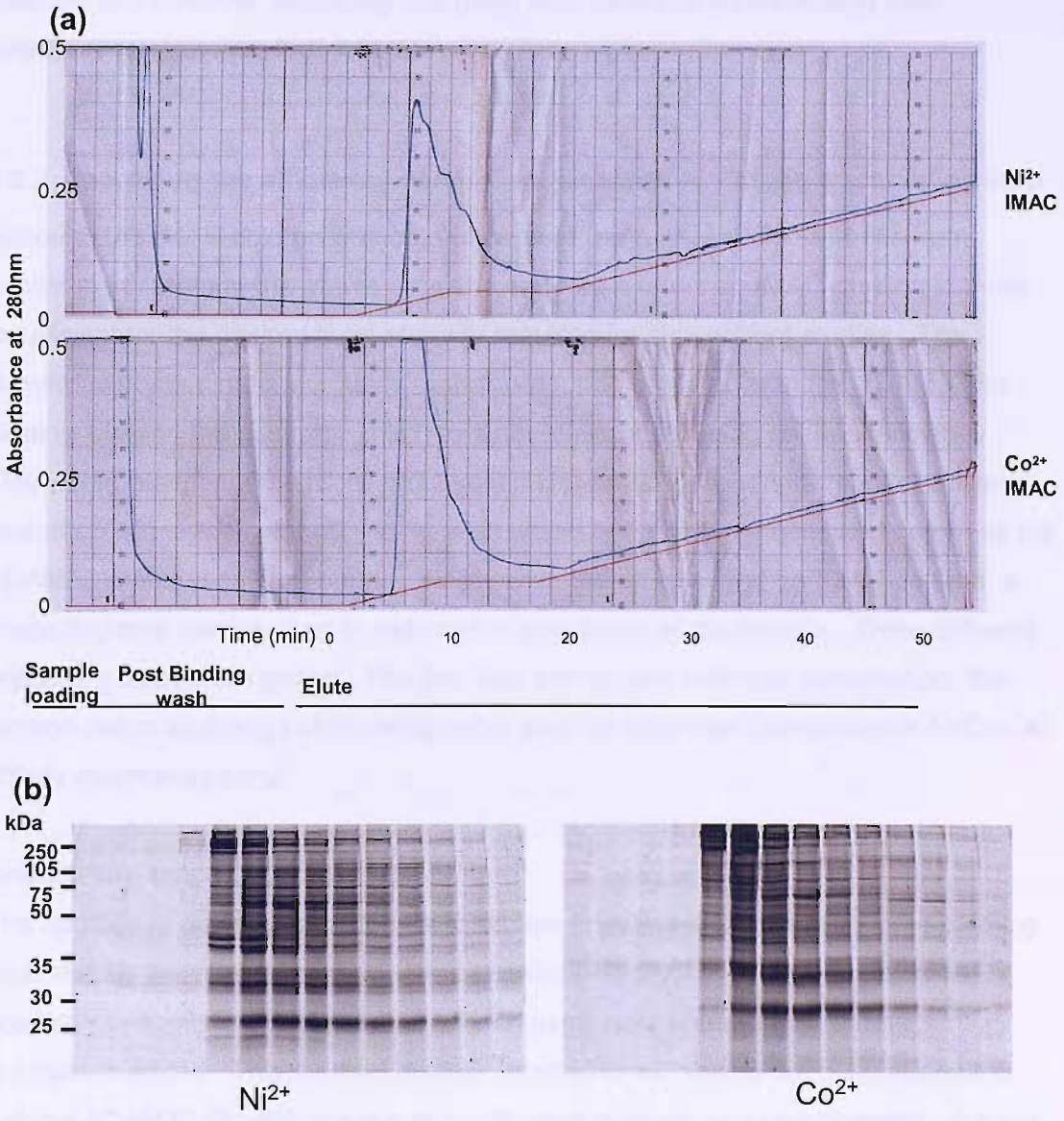

Fig. 3.10. Comparison of the selectivity of IMAC columns loaded with either Ni^{2+} or Co^{2+} ions. Conditioned medium from ADAM33 Pro-MP-His transfectants containing 1mM EDTA was dialysed into 25mM HEPES pH7.9, 0.5M NaCl, 5mM imidazole (binding buffer) overnight at 4°C. This was split in to two equal pools, the first was loaded on to a 1ml Ni^{2+} IMAC column, the second on to a 1ml Co^{2+} IMAC column connected to a FPLC. The columns were washed with binding buffer until the A280nm base line was restored, before being eluted with a gradient of imidazole (5-250mM). The gradient was held at 50mM until the main protein peak had been eluted. The process was monitored using a 280nm UV monitor, and charted as a chromatogram (a). The blue line represents the absorbance at 280nm, with full scale deflection set to 0.5. The red line represents the % of elution buffer going through the column, full scale deflection is 100% (500mM Imidazole in elution buffer). Time 0 represents the start of the elution step. Flow rate 1ml/minute. A sample of the eluted fractions (1-14ml left to right) were solubilised in sample buffer, and separated by SDS PAGE. Proteins were visualised using EZ Blue stain (b).

column, and the eluted fractions remained complex. The relative abundance and pattern of the contaminating bands do however differ between the eluted fractions from the two columns, indicating that there may be some differences in their selectivity for proteins, Fig. 3.10(b).

3.2.3 Improving the efficiency of IMAC loaded with Ni^{2+} using a preceding step

Although the IMAC column was able to capture the ADAM33-Pro-MP-His from conditioned medium, the above data showed that a one step IMAC purification was insufficient for the desired level of purity required for subsequent studies. The numerous contaminating proteins that also bound competed with the ADAM33 for binding sites on the column. This had a net effect of reducing column efficiency. This would have become more problematic and apparent when the purification was scaled up, since the column binding sites would have become occupied before all the ADAM33 protein could be bound. To improve the efficiency of an IMAC column, a preceding step can be used to reduce the complexity of the sample. Three different preceding steps were tested. The first was ammonium sulphate precipitation, the second cation exchange chromatography, and the third was Concanavalin A (Con A) affinity chromatography.

Ammonium sulphate precipitation

The addition of ammonium sulphate to protein mixtures is a crude way of separating proteins into fractions according to their hydrophobicity. In general proteins will gradually precipitate out of solution as increasing concentrations of ammonium sulphate is added. This method is often referred to as "salting out". An attempt to salt out ADAM33 Pro-MP-His out of conditioned medium was unsuccessful. A small protein pellet was recovered at 25% ammonium sulphate saturation, which barely showed the presence of any ADAM33 when slot blotted with the RP2 antibody. No pellets were obtained at 50% and 80% ammonium sulphate saturation, instead the conditioned medium separated into an insoluble lipid phase and an aqueous phase without observable precipitates.

Cation Exchange Chromatography-Resource S

Another way of reducing the complexity of the starting conditioned medium is to use cation exchange chromatography. Cation exchange columns can be used to capture proteins with a net positive charge. These proteins can then be eluted using increasing salt concentrations. In the literature the successful use of cation exchange as a preceding step to IMAC chromatography has been reported[245]. In this

study, when conditioned medium was loaded onto a cation exchange column (Resource S), it was found that ADAM33 could indeed be captured and eluted from the column. SDS-PAGE analysis of the eluted fractions showed the ADAM33 Pro and MP domains migrated as 25kDa and 33kDa species respectively, **Fig.3.11(a)**. In addition to ADAM33, several high molecular weight proteins above 105kDa in molecular weight and a protein that was ~70kDa were also present in the eluted fractions. The ADAM33 containing fractions from the cation exchange column were pooled and subsequently loaded onto an IMAC column and eluted using imidazole. In this case, it was found that using a cation exchange column preceding the IMAC column caused the preferential concentration of the ~70kDa protein over ADAM33 on the IMAC step, **Fig. 3.11(b)**. Therefore the use of cation exchange prior to IMAC was considered to be unsuitable as a preceding step.

Concanavalin A (Con A) affinity chromatography

A complex protein mixture can also be separated using Con A affinity chromatography. Con A is a lectin purified from the Jack bean and has a high affinity for mannosyl and glucosyl chains of polysaccharides. It can be used to select out glycosylated proteins from protein mixtures. Since the ADAM33 MP domain is glycosylated, Con A was used to capture it and remove it from non glycosylated proteins in the medium. Conditioned medium was loaded onto a Con A column, unbound proteins were washed away, and bound proteins were subsequently eluted. The eluted fractions were analysed by SDS-PAGE and proteins were visualised by staining gels with EZ Blue, **Fig.3.12**. The gels showed that Con A successfully captured ADAM33 Pro and MP domains, and these appear as some of the most abundant proteins in the eluted fractions. The ability to recover ADAM33 in the eluted fractions demonstrated that Con A affinity chromatography was an effective preceding step to IMAC in comparison with ammonium sulphate precipitation. If the eluted fractions were shown to be compatible with a subsequent IMAC step then it would also be more effective than cation exchange chromatography as an initial step for purifying ADAM33 Pro-MP-His from conditioned medium.

Con A chromatography -> IMAC

The eluted fractions from the Con A column that contained ADAM33 Pro-MP-His were pooled, and dialysed into IMAC binding buffer containing a very low concentration of imidazole (5mM) which reduced non specific binding. This sample

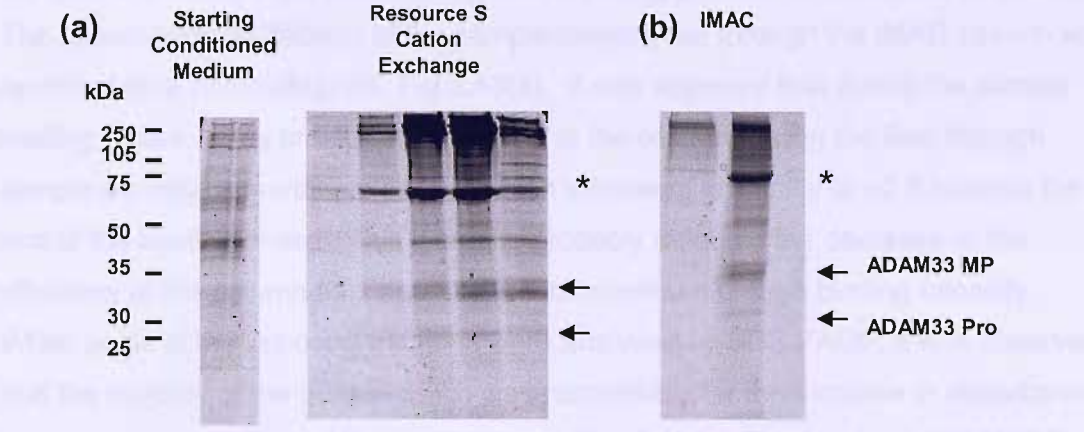

Fig. 3.11. Selection of ADAM33 Pro-MP-His from conditioned medium using cation exchange followed by IMAC. 165ml of conditioned medium from ADAM33 Pro-MP-His transfectants was diluted 1:2 in binding buffer (25mM HEPES pH6.8, 20mM NaCl) and loaded onto a cation-exchange column (Resource S) at a flow rate of 5ml/minute. The column was washed, then bound proteins were eluted with a gradient of NaCl (50-500mM) over 20 minutes at a flow rate1ml/minute. The eluted fractions were analysed by both SDS-PAGE (a), and slot blotted with the RP2 antibody to identify the fractions containing ADAM33. The ADAM33 fractions were pooled and loaded onto an IMAC column and subsequently eluted. The protein fractions eluted from the IMAC column were analysed by SDS-PAGE (b). SDS-PAGE gels were stained with EZ Blue to allow proteins to be visualised. ADAM33 Pro and MP domains are indicated with arrows. A non ADAM33 protein (*) is enriched as a result of the combination of the two chromatographic steps.

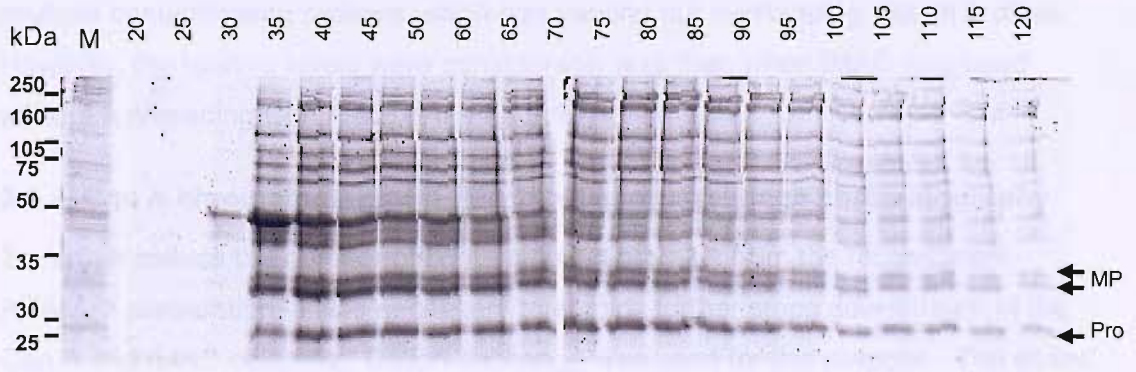

Fig. 3.12. Purification of ADAM33 Pro-MP-His from conditioned medium using Con A affinity chromatography. Conditioned medium (500ml) was loaded onto a pre-equilibrated Con A agarose 4B column, at 4°C with a flow rate of 0.5ml/minute. Unbound proteins were washed away with 10 column volumes of binding buffer and eluted in binding buffer containing 500mM of α-D methyl-mannopyranoside. 1ml fractions were collected. The starting medium (M) and a sample of every 5th fraction (from 20 to 120) were solubilised in sample buffer and 20ul of each was analysed by SDS-PAGE (12.5% gels). Proteins were visualised by staining with EZ Blue. Arrows indicate the ADAM33 Pro and MP domain.

was loaded onto an IMAC column. The unbound proteins were washed away and the bound proteins were eluted using an increasing gradient of imidazole (5-250mM). The absorbance (at 280nm) of the sample passing out through the IMAC column was recorded on a chromatogram, **Fig.3.13(a)**. It was apparent that during the sample loading phase, many proteins did not bind to the column, giving the flow through sample an initial absorbance of ~0.2 which increased gradually to ~0.3 towards the end of the loading phase. This increase probably reflected the decrease in the efficiency of the column as it approached its maximum protein binding capacity. When pools of the unbound fractions were analysed by SDS PAGE, it was observed that the majority of the protein which was responsible for the increase in absorbance from base line were non ADAM33 proteins, **Fig. 3.13(b)**. The levels of ADAM33 Pro and MP domain in the unbound flow through were low compared with the loaded sample in terms of band intensity, suggesting that the majority of ADAM33 in the sample was successfully bound to the column. On the chromatogram, a broad non-symmetrical elution peak was observed as the imidazole concentration was increased. This reflected overlapping peaks of proteins being eluted from the column, and was confirmed by the SDS-PAGE analysis of the eluted fractions. The majority of ADAM33 Pro and MP domains eluted in fractions 6-9, with a low level of protein being eluted before and after this main peak. Recombinant ADAM33 Pro MP-His was the most abundant protein in the eluted fractions, showing significant enrichment in comparison with the initial conditioned medium and Con A column eluate. The fractions containing ADAM33 Pro-MP-His remained fairly complex with multiple contaminating proteins which had varying but overlapping elution profiles. However, the relative levels were considerably less than when IMAC was used without a preceding Con A column, **Fig. 3.10**.

3.2.4 Con A chromatography -> IMAC -> Cation exchange chromatography

To further reduce the number of contaminating proteins from the recombinant ADAM33 preparation, it was necessary to employ further steps downstream of the Con A and IMAC columns. Cation exchange was used for this purpose. The eluted fractions containing ADAM33 Pro-MP-His from the two step Con A and IMAC purification were pooled and dialysed into binding buffer. This was loaded onto a SP Sepharose FF column. Unbound proteins were washed away and bound proteins were eluted off using a gradient of salt (50-500mM NaCl). The procedure was followed by measuring the 280nm absorbance of the sample passing out of the column, and was charted as a chromatogram, **Fig. 3.14(a)**. This showed that the majority of the proteins did not bind to the column, but flowed straight through the

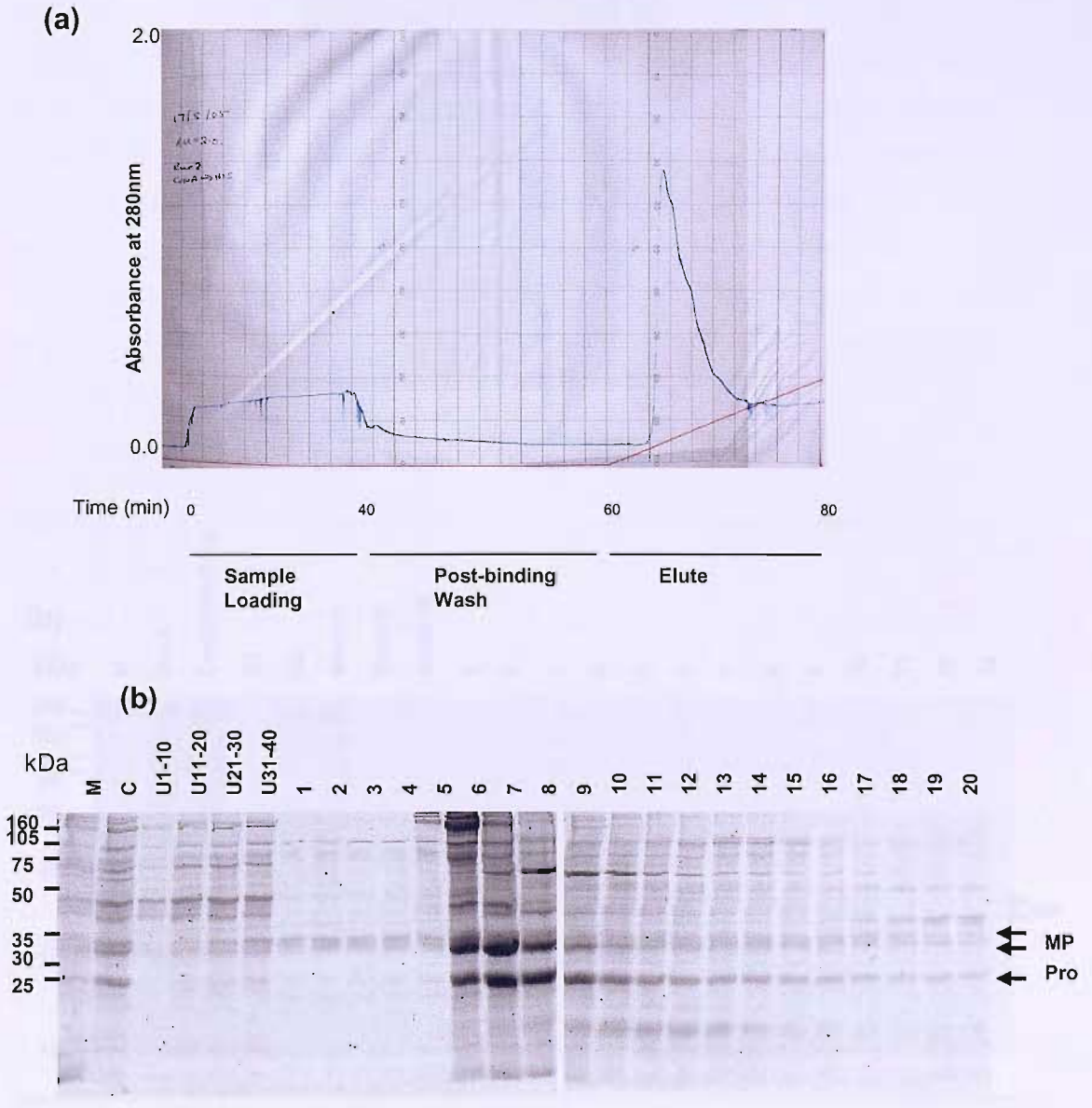

Fig. 3.13. Purification of ADAM33 Pro-MP-His from Con A eluate pool using IMAC. 40ml of dialysed ConA eluate containing ADAM33 Pro-MP-His was loaded on to an IMAC column at 1ml/minute and washed with binding buffer before being eluted using an 5-250mM gradient of imidazole. The chromatogram (a) follows the 280nm absorbance of the sample passing out of the column during the process (blue line). The red line indicates the % of elution buffer going through the column, with full scale deflection set at 100%. The protein complexity of starting conditioned medium (M), dialysed Con A eluate pool (C), pooled IMAC unbound flow through (U) and eluted fractions (1-20ml) were analysed by SDS-PAGE (B) and the proteins were visualised by staining with EZ Blue. Arrows indicate ADAM33 Pro and MP protein bands.

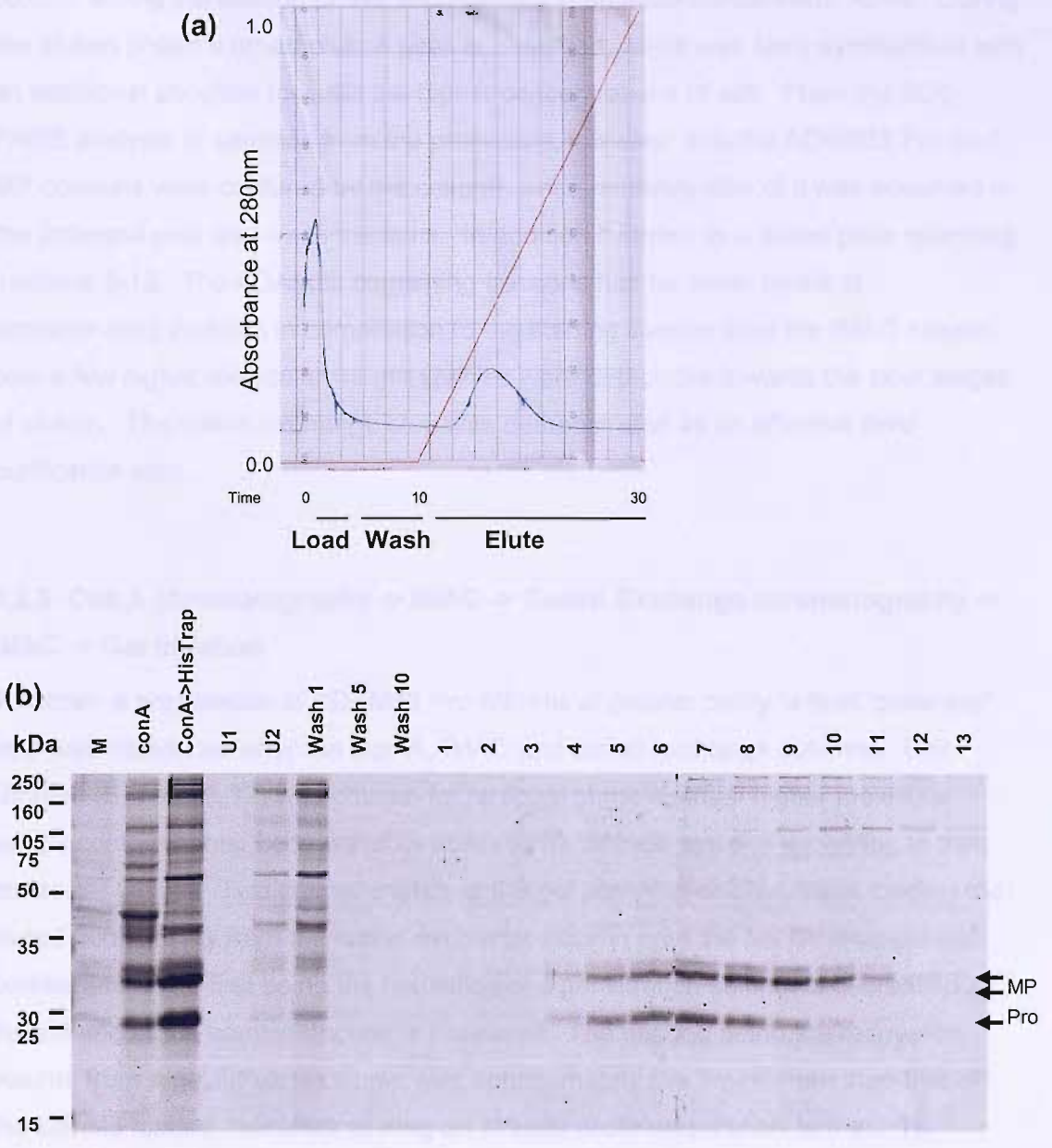

Fig. 3.14. Purification of ADAM33 Pro-MP-His from conditioned medium using Con A affinity chromatography, IMAC and cation exchange chromatography. Conditioned medium was subjected to Con A affinity chromatography followed by IMAC and then cation exchange chromatography. The eluted pool from the IMAC step was loaded onto a SP Sepharose FF cation exchange column at a flow rate of 1ml/minute. The column was washed and the bound proteins were eluted with a gradient of NaCl (50-500mM) over 20 minutes. The absorbance at 280nm of the solution flowing out of the column during this process was recorded on a chromatogram (a). The red line indicates the % of elution buffer going through the column, with full scale deflection set at 100%. The complexity of unpurified conditioned medium (M), dialysed Con A eluate pooled (Con A) , IMAC eluted fractions 5-9 pooled, SP Sepharose FF unbound fractions (U), wash fractions (1,5,10) and eluted fractions (1-20) were analysed by SDS PAGE and visualised by staining with EZ Blue (b). Arrows indicate ADAM33 Pro and MP protein bands.

column during the loading phase and resulted in an absorbance value ~0.45. During the elution phase a broad elution peak is observed, which was fairly symmetrical with an additional shoulder towards the higher concentrations of salt. From the SDS-PAGE analysis of samples from the procedure, it is clear that the ADAM33 Pro and MP domains were captured by the column, since relatively little of it was observed in the unbound pool and wash fractions. In addition it eluted as a broad peak spanning fractions 3-12. The ADAM33 containing fractions had far lower levels of contaminating proteins in comparison to the starting sample from the IMAC column, only a few higher molecular weight species were detectable towards the later stages of elution. The cation exchange step was demonstrated as an effective third purification step.

3.2.5 Con A chromatography -> IMAC -> Cation Exchange chromatography -> IMAC -> Gel filtration

To obtain a preparation of ADAM33 Pro-MP-His of greater purity, a final "polishing" step was introduced after the Con A, IMAC and cation exchange columns. Gel filtration (Superose 12) was chosen for removal of the residual higher molecular weight contaminants, because of its ability to fractionate proteins according to their molecular weight. Two characteristics of the gel polishing column made loading the eluted pool directly from the cation exchange column onto the gel filtration column problematic. The first being the resolution of a gel filtration column is decreased as the volume of the sample applied is increased. The second being the recovered volume from a gel filtration column was approximately five times more than that of the sample loaded, therefore diluting an already dilute preparation further. To counter these issues, the ADAM33 Pro-MP-His fractions containing fractions eluted from the cation exchange step were pooled, and concentrated on the IMAC column. To minimise the volume in which the protein would elute, the protein was eluted using a 500mM step of imidazole, **Fig. 3.15(a)** allowing the majority of the protein to elute in a sharp peak over 2-3ml. The concentration effect of this step could be seen by SDS-PAGE analysis, where barely visible contaminating proteins in the starting sample were now detectable after concentration. A sample of this concentrated preparation was subsequently loaded onto the Superose 12 column. Two peaks were seen eluting from the Superose 12 column, the first at 9ml corresponding to the pre-established void volume of the column, the second containing ADAM33 Pro-MP-His eluted as a symmetrical peak between 14-16ml after loading, **Fig.3.15(b)**.

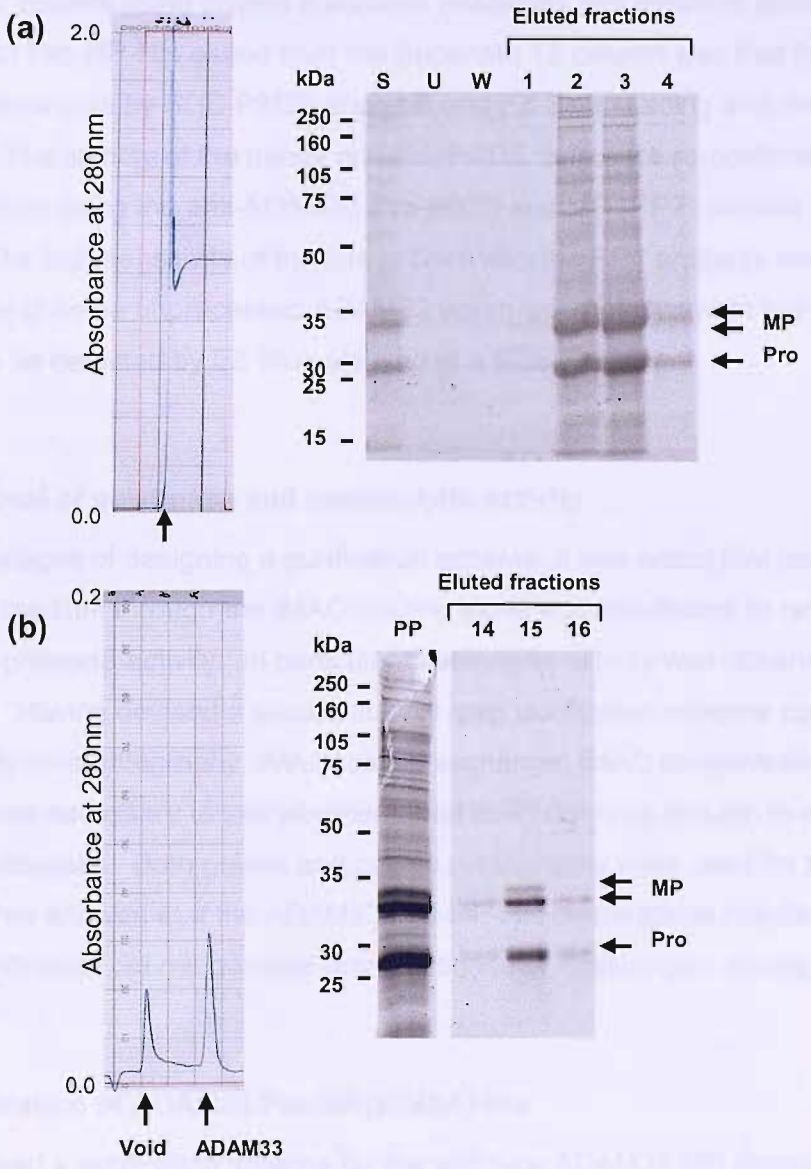

Fig. 3.15. Purification of ADAM33 Pro-MP-His from conditioned medium using Con A affinity chromatography, IMAC, Cation exchange, IMAC concentration and gel filtration. Conditioned medium was subjected to Con A affinity chromatography, then IMAC, followed by cation exchange chromatography. To concentrate this pool the eluted fractions containing ADAM33 Pro-MP-His were pooled and loaded back onto an IMAC column at a flow rate of 1ml/minute. The protein was eluted using 500mM imidazole. (a) The absorbance at 280nm was recorded for the sample flowing out of the column, and charted as a chromatogram, the arrow highlight the elution peak. A sample of each fraction from the column was analysed by SDS-PAGE (12.5% gels). Proteins were visualised by staining gels with EZ Blue. S represents the starting sample, U the unbound pool, W the wash fractions. A sample of the concentrated protein preparation was subsequently loaded onto a Superose 12 column, and eluted at a flow rate of 0.5ml/minute. (b) The absorbance of the column flow through was again charted. Two peaks were seen in the elution phase, one at 9ml and one at 15ml, indicated by the arrows. The 9ml peak corresponded the void volume of the column, and the 15ml peak represented ADAM33 fractions, these were analysed by SDS PAGE (12.5% gels) and EZ blue staining. PP was a sample of the IMAC concentrated partially purified protein that was loaded onto the Superose 12 column. Eluted fractions (14-16) are also shown.

This was in line with the expectations predicted from a calibration run of the Superose 12 column using protein standards (materials and methods section 2.15). The ADAM33 Pro-MP-His eluted from the Superose 12 column was free from visible protein contaminants by SDS-PAGE analysis and EZ Blue staining and deemed of a high purity. The identity of the bands on SDS-PAGE gels were re-confirmed by western blotting using the anti-ADAM33 Pro (RP1) and MP (RP2) domain antibodies, Fig. 3.16. The high sensitivity of the blot probed with the RP1 antibody also revealed the presence of some unprocessed ADAM33 which was not always in high enough quantities to be detected by EZ Blue staining of a SDS-PAGE gel.

3.2.6 Removal of gelatinase and caseinolytic activity

In the early stages of designing a purification scheme, it was noted that passing conditioned medium through the IMAC column alone was insufficient to remove all the residual protease activity. In particular caseinolytic activity was observed in the preparation. Having devised a successful five step purification scheme consisting of Con A affinity chromatography, IMAC, cation exchange, IMAC concentration and gel filtration, it was necessary to test whether it had been rigorous enough to remove the unwanted proteases. Both gelatin and casein zymography were used for this purpose. They showed that the ADAM33 Pro-MP-His preparations resulting from the five step purification did not possess any gelatinase or caseinolytic activity, **Fig.3.17**.

3.2.7 Purification of ADAM33 Pro-MP(E346A)-His

Having devised a purification scheme for the wild type ADAM33 MP domain, the same strategy was used to purify the mutant from conditioned medium. The scheme was shown to work equally well with the mutant protein. Samples from the eluted fractions of each purification step were analysed by SDS-PAGE, **Fig. 3.18**. The mutant migrated to at apparent molecular weight of ~33kDa. Like the wild type, this was larger than expected as predicted by its amino acid sequence alone.

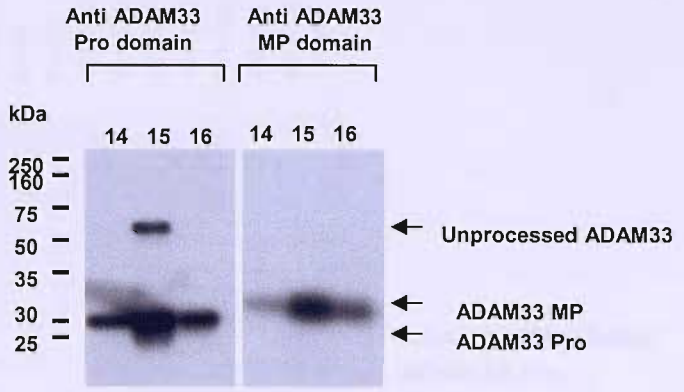

Fig. 3.16. Western blot analysis of purified ADAM33 Pro-MP-His from conditioned medium. Conditioned medium containing ADAM33 Pro-MP-His was purified using a five step process. This involved Con A affinity chromatography, followed by IMAC, then cation exchange chromatography, then concentration of the sample over an IMAC column and lastly gel filtration. The final preparation was analysed by SDS-PAGE, the proteins were transferred to PVDF and subsequently blotted with the anti-ADAM33 Pro and MP antibodies (RP1 and RP2) to confirm the identity of the bands observed by SDS PAGE and protein staining alone.

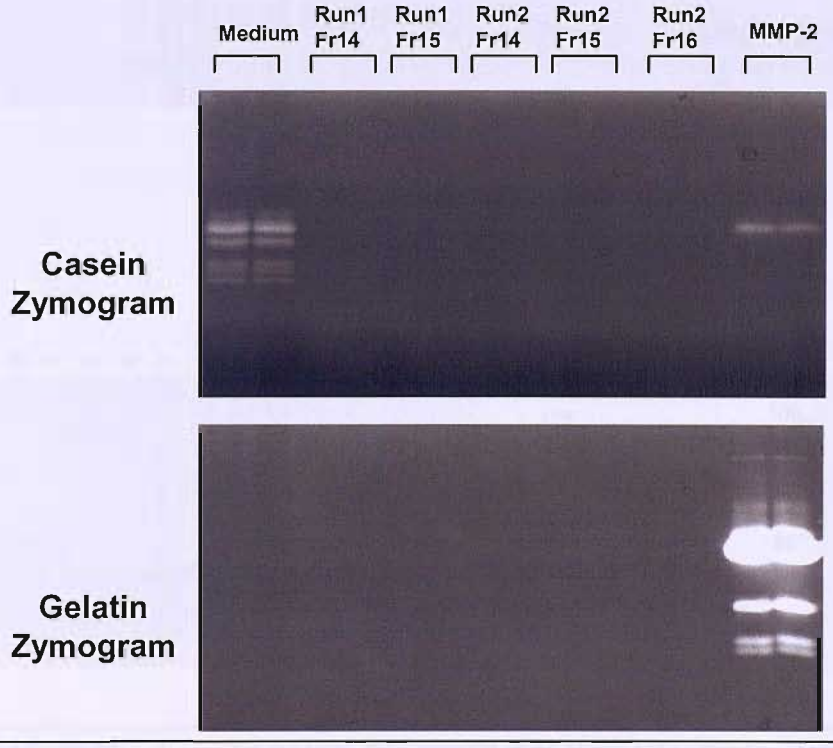

Fig. 3.17. Zymography analysis of purified ADAM33 Pro-MP-His. ADAM33 Pro-His was purified from conditioned medium using the five step process. Purified ADAM33 Pro-MP-His protein fractions (14-16) eluted from the Superose 12 column from two consecutive runs were solubilised in non reducing sample buffer, and separated on 10% SDS PAGE gels containing either casein or gelatin. 5ng of MMP-2 was used as a positive control, and the original conditioned medium from which ADAM33 was purified was also tested. All samples were loaded in duplicate. Gels were washed in 2.5% Triton x-100 solution and distilled water then incubated in assay buffer (50mM Tris-HCl pH7.5, 5mM $CaCl_2$, 1µM $ZnCl_2$, and 0.02% NaN_3) overnight at 37°C. Gels were stained with Coomassie brilliant blue then de-stained. They were then scanned using Bio-Rad GS800 gel scanner. Clear bands indicated the presence of caseinolytic or gelatinase activity.

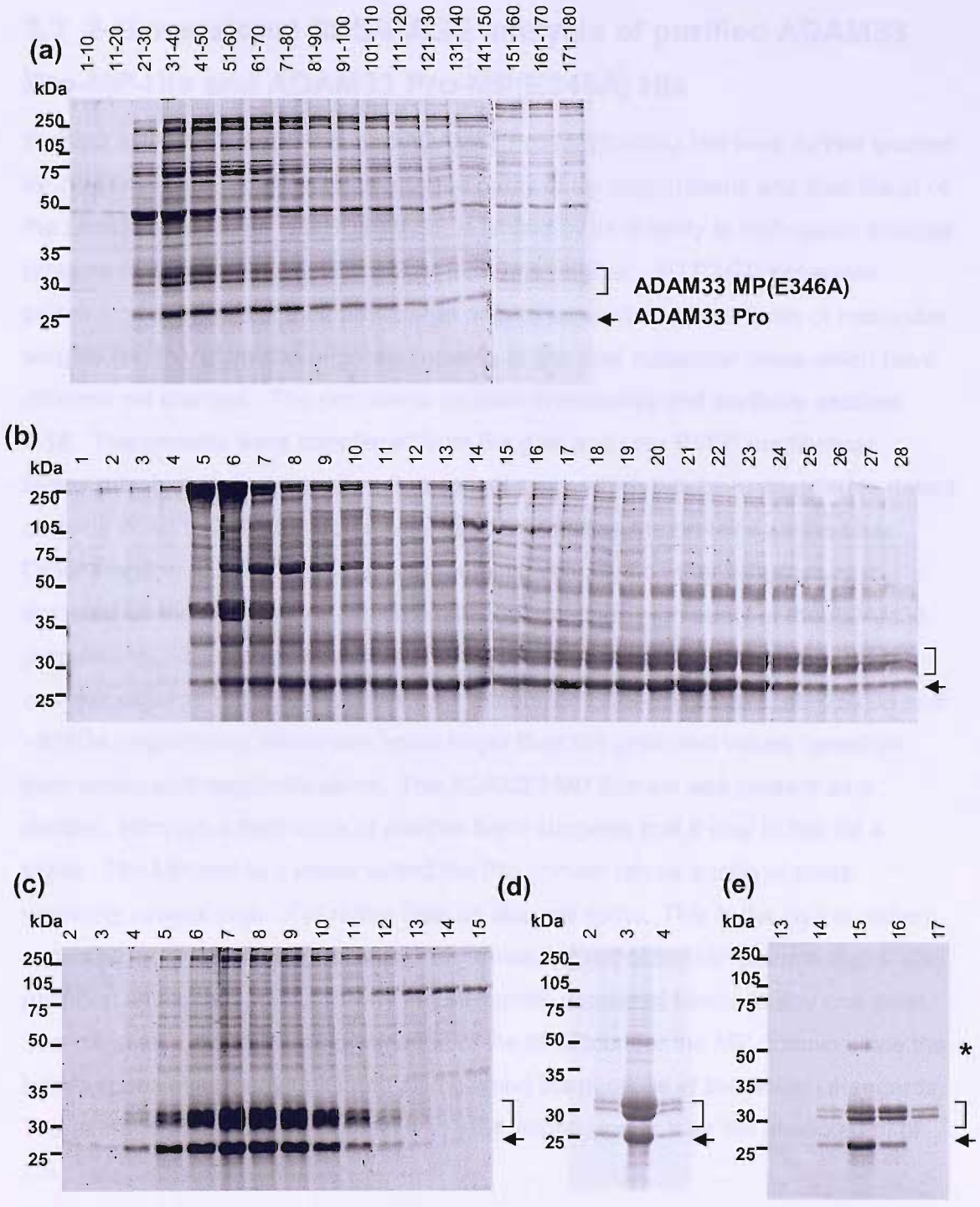

Fig. 3.18. Purification of ADAM33 Pro-MP(E346A)-His. ADAM33 Pro-MP(E346A)-His was purified using the same five step purification scheme that was devised for the wild type protein. Fractions eluted from each column were analysed by SDS-PAGE (12.5% gels) and the protein was visualised by staining with EZ Blue. (a) Con A affinity chromatography, (b) IMAC, (c) Cation exchange chromatography, (d) IMAC concentration, and (e) gel filtration. Lane numbers reflect eluted fraction number. Brackets and arrows indicate ADAM33 MP(E346A) and Pro domain bands respectively. (*) indicates unprocessed ADAM33 Pro-MP(E346A)-His.

3.3 2-Dimensional SDS-PAGE analysis of purified ADAM33 Pro-MP-His and ADAM33 Pro-MP(E346A) His

Purified ADAM33 Pro-MP-His and ADAM33 Pro-MP(E346A)-His were further profiled by 2D SDS PAGE analysis to assess the purity of the preparations and also the pI of the proteins, **Fig. 3.19**. 1D SDS PAGE is limited by its inability to distinguish multiple proteins of the same molecular weight from one another. 2D PAGE separates proteins on the basis of their net charge prior to separation on the basis of molecular weight, and therefore can separate proteins of identical molecular mass which have different net charges. The protocol is detailed in materials and methods **section 2.18**. The proteins were transferred from the gels and onto PVDF membranes. SyproRuby blot stain, a sensitive fluorescent stain, which has been reported to detect proteins down to 2-8ng of protein was used to visualise the proteins on the blots. Other than the ADAM33 Pro and MP domains, virtually no other proteins were detected on the membranes, which again confirmed the high purity of the ADAM33 preparation. The molecular weight of the ADAM33 Pro and MP domains corresponded as expected to previous 1 dimension SDS-PAGE gels, at ~25kDa and ~33kDa respectively, which was again larger than the predicted values based on their amino acid sequence alone. The ADAM33 MP domain was present as a doublet, although a faint trace of another band suggests that it may in fact be a triplet. The MP and to a lesser extent the Pro domain ran as a train of spots spanning several units of pI rather than as discreet spots. This is the typical pattern expected for glycosylated proteins. This spreading out of the MP domain signal also provided an explanation as to why the MP bands appeared fainter at any one point. The effect also made the determination of the pI difficult for the MP domain since the bands spans over many units and also beyond the pI range of the protein standards. The average pI for the Pro domain was ~6.4, slightly lower than the predicted pI of 7.9.

3.4 Glycosylation status of ADAM33 Pro-MP-His and ADAM33 Pro-MP(E346A)-His

The SDS-PAGE analyses of the wild type and mutant ADAM33 Pro and MP domain showed that both domains migrated more slowly than expected by predictions based on their amino acid sequence alone. In addition, the MP domain migrated as several bands, whilst the Pro domain migrated as one thick band, which suggested that it too migrated as multiple bands which were not fully resolved. Surface Enhanced Laser

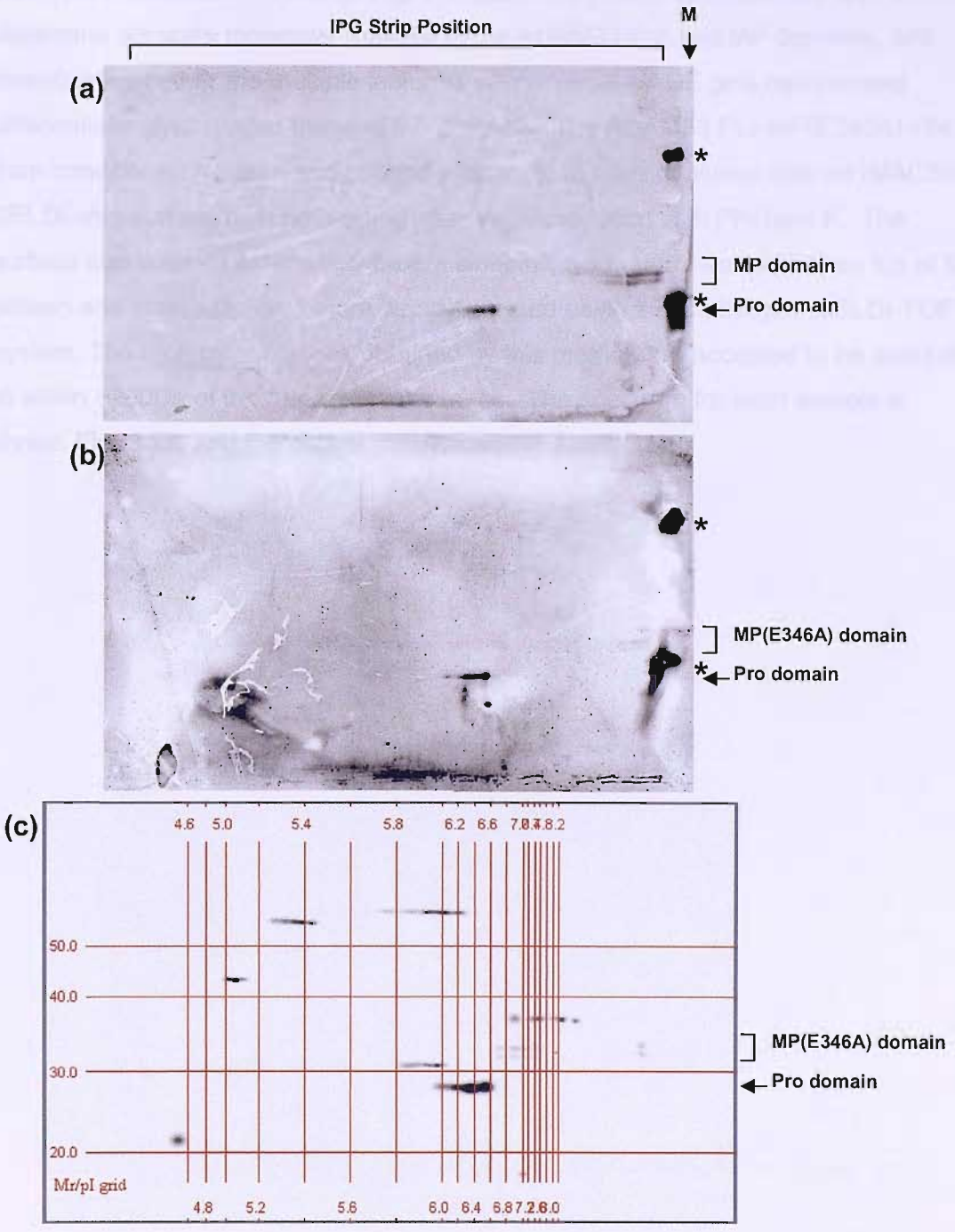

Fig. 3.19. 2D SDS PAGE analysis of purified ADAM33 Pro-MP-His and ADAM33 Pro-MP(E346A)-His. ADAM33 Pro-MP-His and ADAM33 Pro-MP(E346A)-his were purified using the established five step scheme. Proteins were acetone precipitated and resuspended in rehydration buffer. 2µg of (a) ADAM33 Pro-MP-His, (b) ADAM33 Pro-MP(E346A)-His, or (c) ADAM33 Pro-MP(E346A)-His together with 2D PAGE protein standards were loaded onto 3-10NL IPG strips. The proteins were separated by iso-electro-focusing, followed by SDS-PAGE on 12.5% gels. The gels were stained with SyproRuby gel stain (c) or the proteins were subsequently transferred onto PVDF membranes (a)(b). The membranes were stained with Sypro Ruby blot stain, and imaged using the Bio-Rad Versadoc. The position at which the first dimension IPG strip was placed onto the separation gel is shown by the top bracket, (M) highlights the lane on which 1D protein standards were loaded, the 75kDa, and 25kDa standards (*) can clearly be seen. (c) The molecular weight and pI of the 2D PAGE standards were used to construct a molecular weight/pI grid which was used to estimate these properties for the recombinant ADAM33 proteins. This was carried out using PD Quest software (Bio-Rad).

Desorption Ionisation – Time Of Flight (SELDI-TOF) mass spectroscopy was used to determine accurate molecular masses of the ADAM33 Pro and MP domains, and investigate whether the multiple isoforms seen in SDS-PAGE gels represented differentially glycosylated forms of the proteins. The ADAM33 Pro-MP(E346A)-His from conditioned medium and purified preparations were captured onto an IMAC30 SELDI chip surface both before and after deglycosylation with PNGase F. The surface was washed extensively before sinapinic acid matrix was added on top of the protein and allowed to dry before being analysed using the Ciphergen (SELDI-TOF) system. The molecular masses obtained by this method are accepted to be accurate to within ~200Da of the true molecular mass. The spectrum for each sample is shown **Fig. 3.20**, and the data is summarised in **Table 3.1**.

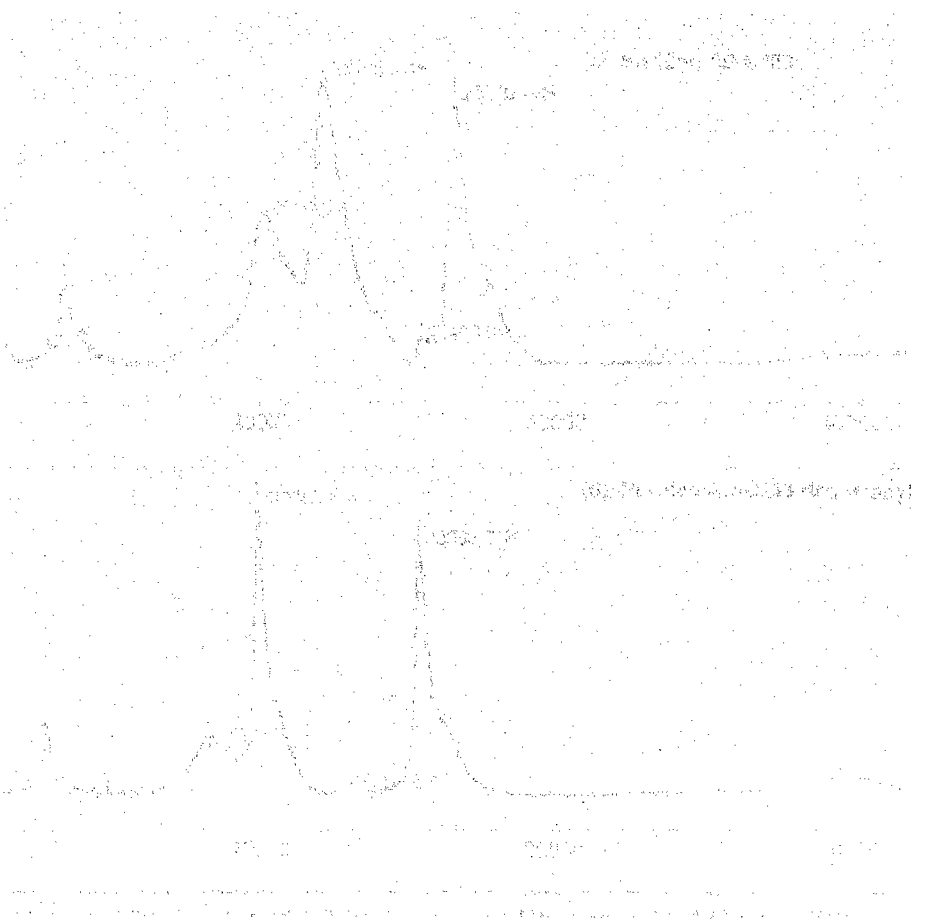

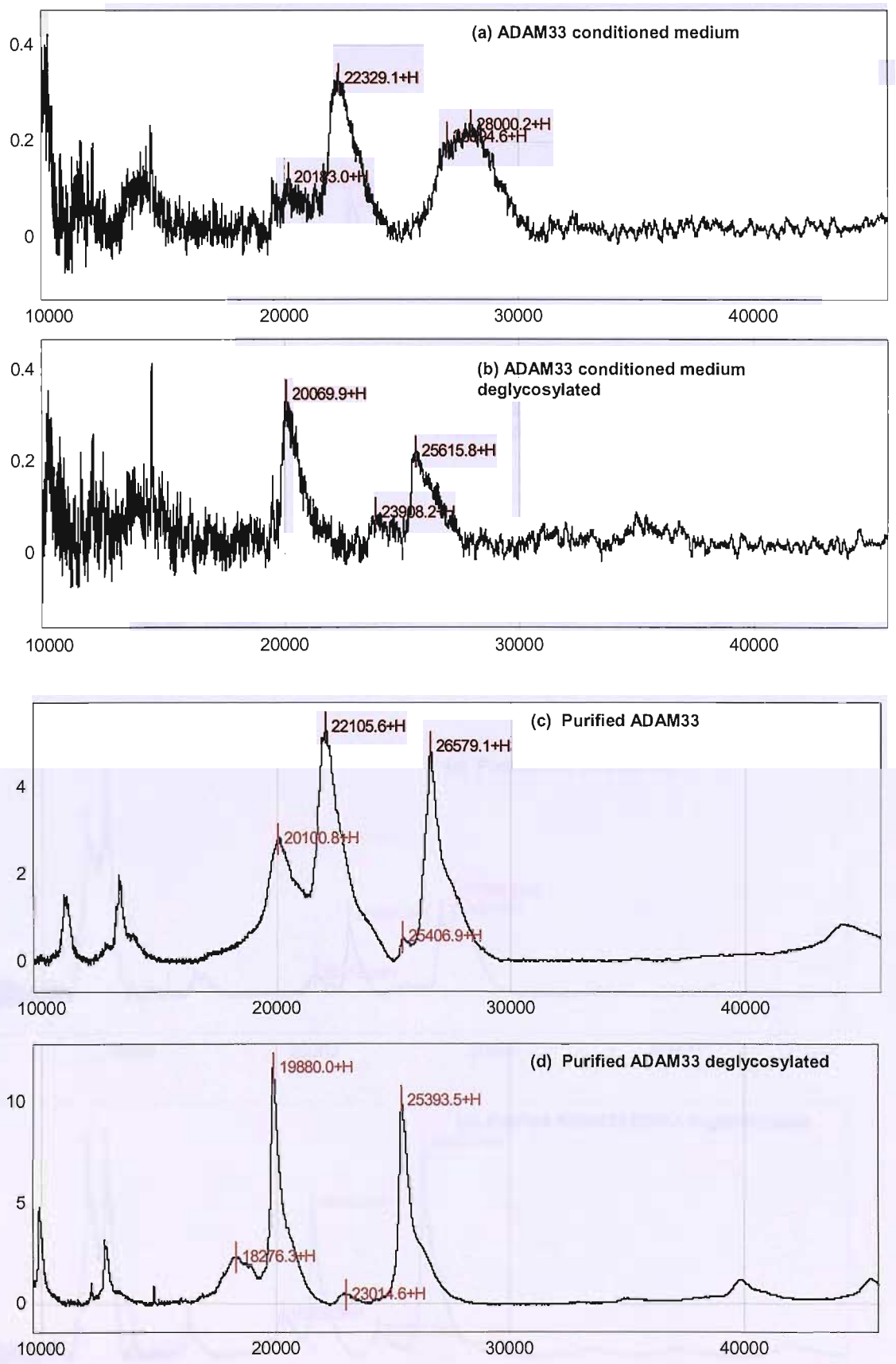

Fig.3.20. SELDI spectra of ADAM33 Pro-MP-His and ADAM33 Pro-MP(E346A)-His. Molecular mass of ADAM33 wild type (a-d) and mutant proteins (e-h) from conditioned medium and purified preparations before and after deglycosylation. Y axis displays intensity, x axis displays charge to mass ratio. Fig. 3.20 continues onto the next page.

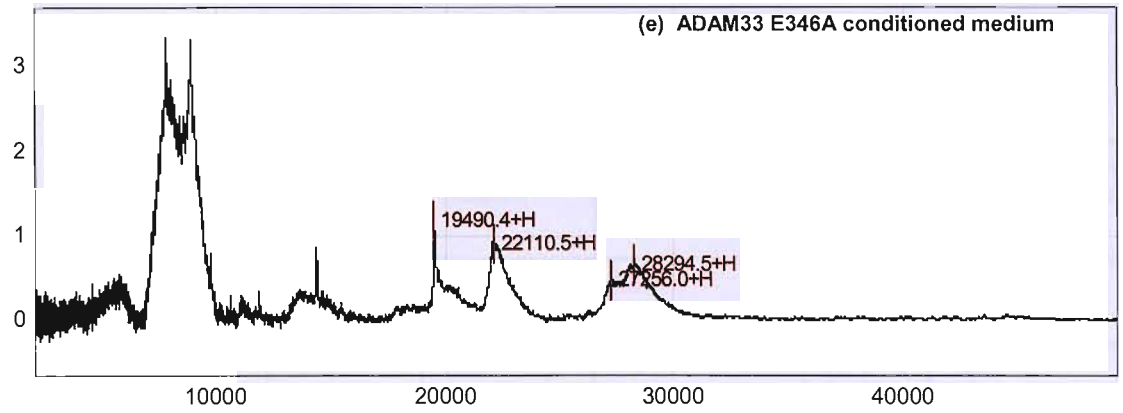
(e) ADAM33 E346A conditioned medium
3
2
1
0
19490.4+H
22110.5+H
28294.5+H
27856.0+H
10000
20000
30000
40000

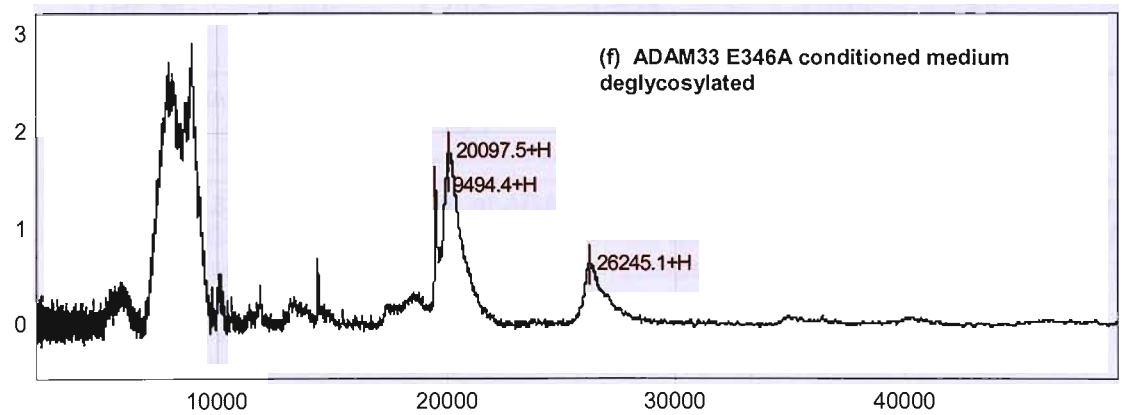
(f) ADAM33 E346A conditioned medium deglycosylated
3
2
1
0
20097.5+H
19494.4+H
26245.1+H
10000
20000
30000
40000

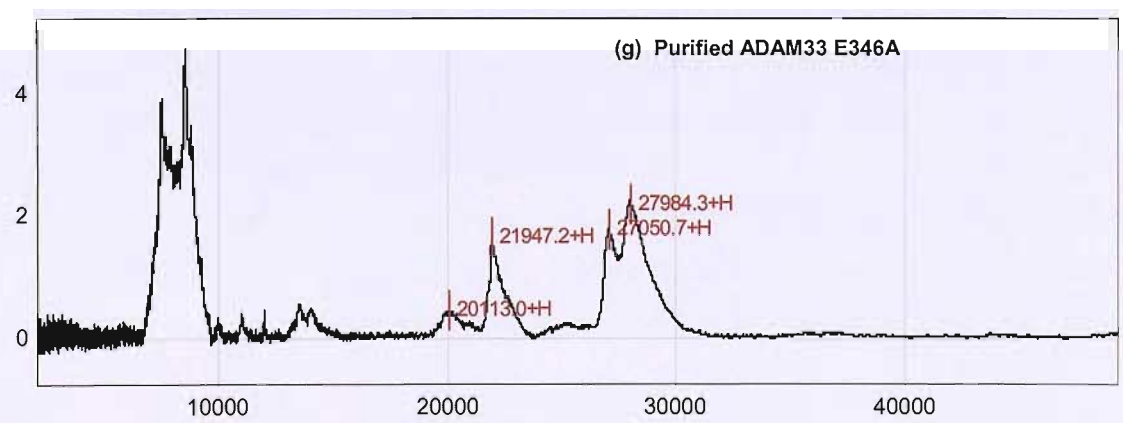
(g) Purified ADAM33 E346A
4
2
0
27984.3+H
27050.7+H
21947.2+H
20113.0+H
10000
20000
30000
40000

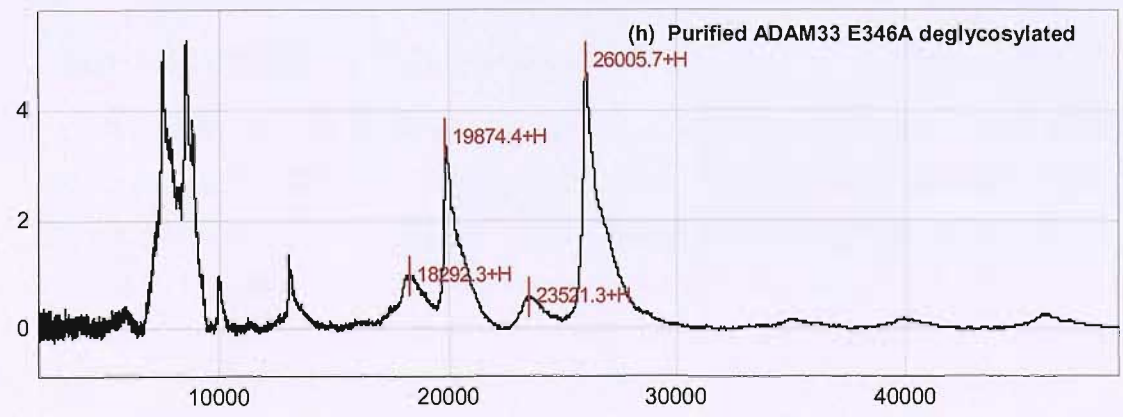
(h) Purified ADAM33 E346A deglycosylated
4
2
0
26005.7+H
19874.4+H
18292.3+H
23521.3+H
10000
20000
30000
40000

	Predicted Mass	Conditioned Medium	Conditioned Medium, Deglycosylated	Purified Protein	Purified Protein Deglycosylated
Pro wt	20.1	20.2 22.3	20.1	20.1 22.1	18.3 19.9
Pro E346A	20.1	19.5 22.1	19.5 20.1	20.1 21.9	18.3 19.9
MP wt	26.0	26.9 28.0	23.9 25.6	25.4 26.6	23.0 25.4
MP E346A	26.0	27.3 28.3	26.2	27.1 28.0	23.5 26.0

Table 3.1. Molecular Mass of ADAM33 species. Conditioned medium and purified ADAM33 Pro-MP-His and the E346A mutant were treated with or without PNGase F. Samples were acetone precipitated and resuspended in lysis buffer (9M Urea 2% CHAPS). These samples were loaded onto Ciphergen IMAC30 chips, washed, mixed with sinapinic acid matrix and read using a laser intensity of 210 units to determine accurate masses for the ADAM33 species. This table summarises the information from the spectra obtained in Fig. 3.20 (a-h), and compares it to the expected molecular masses of the Pro and MP domain as predicted from their amino acid sequences in kDa.

In the conditioned medium samples, two main peaks were observed for the Pro domain from both the wild type and mutant. The peak representing the higher molecular weight species was ~22kDa which was 2kDa larger than expected. Deglycosylating the conditioned medium shifted the maximum of this peak to 20kDa which corresponds with the predicted molecular weight. The purified Pro domain found in the purified protein preparations also showed two peaks, one at 20kDa and a second at 22kDa, the same as those seen in the medium. When these were deglycosylated the observed peaks were reduced to 18kDa and 20kDa. The 20kDa form probably represented the intact Pro domain and was the more prominent peak out of the two; the 18kDa form may have represented a truncated form, derived perhaps from degradation of the sample during the harsh deglycosylation conditions.

The ADAM33 wild type and mutant MP domain found in conditioned medium were expressed predominantly in forms which were greater than their predicted molecular weight by approximately 1-2 kDa. After deglycosylation the mutant MP domain was reduced to a peak of 26kDa, which corresponded to its predicted molecular weight. The molecular weight of the purified mutant MP domain before and after deglycosylation was similar to that seen in the conditioned medium, with an addition species of 23.5kDa. When the wild type MP domain was deglycosylated it was reduced into two species which were slightly smaller than expected, with molecular weights of 23.9kDa and 25.6kDa. The molecular weight of the purified wild type MP domain before deglycosylation was however lower than that found in the conditioned medium at 25.4 and 26.6kDa. After deglycosylation, these were reduced to 23kDa and 25.4kDa. This suggested that in addition to being glycosylated, the wild type MP domain may have been more susceptible to degradation of its N-terminus.

3.5 α2-Macroglobulin binding assay. Testing the activity of purified ADAM33 Pro-MP-His.

Using the α2-Macroglobulin binding assay purified ADAM33 Pro-MP-His was shown to be proteolytically active. When the wild type protease was incubated with α2-Macroglobulin high molecular weight complexes between the two proteins were formed. The samples were analysed by SDS-PAGE and visualised by western blotting using the anti ADAM33 MP domain antibody (RP2), **Fig.3.21**. The molecular weight of the complexes formed were slightly larger than expected (expected ~150kDa). The formation of this complex was dependent on proteolytic activity of the ADAM33. The addition of the metalloproteinase inhibitor 1,10 phenanthroline

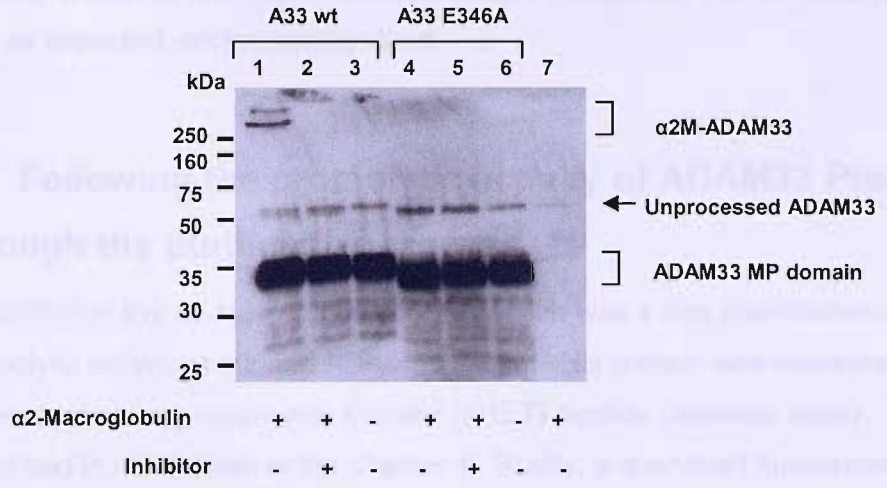

Fig. 3.21. Activity test for purified ADAM33 Pro-MP-His - α2-Macroglobulin assay. 600ng of purified ADAM33 Pro-MP-His and the E346A mutant were incubated at 25°C overnight with 3.5μg of α2-Macroglobulin with (lanes 2 and 5) or without (lanes 1 and 4) the metalloproteinase inhibitor, 1,10, phenanthroline monohydrate. ADAM33 incubated without α2-Macroglobulin (lanes 3 and 6), and α2-Macroglobulin incubated alone (lane 7) were used as negative controls. Samples were solubilised in sample buffer and separated on by SDS-PAGE (12.5% gel), and the proteins were transferred to PVDF membranes and western blotted using the anti ADAM33 MP domain antibody (RP2).

monohydrate inhibited complex formation. The purified ADAM33 Pro-MP(E346A)-His was unable to form high molecular weight complexes with α2-Macroglobulin and was as expected, proteolytically dead.

3.6 Following the proteolytic activity of ADAM33 Pro-MP-His through the purification process.

In addition to the α2-Macroglobulin assay which was a non quantitative method, the proteolytic activity of purified ADAM33 Pro-MP-His protein was measured using a fluorescent energy resonance transfer (FRET) peptide cleavage assay. This assay is described in more detail in the chapter 4. Briefly, a quenched fluorescent peptide which is known to be cleaved by ADAM33 (DABCYL-YRVAFQKLAE(FAM)-NH_2)[235] was incubated with ADAM33. ADAM33 mediated peptide cleavage resulted in the separation of the quencher and fluorophore attached to ends of the peptide, leading to an increase in detectable fluorescence[235]. This assay was used to determine the level of ADAM33 Pro-MP-His activity in the conditioned medium and eluted pools from each of the columns in the purification scheme devised earlier. The results are summarised in **Table 3.2**. The Con A affinity chromatography step enriched for ADAM33 and this is reflected in the increase in specific activity observed between the two steps. However the specific activity of the preparation decreased after the subsequent IMAC step. This was thought to reflect the removal of contaminating proteases which were capable of cleaving the FRET peptide. With the removal of further contaminating proteins using the SP sepharose column the specific activity of the preparation increased by ~6 fold. The specific activity of the preparation eluted from the Superose 12 column was comparable to that obtained from the SP sepharose column when considering the standard deviation of the values, and was inline with what was expected.

	Medium	Con A Eluate	IMAC Eluate	SP Sepharose Eluate	Sup 12 Eluate
Total Activity-RFU/min	108392	35989	2911	1378	535
Std. Dev.	19085.8	3911.2	173.2	171.0	94.5
% Activity Recovered	100	33.2	2.7	1.3	0.5
Specific Activity-RFU/min/ug protein	91	1261	348	2208	1877
Std. Dev	16.0	137.0	20.7	274.0	331.6

Table 3.2 Quantification of proteolytic activity of purified ADAM33 Pro-MP-His

The activity of ADAM33 Pro-MP-His purified from 500ml of conditioned medium was measured using a FRET peptide cleavage assay (as described in detail in **chapter 4**). Proteolytic activity was correlated with the rate at which fluorescence increased. Pooled samples collected at the end of each purification step (Con A affinity chromatography, IMAC, cation exchange (SP Sepharose) and gel filtration (Superose 12) were dialysed into PBS before being assayed. Superose 12 eluate represents the peak eluted fraction. Fluorescence in was measured in relative fluorescence units (RFU), and followed over time using a Bio-Rad iCycler.

3.7 Discussion

3.7.1 Mammalian ADAM33-Fc transfectants

ADAM33 has been identified as an asthma susceptibility gene. It has been hypothesised that it encodes a protein which is important in the remodelling processes that occur in the asthmatic airway. The murine homologue of *ADAM33* is also associated with bronchial hyperresponsiveness. Since some functional association has been demonstrated in humans and mice, it was logical to use mammalian expression systems for recombinant protein expression. This would ensure that the proteins produced had similar post translational modifications to those found in species where ADAM33 is thought to be relevant. The COS-7 and CHO cell lines were chosen as targets for transfection, since they are mammalian cells that have been used successfully for recombinant protein expression in many studies.

The relative level of ADAM33-Fc proteins produced by the transient transfectants was consistently higher in the COS-7 cells relative to the CHO cells, this was perhaps not unexpected. Although the COS-7 and CHO cell lines had been transfected with the same pCDNA3.1 vector only the COS-7 cells express the SV40 large T antigen which allows the episomal replication of the vector which encodes a SV40 origin of replication. Despite this, the level of recombinant protein produced was disappointingly low, reaching only 20ng/ml over 7 days in the most productive transfectant as determined using an anti IgG-Fc ELISA. Western blot analysis of the COS-7 transfectants showed that ADAM33-Fc proteins were accumulating inside the cells, and only relatively small amounts were being secreted. More worryingly, the presence of significant amounts of free Fc in the culture medium made it apparent that the secreted ADAM33-Fc proteins were relatively unstable. This also meant that the quantified levels of ADAM33-Fc in culture medium using the anti-IgG-Fc ELISA were likely to be an overestimate of their true values. The anti IgG-Fc ELISA was used, since recombinant human IgG-Fc was commercially available and could be used as a standard against which the level ADAM33-Fc could be quantified, in contrast recombinant ADAM33 was not available.

The apparent molecular weights of the ADAM33-Fc proteins deduced from the western blots, **Fig. 3.2**, were larger than that predicted by their amino acid sequences. This probably reflected the addition of post translational modifications such as glycosylation. The ADAM33-Fc proteins that accumulated in the cells were

present as the immature unprocessed forms, and could be detected with RP1 and the anti-Fc antibodies. Processing of ADAM proteins to separate the Pro domain from the rest of the protein is thought to be mediated by furin like enzymes as they traffic to the cell surface, or by metalloproteinases after they reach the surface. The secreted ADAM33-Fc was not completely processed and was found as both the immature and processed mature form. These findings agree with work by Garlisi *et al.* who transfected full length *ADAM33* into COS-7 and CHO-K1 cells. They achieved higher levels of recombinant ADAM33 expression in the COS-7 cells relative to the CHO-K1 cells, but found that the COS-7 cells were not as efficient as the CHO-K1 cells at processing the ADAM33 into the mature form by the removal of the Pro domain[236]. Since, the COS-7 cells do not process all the ADAM33 that they secrete, if they were used for ADAM33-Fc production, the unprocessed ADAM33 would have to be subsequently activated with the mecuric compound APMA. In combination with the fact that these cells produce only recombinant protein in the ng range, scaling up ADAM33-Fc expression and production in these cells would have been time consuming, costly and an inefficient process.

3.7.2 Insect cell ADAM33-Fc and ADAM33-His transfectants

ADAM33 ECD-Fc and ADAM33 Pro-MP-Fc transfectants generated using the DES system could express the recombinant protein, but again there were high levels of intracellular accumulation of the immature forms in addition to the secreted forms. The secreted forms of ADAM33 ECD-Fc and ADAM33 Pro-MP-Fc were degraded and both had lost their Fc tags which were required to simplify the downstream purification procedure. The secreted ADAM33 ECD-Fc had also become incorporated into protein aggregates, making these two transfectants unsuitable for scaling up production. Since both mammalian and insect cells had difficulty in producing stable ADAM33-Fc proteins that were secreted in high amounts in the medium, a different tagging epitope was tested to establish whether the intracellular accumulation and protein stability issues could be resolved. It was thought that the cleavage site was in the Fc domain therefore the Fc tag was substituted for a 6x histidine (6xHis) tag. Using the C terminal 6xHis tag, it was possible to get processed ADAM33 to be secreted in high levels into the culture medium with minimal intracellular retention. Being processed removed the further need to activate the ADAM33 after purification. It was interesting to note that when ADAM33 Pro-MP-His was produced in serum containing medium, a species of >250kDa was detected which was not observed when cells were grown in serum free medium. This could represent aggregated protein or perhaps more likely ADAM33 complexed to other

protein species. Serum contains abundant protease inhibitors, some of which can bind irreversibly to proteases such as α2-Macroglobulin. It can be envisaged that such an inhibitor could bind to ADAM33 Pro-MP-His resulting in slower migration through an SDS-PAGE gel. It may be interesting to investigate this further to identify whether there are any relevant ADAM33 inhibitors, or binding partners that are present in serum. This may shed some more light on the biological relevance of ADAM33 and how it is regulated.

3.7.3 Purification of ADAM33 Pro-MP-His

Having generated stable *Drosophila* S2 cell lines expressing ADAM33 Pro-MP His and the equivalent E346A mutant, it was necessary to derive a recombinant protein induction and purification strategy. As a starting point, the methodology used by researchers at the Schering Plough Research Institute (Kenilworth, USA) was used as a guideline. Zou *et al.* and Prosise *et al.* separately published two similar protocols for the induction and purification of ADAM33 Pro-MP-His from conditioned medium in the Journal of Biological Chemistry[205], and Protein Expression & Purification[245] respectively in 2004. The two protocols are summarised in **Table 3.3**.

pH Adjustment Mixed medium 1:1 with S-Buffer A: (25mM HEPES pH6.8, 50mM NaCl, 10% glycerol)	**pH Adjustment** Medium adjusted to pH7.0 by addition of 1M HEPES buffer pH 8.0. Then mixed with Buffer A: (25mM HEPES pH7.0, 10% glycerol, 5mM $CaCl_2$.)
Cation Exchange step. Equilibrated with S-Buffer A. Eluted with NaCl gradient 0.1-0.5M. Adjusted ADAM33 fractions to 20mM imidazole.	**Cation Exchange step.** Equilibrated with Buffer A. Eluted with NaCl gradient 0.1-0.5M. Adjusted ADAM33 fractions to 5mM imidazole.
IMAC step. Equilibrated with 25mM HEPES pH 7.9, 500mM NaCl, 20mM imidazole, 10% glycerol. Eluted with 500mM imidazole.	**IMAC step.** Equilibrated with 25mM HEPES pH 7.9, 500mM NaCl, 5mM imidazole, 10% glycerol, 5mM $CaCl_2$. Eluted with 250mM imidazole.
Concentrated ADAM33 fractions using Ultrafiltration cell.	**Concentrated** ADAM33 fractions using Centriprep unit (MWCO 10kDa) to 5-15mg/ml.
Gel Filtration step. Superdex-75. Eluted with 25mM HEPES pH7.5, 150mM NaCl, 50mM imidazole, 10% glycerol.	**Gel Filtration step.** Superdex-75. Eluted with 25mM HEPES pH7.5, 150mM NaCl, 50mM imidazole, 10% glycerol, 5mM $CaCl_2$.
Zou *et al.* J. Biol. Chem. 2004.	Prosise *et al.* Protein Expr Purif. 2004

Table 3.3 Summary of the published purification strategies for ADAM33 Pro-MP-His.

3.7.4 Inducing agents

Several reagents can be used to induce recombinant protein expression in the *Drosophila Expression System* (Invitrogen), the most common being $CuSO_4$. Both Zou and Prosise chose to use a rather unusual cocktail of $CdCl_2$ and $ZnCl_2$. The main reason for their choice was the known problem associated with purifying his-tagged proteins from medium containing free Cu2+ ions. IMAC is the conventional purification resin of choice for 6xhis tagged proteins because it is rapid, effective, and affordable. However, in addition to activation of the metallothionein promoter, the Cu^{2+} ions also bind to the 6xhis tag tail of the expressed recombinant protein. This disrupts the affinity of the recombinant protein for an IMAC column, since the imidazole ring of the histidine is already co-coordinated with a metal ion, therefore decreasing its affinity for Ni^{2+} ions. In 2000 Lehr *et al.* devised a method to resolve this issue. They showed that by using a non chelated IMAC column, Cu^{2+} ions could be captured from conditioned medium, and the recombinant protein would be pulled out by association[247]. However when this was attempted by Prosise *et al.,* they found that adventitious Cu2+ bound to the ADAM33 and caused a reduction in the specific activity of the purified protease. To overcome this effect, they tried to remove excess Cu^{2+} ions from the medium prior to conventional Ni^{2+}-IMAC, by buffer exchange. However they were unable to capture the protease on IMAC, and interpreted this as an indication that Cu2+ ions remained strongly associated to the 6xhis-tag.

In this study stable ADAM33 S2 cells were generated and recombinant protein expression was induced with 0.5mM $CuSO_4$. The ability of the IMAC column to capture his-tagged ADAM33 from conditioned medium was assessed. Although the literature suggested that the Cu2+ ions would inhibit binding to the IMAC resin, it was not found to be a major issue as shown in Fig. 3.6. We found that ADAM33 from conditioned medium could bind to the Ni^{2+} IMAC column even in the absence of a preceding buffer exchange step, in contrast to previous studies. The most important factor found to affect the IMAC purification step, was actually the concentration of imidazole in the sample loaded on to the column. It was shown that the presence of just 30mM imidazole could completely disrupt recombinant protein binding to the IMAC column, **Fig.3.5(a)**. This concentration was perhaps lower than expected, since 20-40mM of imidazole is routinely added to recombinant protein samples prior to IMAC purification to reduce non specific binding to the resin. This indicated that Cu^{2+} ions may have exerted a minor effect on the his-tag's affinity for the IMAC column.

Schering Plough Research Institute also reported that the addition of a co-inducer $ZnCl_2$ improved the yield of free ADAM33 MP domain relative to Pro-MP complex. This did not greatly enhance purified ADAM33 specific activity, the k_{cat}/k_m was found to be 52±8 M^{-1}/s^{-1} and 58± 11M^{-1}/s^{-1} for $CdCl_2$ induced and $CdCl_2$ and $ZnCl_2$ co-induced ADAM33 respectively. This slight difference in activity comes with the undesirable cost of decreased ADAM33 yield. Also since $CdCl_2$ is more environmentally hazardous than $CuSO_4$, neither $CdCl_2$ or $ZnCl_2$ were used in this ADAM33 expression system, and $CuSO_4$ remained the inducing agent of preference in this study.

3.7.5 Purification process

Small scale purification tests showed that IMAC was suitable for the purification of ADAM33 Pro-MP-His from conditioned medium. However, the eluted recombinant protein did not reach the level of desired purity. Many insect derived proteins co-eluted with ADAM33 into the same fractions. Having demonstrated that the addition of 30mM of imidazole in to the conditioned medium sample (to reduce non specific binding) abolished ADAM33 binding to the IMAC, other methods to increase the efficiency of the IMAC column were tested. The first involved the substitution of the chelated Ni^{2+} ions in the IMAC column for Co^{2+} ions. The bound proteins on the Co^{2+} resin were eluted at marginally lower concentrations of imidazole relative to those bound to the Ni^{2+} resin. This fitted in with the characteristics of Co^{2+} ions which have a lower affinity for histidine than Ni^{2+} ions, a property which allows it to favour tracts of histidines. The protein banding patterns from the Ni^{2+} and Co^{2+} resin eluates did differ, and the complexity of the ADAM33 fractions was slightly increased when Co^{2+} was used. This was particularly true for high molecular weight proteins, which were seen to co-elute in the ADAM33 fractions, Fig. 3.8. This result showed that no real practical advantage was conferred by using Co^{2+} IMAC, and it was either not as specific for histidine tracts as expected, or the insect proteins also contained tracts of histidines. Since cobalt is also more toxic than nickel and the leaching of ions from the column is inevitable, it was decided that Ni^{2+} IMAC would be used in the final purification scheme.

Since the concentration of imidazole had to be kept low to ensure ADAM33 binding to the IMAC column, the purity of recombinant protein eluted from the column was poor. In order to optimise the protocol for the purification of ADAM33, several fractionation techniques were assessed to precede separation on the IMAC column. In the first instance an increasing concentration of ammonium sulphate salt was used

as a quick and crude method of "salting out" proteins from the conditioned medium. Having found it difficult to recover the enzyme from the lipid rich medium using this technique, lectin affinity chromatography using Concanavalin A, and cation exchange chromatography were explored. Cation-exchange was shown to be effective in the published protocols (above), but in this study using cation-exchange as a preceding step to IMAC was less effective, as a protein of ~70kDa co-purified with ADAM33. This discrepancy was likely to be a consequence of differences in the relative levels of ADAM33 protein present in the conditioned medium. Chromatography columns function more efficiently as the proportion of the protein of interest relative to contaminating proteins capable of binding to the resin increases in the sample to be purified. It follows that if the Schering Plough Institute S2 transfectants secreted higher levels of ADAM33 in to the medium, the competitive effect of the contaminating ~70kDa protein would have been less problematic than in a system in which the relative proportions of ADAM33 to contaminating protein was lower. In contrast, Concanavalin A chromatography worked well as a preceding step to IMAC. It selected out glycosylated proteins including ADAM33, and when these were subsequently purified on the IMAC column the ADAM33 eluted as the predominant protein in the fraction.

Having selectively concentrated the ADAM33 protein on the Concanavalin A and IMAC columns, a subsequent cation exchange step was used to improve the purity of the preparation. The protein eluted from the Sepharose FF column was concentrated by passage through an IMAC column, then ADAM33 fractions were loaded on to a Superose 12 gel filtration column, a polishing step used to remove high molecular weight contaminants and aggregated proteins. Two peaks were observed in the chromatogram trace following the absorbance at 280nm of the eluate from the Superose 12 gel filtration column. The first peak eluted at 9ml post loading represented proteins that were unable to penetrate the pores of the Superose 12 matrix. As a result these proteins were not retarded and flowed directly out of the column in the void volume. The second peak eluted at ~15ml post loading represented the pure ADAM33 fraction. The Superose 12 column did not discriminate between fractions containing free MP domain, and those containing Pro-MP complexes like that reported by Zou *et al.* Superose 12 has a higher resolving power than Superdex75 (used by Zou *et al*). So either the column used by Zou had been much longer, since longer columns give better resolution, or more likely in this study only very low levels of free ADAM33 MP domain was present. This is supported by the fact that free mutant MP domain can be observed during the

purification of ADAM33 Pro-MP(E346A)-His, and typically there is more recombinant protein in the conditioned medium from the mutant transfectants.

3.7.6 Yield of recombinant ADAM33 Pro-MP-His

A respectable yield of ~200ug/L of wild type ADAM33 protein was recovered from conditioned insect medium after complete purification. This included the Pro and MP domains, as well as any unprocessed Pro-MP domain complexes. Compared to the 5mg/L of purified MP domain routinely obtained by Schering Plough Institute, there is approximately 25-50 fold difference in yield obtained in this study. There are several plausible explanations. Firstly, the ADAM33 transfectant cell lines used for these two studies were generated independently by transfection and were therefore different cell lines. The DNA transfection technique randomly inserts vectors into host cells. The number of copies accepted by each cell varies, giving rise to a heterogeneous population of cells that show differing levels of recombinant protein expression. Smaller vectors tend to transfect into cells more efficiently and at the same time exert a lower metabolic load on the host cell. In this study, the transfectants were not made from single progenitor cells, or assessed for the level of protein expression. It is possible that stable transfectants generated for this study did not have as many copies of the DNA insert as the Schering Plough Institute's clone. During the selection and expansion stages of generating S2 transfectants, it was also possible that clones which were low to medium expressors were more favourably selected.

Secondly, during protein expression phase, in which the stable transfectants are induced, the cells used were grown in 175cm^2 tissue culture flasks, rather than spinner flasks like those used by the Schering Plough Institute researchers. Spinner flasks ensure more efficient aeration and mixing of the nutrients in the medium, which leads to increased growth rates and cell density of a culture. It was likely that the cell density in 175cm^2 flasks never reached the same density achieved in spinner flasks. Fewer cells, equates to decreased net protein production.

Thirdly, there are more chromatographic steps in the purification scheme devised for this study, than in the commercial studies. It is rare that any chromatographic procedure is 100% efficient, and some loss is to be expected from each step. The more chromatographic steps involved in a purification scheme, the less efficient the whole scheme becomes. In this study a greater degree of purity was chosen at the sacrifice of a higher yield, and the specific activity of the ADAM33 Pro-MP-His preparation was increased by at least 20 fold, **Table 3.2**. This was essential, for

accurate assessment of ADAM33 activity in the absence of other proteases, since even small amounts of a contaminating protease could adversely affect downstream biochemical and functional characterisation. The purification table indicated that only ~0.5% of ADAM33 activity was recovered from the purification, but this is likely to be an underestimate. The conditioned medium is protease rich and since the FRET peptide used for the activity assays can be cleaved by non ADAM33 proteases it is probable that the starting activity level reflects the total activity of several proteases, therefore elevating the starting activity figure. Also, although it appeared that the recovery from the IMAC step was poor, there was some suggestion that the high concentration of imidazole in the sample was not removed effectively by dialysis, and this may have resulted in a decreased level of activity in the FRET peptide assay, since the imidazole can coordinate the zinc ion in the active site.

3.7.8 The association between the Pro and MP domains of purified ADAM33

The ADAM33 pro and MP domains were found to co-elute during all stages of purification, but migrated as separate species on SDS PAGE gels. This strongly suggested that they remained associated, even after being processed. A similar association has been reported for murine ADAM15 [248]. Biotinylated ADAM15 from the cell surface was immunoprecipitated using pro domain antibodies, from ADAM15 transiently transfected COS-7 cells. The pro domain co-precipitated with the ADAM15 species that can also be detected with an anti-cytoplasmic tail antibody, even after it had been processed.

The extent of the association between ADAM33 pro and MP domains may be exaggerated in the absence of the other ADAM protein domains usually found in the full length species. Gonzalez *et al.* have reported that the disintegrin domain of ADAM17 has a role in the removal of the pro domain[249]. They found that the pro domain of ADAM17 had an inhibitory effect on the ADAM17 MP domain, when the two separate species are co-incubated. In peptide cleavage studies, a 30 fold reduction in the inhibitory effect is achieved when the pro domain was co-incubated with ADAM17 MP-disintegrin-cysteine rich domain in the assay. The ability of the disintegrin-cysteine rich domain to facilitate the removal of the pro domain was further demonstrated by its rapid ability to restore proteolytic activity to inactive ADAM17 Pro-MP complexes when added exogenously. It follows that the lack of the disintegrin-cysteine rich domain in this ADAM33 expression system may contribute to the continued association between the two domains.

Since the Pro domains of ADAMs are well known to exert an inhibitory effect on protease activity, the initial concern was that the purified protease would be inactive. However, using the α2-Macroglobulin assay and the FRET peptide assay the purified ADAM33 Pro-MP-His was shown to be active. It may be postulated that the removal of the Pro domain would further increase protease activity. The generation of the ADAM33 Pro-PM-Disintegrin-Cysteine rich-His domain or just the disintegrin-cysteine rich domain could provide more insight in to this.

3.7.9 Molecular weight of purified ADAM33

The SDS PAGE banding pattern and molecular weight profiles of ADAM33 Pro-MP were comparable to previous publications. Both the Pro domain and MP domains were separated out into multiple bands, with the Pro domain bands migrating at ~25kDa, and the MP bands ~33kDa. These were larger than the predicted molecular weight, and are a consequence of glycosylation of the Pro and MP domains, and confirmed with SELDI-TOF mass spectroscopy. The E346A wild type gave a similar banding pattern to the wild type protein, however all the MP domain bands migrated marginally faster than expected. This could be an effect arising from the slight decrease in molecular weight and also partially due to the substitution of a charged residue for an uncharged residue.

Analyses of the molecular weight of the purified ADAM33 wild type and E346A mutant proteins by SELDI-mass spectroscopy also highlighted the apparent disparity between the predicted and observed mass for the wild type protein. The wild type MP domain was consistently flying at a lower molecular weight than predicted. It is therefore interesting to speculate whether ADAM33 could be auto-catalytic and auto-activating like many other MMPs and ADAMs. It is likely that such cleavage occurs at the N terminus of ADAM33 since the C terminus is the 6xHis tag which was necessary for the IMAC purification step and therefore must be intact. The ability of ADAM33 to cleave itself, may be tested by determining whether the wild type proteinase can cleave the mutant form when co-incubated together. In addition the introduction of metalloproteinase inhibitors during the protein expression and harvesting steps could be used to see if auto-catalytic cleavage of ADAM33 can be prevented, and if so whether this protein is as active as the fully processed form. Cleavage of N terminal residues may also explain the apparent spread in the pI of the MP domain highlighted in the 2D PAGE western blots. The first four residues of the N terminus of the MP domain are EARR, one acidic and two basic residues. Losing these charged residues would have an effect on the observed pI.

3.7.10 Proteolytic activity

Having satisfactorily removed insect derived gelatinase and caseinolytic activity from the ADAM33 as demonstrated by zymography, the activity of ADAM33 was assessed using the alpha2-macroglubulin (α2-M) assay. α2-M functions as a key proteinase inhibitor in plasma, covalently trapping active proteinases. High molecular weight complexes were observed with the purified wild type proteinase but not the E346A mutant. This gave confidence that the purified ADAM33 was active. Although it was expected that the complex would consist of the ~100kDa α2-M subunit plus the molecular weight of the ADAM33 Pro-MP domain ~50kDa, the complex observed in the western blot appears to be greater than this, and two bands rather than one were observed. A simple explanation would be that some high molecular weight proteins migrate in to high percentage gels with difficulty, so the molecular weight seen could be an overestimate of the true molecular weight. The presence of multiple α2M-proteinase species have been reported before. It is thought that the trapped proteinase can, under some conditions bridge two α2-M subunits together, although the mechanism by which this occurs is still unclear[250].

3.7.11 Summary

The insect cell expression system was found to produce high levels of stable recombinant ADAM33 protein in contrast to the mammalian expression systems tested. Using this system stable transfectants expressing ADAM33 Pro-MP-His were produced, the recombinant protein harvested and purified to a high standard using a newly devised purification scheme. The most suitable control for ADAM33 Pro-MP-His activity, an inactive mutant ADAM33 was engineered using site directed mutagenesis, and transfected into the same insect expression system and the mutant protein purified similarly to the wild type protein. Initial characterisation studies have demonstrated the retention of proteolytic activity of the purified wild type ADAM33 protein and the inactivity of the mutant protein using the α2-Macrogblulin assay. In addition, the proteins were shown to be glycosylated and whilst the mutant ADAM33 protein was confirmed to be the predicted molecular weight, the wild type protein was found to be less than the predicted, suggesting that the wild type protein is more susceptible to N-terminal cleavage. Sufficient amounts of recombinant ADAM33 Pro-MP-His and the ADAM33 Pro-MP(E346A)-His have been generated to facilitate further investigation into the biochemical and functional behaviour of this

proteinase, which may then shed light onto its role in the airway and why it is implicated in asthma susceptibility.

Chapter 4 Biochemical Characterisation of ADAM33

Using the recombinant ADAM33 Pro-MP-His and ADAM33 Pro-MP(E346A)-His proteins described in chapter 3, the biochemical characteristics of ADAM33 could be investigated. These studies were necessary for understanding the preferred environment in which the ADAM33 enzyme could function. The optimum reaction conditions under which ADAM33 activity assays should be carried out *in vitro*, could also established. The availability of the recombinant enzyme also allowed synthetic and natural inhibitors to be assessed for their ability to abrogate the proteolytic activity of ADAM33, in biochemical assays. Inhibitors were of particular interest for their potential therapeutic implications.

Biochemical characterisation studies are difficult to perform with a method like the α2-Macroglobulin binding assay. In this assay, enzyme activity is not analysed in real-time and it is not easy to quantify substrate turnover. Therefore, it was more practical to use an assay in which the rate of the cleavage of a substrate could be accurately quantified. Although the physiological substrate for ADAM33 has not been identified, ADAM33 has been reported to digest peptides derived from common metalloproteinase substrates such as KL-1, insulin β chain or APP[205]. These peptides can be fluorescently labelled (FRET peptides) and be used as reporters for metalloproteinase mediated cleavage events. The fluorescence emission resulting from ADAM33 digestion of such FRET peptides could be quantified in real-time to assess enzyme activity under different conditions. The aims of this chapter were to

(i) assess the proteolytic activity of the purified ADAM33 *in vitro*, by determining the effect of different biochemical parameters and to compare the activity profiles obtained for ADAM33 with the published literature.

(ii) identify synthetic inhibitors which can inhibit ADAM33 proteolytic activity *in vitro*, which may be useful reagents in studying ADAM33 mediated proteolysis *in vitro* and *in vivo*.

4.1 Assessing ADAM Pro-MP-His activity

To re-confirm that the purified ADAM33 Pro-MP-His was active and that ADAM33 Pro-MP(E346A)-His was proteolytically dead, the purified proteins were incubated with FRET peptide (DABCYL-YRAVFQKLAE(FAM)K-NH_2)[235] at 25°C over a period of

2 hours. The fluorescence emission at 530nm was recorded using an iCycler (Bio-Rad, Hertfordshire, UK), **Fig. 4.1**. All the FRET peptide assays were carried out in 96 well plates typically used for qPCR. This enabled the volume of each reaction to be kept low (20µl), and therefore minimal quantities of the enzyme and peptide reagents were required. This reaction volume is smaller than that typically required for standard 96 well plates, and matches that required for standard 384 well plate formats.

As expected ADAM33 Pro-MP-His was able to cleave the peptide and the detected fluorescence of the reaction increased over time. The increase was steady, and the linear rate remained similar over the course of the assay. The proteolytic activity of ADAM33 could be inhibited by the addition of the zinc chelator 1,10, phenanthroline monohydrate to the reaction at a concentration of 10mM. In contrast, the reaction with the mutant protein and peptide showed no increase in fluorescence over time, and the profile was similar to that seen when peptide was incubated in the absence of enzyme. This lack of fluorescence increase, indicated that the FRET peptide was not cleaved therefore the purified ADAM33 Pro-MP(E346A)-His does not exhibit proteolytic activity. The rate of proteolysis observed was dependent on the enzyme concentration, **Fig. 4.2**.

4.2 Optimising the FRET peptide cleavage assay

4.2.1 Varying divalent cation concentration and ionic strength

The FRET peptide cleavage assay was optimised to yield maximum enzyme activity. The level of free Zn^{2+} and Ca^{2+} ions are known to be important factors in determining metalloproteinase activity. Therefore the concentration of zinc chloride and calcium chloride in the assay buffer were titrated, to study their effects on enzyme activity.

In agreement with the previous ADAM33 activity test **(Fig.4.1**), it was found that when a zinc chelator was added to the reaction to remove free Zn^{2+} ions from the FRET peptide assay, no ADAM33 activity was detectable. If no exogenous zinc chloride is added to the reaction then ADAM33 activity remains low at approximately 73 RFU/minute. ADAM33 activity could be enhanced by ~3 fold by the exogenous addition of zinc chloride at concentrations as low as 10µM, **Fig. 4.3(a).**

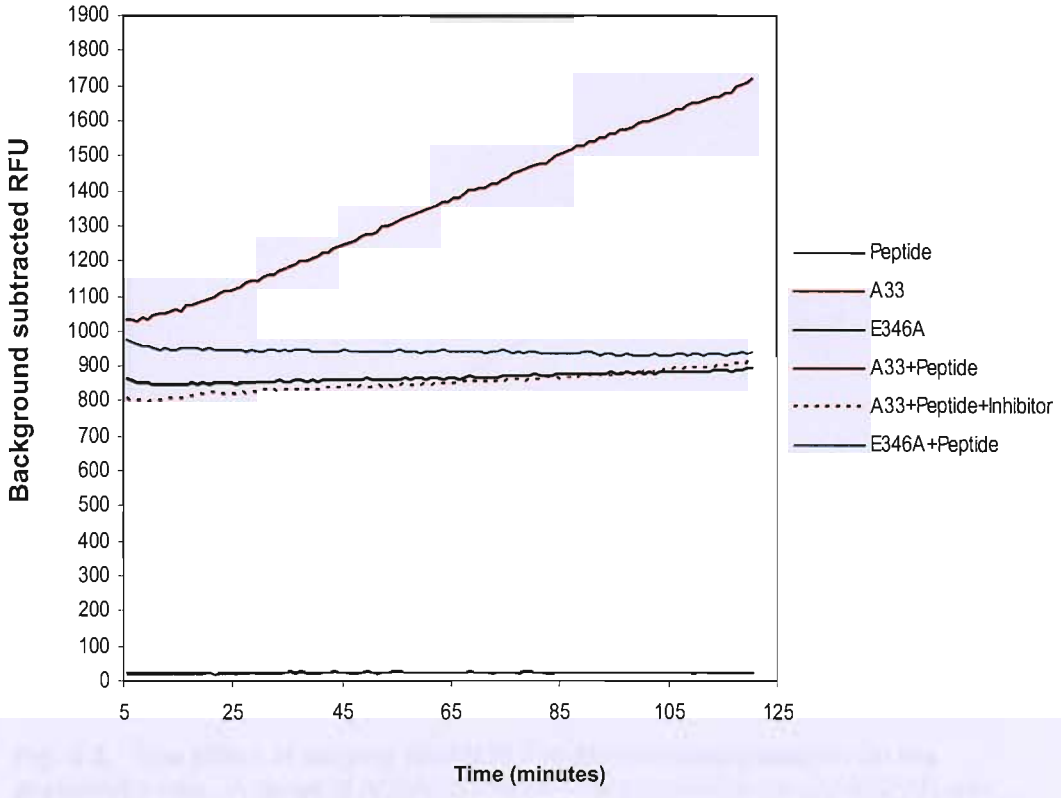

Fig. 4.1. A quantitative ADAM33 activity assay. Purified ADAM33 Pro-MP-His and ADAM33 Pro-MP(E346A)-His were tested in a FRET peptide cleavage assay. 80nM of purified wild type or mutant protein was incubated with 44.4μM of FRET peptide (DABCYL-YRVAFQKLAE(FAM)K-NH_2) in 20mM HEPES pH7.0, 0.5M NaCl and 0.2mg/ml BSA at 25°C. The fluorescence emitted at 530nm over time was measured using the Bio-Rad iCycler. 10mM of 1,10 Phenanthroline monohydrate was used as an inhibitory control.

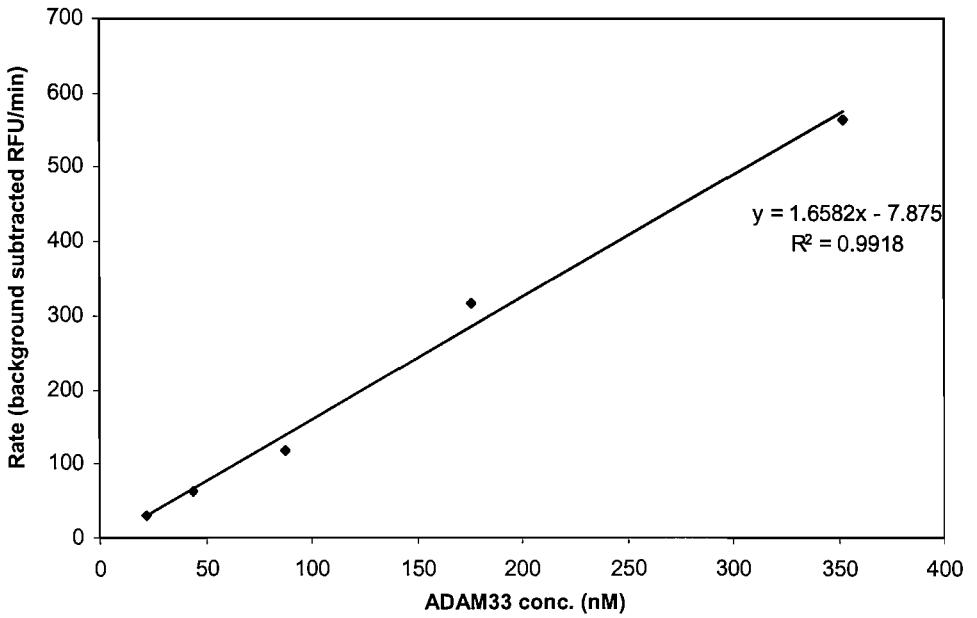

Fig. 4.2. The effect of varying ADAM33 Pro-MP-His concentration on the proteolytic rate. A range of ADAM33 Pro-MP-His concentrations (22-352nM) was tested in the FRET peptide cleavage assay in standard assay buffer at 37°C. The rate of proteolysis in each reaction was measured as a change in the fluorescence at 530nm over time. The above graph represents one experiment carried out in duplicate, the mean of the two values is shown.

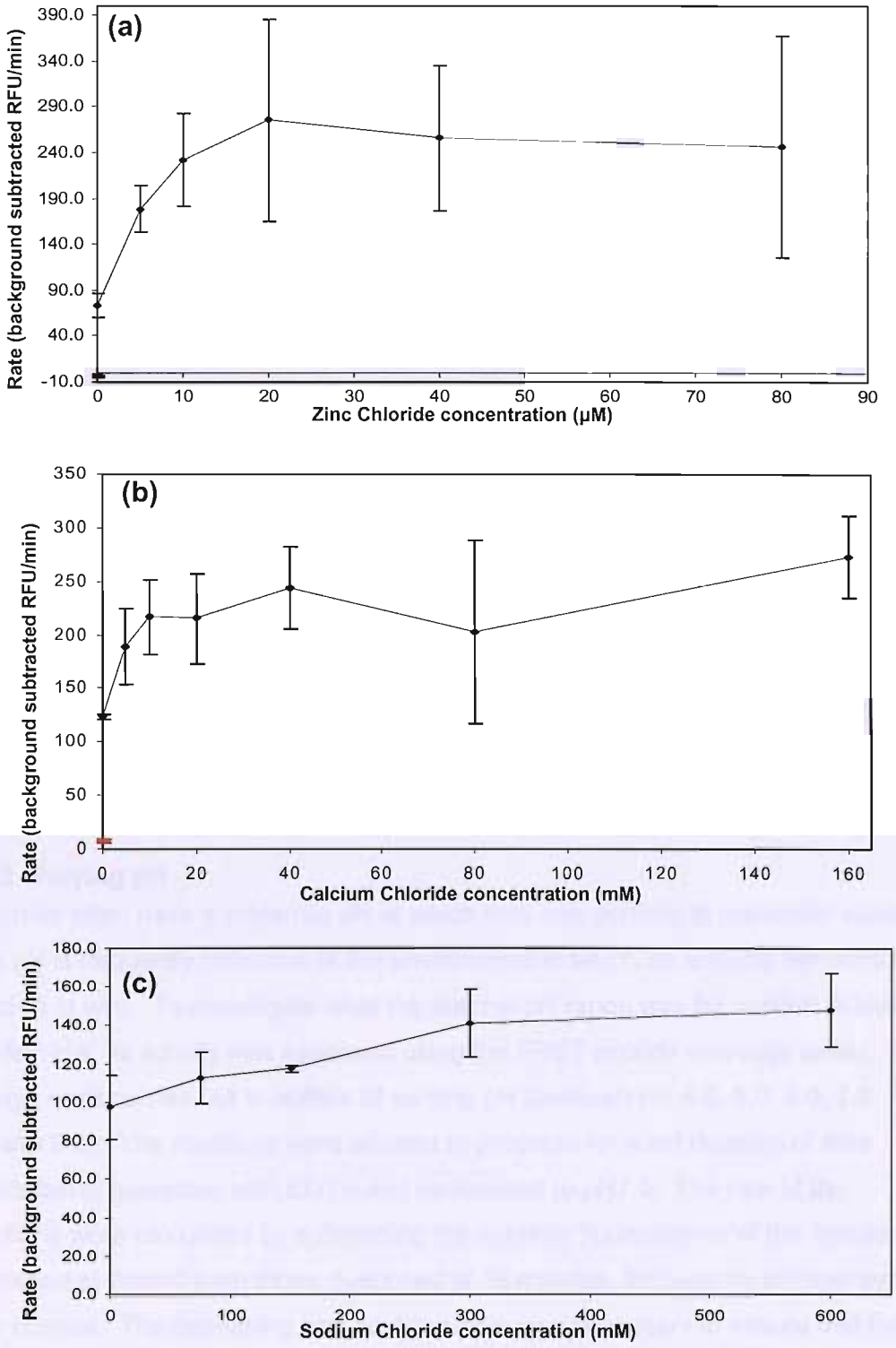

Fig. 4.3. The effect of Zn^{2+}, Ca^{2+}, and sodium chloride on ADAM33 Pro-MP-His activity. The enzymic rate of ADAM33 was measured using a FRET peptide cleavage assay under different buffering conditions. (a) 20mM HEPES pH7.0, 0.5M NaCl, 0.2mg/ml BSA with varying concentrations of $ZnCl_2$ (black). The rate in the presence of 10mM phenanthroline monohydrate, a Zn^{2+} chelator is also shown (red marker). Assay carried out in duplicate, n=2 (b) 20mM HEPES pH7.0, 0.5M NaCl, 0.2mg/ml BSA with varying concentrations $CaCl_2$. The rate in the presence of 5mM EGTA, a divalent cation chelator is also shown (red marker). Assay carried out in duplicate n=2 (except for 0mM $CaCl_2$, where n=1) (c) 20mM HEPES pH7.0 with varying concentrations of sodium chloride. Assay carried out in quadruplicate, n=1. Mean values plotted ± 1 std. deviation.

Although the spread in the data values for each individual condition was quite large, when each of the four individual runs were plotted, it can be seen that they all followed a similar trend. The addition of low concentrations of exogenous zinc chloride increased enzyme activity but when the concentration went above 10-20 μM the enzyme activity declined.

The effect of Ca^{2+} ions on ADAM33 activity was similar to that observed with Zn^{2+} ions. When EGTA, a divalent cation chelator was used to chelate free Ca^{2+} from the reaction, the enzyme activity fell dramatically and was only just within the detection limits of the assay. This may reflect the importance of Ca^{2+} ions but may also re-emphasize the importance of Zn^{2+} ions which can also be sequestered by EGTA. When no exogenous calcium chloride was added to the assay, the enzymic rate was low at ~124RFU/minute. With the addition of 10mM of calcium chloride the enzymic rate increased to ~217RFU/minute, **Fig. 4.3(b)**. Increasing the concentration of calcium chloride maintained the enzymic rate at a high level.

It was found that increasing the ionic strength of the assay buffer by the addition of sodium chloride, also had a slight favourable effect on enzymic activity at concentrations between 75 and 600mM, **Fig.4.3(c).**

4.2.2 Varying pH

Enzymes often have a preferred pH at which they can perform at maximum capacity. This pH is frequently reflective of the environment in which an enzyme performs its function *in vivo*. To investigate what the optimal pH range was for purified ADAM33 Pro-MP-His, its activity was assessed using the FRET peptide cleavage assay. Assays were carried out in buffers of varying pH (between pH 4.0, 5.0, 6.0, 7.0, 7.5, 8.0 and 9.0). The reactions were allowed to progress for a set duration of time before being quenched with EDTA and neutralised to pH7.0. The rate of the reactions were calculated by subtracting the average fluorescence of the reactions quenched at time=0 from those quenched at 16 minutes, followed by division by the time interval. The quenching and neutralisation was necessary to ensure that the changes in fluorescence observed were true reflections of the amount of FRET peptide cleaved and not biased by the pH at which the measurements were made. This was necessary because the fluorescence of FAM (the reporter dye on the FRET peptide), varies with changes in pH **Fig.4.4(a)**. Under low pH conditions, the level of fluorescence emitted by FAM is very low, but this progressively increases with increasing pH, and is high when measured at pH7.0-9.0.

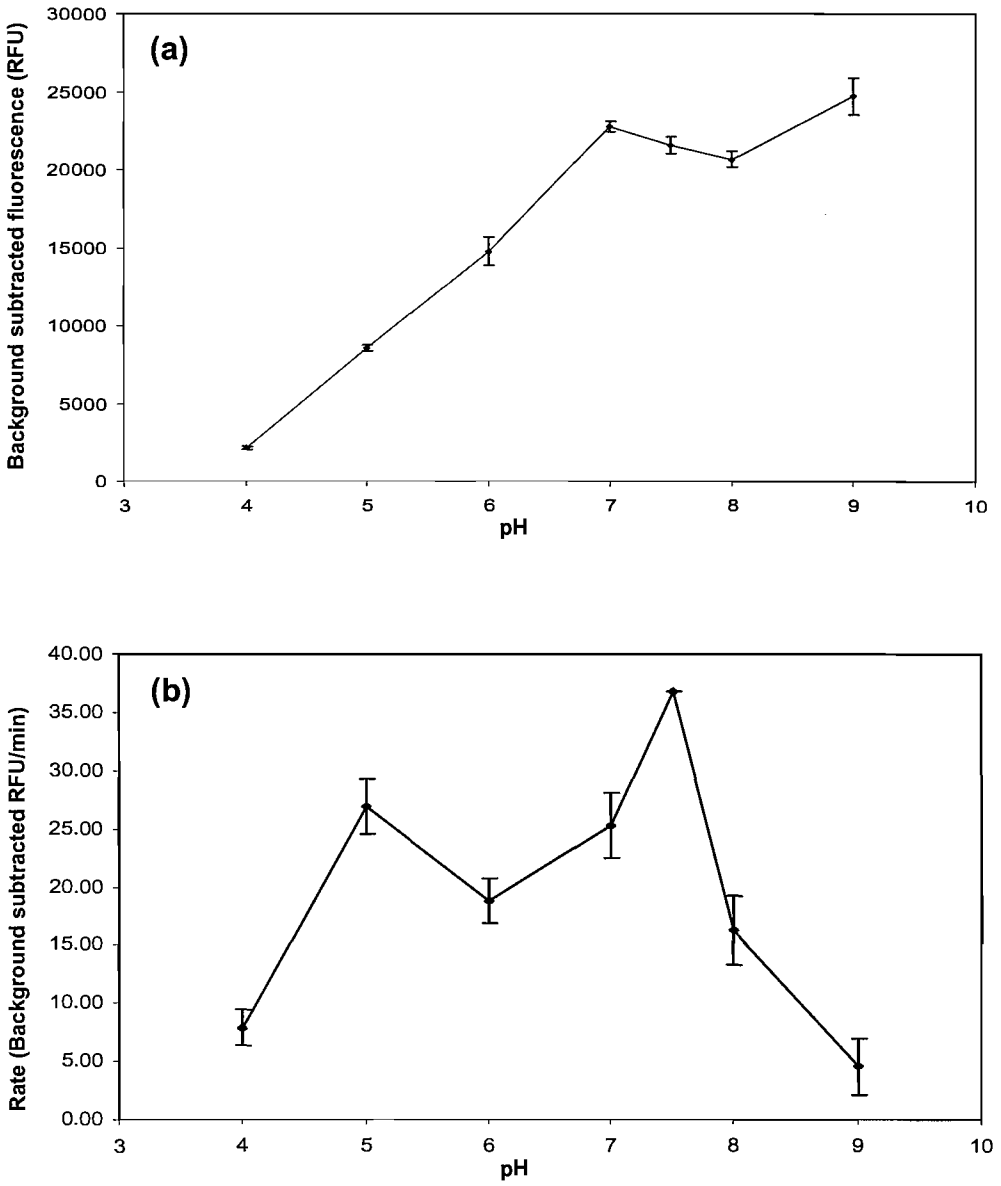

Fig.4.4. The effect of varying pH on reporter fluorescence and the proteolytic activity of ADAM33 Pro-MP-His. (a) Fluorescent cleaved FRET peptide was mixed 1:2 with buffer containing 0.5M NaCl and 100mM of one of the following buffers, sodium acetate pH 4 or 5, MES pH 6.0, HEPES pH 7.0, 7.5 or 8, or Tris-HCl pH 9.0 in triplicate. The emission at 530nm was measured, the mean ± 1 standard deviation is shown (b) 65nM of ADAM33 Pro-MP-His was used per reaction in a FRET peptide assay. Reactions were carried out in 20mM of one of the above buffers and 0.5M NaCl, 0.2mg/ml BSA, 10mM $CaCl_2$, 10μM $ZnCl_2$. Graph represents one experiment carried out in triplicate, mean ± 1 standard deviation is plotted. The data point for pH7.5 is the average of a duplicate, thus standard deviation bars could be displayed for this point.

The plot of enzymic rate against pH showed that the proteolytic activity of the ADAM33 was the lowest under extreme pH conditions, in this case pH4 and 9 **Fig4.4(b).** Otherwise it has a surprisingly broad pH range in which it can function, with an optimal pH range between 5 and 7.5.

4.3 Enzyme Kinetics

The purified ADAM33 Pro-MP-His was tested to establish whether its proteolytic activity followed typical Michaelis-Menten kinetics. A preparation of ADAM33 was dialysed into typical FRET assay buffer without BSA, and then its activity was tested at varying concentrations of FRET peptide substrate. The activity was measured during the initial linear phase of the reaction. The rate obtained in RFU/minute was converted to a function of substrate concentration by the use of a substrate calibration curve. This curve was generated by using the RFU values for trypsin digested FRET peptide at known concentrations, **Fig. 4.5(a)**. The saturation plot shows the measured rate of the enzyme activity as a function of peptide concentration, **Fig.4.5(b)**. ADAM33 Pro-MP-His showed typical saturation kinetics with peptide concentrations between 0.7μM and 22.2 μM. Enzymic activity rapidly increased with substrate concentration, and then gradually reached a plateau. At the highest concentration of peptide tested the enzymic rate unexpectedly decreased. This trend was seen in several experiments (data not shown). This decrease probably reflected some inhibitory effect at high substrate concentration rather than a decrease in intrinsic enzyme activity. To establish the kinetic constants of the enzyme the data from the saturation plot was transformed into a linear form and plotted as a Line-weaver-Burke graph, **Fig. 4.5(c)**. The anomalous data point for the highest substrate concentration was omitted since it was likely to reflect an underestimate of enzyme activity. The data point for the lowest substrate concentration was also omitted, since the Lineweaver-Burke model has a tendency to exaggerate error at low substrate concentrations, in which the enzymic rates are slower. A line of best fit was drawn through the data points, and the equation of the line was calculated. The kinetic constants were calculated from the x and y axis intercepts. The x-axis intercept indicated the -1/km value, and the y intercept gave the value for 1/Vmax. The calculated values for the apparent Km and Vmax for ADAM33 Pro-MP-His were 70μM and 120nM/minute. Using these values Kcat is calculated to be ~2.3×10^{-2} s^{-1} and Kcat/Km to be ~3.3×10^{2} $M^{-1}s^{-1}$.

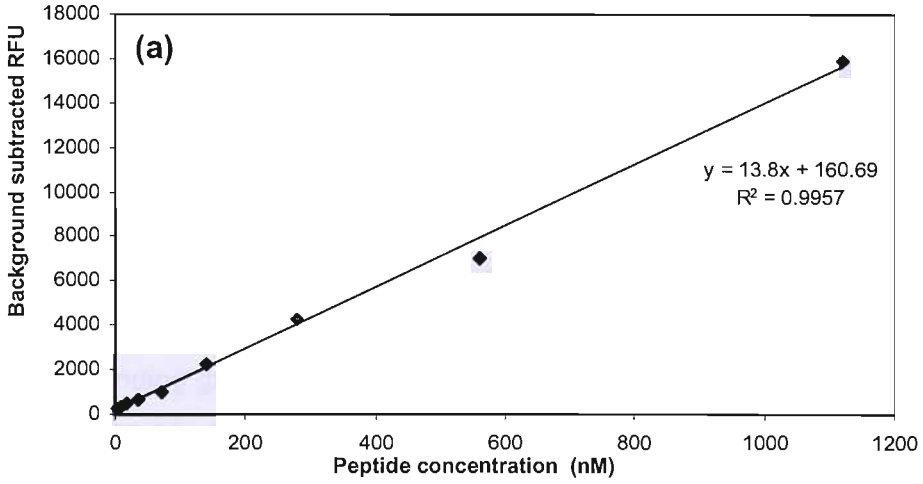

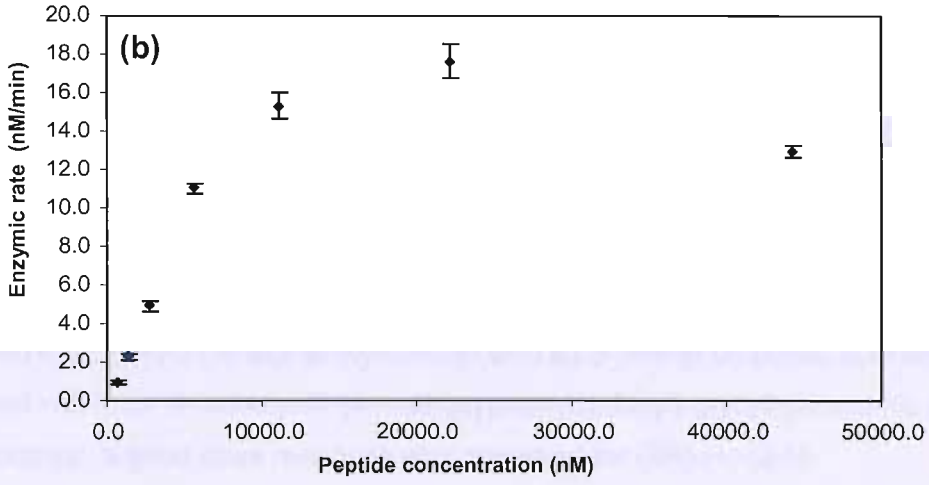

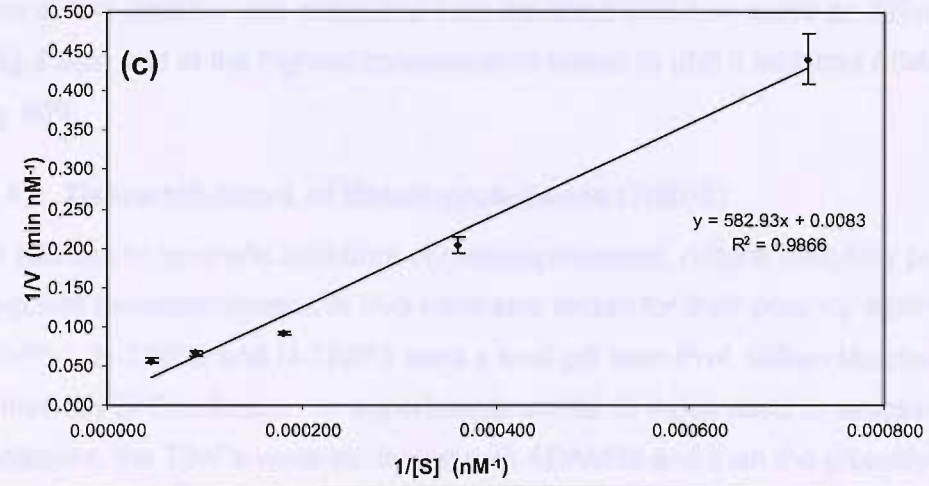

Fig. 4.5. ADAM33 Pro-MP-His enzyme kinetics. (a) Trypsin was used to digest known quantities of FRET peptide to completion. The resulting fluorescence readings were used to construct a calibration curve to show how fluorescence varies with cleaved peptide concentration. This was used to determine the rate at which ADAM33 cleaved the peptide in the kinetic assays. (b) Plot showing how ADAM33 activity varies with substrate concentration. (c) The data from (b) is transformed and used to construct a Lineweaver-Burke plot.

4.4 The potency of metalloproteinase inhibitors

4.4.1 Synthetic inhibitors

Many synthetic metalloprotease inhibitors are commercially available. The selectivity of these inhibitors is influenced by the interaction between the residues in the protease that are in close proximity of the Zn^{2+} ion and the chemical groups on the inhibitor. These interactions stabilise the inhibitor enzyme complex. In this study, a set of four synthetic inhibitors were tested for their potency against ADAM33. These four inhibitors were (i) (2R)-2-[4(-Biphenylylsulfonyl)amino]-3-phenyl propionic acid, the zinc binding group of this compound is the carboxylate ion, (ii) N-Isobutyl-N-(4-methoxyphenylsulfonyl)-glycylhydroxamic acid, (iii) (3R)-(+)-[2-(4-methoxybenzenesulfonyl)-1,2,3,4-tetrahydroisoquinoline-3-hydroxymate and (iv) GM6001; the latter three are hydroxamate compounds. The inhibitors were serially diluted to cover a concentration range of 1.6nM to 5μM and used in a FRET peptide cleavage assay to measure their effect on ADAM33 activity, **Fig.4.6(a).** Three of the inhibitors, (2R)-2-[4(-Biphenylylsulfonyl)amino]-3-phenyl propionic acid, N-Isobutyl-N-(4-methoxyphenylsulfonyl)-glycylhydroxamic acid and GM6001 were shown to be poor inhibitors of ADAM33, with inhibition achieved only at the highest concentration tested. At this concentration, ADAM33 activity could be inhibited by ~40% for (2R)-2-[4(-Biphenylylsulfonyl)amino]-3-phenyl propionic acid and GM6001, and ~60% for N-Isobutyl-N-(4-methoxyphenylsulfonyl)-glycylhydroxamic acid. In contrast, a good dose response was observed for (3R)-(+)-[2-(4-methoxybenzenesulfonyl)-1,2,3,4-tetrahydroisoquinoline-3-hydroxymate. The IC_{50} of this potent inhibitor was estimated from the fitted inhibition curve as 327nM, **Fig.4.6(b)** and at the highest concentration tested (5 μM) it inhibited ADAM33 activity by 90%.

4.4.2 Tissue Inhibitors of Metalloproteinases (TIMPS)

In addition to synthetic inhibitors of metalloproteases, natural inhibitory proteins that regulate metalloproteases *in vivo* were also tested for their potency against ADAM33. TIMP-1, N-TIMP2 and N-TIMP3 were a kind gift from Prof. Gillian Murphy at the University of Cambridge. In experiments similar to those used to assess synthetic inhibitors, the TIMPs were incubated with ADAM33 and then the proteolytic activity was assessed using a FRET peptide cleavage assay. TIMP-1 was tested at 1.8μM to 28nM, N-TIMP-2 was tested at 7.6μM to 28nM, N-TIMP-3 was tested at 1.4μM to 23nM. At the concentrations tested neither TIMP-1 nor N-TIMP-2 were able to inhibit ADAM33 activity, **Fig 4.7(a).**

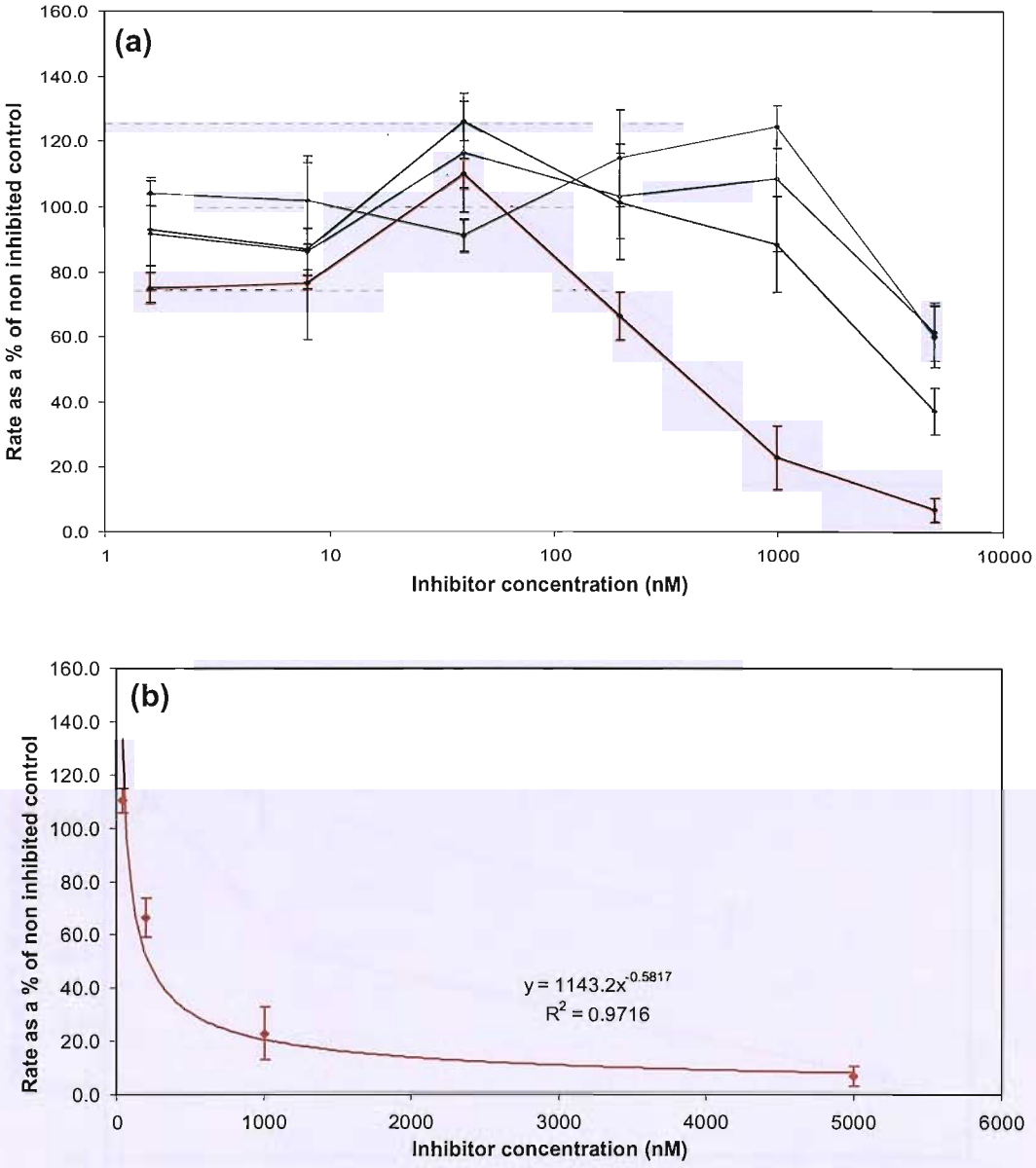

Fig. 4.6. Inhibition of ADAM33 Pro-MP-His using synthetic inhibitors. (a) Four compounds were tested for their ability to inhibit the proteolytic activity of ADAM33 in the FRET peptide assay. Serial dilutions of the compounds covering the range between 1.6nM-5µM were used against 130nM of ADAM33 Pro-MP-His. The assay was carried out in triplicate, and the rate as a percentage of the non inhibited control was plotted using the mean ± 1 standard deviation. The compounds tested were (i) (2R)-2-[4(-Biphenylylsulfonyl)amino]-3-phenyl propionic acid (blue line), (ii) N-Isobutyl-N-(4-methoxyphenylsulfonyl)-glycylhydroxamic acid (green line), (iii) (3R)-(+)-[2-(4-methoxybenzenesulfonyl)-1,2,3,4-tetrahydroisoquinoline-3-hydroxymate] (red line) and (iv) GM6001 (black line). The grey lines on the graphs represent 100% activity (non inhibited controls, mean ± 1 standard deviation). (b)Data from the most potent inhibitor (40nM to 5µM) re-plotted on a linear scale, a curve has been fitted to the data, the equation and R^2 co-efficient is displayed.

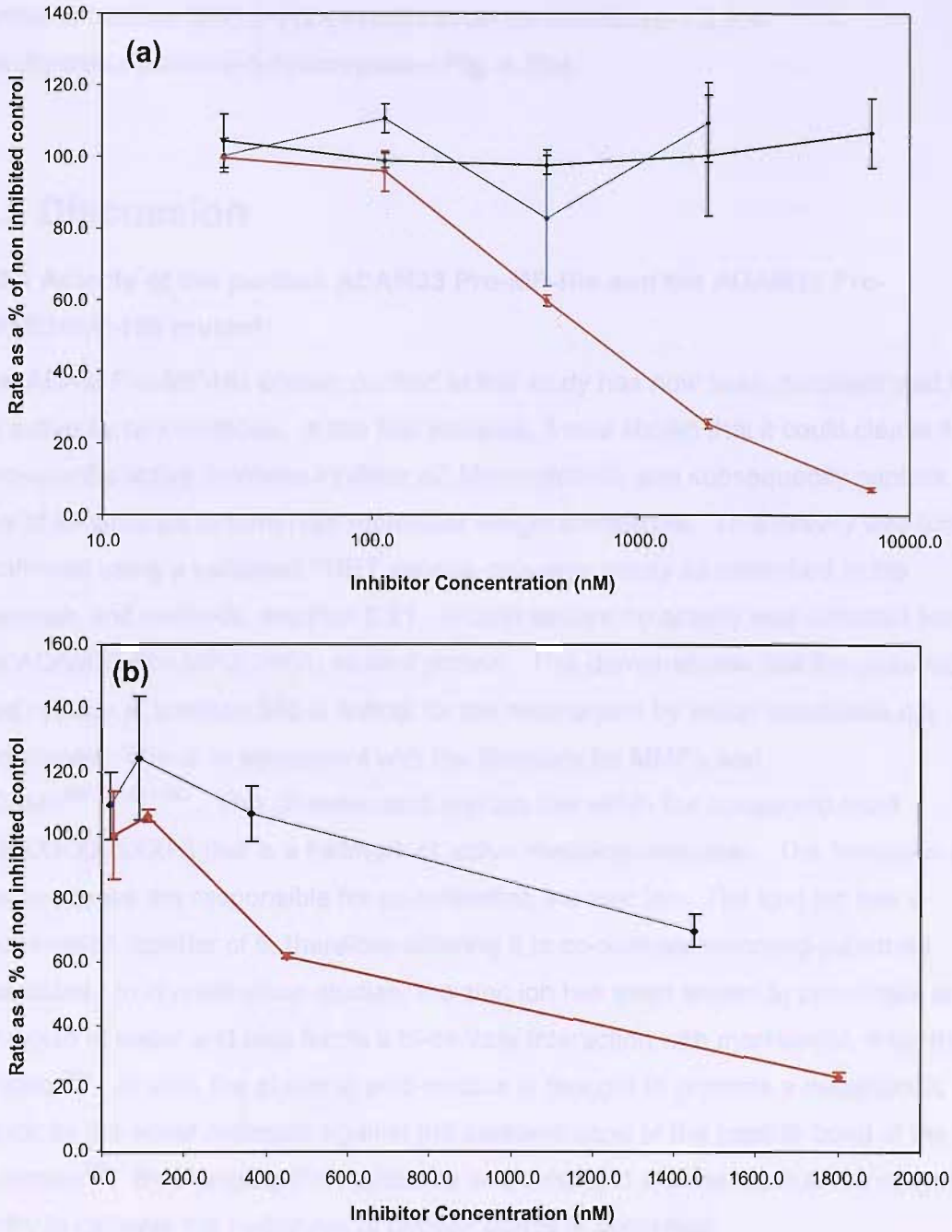

Fig. 4.7. Inhibition of ADAM33 Pro-MP-His by tissue inhibitors of metalloproteinases (TIMPs). TIMP-1, N-TIMP-2 and N-TIMP-3 were tested for their ability to inhibit the proteolytic activity of ADAM33 in the FRET peptide assay. Serial dilutions of the TIMPS were used against 88nM of ADAM33 Pro-MP-His. (a) Graphs showing the data from TIMP-1 (blue line), N-TIMP-2 (green line) and the synthetic inhibitor (3R)-(+)-[2-(4-methoxybenzenesulfonyl)-1,2,3,4-tetrahydroisoquinoline-3-hydroxymate] (red line). The assay was carried out in triplicate (n=3); the mean ± 1 SEM are plotted. (b) Graph showing the data from N-TIMP-3 (blue line) and the synthetic inhibitor (3R)-(+)-[2-(4-methoxybenzenesulfonyl)-1,2,3,4-tetrahydroisoquinoline-3-hydroxymate] (red line). The mean ± 1 standard deviation has been plotted, the graph is representative of one assay carried out in triplicate. TIMPs were kind gifts from Prof. G. Murphy, University of Cambridge.

At the highest concentration tested (1.45 μM) N-TIMP3 was able to inhibit ADAM33 by ~30%. However it appears to a less potent inhibitor in comparison with the potent synthetic inhibitor (3R)-(+)-[2-(4-methoxybenzenesulfonyl)-1,2,3,4-tetrahydroisoquinoline-3-hydroxymate, **Fig. 4.7(b).**

4.5 Discussion

4.5.1 Activity of the purified ADAM33 Pro-MP-His and the ADAM33 Pro-MP(E346A)-His mutant

The ADAM Pro-MP-His protein purified in this study has now been demonstrated to be active by two methods. In the first instance, it was shown that it could cleave the non-specific active protease inhibitor α2-Macroglobulin and subsequently capture one of its subunits to form high molecular weight complexes. This activity was further confirmed using a validated FRET peptide cleavage assay as described in the materials and methods, **section 2.21**. In both assays no activity was detected from the ADAM33 Pro-MP(E346A) mutant protein. This demonstrates that the glutamic acid residue at position 346 is critical for the mechanism by which substrates are hydrolysed. This is in agreement with the literature for MMPs and ADAMs[205;210;251;252]. This glutamic acid residue lies within the conserved motif (HEXXHXXGXXH) that is a hallmark of active metalloproteinases. The histidines in this sequence are responsible for co-ordinating the zinc ion. The zinc ion has a coordination number of 6, therefore allowing it to co-ordinate incoming substrate molecules. In crystallisation studies, the zinc ion has been shown to coordinate one molecule of water and also forms a bi-dentate interaction with marimastat, a synthetic inhibitor[234]. *In vivo*, the glutamic acid residue is thought to promote a nucelophilic attack by the water molecule against the carbonyl bond of the peptide bond of the substrate[253]. By changing this residue to an uncharged alanine residue the enzyme's ability to catalyse the hydrolysis of peptide bonds is abolished.

4.5.2 The effect of cations and ionic strength on enzyme activity

Given the central role of the zinc ion in the catalytic mechanism of ADAM33, the effect of exogenously added zinc ion concentration on enzyme activity was determined. Low concentrations of exogenous zinc chloride in the assay buffer increased ADAM33 activity, but further increases over 10μM had minimal effect. There was a gradual decrease in the level of activity with zinc chloride concentrations above 20 μM, but the spread in the data means that it was not significant in this

study. The study by Zou *et al.* showed a similar trend, with enzyme activity falling with increasing zinc chloride concentration. However, in their study they did not observe an increase in activity at low concentration of zinc chloride. This maybe in part explained by the treatment of the enzyme preparation before use. In this study, ADAM33 protein purified on the final gel filtration step was stored in the elution buffer containing imidazole. Imidazole can co-ordinate the zinc ion and therefore a high concentration imidazole may sequester the zinc ion. This had the advantageous effect of preventing autocatalytic degradation of the ADAM33, but by reducing its activity in this manner, additional zinc chloride may have been required to overcome the inhibitory effect of the imidazole. In the study by Zou *et al.* the concentrated ADAM33 enzyme stock was diluted in a dilution buffer containing 20 μM of zinc chloride before being used in the activity assays. This dilution step may have provided enough zinc ions to overcome the effects of imidazole and thus eliminated the need for further increases of zinc chloride in the assay[235].

The crystal structure of ADAM33 identified a calcium binding site on the metalloproteinase domain of the enzyme. The calcium ion is co-ordinated by residues Asp296, Asn407, Glu213, and the backbone carbonyl oxygen of Cys404[234]. This calcium binding motif is highly conserved among ADAMs and is present in ADAM33's closest related family members, ADAM13 and ADAM19[254]. It is thought that this binding motif increases the stability of the protease[234]. In addition, it can be speculated that the binding of a calcium ion may alter the interaction between the substrate and the enzyme in a favourable manner despite it being some distance from the active site, **Fig. 4.8**. This may explain the improvement in activity in ADAM33 as the availability of calcium ions was increased to 10mM or more. In the study by Zou *et al.* they found that calcium concentration below 10mM inversely affected enzymic rate, and above 10mM the effect was proportional to the enzyme activity. However, this initial adverse effect on enzymic rate was not observed in this study, though the reasons why this is the case, is not completely clear.

Increasing the ionic strength around ADAM33 also improved its activity, possibly by stabilising the charges of some of the residues in the FRET peptide at pH7.0. The trend seen in this study is in agreement with the that reported in the literature over the range of sodium chloride concentration tested[235].

Fig. 4.8. Ribbon structure of the ADAM33 metalloproteinase domain. The metalloproteinase domain of ADAM33 complexed to the inhibitor marimastat (ball and stick) in its active site. The Zn^{2+} ion and the Ca^{2+} ion are depicted as red and yellow spheres respectively. The image was generated using Kinemage software, version 1.39. The 1R55 PTB file depositied by Orth *et al.* (published 2004) was used to create the image.

The optimal ion concentrations that have been determined for ADAM33 can be applied to this particular FRET peptide substrate, but since these conditions have implication not only for the enzyme but also the substrate, different peptide or protein substrates identified in the future may exhibit altered activity profiles. So, whilst the conditions we have found are useful and the most suitable for our immediate studies, the optimal parameters for differing substrates will have to be empirically determined.

4.5.3 The effect of pH on enzyme activity

It is thought that ADAM33 functions on the extracellular surface under normal physiological conditions. Therefore it is logical that the proteinase should function around physiological pH at pH7 to 7.5. In this study the enzyme also showed considerable activity at pH5.0. This was unexpected and differs from the study by Zou *et al.*[235]. The ability of ADAM33 to function at low pH leads one to speculate whether it could be active in the acidic secretory vesicles after having undergone furin mediated maturation. The activity of ADAM19 (the closest human family member to ADAM33) has been shown to be upregulated by autocatalytic processing in the cysteine rich domain[251]. This processing is thought to take place in the secretory pathway. Based on the increasing evidence to suggest that metalloproteinases can be directly influenced by proteolysis other than during Pro domain processing, in addition with the mass spectroscopy data in **Chapter 3, (Fig.3.20)** that shows that mature ADAM33 Pro-MP-His is smaller than the expected size, it is interesting to speculate whether ADAM33 is also under the influence of similar regulatory mechanisms.

4.5.4 Enzyme Kinetics

It was apparent from the saturation plots that high substrate concentration had an adverse effect on ADAM33 activity, under the experimental conditions used for the FRET peptide cleavage assay. At the highest substrate concentration tested, ADAM33 activity decreased relative to that seen at a lower substrate concentration. It is therefore likely that this inhibitory effect reduced the observed activity of ADAM33 at high concentrations. This may explain why the calculated values for Km and Vmax are greater than that estimated directly from the saturation plot alone. The Km value observed was ~14 fold smaller than the reported value for a poorer substrate, the wild type APP peptide (EVHHQKLVFF)[205]. This shows that the modified APP peptide (YEVAHQKLVF) interacts with ADAM33 with higher affinity as expected since it was designed to be a better substrate[235]. The Kcat/Km constant

can be used as a measure of enzyme efficiency. The apparent Kcat/Km that was found in this study ~$3.3x10^2$ $M^{-1}s^{-1}$ was ~100 times less than the reported value in another study[235]. This may be a result of underestimating Kcat in our system, because of the suppressed activity observed at high substrate concentration, since Kcat is calculated by dividing Vmax by the enzyme concentration.

4.5.5 ADAM33 sensitivity to inhibitors- synthetic MMP inhibitors

The ability and potency of a synthetic inhibitor to inhibit a metalloproteinase is largely determined by its ability to bind to the zinc ion in the active site, and make it unavailable for binding substrate. Synthetic inhibitors with a hydroxamate zinc binding group are more potent inhibitors than those which use the carboxylate group to co-ordinate the zinc ion. Although both zinc binding groups can form bi-dentate interactions with the zinc ion, the distance between the two oxygens of the hydroxamate group are ideally spaced to interact with the zinc ion[255]. Therefore this may explain why the carboxylate inhibitor (2R)-2-[4(-Biphenylylsulfonyl)amino]-3-phenyl propionic acid was a poor inhibitor of ADAM33. The order of potency for the three hydroxamate inhibitors were found to be GM6001< N-Isobutyl-N-(4-methoxyphenylsulfonyl)-glycylhydroxamic acid < (3R)-(+)-[2-(4-methoxybenzenesulfonyl)-1,2,3,4-tetrahydroisoquinoline-3-hydroxymate. The ability of the latter inhibitor to be a good inhibitor probably stems from the ability of the residues from the ADAM33 to interact with chemical groups on the inhibitor which could have stabilised the interaction.

One difficulty in using synthetic metalloproteinase inhibitors as research reagents in *in vitro* and *in vivo* systems is that they are not always specific to one metalloprotease, making it hard to assign observed effects to the function of one particular enzyme. In the absence of a more specific inhibitor, it then becomes useful to use several inhibitors of varying overlapping specificities. The involvement of one particular metalloproteinase can then be distinguished from another by studying the sensitivity of the observed effect to different inhibitors.

This study has identified a new inhibitor for ADAM33 with an IC_{50} value of 327nM, whilst demonstrating that a broad spectrum inhibitor GM6001 at comparative concentrations was not particularly effective. GM6001 is a broad spectrum inhibitor which can inhibit MMP1,2,8 and 9 (Ki <0.6nM), MMP-3 (Ki=27nM) [256] as well inhibiting the cleavage of auto-peptide by ADAM19 (IC_{50}=447nM)[257] and the

hydrolysis of recombinant CD40[258] *in vitro* by ADAM17 [258]. Therefore the use of 3R)-(+)-[2-(4-methoxybenzenesulfonyl)-1,2,3,4-tetrahydroisoquinoline-3-hydroxymate in parallel with GM6001 will be extremely useful in further inhibition studies in cell based systems and potentially *in vivo*, to distinguish the effects mediated by other metalloproteases and ADAMs from those of ADAM33. To make this even more effective it would be advantageous to establish the potency of 3R)-(+)-[2-(4-methoxybenzenesulfonyl)-1,2,3,4-tetrahydroisoquinoline-3-hydroxamate against other ADAMs.

4.5.6 ADAM33 sensitivity to inhibitors- Tissue Inhibitors of Metalloproteinases (TIMPS)

Tissue inhibitors of metalloproteinases (TIMPs) inhibit metalloproteinase activity by binding to MMPs in a 1:1 ratio via the N-terminal domain. To date, four TIMPs have been identified TIMP-1,-2,-3 and- 4. In *vivo*, the activities of the MMPs are very much dependent on the balance between the relative levels of MMPs and TIMPs. TIMPs have different specificity profiles against MMPs, and it is reported that they are can also differentially inhibit ADAM proteins[259]. Given the similarity between the MP domain of ADAM proteins and the MMPs this was not wholly unexpected. Studies using *in vitro* cleavage assays show that TIMP-1 and TIMP-3 were able to inhibit ADAM10 mediated cleavage of MBP[244], and that ADAM17 cleavage of a peptide derived from TNFα can be inhibited strongly by TIMP-3 and only very weakly by TIMP-2 and TIMP-4 [260]. In addition recent studies have shown that although TIMP-1 could not inhibit ADAM33, TIMP2 was weakly inhibitory with ki=660nM±150nM, and TIMP-3 and -4 were good inhibitors with Ki= 7nM±1nM and 40±10nM.

In line with the literature, out of the three TIMPs which were tested (TIMP-1, N-TIMP-2 and N-TIMP-3) in this study, N-TIMP3 was the most potent at inhibiting the purified ADAM33 enzyme activity. On the contrary, the tested concentrations of TIMP-2 did not show any inhibition. Since it is a supposedly less potent inhibitor, it could be that its concentration needs to be increased before an effect can be observed. It was somewhat surprising that TIMP-3 could inhibit both ADAM33 and ADAM17, since the two ADAMs are distantly related in the ADAM family and are known to have relatively different substrate specificity profiles. ADAM33 is unable to cleave TNFα and EGF superfamily derived peptides unlike ADAM17 [205]. TIMP-3 is unusual amongst the TIMPs, TIMP-1,-2 and -4 are soluble but once TIMP-3 is secreted it becomes

strongly associated with the extracellular matrix (ECM)[261]. It is therefore in a prime position to influence the storage and release of growth factors from the ECM, and also modulate the migratory and adhesive behaviour of cells secreting MMPs in tissues, as well as general matrix homeostasis. This leaves open the possibility that TIMP-3 could be an important functional inhibitor of ADAM33 catalytic activity *in vivo.*

4.5.7 Summary

The FRET peptide cleavage assay has been used successfully to re-confirm the activity of purified recombinant ADAM33 enzyme. The optimal conditions for *in vitro* enzyme activity in terms of concentration of divalent metal ions (Ca^{2+} and Zn^{2+}), salt concentration (NaCl) and pH have been determined. The hydroxamate compound (3R)-(+)-[2-(4-methoxybenzenesulfonyl)-1,2,3,4-tetrahydroisoquinoline-3-hydroxymate has been described as a potent inhibitor of ADAM33 for the first time. TIMP-3 has also been confirmed as an inhibitor of ADAM33, in agreement with the published literature. Using the information gained regarding the biochemical activity of ADAM33 and the identified inhibitors, the study of ADAM33 can now be directed towards the functional relevance of ADAM33 using cellular models.

Chapter 5 A functional role for ADAM33

A study by Lee *et al.* has demonstrated the presence of ADAM33 in bronchoalveolar lavage (BAL) fluid of both healthy and asthmatic individuals (n=10 and 35 respectively). The level of ADAM33 found was markedly increased in asthmatics in comparison with the normal controls and correlated with decreased lung function (FEV_1). The form of ADAM33 detected was of an unusually low molecular weight at 55kDa and was speculated to be a soluble form of ADAM33 containing the MP domain[232]. This suggested that soluble ADAM33 may be involved in asthma pathogenesis. The purification and characterisation of a recombinant form of ADAM33 has been described in **chapter 3 and 4.** Like the form of soluble ADAM33 found *in* vivo, the recombinant form contains the MP domain but lacks the cytoplasmic tail. Using the recombinant ADAM33 protein as a model of soluble ADAM33, the biological relevance of ADAM33 could be examined in more detail. This chapter was aimed at widening the scope of the study to demonstrate whether:

(i) ADAM33 Pro-MP-His mediated proteolysis could exert a functional effect in a cellular model *in vitro*, and importantly whether the effect seen might be relevant to asthma pathogenesis and airway remodelling.

(ii) the synthetic inhibitors that can antagonise ADAM33 activity in biochemical assays could also interfere with ADAM33 activity in a cellular model.

5.1. Exogenous addition of ADAM33 to epithelial cells

The presence of ADAM33 in the BAL fluid indicated that *in vivo* ADAM33 is in contact with the lumenal surface of the airways. Its increased presence in the asthmatic airway led to the speculation that epithelial cells may be a proteolytic target for soluble ADAM33, and this was the basis for studying the effect of exogenous ADAM33 Pro-MP-His treatment of epithelial cells.

5.1.1 Epithelial cells cultured on tissue culture plastic

In a preliminary experiment, exogenous ADAM33 Pro-MP-His was added to epithelial cells to observe if it could mediate an observable effect. When A549 cells derived from lung carcinoma were seeded onto tissue culture plastic, the cells grew as a typical monolayer with a cobblestone appearance. When these cells were treated

with either buffer, ADAM33 Pro-MP-His (150ng/ml) or ADAM33 Pro-MP(E346A)-His on a daily basis, no marked differences in organisation or morphology of the cells were observed between any of the treatment groups, **Fig.5.1**.

5.1.2 Epithelial cells cultured on matrigel

To simulate a culture environment that bears a little more resemblance to what might occur *in vivo*, instead of seeding the A549 cells directly onto plastic, cells were cultured on growth factor reduced matrigel, a basement membrane like substance derived from the EHS tumour cell line. The A549 cells seeded onto growth factor reduced matrigel were maintained in DMEM containing 1% serum and treated daily with buffer, ADAM33 Pro-MP-His (150ng/ml) or ADAM33 Pro-MP(E346A)-His (150ng/ml). It was found that the A549 epithelial cells that were seeded onto matrigel did not grow as a typical monolayer like that seen when these cells were grown on tissue culture plastic. On matrigel, the epithelial cells adhered and migrated to form a mesh-like network. Over a three day treatment period in which the treatments were renewed daily, the morphology of the cells was observed using light microscopy. The morphology and organisation of the cells were similar regardless of whether cells were treated with ADAM33 Pro-MP-His or the ADAM33 Pro-MP(E346A)-His inactive control, **Fig. 5.2**. However in all cases the epithelial cells gradually changed their organisation and became more aggregated over the course of the experiment.

5.1.3 Differentiated epithelial cell cultures

As A549 cells are alveolar in origin, studies were also undertaken to investigate the effects of ADAM33 on bronchial epithelial cells since asthma is thought to be a disease of the large airways. Primary human epithelial cells derived from bronchial brushings can be grown in transwells as an air-liquid interface (ALI) culture. Under these conditions primary epithelial cells differentiate and cilia can be seen to beat on the apical surface. This is an established *in vitro* model used to mimic the airway epithelium *in vivo*[262]. ALI cultures of differentiated epithelial cells from a healthy individual were provided courtesy of Synairgen Research Ltd (Southampton, UK). Cells were treated both apically and basally with either buffer, ADAM33 Pro-MP-His or ADAM33 Pro-MP(E346A)-His, with treatments being replenished every 1-2 days. Cells were checked daily by light microscopy for changes in cell morphology or organisation, but very little change was observed in the cells from day to day, and between the different treatments.

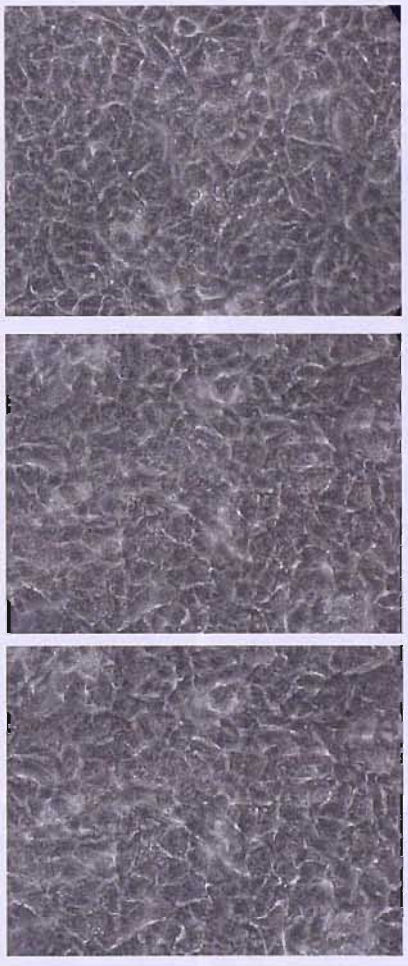

Fig. 5.1. A549 epithelial cells treated with ADAM33. A549 cells were seeded into a 12 well plate and allowed to adhere overnight. The following day, the cells were serum starved in Ultraculture medium for 24 hours, after which they were treated with 20μM of zinc chloride with either a buffer control, ADAM33 Pro-MP-His (150ng/ml) or ADAM33 Pro-MP(E346A)-His (150ng/ml). Cells were re-treated with enzyme daily. Cells were viewed using phase contrast on a inverted Leica light microscope. The panels show the cells at day 3 after the initial treatment and are representative of one experiment carried out in duplicate.

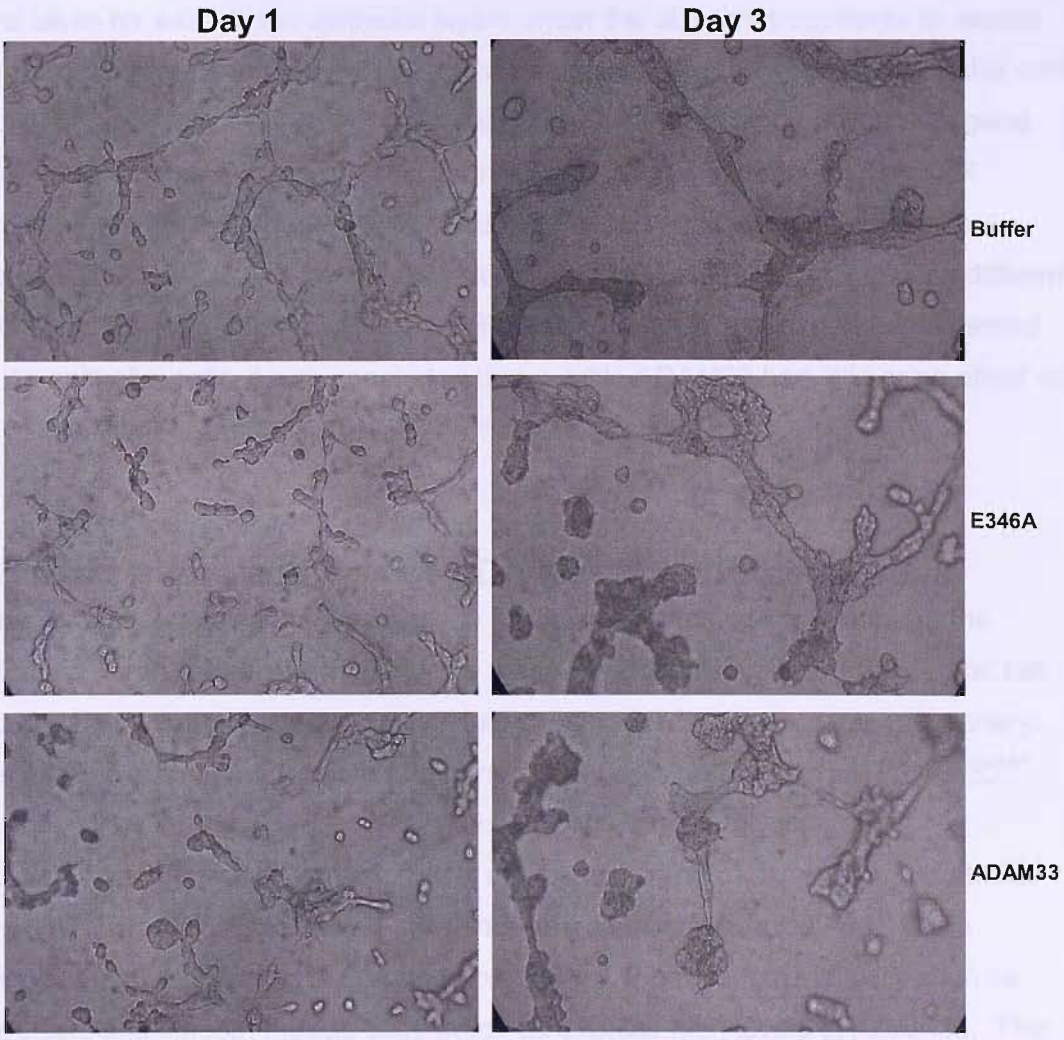

Fig. 5.2. ADAM33 treated epithelial cells grown on matrigel. A549 cells were seeded at $2x10^4$cells/well (96 well plate) onto growth factor reduced matrigel in complete M199 medium containing 1% serum with 20μM $ZnCl_2$, in addition to one of the following, buffer control, ADAM33 Pro-MP-His (150ng/ml) or ADAM33 Pro-MP(E346A)-His. Treatments were replenished on the second day post treatment. Cells were viewed using phase contrast on a inverted Leica light microscope. Panels show images taken 1 and 3 days post treatment. Panels are representative of two experiments, each carried out in duplicate.

As allergen derived proteases have been reported to disrupt the tight junctions between epithelial cells, the possibility that ADAM33 might also affect the epithelial barrier permeability was evaluated. Trans-epithelial resistance (TER) measurements were taken for each of the epithelial layers under the different treatments to assess the permeability and integrity of the epithelial barrier. Typically healthy epithelial cells form tight junctions between adjacent cells and can collectively function as a good barrier and will therefore give high TER readings. In this experiment, the TER readings from the cells treated with ADAM33 Pro-MP-His were similar from those treated with ADAM33 Pro-MP(E346A), although the readings taken between different days could be quite variable, **Fig. 5.3.** Based on the collective experiments carried out on epithelial cells, it was concluded that soluble ADAM33 had little or no effect on the morphology or barrier permeability of epithelial cells.

5.2 Exogenous addition of ADAM33 to endothelial cells

In the remodelled airway, an increase in vascularity is necessary to support the increased fibroblast and smooth muscle mass. Endothelial cells are the central cell type involved in angiogenesis. Initial studies using RT-PCR on primary pulmonary artery lung endothelium indicated that endothelial cells do not express *ADAM33*[181]. This has since been confirmed in the Brooke Laboratory (University of Southampton,UK) using TaqMan qPCR carried out on human vascular endothelial cells (HUVECs) (HM Haitchi and I Puxeddu, personal communication). In the airways, the blood vessels are in close proximity with mesenchymal cells such as fibroblasts and smooth muscle cells which do express high levels of ADAM33. The potential for a secreted form of ADAM33 suggests that endothelial cells can be adjacent to cells releasing a soluble form of ADAM33[232]. So despite their lack of *ADAM33* expression, endothelial cells may still encounter ADAM33 and be a target for its proteolytic activity. Thus, the effect of exogenous ADAM33 Pro-MP-His treatment on endothelial cells *in vitro* was evaluated. All the endothelial cell work was carried out with Dr Ilaria Puxeddu who contributed equally to the study.

5.2.1 The endothelial cell differentiation model

HUVECs routinely passaged on gelatin coated plastic in complete growth medium grew to become a confluent monolayer, and had a cobblestone-like appearance. When grown on top of growth factor reduced matrigel and maintained in medium containing 20% serum, the HUVECs differentiated and distinct changes in their morphology and organisation were apparent. As the HUVECs differentiated they lost

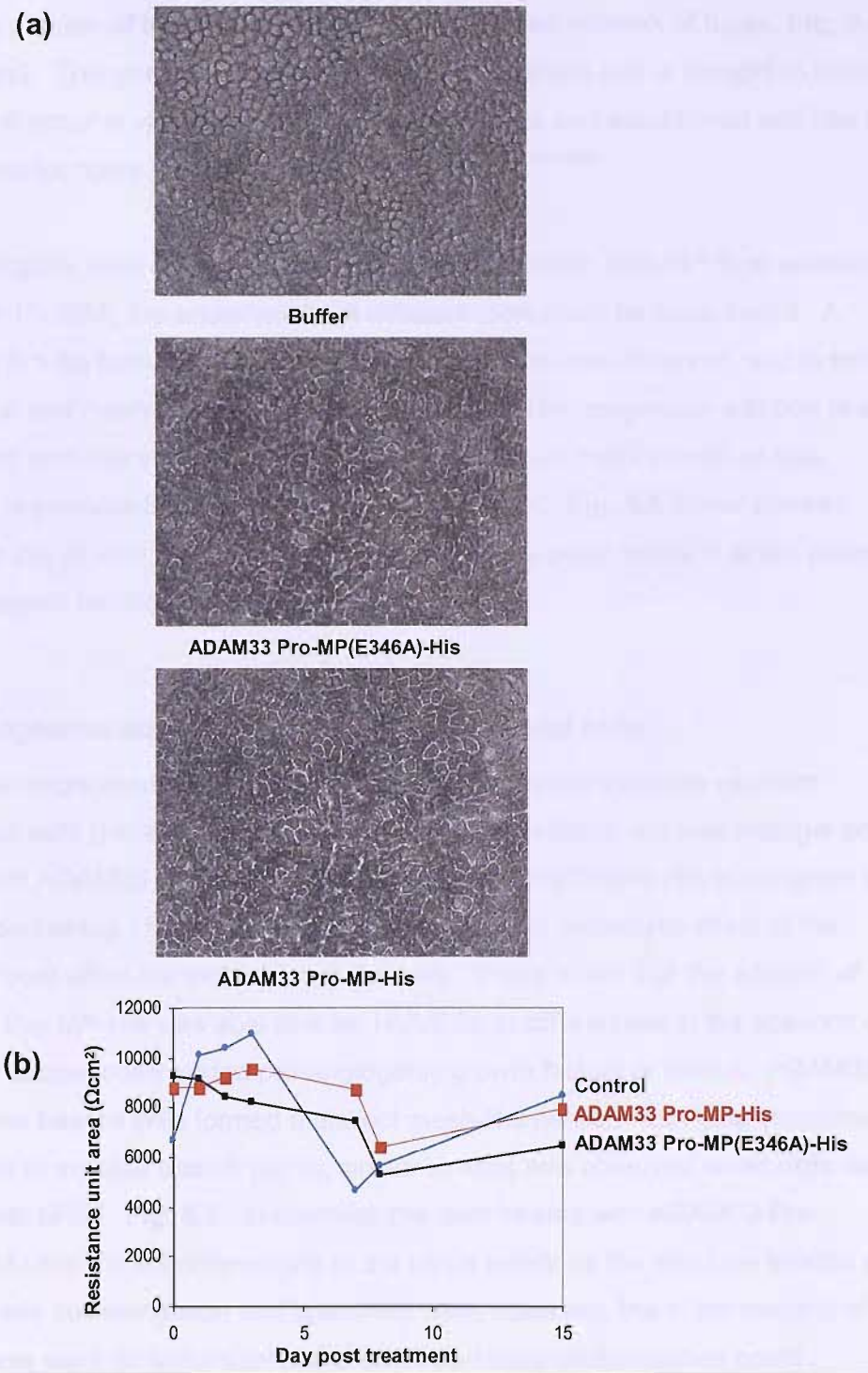

Fig. 5.3. Primary differentiated epithelial cell cultures treated with ADAM33. Bronchial epithelial cells from a normal subject were grown as a differentiated culture using an air-liquid interface differentiation model. Cells were apically and basally treated with either a buffer control, ADAM33 Pro-MP-His (150ng/ml) or ADAM33 Pro-MP(E346A)-His (150ng/ml) in the presence of 20μM $ZnCl_2$ every 1-2days. Cells were checked daily, but very little variation was observed in the organisation or appearance of the cells. (a) Representative photographs taken at day 2 post treatment under phase contrast on an inverted Leica light microscope (x20 objective). (b) Trans-epithelial resistance was measured across the epithelial layer at several time points using an epithelial voltohmmeter (World Precision Instruments Inc. Hertfordshire, UK). Mean values for buffer (blue), ADAM33 Pro-MP-His (red) and ADAM33 Pro-MP(E346A)-His (black) treated cells have been plotted. Results are representative of one experiment carried out in duplicate.

their flat rounded shape and the cells became elongated and connected to each other at a number of branch points forming a mesh-like network of tubes, **Fig. 5.4** (top panels). This phenotypic change is well documented and is thought to mimic the events that occur *in vivo*. This kind of *in vitro* assay is well established and has been used to test for novel pro and anti-angiogenic factors[263-265].

By reducing the level of serum in the culture medium from 20% to 1% or substituting serum for 1% BSA, the endothelial cell differentiation could be suppressed. A reduction in tube formation and hence mesh formation was observed, and in some cases tube and mesh formation were non-existent. The exogenous addition of a pro-angiogenic stimulus such as bFGF-2 into the low serum culture medium was sufficient to promote the cells to become differentiated, **Fig. 5.4** (lower panels). Therefore this *in vitro* system was determined to be a good model in which potential pro-angiogenic factors could be tested.

5.2.2 Exogenous addition of ADAM33 to endothelial cells

In a similar experiment to the epithelial experiment, primary human vascular endothelial cells (HUVECs) were seeded onto growth factor reduced matrigel and treated with ADAM33 Pro-MP-His or ADAM33 Pro-MP(E346A)-His in complete M199 medium containing 1% serum, to observe whether the proteolytic effect of the enzyme could affect the behaviour of the cells. It was found that the addition of ADAM33 Pro-MP-His was able to drive HUVECs to differentiate in the absence of any other exogenously added pro-angiogenic growth factors or stimuli. ADAM33 Pro-MP-His treated cells formed a distinct mesh-like network with tube structures connected at multiple branch points, similar to what was observed when cells were treated with bFGF, **Fig. 5.5**. In contrast, the cells treated with ADAM33 Pro-MP(E346A)-His did not differentiate to the same extent as the wild type treated cells. Occasionally cell elongation and branching were observed, but in the majority of cases these went on to form far fewer tubes and incomplete meshes could sometimes be seen. A complete mesh was considered to be a closed ring, in which several endothelial tubes connected to form an unbroken perimeter. Generally cells treated with ADAM33 Pro-MP(E346A)-His appeared to be similar to the buffer treated controls, but in a number of cases it was noted that the level of cell elongation and spontaneous differentiation was reduced to below that seen in the buffer control. The tube promoting effect of the ADAM33 Pro-MP-His was reproducible in HUVEC cells of differing passages and also confirmed using cells derived from a second donor (data not shown). ADAM33 Pro-MP-His was able to induce differentiation at all three

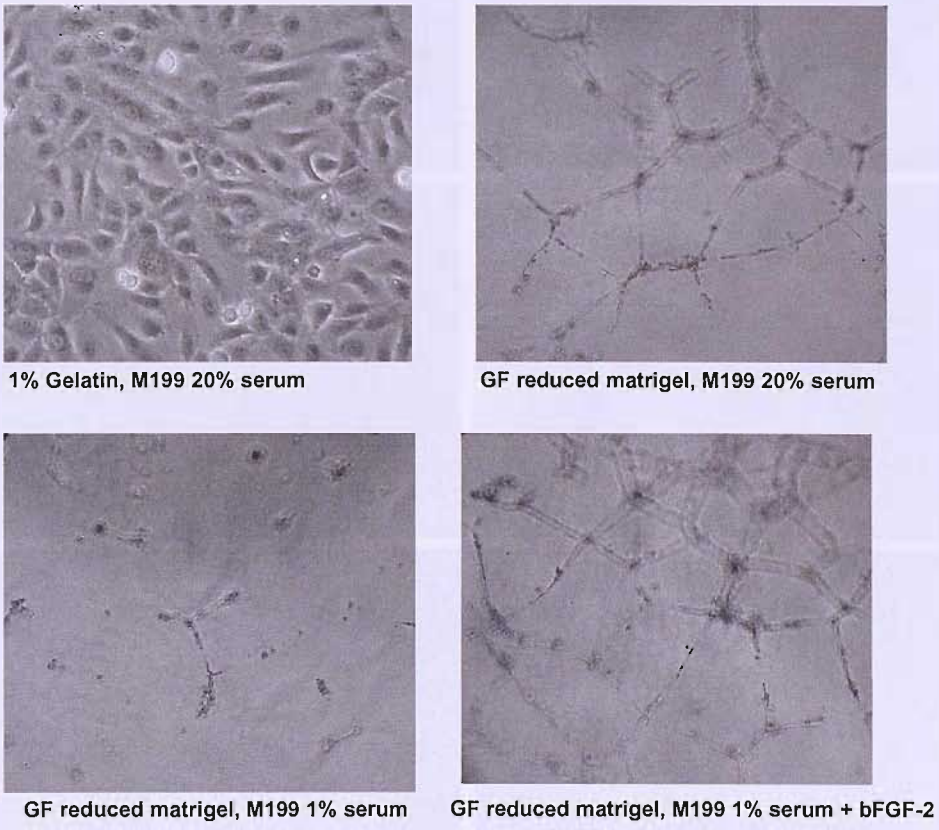

Fig. 5.4. Cultured primary human vascular endothelial cells. Primary HUVECs cultured under different conditions organise themselves differently. Cells grown on 1% gelatin coated plastic and maintained in complete M199 serum containing 20% serum grew as monolayers (top left). Cells maintained in the same medium but grown on growth factor reduced matrigel instead of gelatin differentiated into a network of tubes (top right). By reducing the level of serum in the medium from 20% to 1% the differentiation of the HUVECs was minimised (bottom left). The exogenous addition of a pro-angiogenic factor bFGF-2 into the medium containing 1% serum, induced the HUVECs to differentiate into tubes (bottom right).

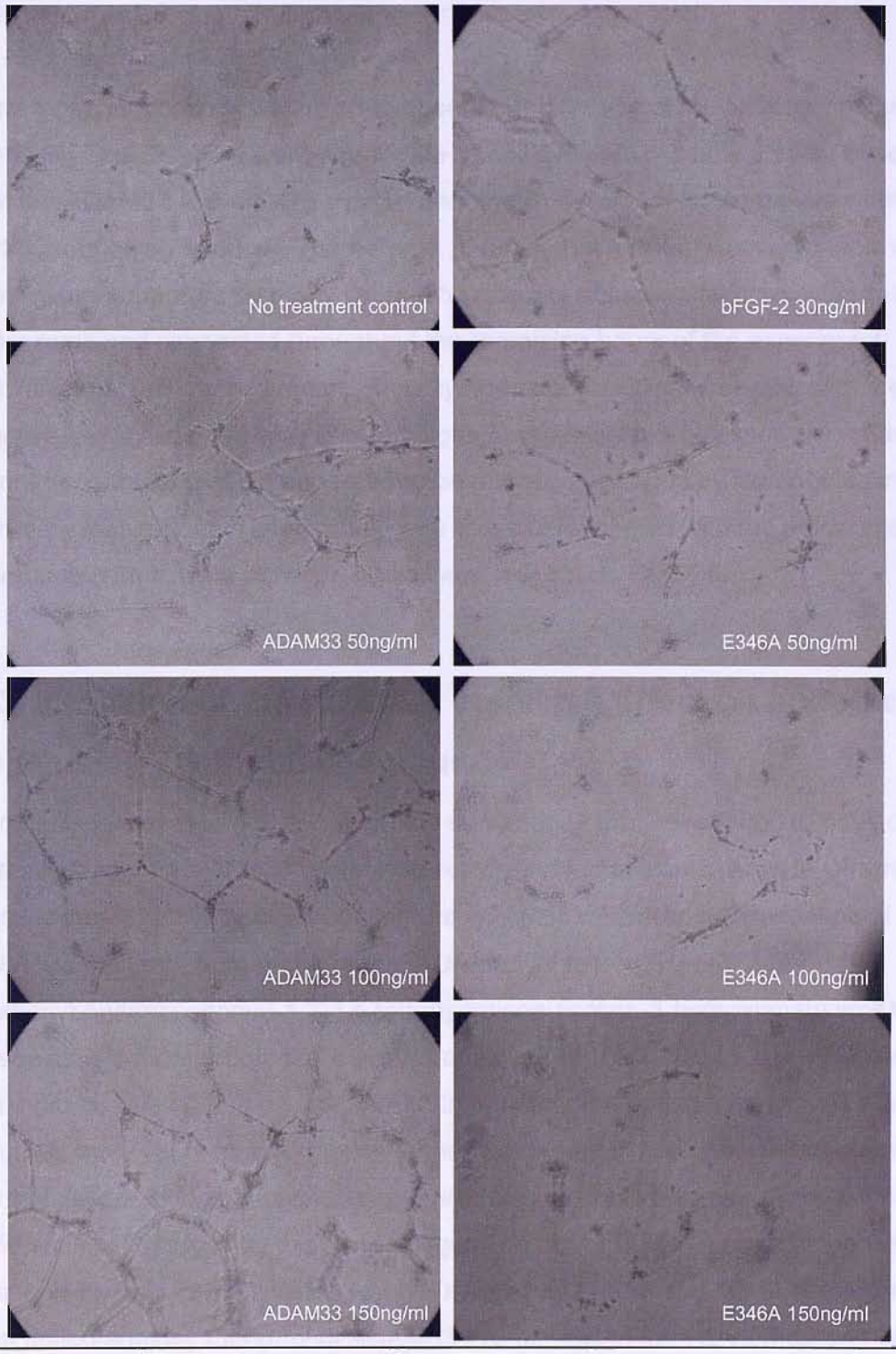

Fig. 5.5. ADAM33 induction of human vascular endothelial cell tube formation. HUVECs were seeded at ~4x10^4 cells/well onto growth factor reduced matrigel coated plastic (96 well plate). Cells were seeded in compete M199 medium containing 1% serum in addition with 20μM $ZnCl_2$ and one of the following treatments: ADAM33 Pro-MP-His (50, 100, 150ng/ml), ADAM33 Pro(E346A)-MP-His (50, 100, 150ng/ml) or bFGF-2 (30ng/ml). Tube formation was allowed to take place overnight. Cells were then viewed under phase contrast on an inverted Leica microscope. Panels are representative of 2 experiments, each carried out in duplicate.

of the concentrations tested (50ng/ml, 100ng/ml and 150ng/ml). There was an indication of a dose response, with the two higher concentrations promoting more complete mesh formation than the lower concentration tested.

Time lapse microscopy was used to observe the kinetics of the tube formation process. The HUVECs were seen to be a very dynamic cell type. It was observed that the ADAM33 Pro-MP-His treated endothelial cells began to organise within the first hour of being seeded. The network of tubes that formed was very stable and tubes were supported by many cells. The majority of tubes that connected to each other remained connected throughout the remaining hours of the experiment, resulting in a well defined mesh. Initially, the endothelial cells treated with the inactive mutant enzyme also showed signs of organisation, however fewer tubes formed and those that did appeared to be thinner, supported by fewer cells and generally less robust in comparison with those cells treated with the active enzyme. Over time connections between tubes were less stable **Fig. 5.6**.

5.3 Inhibition of the ADAM33 mediated effect on endothelial cells using synthetic compounds

Synthetic carboxylate and hydroxamate compounds that were found to have different potencies against ADAM33 proteolytic activity in biochemical assays in **Chapter 4** were tested for efficacy at abrogating the ADAM33 mediated differentiation of HUVECs. Initially, 5μM of the potent ADAM33 inhibitor (3R)-(+)-[2-(4-methoxybenzenesulfonyl)-1,2,3,4-tetrahydroisoquinoline-3-hydroxymate was tested to see its affect on endothelial cell differentiation, **Fig. 5.7**. It was demonstrated that the inhibitor was able to disrupt ADAM33 induced differentiation of HUVECs and returned the level of tube formation to the spontaneous level seen in the buffer control. In addition, the inhibition appeared to be selective as it did little to inhibit the differentiation induced by the pro-angiogenic factor bFGF-2. A dose response for this inhibitor was demonstrated when 50nM, 500nM, 5μM and 50μM of this inhibitor was tested against 150ng/ml of ADAM33 Pro-MP-His in the HUVEC differentiation assay, **Fig. 5.8(a)**. It was found that at the two lower concentrations the HUVECs were still able to differentiate into tube like structures but the walls of the mesh appeared to be more fragile with decreased thickness than those seen in the no-inhibitor control. When the inhibitor was present at 5μM, not only were the walls of the mesh thin, the number of complete meshes formed was also markedly decreased. This resembled the ADAM33 Pro-MP(E346A)-His treated cells. At an

inhibitor concentration of 50μM, the effect of the exogenous ADAM33 treatment was completely antagonised and the level of endothelial cell differentiation was below that expected from spontaneous differentiation (by comparison with the buffer treated control). The intrinsic ability of the endothelial cells to differentiate however, was not substantially affected by this inhibitor and differentiation could be induced when cells were treated simultaneously with bFGF-2 and the inhibitor.

The efficacy of three other protease inhibitors ((2R)-2-[4(-Biphenylylsulfonyl)amino]-3-phenyl propionic acid, N-Isobutyl-N-(4-methoxyphenylsulfonyl)-glycylhydroxamic acid and GM6001 at inhibiting the effects of ADAM33 in this *in vitro* assay were also determined. The inhibitors were tested at 5μM and 50μM against 150ng/ml of ADAM33 Pro-MP-His, see **Fig. 5.8(b)(c)**. It was found that (2R)-2-[4(-Biphenylylsulfonyl)amino]-3-phenyl propionic acid could inhibit the ADAM33 mediated effect, but it was less potent than (3R)-(+)-[2-(4-methoxybenzenesulfonyl)-1,2,3,4-tetrahydroisoquinoline-3-hydroxymate. The inhibitory effects of N-Isobutyl-N-(4-methoxyphenylsulfonyl)-glycylhydroxamic acid and GM6001 were even less pronounced.

5.4 Quantification of endothelial cell tube formation

Assessment of endothelial cell tube formation experiments has been for many years largely descriptive and subjective. More recently, computer assisted image analysis of the experiments has become available to allow increased consistency in assessment[266]. Based on the results shown in **Figures 5.5 – 5.8**, the number of complete meshes was the parameter which was most influenced by ADAM33, therefore further experiments were performed to quantify the effect of ADAM33 Pro-MP-His and the mutated enzyme on endothelial tube formation in the absence or presence of (3R)-(+)-[2-(4-methoxybenzenesulfonyl)-1,2,3,4-tetrahydroisoquinoline-3-hydroxymate. When the Leica Qwin v3 software package became available in our laboratory, images taken at the endpoint of these experiments were analysed for mesh formation, **Fig. 5.9**. This revealed that ADAM33 Pro-MP-His (150ng/ml) significantly ($p<0.01$) promoted endothelial cell tube formation whereas the mutant was without effect. As suggested in preliminary experiments, (3R)-(+)-[2-(4-methoxybenzenesulfonyl)-1,2,3,4-tetrahydroisoquinoline-3-hydroxymate (5μM) significantly ($p<0.01$) inhibited the pro-angiogenic effect of ADAM33 Pro-MP-His, but had no effect on the activity of FGF2, **Fig.5.9**.

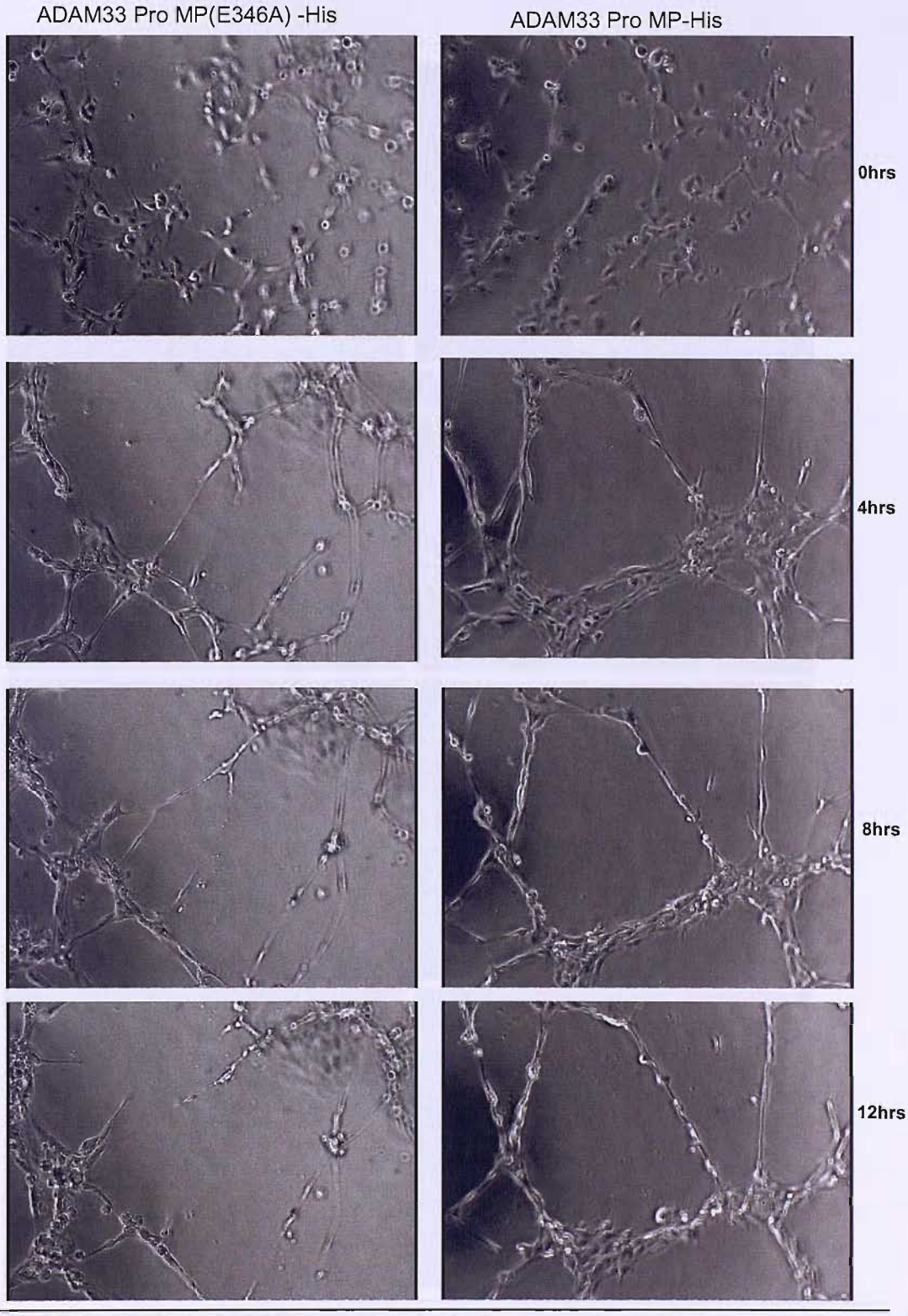

Fig. 5.6. Time lapse of ADAM33 induced HUVEC tube formation. HUVECs were seeded onto a layer of polymerised growth factor reduced matrigel in complete M199 medium containing 1% serum (in a 96 well plate). The cells were treated at the time of seeding with ADAM33 Pro-MP-His or ADAM33 Pro-MP(E346A)-His at 150ng/ml in the presence of 20μM zinc chloride. The cells were put in a heated chamber (37°C) with 5% CO_2 and imaged over a period of 12 hours, with one image being taken every 5 minutes (Olympus IX81 microscope with a motorised stage, ORCA-AG firewire digital camera). The panels above show the images of the cells taken at time = 0, 4, 8, 12 hours and are representative of one experiment.

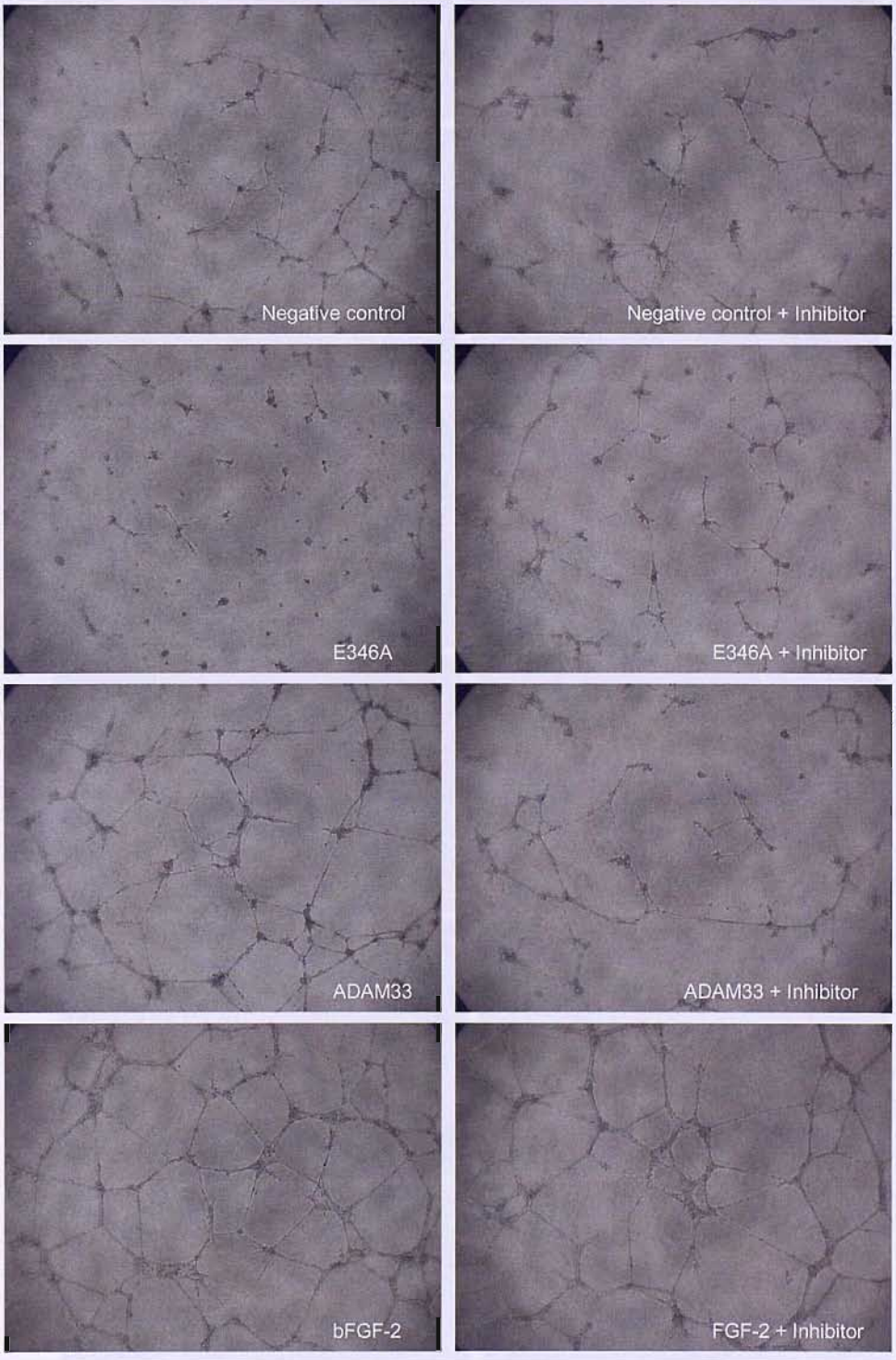

Fig. 5.7. Inhibition of ADAM33 mediated tube formation by the hydroxamate compound (3R)-(+)-[2-(4-methoxybenzenesulfonyl)-1,2,3,4-tetrahydroisoquinoline-3-hydroxymate]. HUVECs (passage 3) were seeded at $2x10^4$/well (96 well plate) onto growth factor reduced matrigel coated wells. Cells were seeded in complete M199 medium containing 1% serum, in addition with 20μM $ZnCl_2$, with or without the hydroxamate compound and one of the following treatments; buffer (negative control), ADAM33 Pro-MP-His (150ng/ml), ADAM33 Pro-MP(E346A)-His (150ng/ml) or bFGF-2 (30ng/ml). Tube formation was allowed to take place overnight and then images were captured under phase contrast on an inverted Leica microscope. Data are representative of one experiment carried out in duplicate.

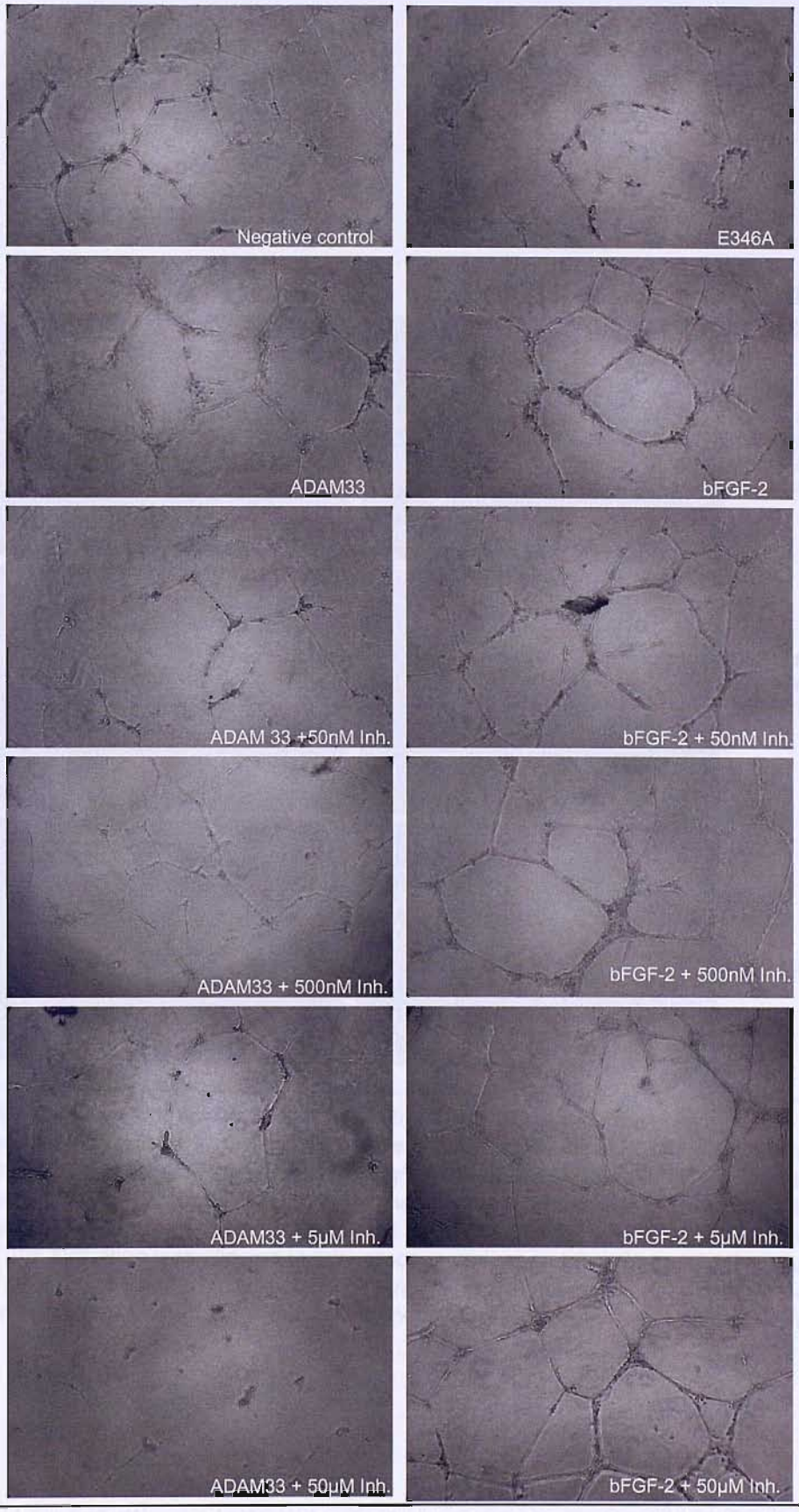

Fig. 5.8(a) Inhibition of ADAM33 mediated tube formation with carboxylate and hydroxamate compounds. HUVECs (passage 4) were seeded in M199 medium containing 1% serum in addition with 20μM ZnCl2, and one of the following treatments; buffer (negative control), ADAM33 Pro-MP-His (150ng/ml), ADAM33 Pro-MP(E346A)-His (150ng/ml) or bFGF-2 (30ng/ml). The inhibitor (3R)-(+)-[2-(4-methoxybenzenesulfonyl)-1,2,3,4-tetrahydroisoquinoline-3-hydroxymate was tested in the range of 50nM-50μM. Tube formation was allowed to take place overnight and then the cells were imaged under phase contrast on an inverted Leica microscope. Data representative of one experiment carried out in duplicate.

(a)

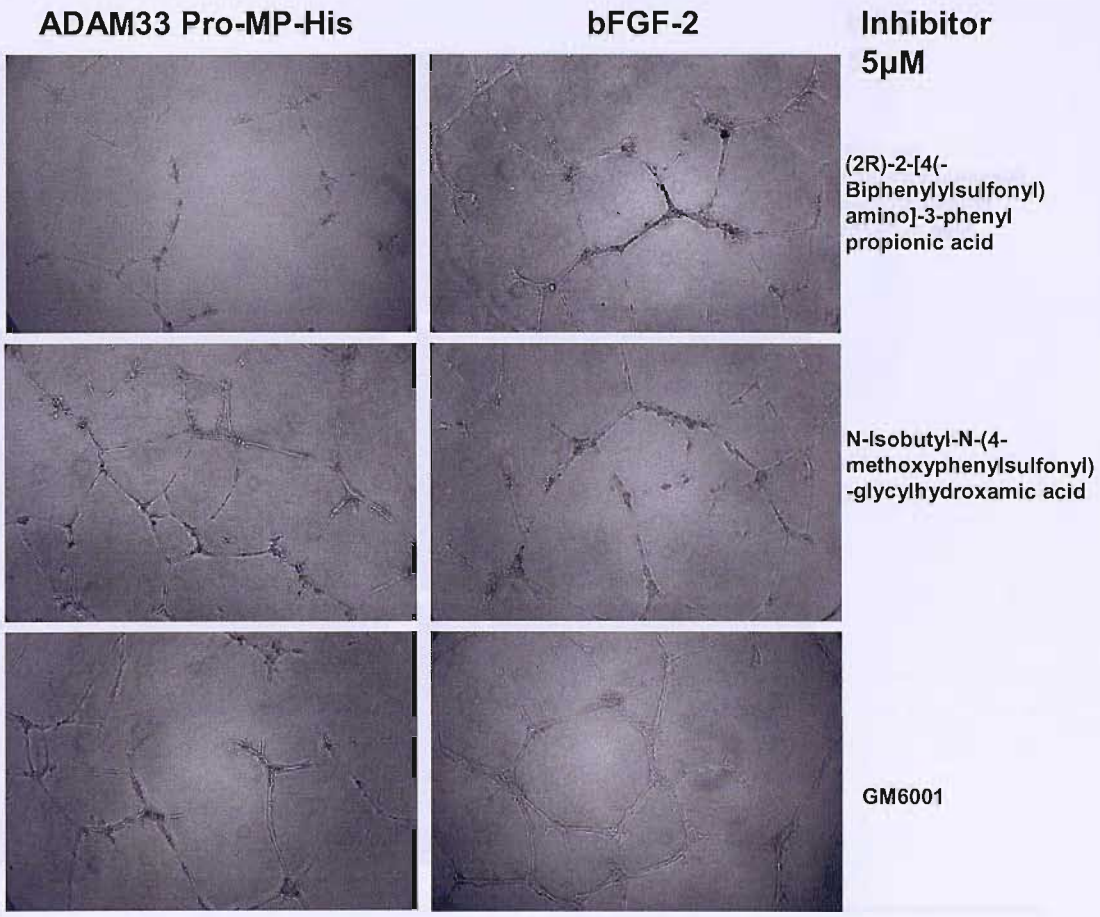

Fig. 5.8(b) Inhibition of ADAM33 mediated tube formation with carboxylate and hydroxamate compounds. Cells were seeded as described in (a). Cells were treated with 20μM ZnCl2 and ADAM33 Pro-MP-His (150ng/ml) in addition to one of the following synthetic compounds (2R)-2-[4(-Biphenylylsulfonyl)amino]-3-phenyl propionic acid, N-Isobutyl-N-(4-methoxyphenylsulfonyl)-glycylhydroxamic acid or GM6001 at (b) 5μM or (c) 50μM (see next page). Tube formation was allowed to take place overnight and then imaged using phase contrast on a Leica inverted microscope. (For non controls and comparison with (3R)-(+)-[2-(4-methoxybenzenesulfonyl)-1,2,3,4-tetrahydroisoquinoline-3-hydroxymate see Fig. 5.9(a).

(b)

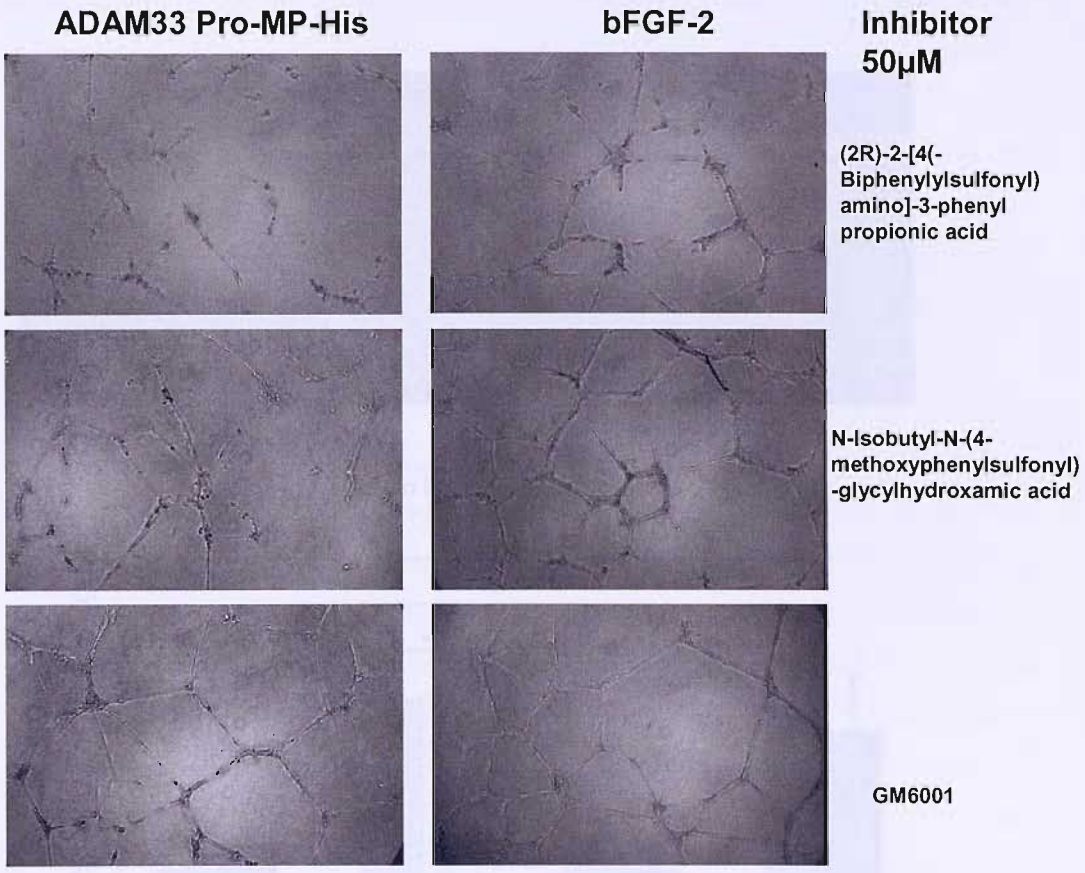

Fig. 5.8(c) Inhibition of ADAM33 mediated tube formation with carboxylate and hydroxamate compounds. See legend of Fig. 5.8(b). This experiment was performed once in duplicate where only one field of view was photographed per well. Therefore quantification of the images and statistical analyses of the data were not carried out.

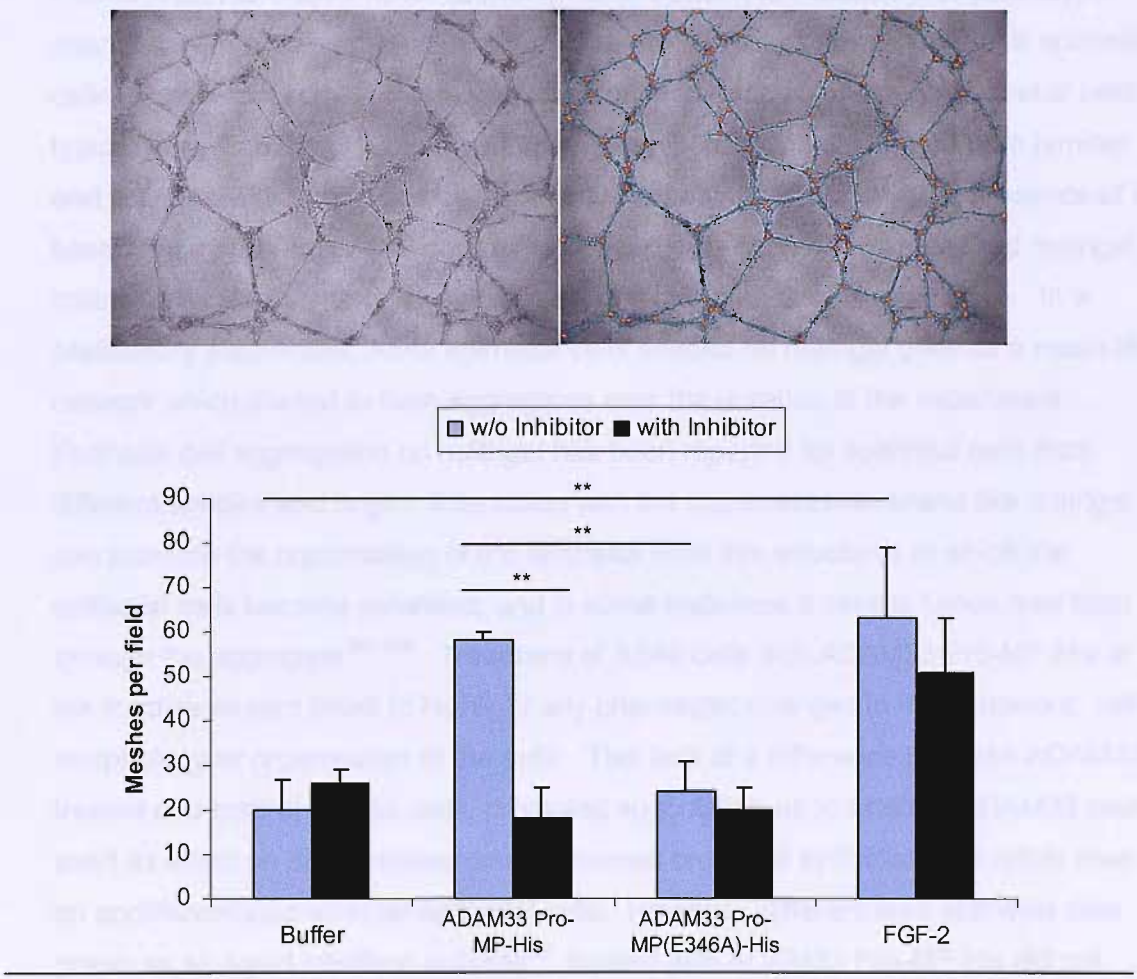

Fig. 5.9. Quantification of ADAM33 mediated endothelial cell tubulogenesis. Endothelial cell tube formation induced by ADAM33 Pro-MP-His (150ng/ml) and bFGF-2 was quantified using computer assisted image analysis (Leica Qwin v3). The tubes and branch points were identified by the software (top panels). Mesh formation was chosen as the parameter to assess the angiogenic activity of ADAM33. A mesh was considered to be where the endothelial tubes form an unbroken perimeter around an open area. The effect of the (3R)-(+)-[2-(4-methoxybenzenesulfonyl)-1,2,3,4-tetrahydroisoquinoline-3-hydroxamate (5μM) to inhibit tube formation was also assessed. The graph shows the mean and standard deviation of three experiments carried out in duplicate, n=3. Statistical test used was the parametric ANOVA test, with Tukey-Kramer multiple comparisons test correction. ** P<0.01.

5.5 DISCUSSION

5.5.1 Effect of ADAM33 on epithelial cells

In an initial simple experiment, A549 epithelial cells which do not express ADAM33[227] were grown as monolayers on tissue culture plastic, and treated with either ADAM33 Pro-MP-His, ADAM33 Pro-MP(E346A)-His or buffer. No indications of phenotypic changes were observed. A different culture model which allowed the A549 epithelial cells to grow to resemble the *in vivo* situation more was also tested. Epithelial cells typically grow on top of a basement membrane predominantly formed from laminin and collagen IV which allows epithelial cells to polarise. To mimic the presence of a basement membrane, A549 cells were seeded onto growth factor reduced matrigel, a matrix with many common components found in the basement membrane. In a preliminary experiment, A549 epithelial cells seeded on matrigel grew as a mesh-like network which started to form aggregates over the duration of the experiment. Epithelial cell aggregation on matrigel has been reported for epithelial cells from different species and origin. Interaction with the basement membrane like matrigel can promote the organisation of the epithelial cells into structures in which the epithelial cells become polarised, and in some instances a central lumen may form through the aggregate[267-269]. Treatment of A549 cells with ADAM33 Pro-MP-His or the inactive mutant failed to highlight any phenotypic changes in the behaviour, cell morphology or organisation of the cells. This lack of a difference between ADAM33 treated and control treated cells, prompted speculation as to whether ADAM33 could exert its effect on differentiated primary human bronchial epithelial cells rather than on undifferentiated alveolar epithelial cells. However, differentiated epithelial cells grown as air-liquid interface cultures[262] treated with ADAM33 Pro-MP-His did not show macroscopic differences in their morphology or organisation or epithelial integrity when compared with the mutant enzyme and buffer treated controls. Having obtained no functional evidence to suggest a role for ADAM33 Pro-MP-His in epithelial cell models, further investigation using other types of functional readouts or microscopic changes were not pursued. However, this has not excluded the possibility that ADAM33 may exert an effect on epithelial cells, and other assays may be needed to examine the treated cells. For example, gene expression studies or ELISAs may be used to assess the release of growth factors and cytokines from epithelial cells treated with ADAM33. Considering the sheddase activity of ADAMs, it is conceivable that ADAM33 may influence the release of growth factors and cytokines which epithelial cells are capable of producing such as FGF, ET-1, PDGF,

IGF, TGFβ, IL-6 and IL-8 [88], and changes in their levels may contribute to airway inflammation and the airway remodelling processes.

5.5.2 Effect of ADAM33 on endothelial cells

The remodelling features in the airway, such as increased smooth muscle mass can only occur when supported by increased vascularisation of the tissue. In a study carried out by Hoshino *et al.*, immunohistochemical analysis of bronchial biopsy sections from 16 asthmatic individuals showed increased vessel formation in comparison with 9 normal controls[80]. Another study by Hashimoto *et al.* showed that this increased vascularity in asthmatics was not confined to the large airways, but also extended into the medium and small airways in lung specimens obtained from surgery[270].

In vivo, an endothelial cell monolayer lines the lumenal surface of every blood vessel. Like epithelial cells, these reside on top of a basement membrane. Beneath this basement membrane are cell layers consisting of fibroblasts, pericytes and smooth muscle cells. It was speculated that their close proximity to the mesenchymal cells which do express ADAM33[227;227;229] may make them a target for membrane bound and soluble ADAM33[232] released from smooth muscle cells and fibroblasts. To address this, a well established *in vitro* model of angiogenesis, the HUVEC differentiation assay was taken to test for angiogenic properties of ADAM33. Endothelial cells are central to angiogenesis and their differentiation is fundamental for the process. Using this model, a functional effect of ADAM33 was demonstrated for the very first time. ADAM33 mediated proteolysis stimulated endothelial cell differentiation into a network of tubes in the absence of any pro-angiogenic stimulus. The ability of ADAM33 to promote endothelial cell differentiation has since been shown to extend beyond umbilical vein derived endothelial cells. Preliminary studies show that ADAM33 is able to promote angiogenesis in murine micro-vascular cells and also in human embryonic lung explant tissues where vessel formation is in the context of stromal cells (Pang, Puxeddu and Haitchi unpublished).

The mechanism by which ADAM33 proteolysis mediates its pro-angiogenic effect is not yet clear. Although ADAM proteins are not typical growth factors, they do possess sheddase activity which could cleave growth factors from the surface of cells. It is therefore possible that the release of pro-angiogenic growth factors which promote angiogenesis and vessel formation may be responsible for the ADAM33

mediated effect. Or alternatively, ADAM33 may be able to remodel the immediate extracellular matrix environment to facilitate angiogenesis. Many matrix metalloproteinases including MMP2 and 9 and MT1-MMP have been shown to play important roles in assisting the formation of new vessels [271;272]. The extracellular matrix (ECM) needs to be re-modelled as cells invade into the tissue during the initial vessel formation process. Degradation of the matrix can also release growth factors sequestered in the ECM such as members of the pro-angiogenic fibroblast growth factor (FGF) and vascular endothelial growth factor (VEGF) families which can go onto promote angiogenesis[273;274]. Although the exact pathway in which ADAM33 mediated proteolysis exerts its function is yet to be determined, time lapse microscopy used to track the formation of the tubes *in vitro*, suggests that the apparent increase in tube formation in ADAM33 Pro-MP-His treated cells may stem from its ability to stabilise the tubes. ADAM33 Pro-MP(E346A)-His treated endothelial cells also appear to begin to organise into tubes at the earlier time points, but the structures are fragile and unstable with a tendency to regress unlike those formed in the presence of active ADAM33.

ADAM33 is not the first ADAM capable of promoting angiogenesis to be identified. ADAM15, the closest relative to ADAM33 after ADAM19 and ADAM12 in humans has also been shown to facilitate the process. Knock-out mice deficient in *Adam15* have a normal phenotype under standard conditions. However, under pathological conditions, its pro-angiogenic properties can be unmasked. Under a hypoxic stress model of retinopathy, the retinas of the mice formed significantly fewer vessels than in the wild type mice. Furthermore, in a tumour model the *Adam15* knockout mice carried a much lower tumour burden than the wild type mice, consistent with decreased angiogenesis[275]. In human disease, ADAM15 has been found to be constitutively expressed in the synovial tissues from rheumatoid arthritis patients with a direct linear correlation with the vascular density in the synovial tissues. *ADAM15* expression can also be regulated by VEGF signalling through VEGFR-2 in both HUVECs and synovial fibroblasts[276], suggesting that it may have a role downstream of VEGF signalling. Although such studies have yet to be carried out with *ADAM33*, it is known that metalloproteinases often have distinct but overlapping specificities and it may be speculated that ADAM33 and ADAM15 may have overlapping functions either under normal or pathological conditions.

In the HUVEC differentiation assays, the cells treated with the mutant ADAM33 enzyme can in some instances show less spontaneous differentiation when

compared with the buffer treated control. Although not the only explanation, it is interesting to speculate whether this may suggest that the mutant can act as a dominant negative form of the protein, reducing basal activity further. The closest homolog to ADAM33; *Xenopus* ADAM13 also exhibits a similar dominant negative effect when the critical glutamic acid residue has been substituted by an alanine residue. Proteolytically active ADAM13 is required for neural crest cell migration, but the presence of mutant ADAM13 inhibits this migration[210]. It could be envisaged that the mutant may bind to the target substrate and in doing so mask the proteolytic cleavage site making it unavailable to any other active proteases. Whether the ADAM33 Pro-MP(E346A)-His is a true dominant mutant could be determined by simultaneously treating HUVECs with both the wild type and inactive mutant ADAM33 and observing whether tube formation occurs under such conditions. If it is proven to be such, the mutant enzyme may become a useful inhibitor against ADAM33 mediated proteolysis.

5.5.3 Inhibition of ADAM33 mediated endothelial cell differentiation

Inhibition of ADAM33 activity by (3R)-(+)-[2-(4-methoxybenzenesulfonyl)-1,2,3,4-tetrahydroisoquinoline-3-hydroxymate could be translated from biochemical studies into a functional HUVEC differentiation assay. The inhibitory effect was dose dependent and reproducible. It did not affect the intrinsic ability of cells to differentiate, since cells treated with this inhibitor were still able to respond to bFGF-2. It would therefore be of interest to study its specific effects further, and to evaluate whether this inhibitor is effective in *in* vivo models of angiogenesis and if it has the potential to slow the progress of the remodelling events seen in some cases of asthma. However, it must be noted that the problem with hydroxamate inhibitors is that they are often capable of inhibiting a number of MMPs. In this case, the inhibitor is also known to inhibit MMP-8[277]. MMP8 is the neutrophil collagenase, but it can also be expressed by fibroblasts and endothelial cells[278]. However, to date there is no evidence yet to suggest that MMP8 is involved in angiogenesis.

In one experiment the other inhibitors, ((2R)-2-[4(-Biphenylylsulfonyl)amino]-3-phenyl propionic acid, N-Isobutyl-N-(4-methoxyphenylsulfonyl)-glycylhydroxamic acid and GM6001 were found to be capable of inhibiting ADAM33 mediated endothelial cell differentiation at 5μM and 50μM. However these inhibitors were not as potent as (3R)-(+)-[2-(4-methoxybenzenesulfonyl)-1,2,3,4-tetrahydroisoquinoline-3-hydroxymate. When cells were treated simultaneously with bFGF-2 and the inhibitors tube formation was still observed, suggesting that they were not acting on

the same pathway as the bFGF-2 induced response. However, the results with these inhibitors were not always consistent, and a previous pilot experiment showed that whilst (3R)-(+)-[2-(4-methoxybenzenesulfonyl)-1,2,3,4-tetrahydroisoquinoline-3-hydroxymate could inhibit endothelial cell differentiation the other inhibitors had no inhibitory effect (data not shown).

Some caution is necessary when interpreting the data, since MMPs, and in particular MMP2 and 9 which are also important in the process of angiogenesis[279] can also be inhibited by some of these synthetic inhibitors. ((2R)-2-[4(-Biphenylylsulfonyl)amino]-3-phenyl propionic acid is a potent inhibitor of MMP2 and MMP9, and GM6001 is a broad spectrum MMP inhibitor, but neither inhibit the ADAM33 mediated response as effectively as (3R)-(+)-[2-(4-methoxybenzenesulfonyl)-1,2,3,4-tetrahydroisoquinoline-3-hydroxymate. It is therefore apparent that the pro-angiogenic response can be largely attributed to ADAM33 activity and not by other MMPs. In the future it would be worth testing a lower concentration of inhibitor, for example 1μM. The biochemical data from suggests that at this concentration, (3R)-(+)-[2-(4-methoxybenzenesulfonyl)-1,2,3,4-tetrahydroisoquinoline-3-hydroxymate would inhibit ADAM33 by ~80%, whereas the other inhibitors would show minimal inhibition of ADAM33 at this concentration, see **chapter 4, Fig. 4.6**.

5.5.4 Summary

The first functional role for ADAM33 mediated proteolysis has been described here. Soluble ADAM33 containing the MP domain has been shown to cause the rapid induction of endothelial cell differentiation *in vitro*. A potent ADAM33 inhibitor (3R)-(+)-[2-(4-methoxybenzenesulfonyl)-1,2,3,4-tetrahydroisoquinoline-3-hydroxymate that was identified in **chapter 4** was capable of selectively inhibiting the ADAM33 induced endothelial cell differentiation *in vitro*. No effects of ADAM33 treatment were observed on epithelial cells and suggested the effects of ADAM33 are cell type specific. This is exciting since an increase in vascularity of the airway has been associated with asthma and disease severity. The potential for ADAM33 to contribute to this process implies that ADAM33 may play a role in disease progression via a 'gain of function' effect. The exact mechanism by which ADAM33 mediates its effect will be clearer once its relevant target substrate has been identified.

Chapter 6 Profiling ADAM33 Pro-MP-His specificity

Following on from the demonstration of a role for ADAM33 in angiogenesis, the research effort was focused on trying to explain the mechanism by which it mediated the effect. Being a proteolysis-dependent effect, the identification of the target substrate(s) was key to understanding the mechanism. Finding the physiological substrate(s) for an orphan proteinase is a difficult process. One commonly employed strategy is the screening of candidate peptides and proteins based on the specificity of closely related proteinases. Although this method of screening is useful, it is biased in favour of pre-identified substrates and may reduce the likelihood of identifying novel substrates, since not all peptide sequences are considered equally. The candidate approach has already been undertaken for ADAM33 by Zou and colleagues. Although peptide substrates were identified, efficient cleavage of these in recombinant cell models could not be confirmed[205]. The relevant substrate is therefore yet to be found. To increase the breadth of the search for substrate proteins and eliminate some of the initial bias, a high throughput screening process can be put into place before the selection of potential proteins for testing. This involves screening a large random library of peptides to identify cleaved peptides. These peptides can then be aligned to produce a cleavage consensus sequence. Candidate proteins containing this consensus sequence can then be tested as substrates. This kind of approach is the basis for the work carried out for this chapter. Thus the aims of this chapter were to:

(i) identify a cleavage consensus for ADAM33 using a high throughput screen.

(ii) validate candidate substrates which may have a relevance to asthma and angiogenesis.

6.1 Screening the 10,000 member PNA-FRET peptide library

A PNA-FRET peptide library was developed by Prof. Mark Bradley's research group at the University of Edinburgh. This is described in more detail in materials and methods section **2.22**. The library consists of 10 000 members, each member of the library has a 6 amino acid peptide. The N and C terminal amino acids were fixed to be serine and alanine respectively, and the four remaining residues were random sequences chosen from 10 amino acids which were chosen to be biochemically representative of the 20 amino acids. To establish whether ADAM33 was capable of

degrading some of the peptides in the library, the enzyme and library were incubated together in solution, and the net fluorescence of this mixture was monitored at several time points, **Fig 6.1**. The fluorescence of the FAM was shown to increase gradually over time. A similar increase in fluorescence was not observed when the library was incubated in the absence of ADAM33, or when ADAM33 was incubated with a smaller subset of peptides (data not shown). This demonstrated that ADAM33 had activity that was specific towards members of the 10,000 PNA-peptide library. However, in this solution based system it was not possible to determine the sequence of the cleaved peptides, since the peptide emitting the fluorescence could not be distinguished from any other peptide in the library.

6.2 PNA-peptide Microarray

To identify which of the peptides in the PNA- FRET peptide library were cleaved, a similar solution based assay was carried out as before with an incubation time of 1 hour at 37°C. The library was subsequently hybridised onto a DNA microarray, transforming the solution based assay into an analysable 2D platform. Each member of the library bound to its own unique spot on the DNA microarray as dictated by their PNA tag, and allowed the fluorescence emitted from both the reporter dye (FAM) and quencher dye (TAMRA) of each member to recorded using a microarray scanner. The library treated with the ADAM33 Pro-MP(E346A)-His was used as a negative control. A global normalisation was applied to the data (which assumes that overall the fluorescence in the two channels should be similar) from the treated and control libraries and the two microarrays were subsequently compared. Poorly hybridised members of the microarray were manually excluded (382 spots, including 5 in which both duplicate spots of a library member were excluded). The FAM/TAMRA ratio of the spots on the treated and control microarrays were plotted against each other, **Fig.6.2**. The majority of spots fell close to the hypothetical identity line which indicated that the FAM/TAMRA ratio was the same or similar in both the ADAM33 and mutant treated samples. The absence of change in the fluorescence ratio detected between the two fluorescent channels showed that the majority of peptides (corresponding to these spots) had not been cleaved. For spots falling further away from the identity line there was an overall tendency to fall just below the line which

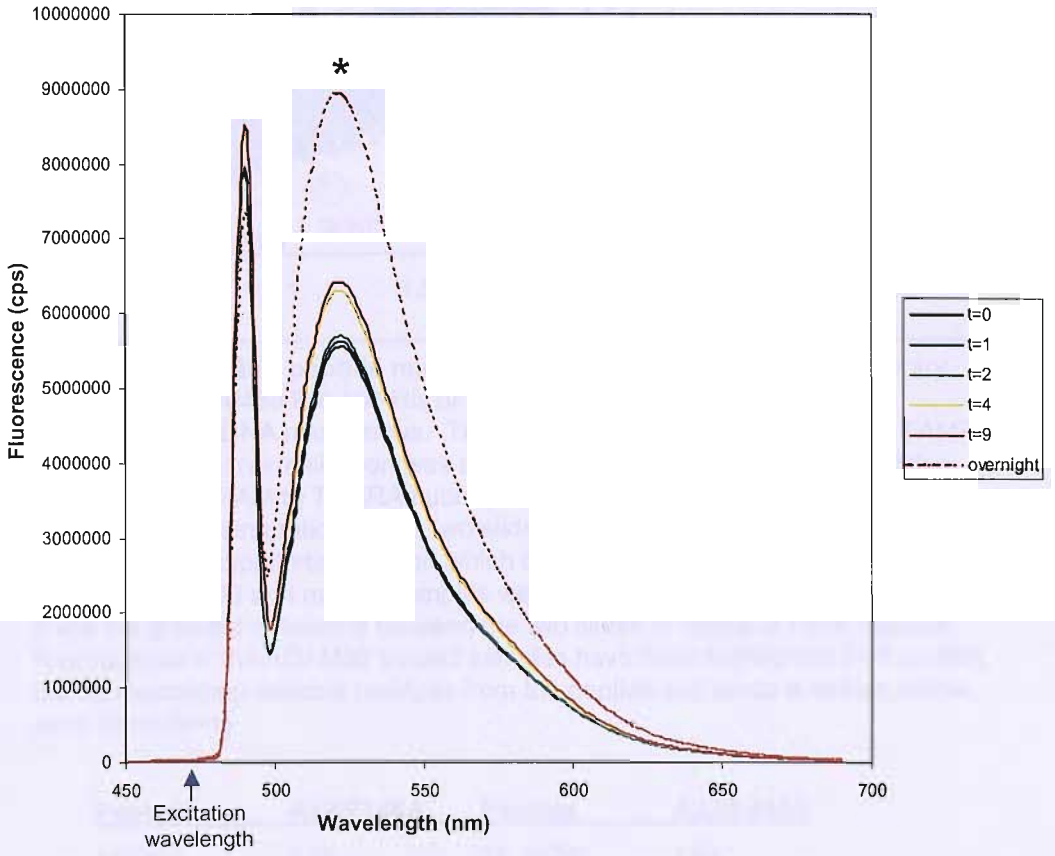

Fig. 6.1. ADAM33 Pro-MP-His cleaves PNA-FRET peptide library in solution. ~155nM of ADAM33 Pro-MP-His was mixed with ~400nM of PNA-peptide library in a quartz cuvette. This was placed into a Fluormax fluorescent spectrophotometer. The sample was excited at 490nm, and the emission spectrum of the sample was recorded at time (t) = 0,1,2,4,9 minutes and again after an overnight incubation at 37°C. The emission peaks (*) are shown in the graph above. The initial peak observed at 490nm was typical of bleed through from the excitation wavelength. (n=1)

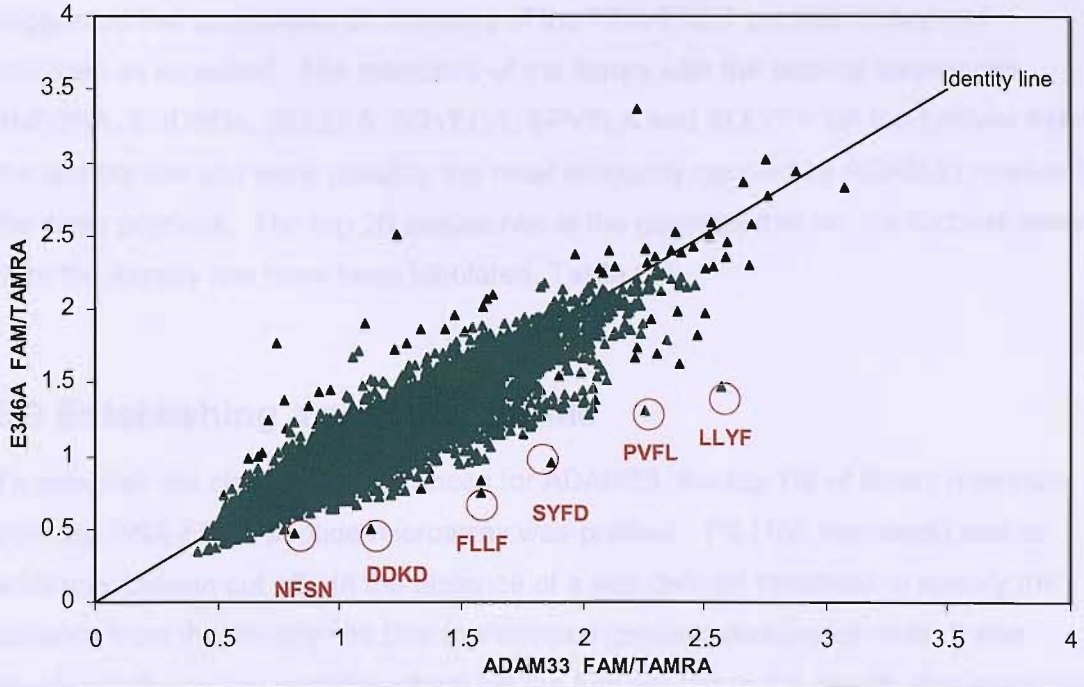

Fig. 6.2. PNA-FRET peptide microarray analysis. The PNA-peptide library treated with ADAM33 Pro-MP-His or ADAM33 Pro-MP(E346A)-His was hybridised onto DNA microarrays. The slides were scanned for FAM and TAMRA emission. Global normalisation was applied to the data from each of the slides and the ratio of FAM to TAMRA fluorescence was found for each spot on each array. The resulting ratios for the two slides have been plotted. The identity line represents the hypothetical line on which data points would lie if the signal from both the ADAM33 and mutant samples were equivalent. The peptides which show the greatest difference between the two slides in favour of more reporter fluorescence in the ADAM33 treated samples have been highlighted (red circles), the corresponding variable residues from the peptide sequence is written below each circle.(n=1)

Peptide	A33/E346A	Peptide	A33/E346A
1.DDKD	2.25	11. SKFV	1.64
2. FLFF	2.13	12. NFYF	1.63
3. DKKL	1.98	13. PNLP	1.62
4.NFSN	1.91	14. KPAF	1.62
5. LLYF	1.75	15. PSDP	1.61
6. PVFL	1.75	16. FKLV	1.61
7. SVFS	1.72	17. NNVY	1.61
8. PADY	1.72	18.NKFD	1.61
9. LYNL	1.67	19. LFAY	1.60
10. DLKF	1.65	20. SAAA	1.58

Table 6.1. Top 20 cleaved peptides from the PNA-FRET peptide microarray screen. The 20 peptides that fell furthest away from the identity line (Fig. 6.2) are listed. The FAM/TAMRA ratio from the ADAM33 Pro-MP-His treated microarray was divided by the FAM/TAMRA ratio from the ADAM33 Pro-MP(E346A)-His treated array to give an indication of distance from the identity line. The larger the value the further the deviation from the line.

suggested that proteolysis of members of the PNA-FRET peptide library had occurred as expected. The members of the library with the peptide sequences SNFSNA, SDDKDA, SFLLFA, SSYFDA, SPVFLA and SLLYFA fell the furthest below the identity line and were possibly the most efficiently cleaved by ADAM33 relative to the other peptides. The top 20 sequences of the peptides that fell the furthest away from the identity line have been tabulated, **Table 6.1**.

6.3 Establishing a specifity profile

To establish the cleavage preferences for ADAM33, the top 1% of library members from the PNA-FRET peptide microarray was profiled. 1% (108 members) was an arbitrarily chosen cut off. In the absence of a well defined threshold to specify the distance from the identity line that represented genuine cleavage events, it was decided that only the peptides which fell the furthest below the identity line would be considered and used to generate a consensus sequence.

Using these peptides, the frequency at which an amino acid occurred at each of the variable positions was recorded, **Fig. 6.3**. The variable N-terminal residue was found to be frequently occupied by both the hydrophobic residues phenylalanine and valine, but tyrosine was rarely present. In the adjacent position the hydrophobic residue phenylalanine and positively charged residue lysine were found to frequently occupy this position, with a small preference for the former. In the third variable position, very hydrophobic amino acids such as phenylalanine and leucine were found the most often, with other hydrophobic residues and uncharged and non polar residues preferred over charged and polar residues. The amino acid profile for the fourth amino acid position was again dominated by the hydrophobic residues phenylalanine and leucine. This data suggested that the ADAM33 cleavage consensus sequence may be (F/V - F/K - F/L - F/L). It was noted that since the cleavage site of the peptides were not known, this linear alignment of the peptides based purely on their amino acid sequence may not necessarily reflect the exact consensus sequence. To obtain the true consensus sequence the peptides should be aligned in accordance to the ADAM33 cleavage site within them. Nevertheless the consensus obtained gave an indication that hydrophobic residues in the substrate are important for ADAM33 mediated cleavage.

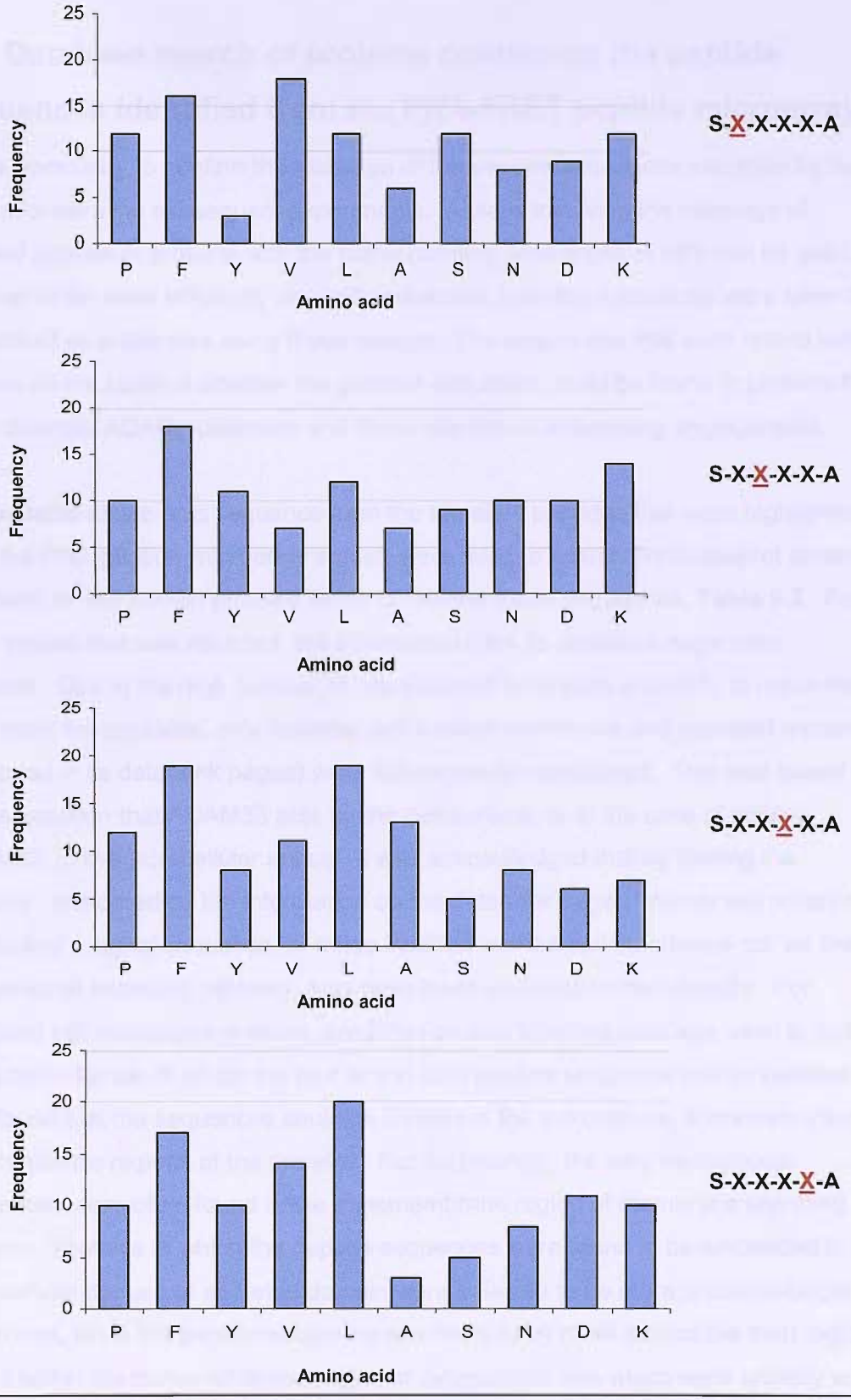

Fig. 6.3. Amino acid sequence analysis of top 1% of cleaved peptides from the PNA-FRET peptide library. 108 peptides from the PNA-peptide library that were cleaved most efficiently by ADAM33 were analysed. The frequency that a particular amino acid occurred in a specific position in the peptide was plotted. X denotes the amino acid position that corresponds to the adjacent graph. The members of the library were 6 amino acids in length, the first and last amino acids were fixed to be serine and alanine respectively, the remaining four residues were variable.

6.4 Database search of proteins containing the peptide sequences identified from the PNA-FRET peptide microarray

It was necessary to confirm the cleavage of the peptide sequences identified by the PNA microarray in subsequent experiments. Assays involving the cleavage of purified peptide or proteins with the corresponding sequences *in vitro* can be used. Several of the most efficiently cleaved sequences from the microarray were taken to be verified as substrates using these assays. The sequences that were tested were chosen on the basis of whether the putative sequence could be found in proteins that were potential ADAM substrates and those capable of influencing angiogenesis.

The variable amino acid sequence from the top eight peptides that were highlighted from the PNA-peptide-microarray screen were used to search the Swissprot protein databank to find human proteins which contained these sequences, **Table 6.2**. For each protein that was returned, the information from its databank page were checked. Due to the high number of hits obtained from such a search, to make the data more manageable, only potential cell surface membrane and secreted proteins (as stated in its databank pages) were subsequently considered. This was based on the assumption that ADAM33 acts on the cell surface, or in the case of soluble ADAM33, in the extracellular space. It was acknowledged that by limiting the proteins considered by the information on the databank pages, membrane proteins that lacked a signal sequence, or those inserted into the cell membrane not via the conventional secretory pathway, may have been excluded unintentionally. For identified cell membrane proteins, predicted protein topology data was used to find the protein domain in which the four amino acid peptide sequence was embedded. It was found that the sequences could be located in the extracellular, transmembrane or cytoplasmic regions of the proteins. Not surprisingly, the very hydrophobic sequences were often found in the transmembrane region of membrane spanning proteins. Proteins in which the peptide sequences were found to be embedded in the extracellular domain or secreted domain were believed to be more probable target substrates, since the peptide sequence was likely to be more accessible than regions buried within the transmembrane region or cytoplasmic tails which were unlikely to encounter the active ADAM33 proteinase. Some of the proteins found by this search fitted the profile of suspect metalloproteinase targets such as extracellular matrix components and cell surface growth factors and their receptors. The extracellular matrix components highlighted included collagen type IV, V, XI and laminin. The growth factors, their receptors and cell surface proteins included EGF,

Table 6.2. Proteins containing amino acid sequences taken from the microarray.
Human proteins containing the peptide sequences specified were found by using the NCBI protein BLAST program to search the Swissprot protein sequence databank. Secreted and plasma membrane proteins were identified. Where possible the protein domain in which the peptide sequence was found and tissue expression were noted down. ECD, TM, and Cyt represent the extracellular, transmembrane and cytoplasmic domains respectively. The amino acid sequence of the peptides have been written in single letter code.

Proteins containing DDKD	Region	Note
C5a anaphylatoxin chemotactic receptor	ECD	
Cadherin-11	ECD	Brain
Chondroitin sulfate proteoglycan 5	ECD	Brain
Neuropilin-2	ECD	
Roundabout homolog 1	ECD	Widely except kidney
Sodium/potassium-transporting ATPase alpha-3 chain	Cyt	
Transient receptor potential cation channel subfamily M(7)	Cyt	
Anion exchange protein 3	Cyt	Failing ventricle
Toll/interleukin-1 receptor 8	Cyt	Lung, Gut, Kidney (epithelial tissues)
G protein-coupled receptor kinase 7	lipid anchor	Retina
Dentin matrix acidic phosphoprotein 1	Secreted	Teeth
Thrombospondin-1	Secreted	
Potassium voltage-gated channel subfamily A member 1	not in TM	

Proteins containing FLLF	Region	Note
Aquaporin-0	ECD	Lens fiber gap junctions
Hephaestin	ECD	Breast, colon, bone, fibroblasts
IgG receptor FcRn large subunit p51	ECD	
Inactive dipeptidyl peptidase 10	ECD	Brain, Serum, Pancreas, Spinal cord, Adrenal gland
Low-density lipoprotein receptor-related protein 4	ECD	Brain
Low-density lipoprotein receptor-related protein 5	ECD	Widely including liver
Low-density lipoprotein receptor-related protein 6	ECD	Cuts in 2 sites
Nodal modulator 1	ECD	Colon tumour
Nodal modulator 3	ECD	
Olfactory receptor 5P2	ECD	Tongue
Pro-epidermal growth factor	ECD	Cuts in LDL class region
Retinoic acid early transcript 1G	ECD	Colon
Vomeronasal type-1 receptor 1	ECD	Olfactory mucosa, Brain, lung, kidney
ATP-binding cassette sub-family G member 4	ECD/TM	
Olfactory receptor 4K17	ECD/TM	
Olfactory receptor 5V1	ECD/TM	
Olfactory receptor 10H5	TM	
Acetylcholine receptor subunit delta	TM	
Activin receptor type 1B	TM	Widely
ADAM 20	TM	Testis
Adenylate cyclase type 4	TM	
Aquaporin-12A	TM	Pancreas
ATP-binding cassette sub-family A member 3	TM	Lung, Brain, Kkeletal Muscle, Pancreas, Heart
ATP-binding cassette sub-family A member 7	TM	Leulocytes, Spleen, Thymus, Lymph nodes, Brain
Bestrophin-4	TM	Colon, weakly in other tissues
Choline transporter-like protein 3	TM	
Choline transporter-like protein 4	TM	
Corticotropin-releasing factor receptor 2	TM	
Endothelin B receptor-like protein 1	TM	Brain, Spinal cord
Equilibrative nucleoside transporter 2	TM	Placenta, Brain, Heart, Ovary
Gamma-aminobutyric-acid receptor subunit gamma-3	TM	
Gap junction alpha-10	TM	
Glucose transporter type 4	TM	Skeletal and Cardiac muscle, Fat
Limb region 1 protein homolog	TM	Widely, highly in Heart, P+D88ancreas
Mannose-P-dolichol utilization defect 1	TM	
Melatonin-related receptor	TM	Brain
Motile sperm domain-containing protein 3	TM	
Neuronal voltage-gated calcium channel gamma-like subunit	TM	
Olfactory receptor 10A4	TM	Tongue
Olfactory receptor 10H1	TM	
Olfactory receptor 10H2	TM	
Olfactory receptor 10Q1	TM	
Olfactory receptor 10S1	TM	

Olfactory receptor 1E1	TM	
Olfactory receptor 2A12	TM	
Olfactory receptor 2L13	TM	
Olfactory receptor 2T3	TM	
Olfactory receptor 2T34	TM	
Olfactory receptor 4A4	TM	
Olfactory receptor 4A47	TM	
Olfactory receptor 4D1	TM	
Olfactory receptor 4Q3	TM	
Olfactory receptor 5L1	TM	
Olfactory receptor 5L2	TM	
Olfactory receptor 5T1	TM	
Olfactory receptor 5T3	TM	
Olfactory receptor 6B2	TM	
Olfactory receptor 6B3	TM	
Olfactory receptor 6K6	TM	
Olfactory receptor 7A10	TM	
Olfactory receptor 7G1	TM	
Olfactory receptor 8A1	TM	
Olfactory receptor 8B4	TM	
Olfactory receptor 8D1	TM	Tongue
Olfactory receptor 8D2	TM	Tongue
Olfactory receptor 8G1	TM	
Olfactory receptor 8G2	TM	
Olfactory receptor 9K2	TM	
Olfactory receptor 9Q1	TM	
Organic cation transporter 3	TM	Widely
Palmitoyltransferase ZDHHC15	TM	Lung, Placenta, Kidney, Liver, Heart, Brain
Palmitoyltransferase ZDHHC2	TM	Ubiquitous
Phosphatidylserine synthase 1	TM	
Polycystic kidney disease and receptor for egg jelly-related	TM	Testis
Potassium voltage-gated channel subfamily D member 1	TM	Widely
Potassium voltage-gated channel subfamily D member 2	TM	Brain
Potassium voltage-gated channel subfamily D member 3	TM	Heart, Brain, Pancreas, Kidney, Skeletal muscle
Probable G-protein coupled receptor 1	TM	Brain
Probable G-protein coupled receptor 144	TM	
Probable palmitoyltransferase ZDHHC20	TM	
Prostaglandin E2 receptor	TM	Kidney, Lung, Spleen, Skeletal muscle
Protein phosphatase 1 regulatory subunit 3A	TM	Heart and Skeletal muscle
Putative euronal cell adhesion molecule	TM	
Putative Taste receptor type 2 member 12	TM	Tongue, Palate Epithelium
Rhomboid-related protein 1	TM	Heart, Brain, Kidney, Skeletal muscle
Secretory carrier-associated membrane protein 1	TM	Widely including Brain
Sodium/hydrogen exchanger 3	TM	
Sodium/hydrogen exchanger 5	TM	Brain, Testis, Spleen, Skeletal muscle
Sodium-dependent dopamine transporter	TM	
Sodium-dependent noradrenaline transporter	TM	
Sodium-dependent phosphate transport protein 4	TM	
Sodium-dependent serotonin transporter	TM	
Solute carrier family 13 member 4	TM	Placenta, Testis, Heart
Sterolin-1	TM	Liver, Small Intestine, Colon
Sulfonylurea receptor 1	TM	
Sulfonylurea receptor 2	TM	
Taste receptor type 2 member 13	TM	Tongue, Palate epithelium
Taste receptor type 2 member 38	TM	Tongue
Thyrotropin-releasing hormone receptor	TM	
Trace amine-associated receptor 8	TM	Kidney, Brain
Trace amine-associated receptor 9	TM	
Transmembrane protein 17	TM	
Transmembrane protein 41A	TM	
Tumor necrosis factor receptor superfamily member 9	TM	T cells-activated
Voltage-dependent N-type calcium channel subunit alpha-1B	TM	Central nervous system
Voltage-dependent P/Q-type calcium channel subunit alpha-1A	TM	Brain
Voltage-dependent R-type calcium channel subunit alpha-1E	TM	Neurones, Kidney

Sodium/potassium-transporting ATPase alpha-2	TM/lumenal	
Sodium/potassium-transporting ATPase alpha-3	lumenal	
Olfactory receptor 12D3	Cyt	
Probable G-protein coupled receptor 119	Cyt	
B7 homolog 2	Signal peptide	Widely
CD19	Signal peptide	B cells
CD1e	Signal peptide	Thymocytes
CTLA-4	Signal peptide	Lymphoid tissues
Gamma-aminobutyric-acid receptor subunit alpha-2	Signal peptide	
Kremen protein 2	Signal peptide	
Surface IgM associated protein	Signal peptide	B cells
NKG2D ligand 1 precursor	lipid anchor	widely
NKG2D ligand 3	lipid anchor	
Phosphorylase kinase alpha L subunit	lipid anchor	Liver
Intelectin-1	lipid anchor	Widely, specifically Intestine
Arylsulfatase F	Secreted	
Coagulation factor VIII	Secreted	Plasma
Complement C1q subcomponent subunit B	Secreted	Plasma
Complement C1q subcomponent subunit C	Secreted	Plasma
Complement C1q tumor necrosis factor-related protein 3	Secreted	Plasma
Complement factor I precursor	Secreted	Plasma
Guanylin	Secreted	Ileum, Colon, Plasma
Hepatic triacylglycerol lipase	Secreted	
Intelectin-2	Secreted	Small intestine
Interleukin-24	Secreted	upregulated in melanoma
Mesothelin	Secreted	Lung, Heart, Placenta, Kidney
Microfibrillar-associated protein 2	Secreted	Secreted
NKG2D ligand 2	Secreted	Cancer tissues
Phospholipase A1 member	Secreted	Placenta, Prostate, Liver
Serine protease 23	Secreted	
Sushi repeat-containing protein SRPX2	Secreted	
Tenascin-X	Secreted	2 Cut sites. Foetal adrenal galnds, Testis, Muscle
Thyroglobulin	Secreted	Thyroid
Receptor expression-enhancing protein 6	not in TM	

Protein containing SYFD	Region	Note
Atrial natriuteric peptide-converting enzyme	ECD	Heart myocytes
Cadherin-23	ECD	Retina, Cochlea
Potassium channel subfamily K member 13	TM	Ubiquitous
Probable G-protein coupled receptor 156	Cyt	Ubiquitous, high in brain and testis
Short transient receptor potential channel 1	Cyt	Ubiquitous
Short transient receptor potential channel 3	Cyt	Brain, Lung, Ovary, Colon, Small intestine, Prostate, Placenta,Testis
Short transient receptor potential channel 5	Cyt	Brain
Short transient receptor potential channel 7	Cyt	
Toll-like receptor 10 precursor	Cyt	Spleen, Lymph nodes, Thymus, Tonsil, Lung
Group XIIB secretory phospholipase A2-like protein	Secreted	Liver, Kidney, Small intestine
Platelet-derived growth factor receptor-like protein	Secreted	Colon, Lung, Liver
von Willebrand factor	Secreted	Cuts in col type I and III binding domain. Plasma

Proteins containing DKKL	Region	Expression / Comment
CD320 antigen	ECD	Follicular dendritic cells
Fibroblast growth factor receptor 3	ECD	Brain, Kidney, Testis, Embryonic lung, Kidney, Brain, Intestine
Gamma-aminobutyric-acid receptor subunit gamma-3	ECD	
Glutamate receptor delta-2 subunit	ECD	Central nervous system
Low-density lipoprotein receptor-related protein 1B	ECD	Brain, Salivary gland, Thyroid
ATP-binding cassette transporter 2	TM	
Transmembrane protein 111	TM	
XK-related protein 9	TM	
Probable G-protein coupled receptor 157	TM/Cyt	
ADAM 17	Cyt	Ubiquitous
Brain-specific angiogenesis inhibitor 1	Cyt	Brain
Brain-specific angiogenesis inhibitor 3	Cyt	Brain, Heart
Gap junction alpha-9 protein	Cyt	Neurons
Myoferlin	Cyt	Skeletal muscle, Lung, Kidney, Brain, Placenta
Sodium/potassium/calcium exchanger 3	Cyt	Brain, Aorta, Uterus, Intestine

Carbonic anhydrase 4	lipid anchor	Endothelium (in eyes)
GPI-anchored membrane protein 1	lipid anchor	
Wnt-16	Secreted	Peripheral lymphoid organs, Kidney
Angiogenic factor with G patch and FHA domains 1	Secreted	Endothelial, Vascular smooth muscle cells, Osteoblasts
Apolipoprotein B-100	Secreted	Plasma
Coagulation factor XIII B	Secreted	Plasma
Ectonucleotide pyrophosphatase/phosphodiesterase family(5)	Secreted	
ER degradation-enhancing alpha-mannosidase-like 2	Secreted	
FAM20C	Secreted	
Laminin subunit alpha-1	Secreted	
Signal peptide, CUB and EGF-like domain-containing protein 1	Secreted	Associated with ECM. Endothelial cells
Signal peptide, CUB and EGF-like domain-containing protein 2	Secreted	Broad including endothelial cells
Signal peptide, CUB and EGF-like domain-containing protein 3	Secreted	Osteoblasts
Tumor suppressor TSBF-1	Not in TM	

Proteins containing NFSN	Region	Note
ADAM15	ECD	Ubiquitous, Endothelium, Smooth muscle
G protein coupled receptor 64	ECD	Epididymis
P2X purinoceptor 5 (ATP receptor)	ECD	Brain, Immune system
CD1a antigen	ECD	T cells
Toll-like receptor 8	ECD	Brain, Heart, Lung, Liver, Placenta, Immature DCs and Monocytes
Toll-like receptor 5	ECD	Ovary, Blood leukocytes
CD1c antigen	ECD	Thymopcytes, T cells
GPR155	TM	Eye, Brain
Taste receptor type 2 member 10	TM	Tongue, Palate epithelium
Taste receptor type 2 member 44	TM	Tongue
Taste receptor type 2 member 45	TM	Tongue
Aquaporin 1	TM	Kidney, Heart, Lung, Pancreas
FAM74A1	TM	
Proteocadherin beta 1	Cyt	
Taste receptor type 2 member 47	Cyt	Tongue
Taste receptor type 2 member 14	Cyt	Tongue, Palate epithelium
Taste receptor type 2 member 43	Cyt	Tongue
Taste receptor type 2 member 46	Cyt	Tongue
Taste receptor type 2 member 50	Cyt	Tongue
Taste receptor type 2 member 48	Cyt	Tongue
Coagulation factor V	Secreted	
Ligand-binding protein RYA3	Secreted	Nasal septal epithelium
Granzyme B	Secreted	T cells NK cells
Slit homolog 2 protein precursor	Secreted	Foetal lung and Kidney, Spinal cord weaker in other tissues
Interphotoreceptor matrix proteoglycan 1	Secreted	Retina
Granzyme H	Secreted	T cells
Bactericidal/permeability-increasing protein-like 2	Secreted	epidermis of inflamed skin with psorasis
Peptidyl-glycine alpha-amidating monooxygenase	Secreted or on membrane	
Thromboxane-A-synthase	Not in TM	Platelets, Lung, Kidney, Macrophages and Lung fibroblasts

Proteins containing LLYF	Region	Note
Abhydrolase domain-containing protein 13	ECD	
Adrenomedullin receptor	ECD	Heart, Skeletal muscle, Immune system, Liver, Adrenal gland
CD109	ECD	widely
Choline transporter-like protein 4	ECD	
Low-density lipoprotein receptor-related protein 2	ECD	Absorptive epithelia
Lymphocyte antigen 75 precursor	ECD	Spleen, Thymus, Lymphocytes
Sarcospan isoform 1	ECD	Heart, Skeletal muscle
Voltage-dependent T-type calcium channel subunit alpha-1I	ECD/TM	Brain
Solute carrier organic anion transporter family member 1A2	TM	
Transmembrane 4 L6 family member 18	TM	
Calcium-activated potassium channel subunit alpha 1	TM	Widely except myocytes
cGMP-gated cation channel alpha 1	TM	Retina
C-type lectin domain family 5 member A	TM	Peripheral blood monocytes
Cysteinyl leukotriene receptor 1	TM	Widely
Excitatory amino acid transporter 1	TM	Brain
Excitatory amino acid transporter 5	TM	Retina, lower in Brain, Liver, Heart
Frizzled-6	TM	Widely
Immunoglobulin superfamily member 2	TM	DCs, T cells, Monocytes, Granulocytes, Epithelial cells
NIPA-like protein 2	TM	only partially in TM

NIPA-like protein 3	TM	only partially in TM
Olfactory receptor 6K3	TM	
P2X purinoceptor 2	TM	Neurons
Polycystic kidney disease 2-like 2 protein	TM	Controversial. Brain, Kidney, widely
RING finger protein 103	TM	Brain
RING finger protein 182	TM	
SID1 transmembrane family member 2	TM	
Signal peptide peptidase-like 2A	TM	
Sodium/potassium/calcium exchanger 1	TM	Retina
Sodium-dependent dopamine transporter	TM	Neurones
Solute carrier organic anion transporter family member 1B1	TM	Liver
Solute carrier organic anion transporter family member 1B3	TM	Liver
Taste receptor type 2 member 3	TM	Tongue, Stomach, Gut
Transient receptor potential cation channel subfamily V (4)	TM	
Transmembrane 4 L6 family member 1	TM	Endothelial cells, Carcinoma of the Lung, Breast, Colon, Ovaries
Transmembrane 9 superfamily protein member 4	TM	
Voltage-dependent T-type calcium channel subunit alpha-1G	TM	High in Brain, moderate in Lung, Placenta, Kidney
Voltage-dependent T-type calcium channel subunit alpha-1H	TM	Kidney, Liver, Heart, Brain, (isoform 2 Testis)
Transient receptor potential cation channel subfamily M (4)	Cyt	Widely
Glutamate receptor, ionotropic kainate 1	Signal peptide	Brain
Semaphorin-6A precursor	Signal peptide	
Apolipoprotein M	Secreted	Plasma, Liver, Kidney
Bone morphogenetic protein 15	Secreted	Ovary
Collagen alpha-2(IV) chain	Secreted	Basement membrane component
Complement C4-A precursor	Secreted	Plasma Cut in C4 gamma chain
Complement C4-B precursor	Secreted	Plasma Cut in C4 gamma chain
Growth/differentiation factor 3	Secreted	
Phosphatidylcholine-sterol acyltransferase	Secreted	Blood
Polypeptide N-acetylgalactosaminyltransferase 1	Secreted, or golgi membrane	
Multidrug resistance-associated protein 9	Not in TM	Testis, Brain, Breast cancer
Transmembrane protein 145	Not in TM	

Proteins containing PVFL	Region	Note
CD8 alpha chain	ECD	T cells
DnaJ homolog subfamily C member 16	ECD	
Ephrin type-A receptor 8	ECD	
Olfactory receptor 1B1	ECD	
Olfactory receptor 2Y1	ECD	
Polycystic kidney and hepatic disease 1	ECD	Kidney, Pancreas
Protocadherin beta 1	ECD	
Protocadherin beta 12	ECD	
Protocadherin beta 13	ECD	
Protocadherin beta 2	ECD	
Protocadherin beta 7	ECD	
Protocadherin beta 8	ECD	
Protocadherin Fat 2	ECD	
Protocadherin LKC	ECD	Liver, Kidney, Small intestine, Colon
Protocadherin-16	ECD	Fibroblast specific
Activin receptor type 1B precursor	TM	Widely, Lung, Brain, Kidney, Liver
C-C chemokine receptor type 11	TM	Heart, Lung, Small intestine, Spleen, Colon,Sskeletal muscle
Ferroportin-1	TM	Placenta, Muscle, Spleen, Intestine
FMLP-related receptor I	TM	Lung, Neutophils, Spleen, Testis
Folate transporter 1	TM	Placenta, Liver, Lung
Glucagon receptor	TM	
Leukotriene C(4) transporter	TM	Lung, Testis, Peripheral blood mononuclear cells
Mas-related G-protein coupled receptor member X2	TM	only partially TM. Nervous system
Metabotropic glutamate receptor 7	TM	Brain
Monocarboxylate transporter 1	TM	Widely
Monocarboxylate transporter 2	TM	Testis, low in other tissues (widely)
Monocarboxylate transporter 3	TM	Retinal epithelium
Monocarboxylate transporter 4	TM	Skeletal muscle
Olfactory receptor 2D2	TM	
Olfactory receptor 56B4	TM	only partially TM
Potassium channel subfamily T member 1	TM	Liver, Brain, Spinal chord, Skeletal muscle
Probable G-protein coupled receptor 153	TM	

Probable G-protein coupled receptor 160	TM	
Protein YIPF6	TM	
Sodium- and chloride-dependent GABA transporter 2	TM	Kidney,Liver, Brain
Sulfonylurea receptor 1	TM	
Sulfonylurea receptor 2	TM	Heart
Taste receptor type 2 member 9	TM	Taste buds, Palate epithelium
Thiamine transporter 1	TM	ubiquitous
Transmembrane protein 126A	TM	
Beta cysteine string protein	lipid anchor	Testis
Type I inositol-1,4,5-trisphosphate 5-phosphatase	lipid anchor	Brain
CD20 antigen-like 2	Cyt	Testis, Pancreas, Heart, Brain
Vanilloid receptor-like channel 2	Cyt	
Voltage-dependent L-type calcium channel subunit alpha-1S	Cyt	Skeletal muscle
Neuronal acetylcholine receptor subunit alpha-2	Signal peptide	
Collagen alpha-1(V) chain	Secreted	Ubiquitous
Collagen alpha-1(XI) chain	Secreted	Cartilage, Placenta
Interleukin-1 beta	Secreted	Inflammatory cells
Laminin subunit gamma-3 (Laminin 12 gamma 3 subunit)	Secreted	Widely including, Lung, Skin, Heart
Phosphatidylcholine-sterol acyltransferase	Secreted	Plasma
Procollagen C-endopeptidase enhancer 1	Secreted	
Membralin	Not in TM	

Proteins containing SVFS	Region	Note
ATPase class I type 8B member 4	ECD	Ubiquitous
Brain-specific angiogenesis inhibitor 1	ECD	Brain
Chemokine receptor-like 1	ECD	Brain, Cartilage
Contactin-2	ECD	Neurones
CUB and sushi domain-containing protein 3	ECD	Widely
Glutamate receptor, ionotropic kainate 3	ECD	Synapse
Integrin alpha-10	ECD	Heart, Muscle, Cartilage
Interferon-alpha/beta receptor alpha chain	ECD	Ubiquitous
P2X purinoceptor 2	ECD	
Plexin-B1	ECD	Foetal kidney, Lung, Brain, Liver
Probable G-protein coupled receptor 114	ECD	
Probable G-protein coupled receptor 45	ECD	Brain
Protocadherin gamma A2	ECD	
Receptor tyrosine-protein kinase erbB-3	ECD	Brain, Epithelium
Receptor tyrosine-protein kinase erbB-4	ECD	Widely
Visual pigment-like receptor peropsin	ECD	Eye
Endothelial differentiation G-protein coupled receptor 5	TM	
Gamma-aminobutyric-acid receptor subunit rho-2	TM	
Membrane-associated transporter protein	TM	Melanocytes
Olfactory receptor 4B1	TM	
Olfactory receptor 52J3	TM	
Olfactory receptor 7G1	TM	
Potassium voltage-gated channel subfamily KQT (2)	TM	Brain
Potassium voltage-gated channel subfamily KQT (5)	TM	Brain, Skeletal muscle
Potassium voltage-gated channel subfamily S (1)	TM	Widely except Skeletal muscle
Sodium channel protein type 8 subunit alpha	TM	
Sphingosine 1-phosphate receptor Edg-1	TM	Epithelium, Endothelial cells, Vascular smooth muscle cells, Fibroblasts
Lysosome-associated membrane glycoprotein 2	lumenal	Placenta, lung, liver, kidney, brain, skeletal muscle
Tetraspan transmembrane protein L6H	TM/Cyt	Intestine, Pancreas
Amphoterin-induced protein 1	Cyt	Neurones
Amphoterin-induced protein 2	Cyt	Breast, Ovary, Cervix, Uterus, Lung, Colon, Rectum
Basic fibroblast growth factor receptor 1	Cyt	
Cadherin-21	Cyt	
Fibroblast growth factor receptor 2	Cyt	
Glucagon-like peptide 1 receptor	Cyt	
Melatonin-related receptor	Cyt	Brain
Multidrug resistance protein 1	Cyt	Liver, Kidney, Brain, Small intestine
Otoferlin	Cyt	Brain, Heart, Skeletal muscle, Placenta, Kidney
Plasma membrane calcium-transporting ATPase 3	Cyt	Brain, Foetal skeletal muscle
Receptor-transporting protein 1	Cyt	
Taste receptor type 2 member 41	Cyt	Tongue
Calcium and integrin-binding protein 1	lipid anchor	Ubiquitous
Contactin-1	lipid anchor	Neurones

Alpha-2-antiplasmin	Secreted	Liver, Plasma
Autoprothrombin IIA	Secreted	Liver, Plasma
Collagen alpha-3(VI) chain	Secreted	
Complement C1q subcomponent subunit A	Secreted	Plasma
Complement C1q subcomponent subunit C	Secreted	Plasma
Dystroglycan	Secreted	Widely
Mucin-2	Secreted	Intestine, Colon, Bronchus, Gall bladder, Cervix
Nociceptin	Secreted	Brain, Spinal cord
Reelin	Secreted	Brain, Liver
Tectonic-1	Secreted	
Tenascin-X	Secreted	Adrenal gland, Testis, Muscle
O-acyltransferase domain-containing protein 4	Not TM	
Chloride anion exchanger	Not TM	
Limbin	Not TM	

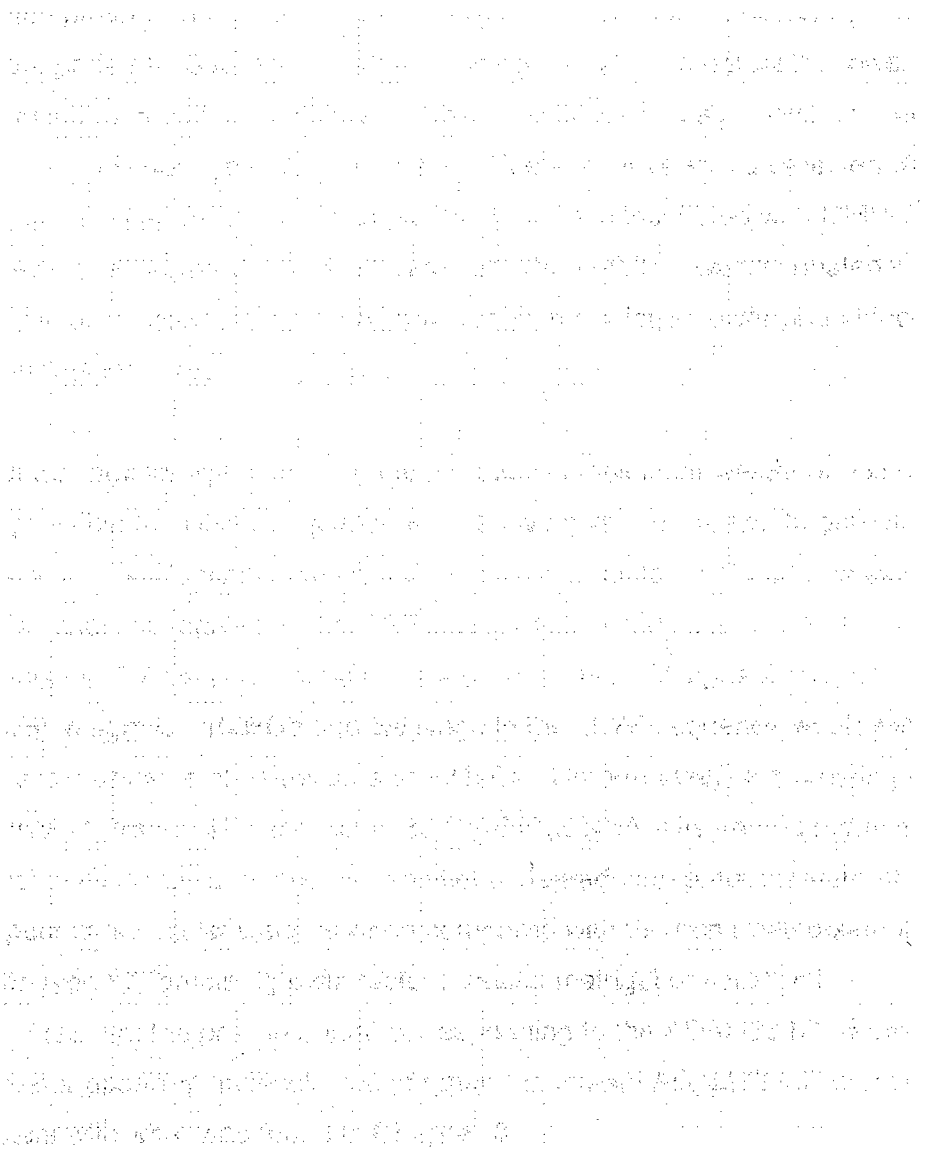

FGFR-3 and VEGF-R2. ADAM15 was also found within the list. Collagen IV, laminin and ADAM15 sequences were taken for evaluation as substrates for ADAM33.

6.5 Digestion of extracellular matrix components in solution

In an attempt to validate the PNA-peptide microarray data, collagen type IV, laminin, matrigel and fibronectin were taken independently and incubated with ADAM33 Pro-MP-His in solution to study whether they could act as potential substrates of ADAM33. Fibronectin was not identified in the peptide library screen and was used as a negative control. Each peptide was incubated with ADAM33 for 8.5 hours before the reactions were stopped by solubilisation in reducing SDS-PAGE sample buffer and denaturation at 95°C. The products were analysed by SDS-PAGE and the separated proteins visualised by staining with EZ Blue stain to detect the more abundant proteins. Subsequent silver staining was used to detect the lower abundance protein species, **Fig. 6.4**. MMP-2 was used as a positive control for the cleavage of collagen type IV. Both the EZ Blue and silver stains detected cleaved fragments of collagen IV in the sample that had been incubated with MMP-2. However these fragments were not detected when MMP-2 was incubated with growth factor reduced matrigel, and may reflect the relative lower abundance of collagen type IV in the matrigel sample.

The human laminin alpha 1 chain has a predicted molecular weight of ~337kDa, cleavage within the DKKL sequence would have given rise to two fragments of ~196 and 141kDa. The laminin gamma 3 chain has a predicted molecular weight of ~172kDa and cleavage within the PVFL sequence would have given rise to two fragments of ~70kDa and ~101kDa. For collagen type IV alpha 2, the predicted molecular weight is ~168kDa and cleavage in the LLYF sequence would have given rise to two fragments of ~146kDa and ~21kDa. Unfortunately, the protein profiles for the ADAM33 Pro-MP-His and ADAM33 Pro-MP(E346A)-His treated matrix proteins were not significantly different. No additional degradation products were observed at the expected molecular weights when compared with the non treated samples for collagen type IV, laminin, growth factor reduced matrigel or fibronectin.
It was noted that the protein bands corresponding to the ADAM33 MP domain did run at a greater apparent molecular weight than the mutant ADAM33 MP domain, consistent with what was found in **Chapter 3**.

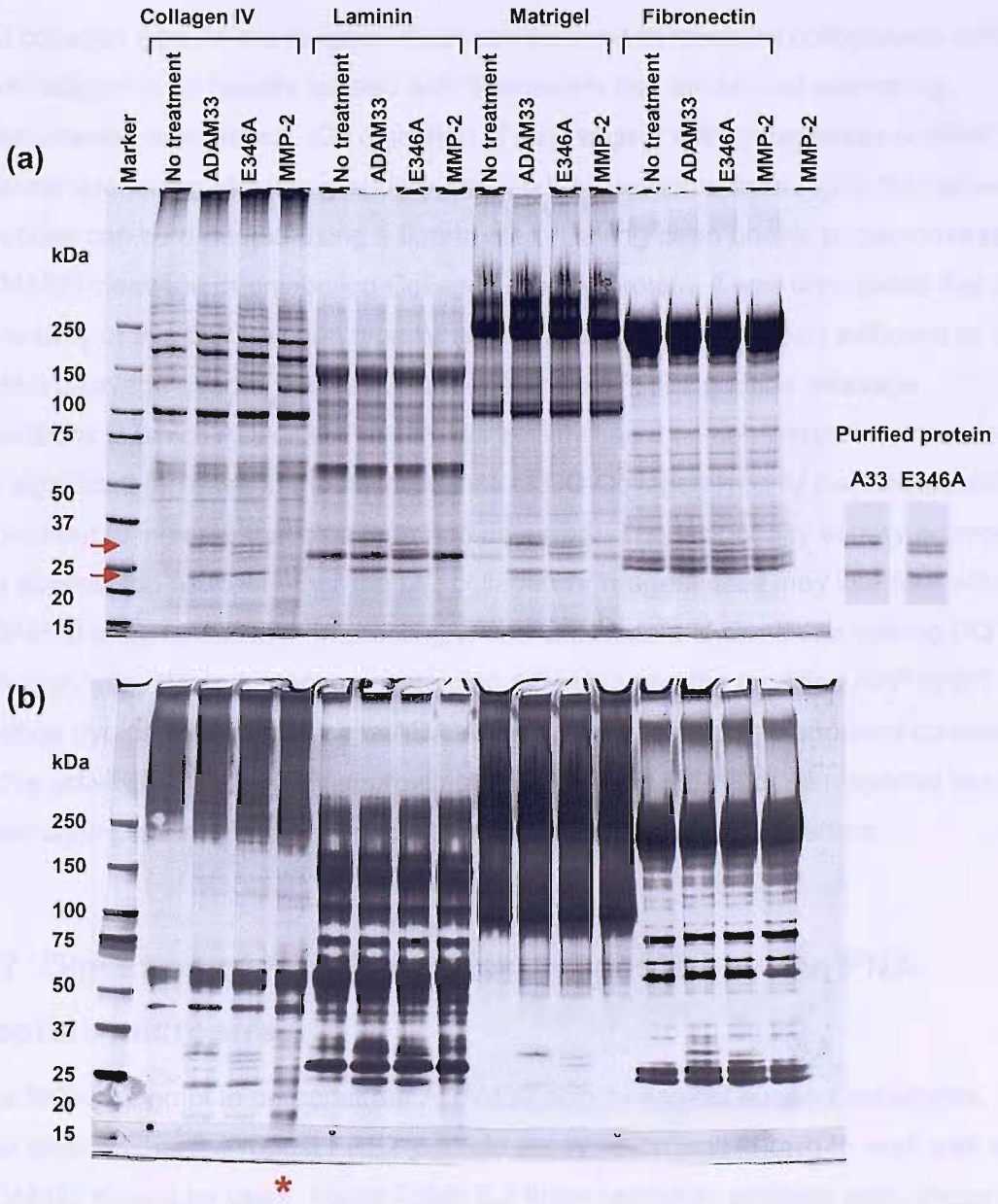

Fig. 6.4. Extracellular matrix components as target substrates for ADAM33. 395nM of ADAM33 Pro-MP-His was incubated with 15µg Collagen Type IV, 7µg laminin, 15µg growth factor reduced matrigel or 14µg of fibronectin for 8.5 hours at 37°C. No treatment and ADAM33 Pro-MP(E346A)-His treatment were used as negative controls, treatment with 10ng of active MMP-2 was used as a positive control. Reactions were stopped with the addition of 5x SDS-PAGE sample buffer, and half of each sample was analysed by SDS-PAGE on a 4-15% Criterion gradient gel (Bio-Rad). Proteins were initially visualised by staining with EZ Blue stain (a), then subsequently visualised by silver staining to detect low abundance proteins (b). The SDS-PAGE protein profiles of purified ADAM33 Pro-MP-His and ADAM33 Pro-MP(E346A)-His are shown on the right of the experimental gel as a reference. Gels were imaged using the Bio-Rad GS800 scanner. Arrows point to the ADAM33 Pro domain, and the MP domain doublet. Note that the doublet for the mutant migrates faster than the wild type. (*) denotes the lanes is which multiple cleavage products can be observed as a result of MMP-2 mediated cleavage.

6.6 Digestion of DQ collagen type IV

DQ collagen type IV is a reagent which can be used to measure collagenase activity. The collagen is so heavily labeled with fluorescein that an internal quenching phenomenon is achieved. On digestion of this reagent with collagenase or MMP, the internal quenching effect is gradually lost, and the emission from highly fluorescent peptides can be detected using a fluorimeter. Having been unable to demonstrate ADAM33 cleavage of unlabelled Collagen type IV protein, it was anticipated that the sensitivity of this DQ collagen type IV activity assay may have been sufficient to detect cleavage events. However, under standard FRET peptide cleavage conditions in which ADAM33 Pro-MP-His activity could be demonstrated, there was no significant increase in the fluorescence of DQ Collagen type IV over the duration of an hour to indicate that cleavage had occurred. The lack of any activity prompted the speculation as to whether the DQ collagen IV reagent itself may interfere with ADAM33 enzyme activity. Interestingly, one experiment showed that spiking DQ collagen type IV into a reaction containing ADAM33 and the modified APP FRET peptide (typically used to assess ADAM33 activity[235]) caused an apparent decrease in the activity of ADAM33 by approximately 9 fold, **Fig 6.5**. A dose response has not been attempted in this case, but could be carried out to verify the effect.

6.7 Digestion of FRET peptides suggested by the PNA-peptide microarray

In a further attempt to demonstrate ADAM33 activity against suspect substrates, it was decided that the robust FRET peptide assay which was known to work well with ADAM33 should be used. Using **Table 6.2** three candidate proteins were chosen, these were Collagen type IV, laminin and ADAM15 from which FRET peptides similar to the one used in previous activity assay (**chapter 4**) were to be synthesised (Severn Biotech). These candidates were chosen on the basis that the predicted cleavage sites were expected to lie in the accessible extracellular space. In addition, these candidates fitted in with the profile of typical ADAM family substrates. Furthermore, interactions with these proteins are known to be critical in angiogenesis, or in the case of ADAM15, has been shown to play a known role in angiogenesis under pathological conditions. Unfortunately, the laminin peptide was problematic for synthesis and could not be tested within the time frame of this study, therefore only the ADAM15 and collagen type IV peptides were investigated.

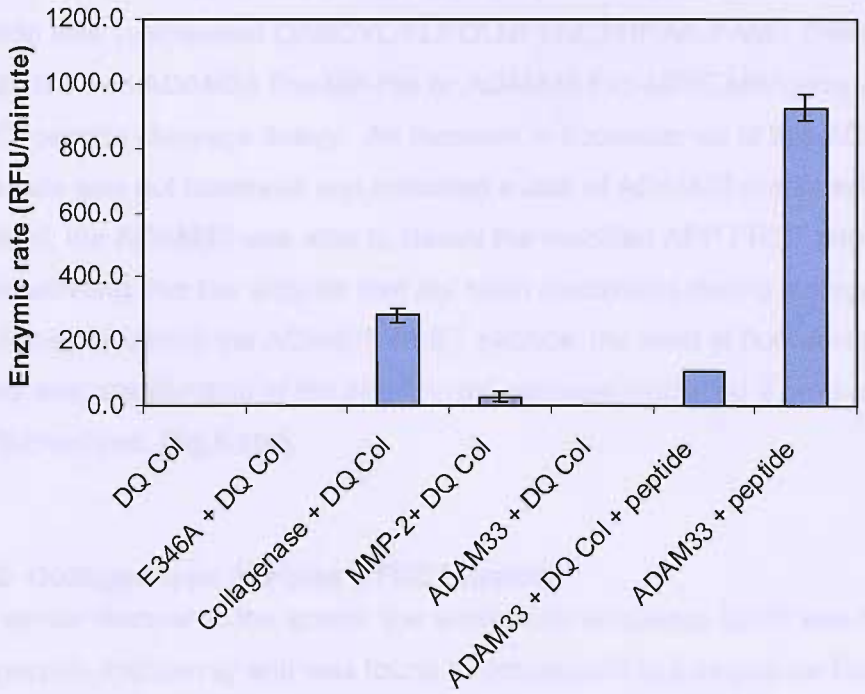

Fig. 6.5. Cleavage assay using DQ collagen type IV. DQ Collagen type IV (Invitrogen) was incubated at a concentration of 0.1mg/ml with 174nM of ADAM Pro-MP-His or ADAM33 Pro-MP(E346A) at 37°C for 1 hour using a iCycler (Bio-Rad). The fluorescence emission at 520nM was recorded every minute throughout the duration of the experiment. DQ Collagen type IV incubated alone was used as a negative control, active MMP-2 (15nM) and collagenase (8µg/ml) from *Clostridium histolyticum* were used as positive controls for DQ collagen type IV digestion. ADAM33 Pro-MP-His was also incubated with FRET peptide DABCYL-YRVAFQKLAE(FAM)K-NH2 to demonstrate that the enzyme was active. The graph represents mean rates ± 1 s.d. obtained from one experiment carried out in triplicate. One data point was excluded from the ADAM33 + DQ Col + peptide data due to an anomalous result. The lack of ADAM33 Pro-MP-His mediated collagen type IV digestion is also representative of another two similar experiments.

6.7.1 ADAM15 FRET peptide

The amino acid sequence NFSN was identified from the PNA-FRET peptide microarray. It corresponded to a sequence found in ADAM15. The NFSN sequence was elongated to span more of the ADAM15 sequence and the following FRET peptide was synthesised DABCYL-FLPGLNFSNCSRRAK-FAM. This peptide was incubated with ADAM33 Pro-MP-His or ADAM33 Pro-MP(E346A)-His in a typical FRET-peptide cleavage assay. An increase in fluorescence of this ADAM15 substrate was not observed and indicated a lack of ADAM33 mediated cleavage. In contrast, the ADAM33 was able to cleave the modified APP FRET peptide efficiently demonstrating that the enzyme had not been inactivated during storage. In all the reactions containing the ADAM15 FRET peptide, the level of fluorescence decreased slowly over the duration of the experiment, perhaps indicating a gradual bleaching of the fluorophore, **Fig.6.6(a).**

6.7.2 Collagen type IV alpha 2 FRET peptide

In a similar manner to the above, the amino acid sequence LLYF was identified from the peptide microarray and was found to correspond to a sequence found in collagen type IV alpha 2. The LLYF sequence was elongated at the N and C-terminus to match the collagen type IV sequence, and the following FRET peptide was synthesised DABCYL-WSGYSLLYFEGEGKK-FAM. This peptide was incubated with ADAM33 Pro-MP-His or ADAM33 Pro-MP(E346A)-His in a typical FRET-peptide cleavage assay. A slow rate of fluorescence increase was observed when this collagen FRET peptide was incubated with either ADAM33 Pro-MP-His or ADAM33 Pro-MP(E346A)-His. The rate of the increase did not differ significantly between the two treatments or from the rate observed when the collagen FRET peptide was incubated in the absence of any enzyme, **Fig. 6.6 (b).** It is unclear why the fluorescence of the peptide should increase, but from the data it appears that the peptide may have limited stability and perhaps be susceptible to non-enzymic degradation.

6.7.3 Varying pH

Each peptide substrate will have its own individual biochemical preferences for the conditions in which it can be cleaved by an enzyme. One of these parameters is pH. To test whether ADAM33 could be made to cleave ADAM15 or collagen type IV FRET peptide under different pH, FRET assays were carried out under the standard conditions, but in a range of buffers differing in pH (pH4, 5, 6, 7, 7.5, 8, and 9) in the

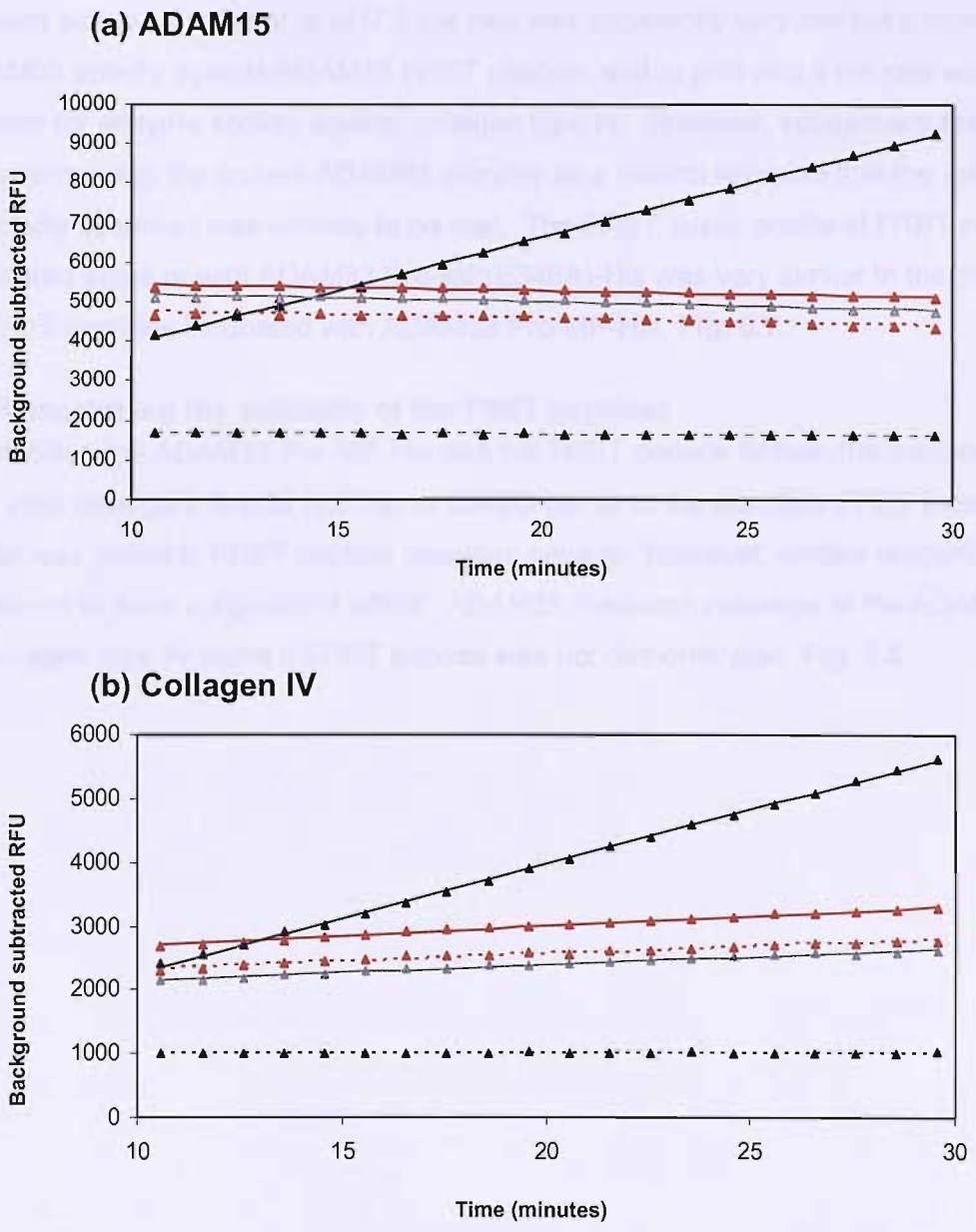

Fig. 6.6. Testing ADAM15 and Collagen IV FRET peptides as substrates for ADAM33. FRET peptide cleavage assays were carried out by incubating 88nM of ADAM33 Pro-MP-His (solid lines) or ADAM33 Pro-MP(E346A)-His (dashed lines) with 4.4μM peptide at 37°C in assay buffer (20mM HEPES pH7.0, 0.5M NaCl, 10mM $CaCl_2$, 10μM $ZnCl_2$, 0.2mg/ml BSA). Fluorescence was measured over time using a Bio-Rad iCycler. (a) The ADAM15 FRET peptide DABCYL-FLPGLNFSNCSRRAK-FAM and the (b) Collagen IV FRET peptide DABCYL-WSGYSLLYFEGEGKK-FAM were tested as substrates for ADAM33. Data obtained when the test peptides were incubated in the presence of enzyme are shown in red. FRET peptides incubated in the absence of enzyme were used as a control and are shown in grey. The APP modified peptide **(see chapter 4)** was used as a positive control to demonstrate enzyme activity and are shown in black. These graphs are plotted from one experiment for each test peptide (carried out in at least duplicate), and the trends observed are representative of two independent experiments.

same manner as the pH optimisation assays were carried out in **Chapter 4**. Under most pH conditions, the rates observed were negative indicating the absence of enzyme activity. However at pH7.5 the rate was apparently very low but positive for ADAM33 activity against ADAM15 FRET peptide, and at pH8 and 9 the rate was positive for enzyme activity against collagen type IV. However, subsequent testing at those pHs using the mutant ADAM33 enzyme as a control revealed that the low level of activity observed was unlikely to be real. The FRET assay profile of FRET peptide incubated alone or with ADAM33 Pro-MP(E346A)-His was very similar to the profile of FRET peptides incubated with ADAM33 Pro-MP-His, **Fig. 6.7**.

6.7.4 Increasing the solubility of the FRET peptides

To stabilise the ADAM33 Pro-MP-His and the FRET peptide further, the addition of a non-ionic detergent Brij-35 (0.01%) or DMSO (20%) to the standard FRET assay buffer was tested in FRET peptide cleavage assays. However, neither reagent appeared to have a significant effect. ADAM33 mediated cleavage of the ADAM15 or collagen type IV alpha 2 FRET peptide was not demonstrated, **Fig. 6.8**.

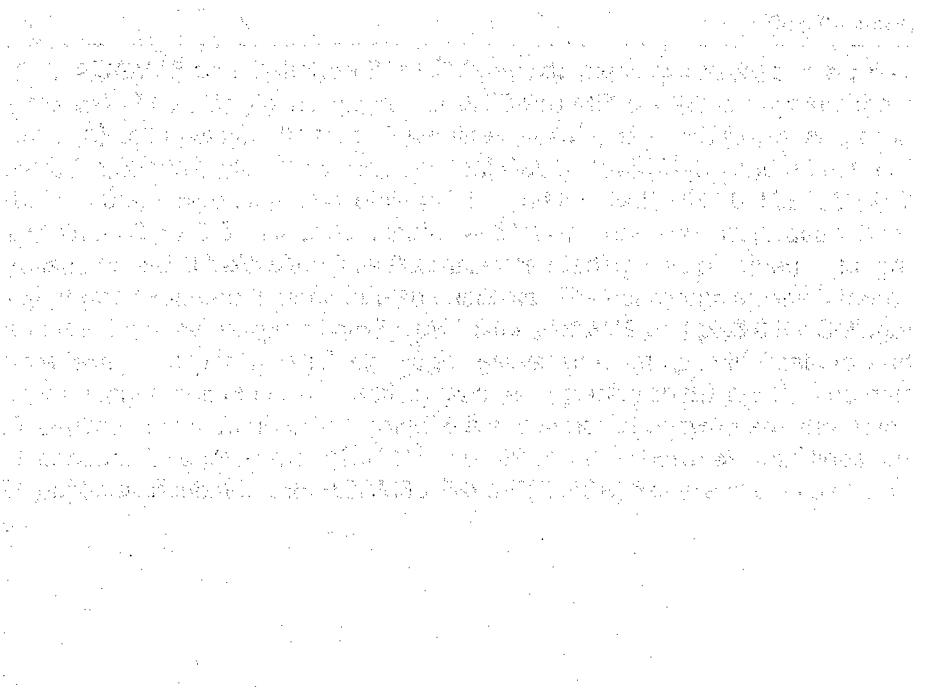

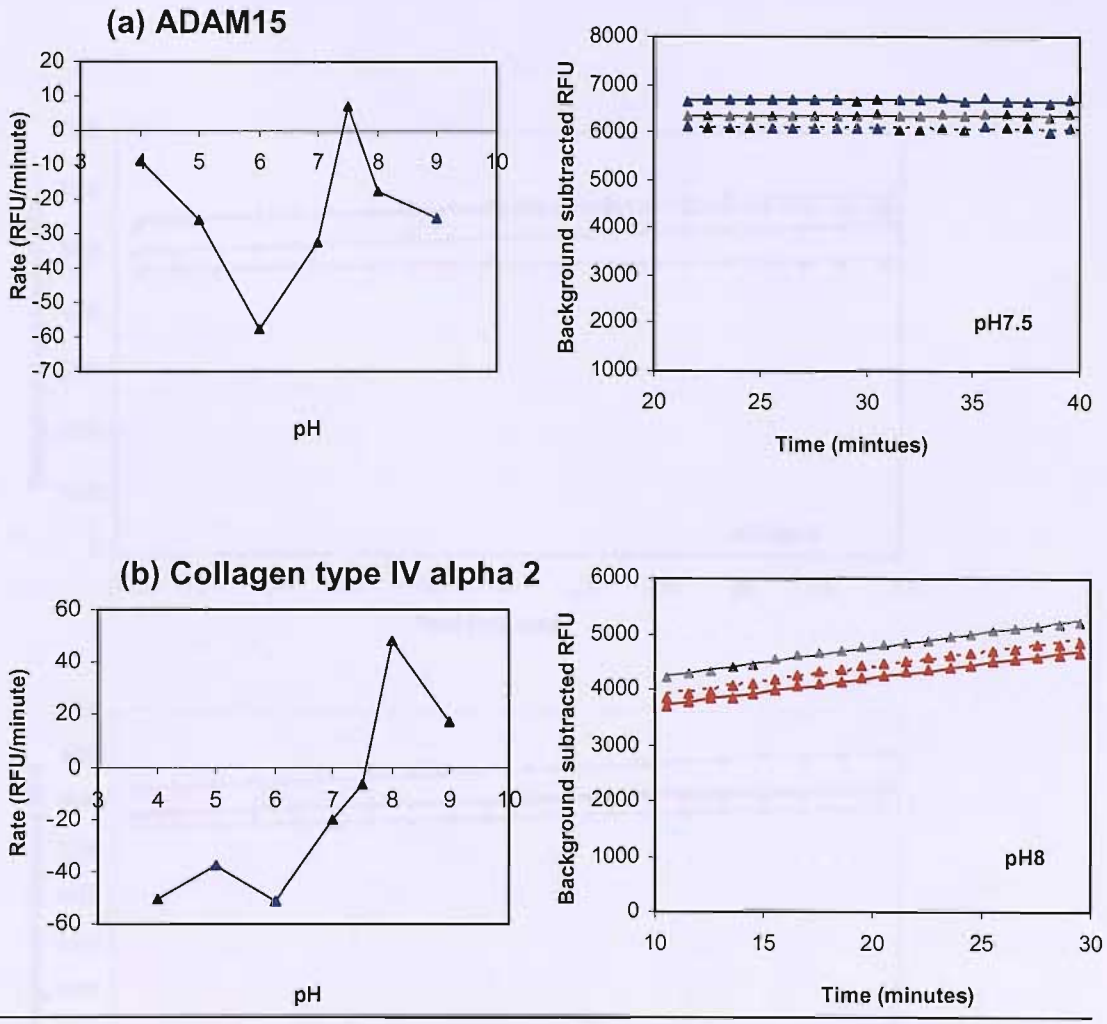

Fig. 6.7. ADAM15 and Collagen IV FRET peptide cleavage assays in buffers of different pH. The catalytic activity of ADAM33 Pro-MP-His (88nM) against the (a) ADAM15 (b) collagen type IV alpha 2 peptides (4.4μM) in a FRET cleavage assay were measured in 20mM buffer, 0.5M NaCl, 10mM $CaCl_2$, 10μM $ZnCl_2$ and 0.2mg/ml BSA. The buffers used were sodium acetate pH 4.0 and 5.0, MES pH6.0, HEPES pH 7.0, 7.5, 8.0 and Tris-HCl pH9.0. After 30 minutes at 37°C the reactions were quenched and neutralised to pH7.0 before the final fluorescence reading was obtained. The graphs represent one experiment carried out in duplicate. The conditions at which there appeared to be some enzyme activity, pH7.5 for ADAM15 and pH8.0 for Collagen type IV, were taken and typical FRET cleavage assays were set up in triplicate to verify whether the presence of enzyme activity was real (graphs on the right). The data from FRET peptides that had been incubated in the absence of enzyme are shown in grey; FRET peptides incubated with ADAM33 Pro-MP-His are shown as solid lines, and FRET peptides incubated with ADAM33 Pro-MP(E346A)-His are shown as dashed lines.

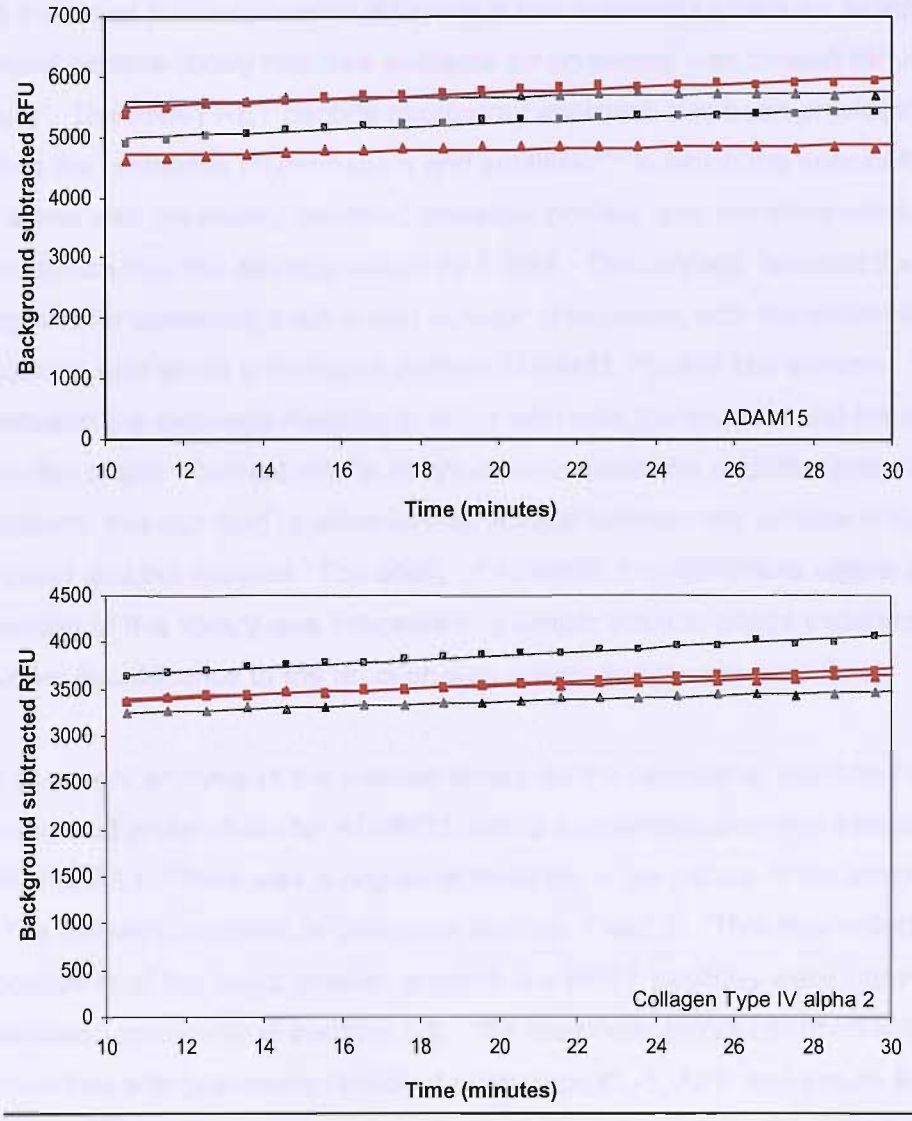

Fig. 6.8. The effect of Brij35 and DMSO on ADAM15 and Collagen type IV FRET peptide cleavage assays. ADAM33 Pro-MP-His (red) and ADAM33 Pro-MP(E346A)-His (grey) enzyme (88nM)were incubated with ADAM15 or collagen type IV alpha 2 FRET peptide (4.4μM) at 37°C, in 20mM HEPES pH7.0, 0.5M NaCl, 10mM $CaCl_2$, 10μM $ZnCl_2$, 0.2mg/ml BSA in the presence of either 0.01% Brij35 (triangles) or 20% DMSO (squares). The fluorescence emission was recorded using a Bio-Rad iCycler. Data representative of one experiment carried out in duplicate.

6.8 Discussion

6.8.1 Screening the PNA-FRET peptide library

To maximise the likelihood of obtaining a true specificity profile for ADAM33, the largest peptide library that was available for screening was chosen for use in this study. The PNA-FRET peptide microarray approach has been previously validated using the proteases chymopapain and subtilisin[242] in which the specificity was found to agree with previously identified cleavage profiles, and therefore provided a level of confidence that this strategy would be fruitful. This strategy reduced the time required for screening such a vast number of peptides, with the additional benefit of requiring only small amounts of purified ADAM33 Pro-MP-His enzyme. Furthermore, it allowed the cleavage reaction to occur with both the enzyme and the peptides in solution phase. Current similar methods immobilise the peptide library onto solid supports, this can lead to adverse interactions between the surface of the solid support and the enzyme. The ability of ADAM33 Pro-MP-His to cleave at least one member of this library was indicated in a simple solution phase experiment, in which the net fluorescence of the reaction was shown to increase over time.

Subsequent analysis of the cleaved library on the microarray platform highlighted the amino acid preferences for ADAM33, with a suggested consenus sequence of (F/V-F/K, F/L,F/L). There was a degree of flexibility in the nature of the amino acids found in the different positions (in particular position 1 and 2). This may reflect the uncertainty of the exact position in which the FRET peptides were cleaved, as discussed previously in **section 6.3.** The specificity profile obtained did bear similarities with previously identified substrates KL-1, APP and insulin B chain peptides[205], with predominantly hydrophobic residues at the C terminal end of the peptides (*denotes cleavage site):

KL-1	PPVAA * SSLRN
APP	YEVHH * QKLVF
Insulin β chain	HLVEA * LYLVC

In addition, the hydrophobic nature of the obtained profile is in agreement with the profile obtained in a study where the APP peptide was subjected to positional scanning using alanine substitutions. In that study, position P3 in the sequence favoured valine, and position P1, 2' and 4' favoured hydrophobic residues[235]. This does not mean that charged residues can not be accommodated since the modified

APP peptide which proved to be a very good substrate for ADAM33 had the sequence YEVAH * QKLAE. This contains both negatively charged glutamic acid and positively charged lysine. The positively charged residues found to be in PNA-peptides identified from the library screen also support this. It is not known whether the flexibility in amino acid usage seen in the suspect peptides would translate to the protein substrates to the same degree. This is because the conformation of a protein is more constrained by the rest of the protein structure and may be less plastic than peptides in solution.

It was unclear why some PNA-peptides were observed to fall above the identity line. This would suggest that the FAM/TAMRA ratio of those particular peptides were higher in the mutant ADAM33 enzyme treated library than the equivalent in the ADAM33 wild type treated library. The results need to be verified through repetition of the experiment, but one interesting explanation of the results could be that the mutant enzyme was binding to some PNA-peptides, and in the absence of the ability to cleave them, it may have interfered with the FRET process leading to an increase of fluorescence above untreated levels during the scanning of the microarrays.

6.8.2 Validating the substrates from the PNA-peptide library - Extracellular matrix proteins

The top eight peptide sequences highlighted by the PNA-FRET peptide library screen were used to search the protein database. A large number of hits were returned from each peptide sequence due to the short length of the peptide. To identify candidate substrates, the list of proteins were narrowed down by eliminating the least likely protein substrates based on the current knowledge of ADAMs. Proteins in which the variable peptide sequence was found to be in an intracellular domain or within the transmembrane domain were not considered. Even after this process the number of hits was very high and it was not practical to screen every protein on the list. Therefore, the proteins which appeared to be highly plausible substrates and those which were easiest to screen were tested. Initially the proteins chosen were collagen type IV and laminin.

These matrix proteins were chosen since it is becoming evident that in addition to ADAM proteins' ability to be sheddases, they also have the capability to re-model the extracellular matrix. Three members of the ADAM family, ADAM12, ADAM10 and ADAM15 have been reported to degrade both collagen type IV and fibronectin in

zymography assays[280]. ADAM12 has been implicated in pathology, although its function is yet to be established. Its expression is elevated in patients with breast and bladder cancer and correlates with disease progression[280;281], and so it has been suggested that ADAM12 may play a role in tumour progression. Bovine ADAM10 can cleave collagen type IV when the two are co-incubated in solution. The degraded fragments can be detected by silver staining of SDS-PAGE protein gels, and the identity of the fragments are detectable by anti-collagen IV antibodies[282]. In a similar manner, there has been one report of ADAM15 mediated degradation of collagen type IV[283]. In that study, ADAM15 was speculated to aid the migration of glomerular mesengial cells by degrading the local extracellular matrix during renal disease progression. The ability of ADAMs to influence the processes of invasion and matrix degradation fits in with the hypothesis that ADAM33 may have a role in angiogenesis and airway remodelling. The degradation of the local matrix to permit invasion of the endothelial cells into the surrounding tissue is a key process during the formation of new capillaries.

Like collagen IV, laminin is a major constituent of the basement membrane that must be degraded during the initial stages of angiogenesis to allow endothelial cell invasion into the surrounding tissue. ADAM9 is a proteinase which again like many of its related family members is associated with tumour cell invasion and migration. Mozzocca and colleagues demonstrated that recombinant ADAM9 could degrade laminin using zymography[211].

In this study, when purified human collagen type IV, laminin and growth factor reduced matrigel were taken and incubated with ADAM33 Pro-MP-His, no cleavage of the matrix proteins was detected when the proteins were analysed by SDS-PAGE. Although disappointing, it did not exclude the possibility that the assay lacked the required level of sensitivity. Western blotting using polyclonal laminin or collagen type IV antibodies is more sensitive and should be considered for similar experiments in the future. Another possibility was that in solution phase, the folding of the matrix proteins were spatially different from the polymerised states that would be encountered *in vivo,* and hence may not be conducive for cleavage. In addition, it is not possible to exclude the possibility that protein fragments were below the detection limit of the SDS-PAGE method, in terms of sensitivity and molecular weight.

To increase the sensitivity of the detection, DQ collagen type IV was tested as a substrate for ADAM33. Although this substrate could be digested by collagenase and MMP-2, it was not digested by ADAM33. In one experiment, it was apparent that some property of the reagent reduced the proteolytic activity of ADAM33 considerably. Although the inhibitory action is still to be verified and explained, it was apparent that DQ collagen type IV was not a good substrate for use in measuring the activity of ADAM33.

6.8.3 Validating the substrates from the PNA-peptide library - FRET peptides

Parallel to cleavage studies using purified extracellular matrix proteins, peptide sequences from collagen type IV and laminin were chosen to be synthesised into FRET peptides (Severn Biotech). Since it has previously been shown that ADAM33 cleaves longer peptides more efficiently[235], the variable peptide sequences identified from the microarray were extended at both the N and C termini to make 14-mer peptides corresponding to the matrix proteins. Due to the difficulty in the synthesis and labelling of the laminin FRET peptide, evaluating this peptide was not possible. Instead, ADAM15, another hit from the microarray was synthesised as a FRET peptide and tested. As discussed in the previous chapter, ADAM15 has an identified role in angiogenesis in pathological conditions, although how it mediates its function is not fully understood. There is some indication that ADAM15 may play a role in capillary regression during angiogenesis. The knock down of ADAM15 using si-RNA can lead to delayed regression of an endothelial tube network in a collagen gel[76]. Therefore cleavage of ADAM15 may disrupt this process and lead to the stabilisation of new vessels. The collagen type IV and ADAM15 peptides were tested in standard FRET peptide cleavage assays to assess them as candidate substrates. Under the standard conditions no ADAM33 mediated cleavage was observed. Subsequently pH and solubility parameters were investigated, but again no ADAM33 Pro-MP-His activity was observed. Although cleavage of peptide sequences obtained from the PNA-peptide microarray screen has not been confirmed, it is worth noting that FRET peptides used in the microarray screen unlike those tested in this experiment had an additional PNA peptide tag. The pesudo-peptide nature of this tag gives it the potential to interact with the peptide or ADAM33 in solution to make the environment more conducive to cleavage, perhaps in a similar manner to how the adjacent protein chains of a real substrate could. Therefore, the experiments carried out here did not serve as a direct test to confirm the cleavage observed in the PNA microarray screen, and the results from these experiments do not provide conclusive evidence that the peptides were false positives in the peptide screen.

In this instance, the consensus sequence obtained was not used to identify potential substrates for ADAM33, which was one of the original intentions of the study. The flexibility of the consensus sequence and the issue with peptide alignment discussed previously, meant that it was necessary to confirm the cleavage of peptides used to construct the consensus sequence prior to the evaluation of proteins containing it. It is likely that a peptide possessing the consensus sequence could as expected be a more efficient substrate than those tested in this study. It would therefore be worthwhile to evaluate these as purified PNA-FRET peptides to confirm cleavage, and to identify potential substrates for ADAM33 from a database search for proteins containing the consensus sequence.

In addition, the peptides and proteins that were selected from the PNA microarray for further testing were chosen on the basis that they are known to influence angiogenesis. In future studies it is also worth considering proteins which are thought to be implicated in asthma susceptibility, such as inactive dipeptidyl peptidase 10 (DPP10). *DPP10* is an asthma susceptibility gene that was identified in 2003 by positional cloning. Its function is not well defined although it is expressed at low levels in the trachea and is capable of regulating potasssium channels. Whether it may be implicated in regulating smooth muscle contraction in the airway is yet to be investigated, but it is interesting to speculate whether ADAM33 may be able to influence BHR via DPP10[284;285].

Lastly, it is also important to take into account the limitations of a biochemical approach to substrate identification based on peptides. Identification of a cleaved sequence using this approach, may not necessarily translate into a cleavable sequence when found within a protein, since other factors such as protein folding may influence accessibility to the sequence and re-iterates the need for protein based substrate validation.

6.8.4 Summary

The microarray data has brought a number of proteins of interest to light. This includes extracellular matrix proteins such as laminin, collagens, growth factors and their receptors, which are conceivable ADAM targets and other proteins implicated in asthma susceptibility. It can easily be envisaged how cleavage of collagen type IV and laminin could contribute to the pro-angiogenic effect of ADAM33 observed in the previous chapter. With their availability in the laboratory, these matrix proteins were

the first of the substrates to be investigated. Using the simplest solution based cleavage assay and FRET peptide cleavage assays, ADAM33 mediated cleavage of the matrix proteins and ADAM15 were not observed.

Although such methods have been used in the past for other ADAM proteins, every proteinase is unique and it is possible that the conditions under which cleavage is achieved may require a very specific set of conditions which were not tested in this study. It is believed that the cleavage of members of the PNA-FRET peptide library was real, and that ADAM33 mediated cleavage is the most likely explanation for the increase in the fluorescence of the solution, in which the library and the ADAM33 were co-incubated. Efforts to demonstrate cleavage of individual proteins and peptides have been inconclusive. However, there remains a lot of potential in optimising the PNA-peptide microarray screening approach and validating its results. Especially when the data produced contains candidate proteins which fit appropriately with the current understanding of ADAMs and angiogenesis and its potential role in asthma remodelling.

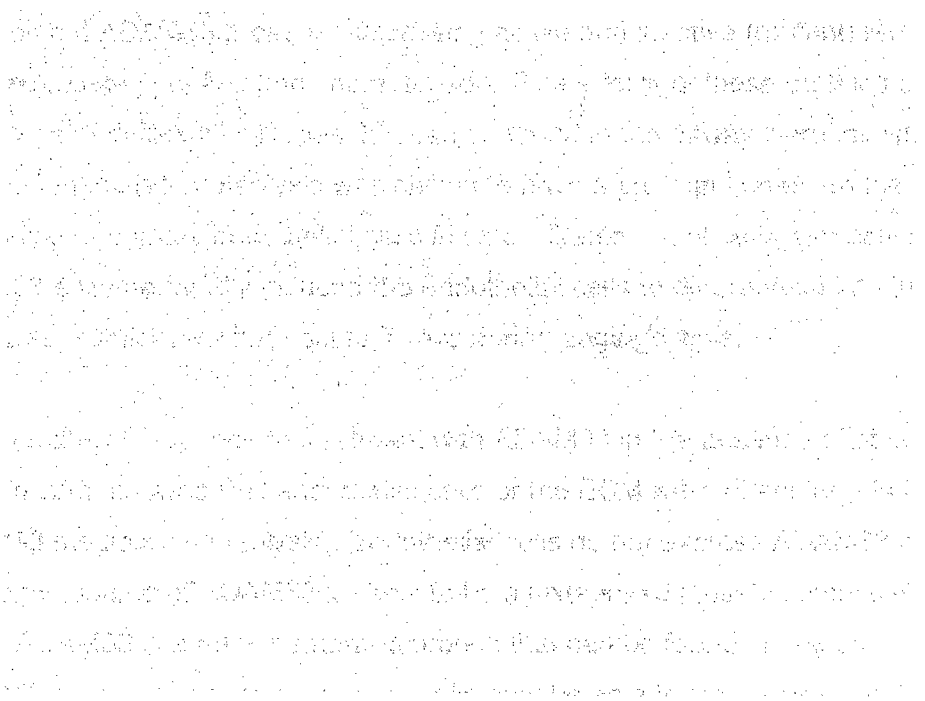

Chapter 7 Final discussion

7.1 Unravelling the function of ADAM33

At the start of this project back in 2003, a novel asthma gene, *ADAM33*, had been brought to attention. It was the first positionally cloned asthma susceptibility gene and rapidly became a topic of hot interest. Subsequently many genetic studies have shown *ADAM33* to be associated with asthma in different populations[183;184;187], COPD[196] and implicated it in the maintenance of lung function of the general population[192], raising the profile of this candidate.

What is somewhat surprising is that since its discovery little progress has made in the understanding of the functional role of ADAM33. A correlation between the ADAM33 level in BAL fluid and disease severity remains one of the few pieces of non-genetic evidence to support a role for ADAM33 in disease. Reports of a correlation between ADAM33 protein levels in the asthmatic airway epithelium remain controversial, and have not been reproducible in our lab[229;230]. An *Adam33* knock-out mouse model has yielded no functional clues; the animals were asymptomatic with normal growth and development[233].

To progress the understanding of ADAM33 function, a reductionist approach was taken in this study. With the literature strongly indicating a role for the MP domain, recombinant ADAM33 proteins possessing active and inactive (mutant) MP domains were expressed, purified and characterised. The effects of these proteins on the phenotype of different cell types that can be found in the airway were investigated. ADAM33 mediated proteolysis was shown to have a profound effect on the phenotype of primary endothelial cells *in vitro*. Treatment of cells with active ADAM33 enzyme rapidly induced the endothelial cells to differentiate into tube like structures, mimicking what occurs *in vivo* during angiogenesis.

The endothelial response to treatment with ADAM33 in the absence of other cell types *in vitro,* showed that endothelial cells or the ECM were direct targets for ADAM33 mediated proteolysis. Endothelial cells do not express ADAM33 and in the airway the source of ADAM33 is likely to be a juxtaposed mesenchymal cell. Full length ADAM33 is a transmembrane protein that can be found on the cell surface. ADAM33 expressed in mesenchymal cells may be able to cleave proteins from the endothelial cells in trans, releasing growth factors and cytokines which are implicated in endothelial differentiation. Although ADAM proteins typically cleave in cis (proteins

on the same cell as itself), cleavage of substrates in trans has previously been demonstrated for ADAM10, in the cleavage of ephrin-A5. Signalling resulting from ephrin and ephrin receptor signalling results in the repulsion between the two interacting cells changing cell attachment and migratory characteristics. Typically ADAM10 and the ephrin-A5 receptor Eph-A3 do not associate with each other when expressed on the same cell. However when Eph-A3 binds its ligand ephrin-A5 on an adjacent cell, ADAM10 is able to associate with the complex with high affinity using its cysteine rich domain. This subsequently results in the ADAM10 mediated cleavage of ephrin-A5 releasing it from the adjacent cell[286]. In this mechanism the cysteine rich domain brings the ADAM and its substrate into close proximity to facilitate cleavage. This serves as an example of the "beloved liberator" model of ADAM proteolysis, in which protein domains other than the MP domain serve to regulate proteolytic specificity. In addition to cleaving cell surface molecules in trans, ADAM33 may also cleave substrates in the extracellular space such as ECM proteins and pro-angiogenic growth factors anchored to the ECM. The degradation of the local ECM and adjacent basement membrane is an important initial step in angiogenesis, and is required to permit endothelial cell migration. A pictorial depicting these possible mechanisms is shown in **Fig. 7.1**.

To complement the functional assays, the confirmation of a biologically relevant substrate was attempted as part of this study. A novel PNA-peptide microarray approach was used to screen peptides as potential substrates. The cleaved sequences were aligned and a cleavage consensus sequence was obtained for ADAM33. Reassuringly, the sequence bears similarity with the specificity profile proposed by Zou and colleagues[235]. Preliminary analysis suggested that putative ADAM substrates such as extracellular matrix proteins and ADAMs with known roles in angiogenesis, contain sequences which may be cleaved by ADAM33. Initial experiments carried out to test these substrates have been inconclusive. Ongoing efforts are being made to identify the substrate as it has great importance in furthering the understanding of ADAM33 function, and also for increasing the prospect of developing an effective therapeutic.

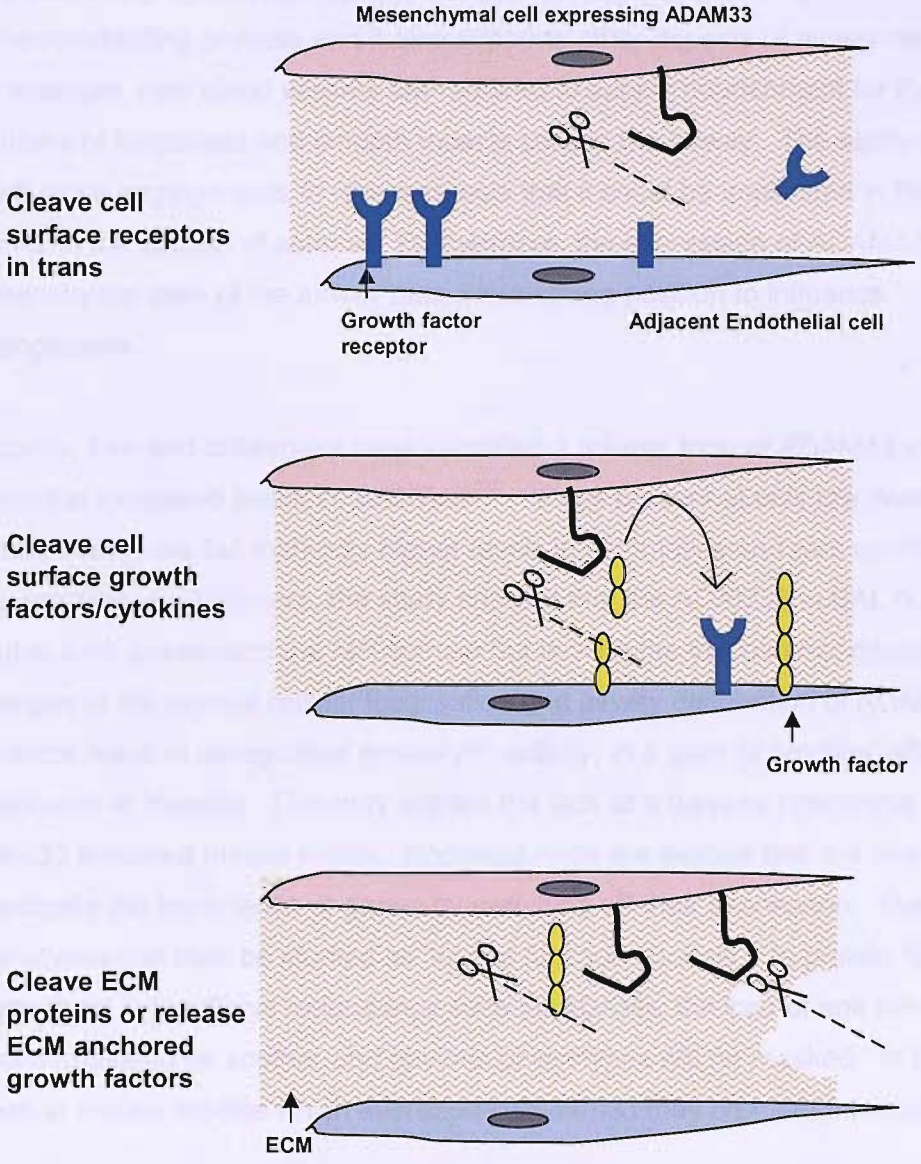

Fig. 7.1. Mechanisms by which ADAM33 expressed by mesenchymal may exert an effect on endothelial cells. The mesenchymal cells adjacent to endothelial cells are a source of ADAM33 in the airway. This pictorial represents potential ways in which ADAM33 proteolysis could affect the behaviour of the endothelial cells and promote them to differentiate. The ADAM33 may cleave endothelial cell surface growth factors, their receptors of cytokines in trans, or it may release pro-angiogenic growth factors from the surrounding extracellular matrix, or it may degrade extracellular matrix proteins directly to facilitate endothelial cell migration.

7.2 A role for ADAM33 in asthma and airway remodelling

An increase in the vascularity seen in asthmatic airways indicates that there is an increase in angiogenesis in asthma which is correlated to severity [80;270]. This is part of the remodelling process and it also supports other aspects of airway remodelling. For example, new blood vessels are required to supply nourishment for the increased numbers of fibroblasts and smooth muscle cells in the airway. The ability of ADAM33 to influence angiogenesis *in vitro* suggests that it could be implicated in this process *in vivo,* in the context of asthma. Furthermore, the expression of ADAM33 in mesenchymal cells of the airway puts it in a strong position to influence angiogenesis.

Recently, Lee and colleagues have identified a soluble form of ADAM33 which is present in increased levels in BAL fluid[232]. It was present at only low levels in normal individuals but markedly higher levels in asthmatics and was correlated with lung function. Furthermore, the study showed that the ADAM33 in BAL fluid was a soluble form possessing the MP domain but lacking the cytoplasmic domain. Changes to the normal cellular localisation and airway distribution of ADAM33 may therefore result in deregulated proteolytic activity, in a 'gain of function' effect which contributes to disease. This may explain the lack of a disease phenotype in the *Adam33* knockout mouse model. Knockout-mice are models that are used to investigate the importance of genes by switching off their expression. The resulting phenotypes can then be studied as 'loss of function' models. In protein families where there is functional redundancy such as ADAMs, the loss of one member may be compensated by another and obvious phenotypes will be masked. In light of this, knock-in mouse models which overexpress *Adam33* may be more informative.

7.3 The deregulation of ADAM33 in asthma

ADAM33 is produced in mesenchymal cells. As discussed above, a soluble form can also be found in BAL fluid from asthmatic patients. This suggests that soluble ADAM33 can be distributed throughout the airway in the disease setting. The loss of normal spatial regulation of ADAM33 may allow it to cleave its physiological substrate in an unregulated manner. Alternatively, ADAM33 may encounter proteins, which are not normally ADAM33 substrates due to their spatial separation. These may be extracellular proteins or proteins on the surface of other cells which do not express ADAM33. In the airway, the close proximity between mesenchymal cells expressing soluble ADAM33 and endothelial cells, suggests that the latter may be subjected to

high levels of active ADAM33 *in vivo*. Given the pro-angiogenic activity of ADAM33, it is plausible that the increase in vascularity in asthmatic airways may be partly attributed to deregulated activity of soluble ADAM33.

If the deregulation of soluble ADAM33 can contribute to the increased vascularity in the asthmatic airway, then the question of why it is deregulated is important. Although soluble ADAM33 has been described the process by which it is generated is yet to be elucidated. Possibilities include the alternative splicing of mRNA transcripts and the shedding of ADAM33 from the cell surface of the protein. There is evidence to support both these mechanisms in the release of soluble ADAM proteins. A mRNA transcript for a putative soluble form of ADAM33 has been described in airway fibroblasts[228]. In addition, soluble forms of ADAMs generated by differential splicing have also been reported for ADAMs, such as ADAM-9 and ADAM12. *Xenopus* ADAM13 the closest relative of ADAM33 sheds itself from the cell surface in a mechanism dependent on its own proteolytic activity[287]. It is thought that ADAMs may need to traffic to the cell surface in order to be shed by a sheddase (which are typically ADAM proteins). There is some evidence to suggest that the cytoplasmic tails of ADAM33 proteins can mediate ADAM33 dimerisation (Gill Murphy personal communication). Therefore, the dimerisation of ADAM33 on the cell surface may regulate the shedding of ADAM33 into the extracellular space. Genetically encoded changes to the cytoplasmic tail of ADAM33 may interfere with ADAM33 trafficking or its dimerisation and could be a potential mechanism by which the shedding of ADAM33 can become deregulated. **Fig. 7.2** depicts how ADAM33 deregulation may be implicated in airway remodelling.

7.4 Can endothelial cells capture deregulated soluble ADAM33?

In addition to the aberrant spatial localisation of ADAM33 in the airway it is interesting to speculate whether endothelial cells can capture the soluble ADAM33 which it encounters. This could increase the local concentration of soluble ADAM33, and direct its activity towards the endothelial cell surface proteins and its immediate ECM. The persistence of ADAM33 activity on the endothelial cell surface may amplify the effect of the presence of deregulated ADAM33 and promote the migration and invasion processes of angiogenesis. Although ADAM33 capture by endothelial cells has not been investigated in this study, recent studies by other groups provide some evidence that this maybe plausible.

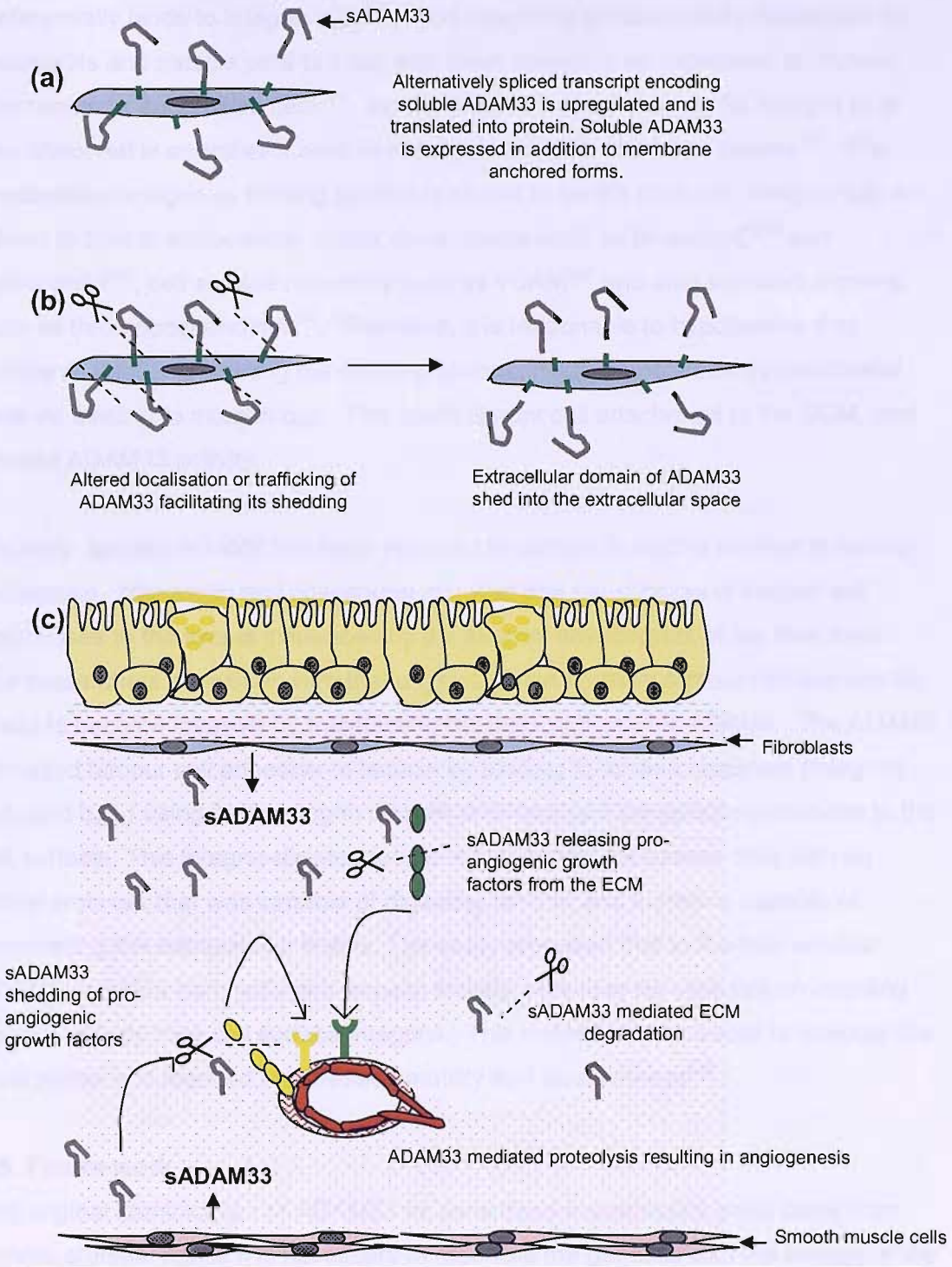

Fig. 7.2. Deregulated ADAM33 proteolysis. (a) In airway fibroblasts, alternative splicing may generate a a splice variant coding for soluble form of ADAM33. Upregulation of this transcript may arise from SNP polymorphisms in ADAM33, and increase its expression in the airway. (b) Alternatively, aberrant trafficking of ADAM33 to the cell surface may increase the shedding of ADAM33, leading to the release of soluble ADAM33 (sADAM33) into the airway tissue. (c) In the asthmatic airway mesenchymal cells may release soluble ADAM33 (sADAM33). This sADAM33 gets distributed aberrantly in the asthmatic airway and its proteolytic activity is no longer tightly controlled. It may cleave pro-angiogenic growth factors from the surface of nearby endothelial cells, or release ECM anchored growth factors which can signal to the endothelial cells. sADAM33 may also degrade the ECM to facilitate the migration or invasion of endothelial cells and promote angiogenesis.

Bridges and colleagues have reported that the disintegrin domain of ADAM33 preferentially binds to integrin $\alpha_9\beta_1$[207]. This integrin is predominately expressed on neutrophils and muscle cells but has also been shown to be expressed on human microvascular endothelial cells[288]. Immunohistochemical staining for integrin α_9 is also observed in endothelial cells from lung, brain, skin and heart tissues[289]. The predominant integrin α_9 binding partner is known to be the β_1 chain. Integrin $\alpha_9\beta_1$ is known to bind to extracellular matrix components such as tenascin-C[290] and osteopontin[291], cell surface receptors such as VCAM[292] and also secreted proteins such as thromobospondin-1[289]. Therefore, it is reasonable to hypothesise that soluble ADAM33 containing the disintegrin domain maybe captured by endothelial cells via binding to integrin $\alpha_9\beta_1$. This could disrupt cell attachment to the ECM, and localise ADAM33 activity.

Recently, soluble ADAM9 has been reported to behave in such a manner in cancer metastasis. Mazzocca and colleagues reported that the success of tumour cell metastases to the liver is influenced by the stromal environment of the liver itself. The researchers showed *in vitro* that a typically non invasive tumour cell line can be made to become invasive by transfecting the cells with soluble ADAM9. The ADAM9 disrupted tumour cell adhesion to laminin by binding to laminin receptors (integrins $\alpha_6\beta_4$ and $\alpha_2\beta_1$) using its disintegrin domain and localised the soluble proteinase to the cell surface. This integrin-disintegrin interaction armed the tumour cells with an active protease that was capable of digesting laminin and therefore capable of remodelling the extracellular matrix. The study proposed that in the liver soluble ADAM9 secreted from activated hepatic stellate cells may be captured on invading tumour cells by their cell surface integrins. This increased their ability to remodel the local matrix and resulted in increased motility and invasiveness[211].

7.5 Future work

The original identification of *ADAM33* as an asthma susceptibility gene came from genetic studies, hence it is necessary to reconcile the genetics with the biology of the disease. In the original paper that described *ADAM33*, both coding and non coding SNPs were found to be associated with asthma [181]. Non-coding SNPs have the potential to modulate mRNA splicing patterns which may lead to the generation of soluble forms of ADAM33 which are no longer regulated by the cell which secretes them. In addition SNPs (T1 and T2) encoding amino acid substitutions in cytoplasmic tail of *ADAM33* were found to be associated with asthma in the US population. It is conceivable that these SNPs may potentiate trafficking of the

ADAM33 proteins to the cell surface and modulate their ability to dimerise. To test the whether these SNPs can cause the deregulation of ADAM33, *ADAM33* engineered with these SNPs should be studied in transfected cell models *in vitro*.

To complement these *in vitro* studies, the distribution of ADAM33 protein in the airway should be investigated more thoroughly. Comparisons can be made between the spatial localisation of the regulated transmembrane ADAM33 and the deregulated soluble ADAM33 in the airways of asthmatic and normal individuals. Immunohistochemistry data for ADAM33 carried out on bronchial biopsies could then be related back to specific *ADAM33* SNP genotypes of the subjects, to establish whether the *in vivo* data corresponds to the *in vitro* data.

The evidence for a functional role for ADAM33 in angiogenesis has been based on *in vitro* studies. *In* vivo, the outcome of ADAM33 mediated proteolysis on the behaviour of endothelial cells will be influenced by its microenvironment and the signals it receives from neighbouring cells, such as pericytes and smooth muscle cells as well as the ECM. It is now important to demonstrate that the pro-angiogenic effect observed is not only an *in vitro* phenomenon, but translates through to *in vivo* models. Many *in vivo* models exist including the chick chorio-allantoic membrane assay and tumour growth models. These can be used to study the ADAM33 effect further.

7.6 Conclusion

Research into ADAM33 and its role in asthma and bronchial hyperresponsiveness is now in an exciting phase. A functional role for ADAM33 has been demonstrated for the first time. The capability of ADAM33 to promote angiogenesis is fitting with the genetic studies which show that it is associated with asthma and airway remodelling. Furthermore, it may serve to explain the association between *ADAM33* and COPD, in which the vascular area of the airway is significantly increased relative to normal controls[270]. The importance of angiogenesis and its regulation broadens the range of pathologies in which ADAM33 could be implicated, the most obvious being cancer.

Reference List

1. Asthma UK. 2004. Where do we stand? Asthma in the UK today. Report.

2. Global initiative for asthma. 2005. Global strategy for asthma management and prevention. Report.

3. Goldsby,R., T.Kindt, and Osbourne BA. 2000. Kuby Immunology. W.H. Freeman and Company.

4. Hilman, B. NHLBI guidelines for diagnosis and management of asthma. 1997. Bethesda Md: National Heart, Lung and Blood Institute 1997. NIH publication no.97-4051.

5. Salvi ,S., A.Sampson, and S.Holgate. 2001. Encylopedia of Life Sciences, Asthma. Wiley & Sons Ltd.

6. Hargreave,F.E., E.H.Ramsdale, P.J.Sterk, and E.F.Juniper. 1985. Advances in the use of inhalation provocation tests in clinical evaluation. *Chest* 87:32S-35S.

7. Howarth,P.H., J.Wilson, R.Djukanovic, S.Wilson, K.Britten, A.Walls, W.R.Roche, and S.T.Holgate. 1991. Airway inflammation and atopic asthma: a comparative bronchoscopic investigation. *Int. Arch. Allergy Appl. Immunol.* 94:266-269.

8. Jeffery,P.K., A.J.Wardlaw, F.C.Nelson, J.V.Collins, and A.B.Kay. 1989. Bronchial biopsies in asthma. An ultrastructural, quantitative study and correlation with hyperreactivity. *Am. Rev. Respir Dis.* 140:1745-1753.

9. Foresi,A., G.Bertorelli, A.Pesci, A.Chetta, and D.Olivieri. 1990. Inflammatory markers in bronchoalveolar lavage and in bronchial biopsy in asthma during remission. *Chest* 98:528-535.

10. 2003. The ENFUMOSA cross-sectional European multicentre study of the clinical phenotype of chronic severe asthma. European Network for Understanding Mechanisms of Severe Asthma. *Eur Respir J* 22:470-477.

11. Reid,M.J., R.B.Moss, Y.P.Hsu, J.M.Kwasnicki, T.M.Commerford, and B.L.Nelson. 1986. Seasonal asthma in northern California: allergic causes and efficacy of immunotherapy. *J Allergy Clin. Immunol.* 78:590-600.

12. Sporik,R., T.A.Platts-Mills, and J.J.Cogswell. 1993. Exposure to house dust mite allergen of children admitted to hospital with asthma. *Clin. Exp. Allergy* 23:740-746.

13. Atkinson,R.W., D.P.Strachan, H.R.Anderson, S.Hajat, and J.Emberlin. 2006. Temporal associations between daily counts of fungal spores and asthma exacerbations. *Occup. Environ. Med.* 63:580-590.

14. Negrao-Correa,D. 2001. Importance of immunoglobulin E (IgE) in the protective mechanism against gastrointestinal nematode infection: looking at the intestinal mucosae. *Rev. Inst. Med. Trop. Sao Paulo* 43:291-299.

15. Allergy: the unmet need. A report of the Royal College of Physicians Working Party on the Provision of allergy services in the UK . 2003. Royal College of Physicians.

16. Pearce,N., J.Pekkanen, and R.Beasley. 1999. How much asthma is really attributable to atopy? *Thorax* 54:268-272.

17. Bradding,P., J.A.Roberts, K.M.Britten, S.Montefort, R.Djukanovic, R.Mueller, C.H.Heusser, P.H.Howarth, and S.T.Holgate. 1994. Interleukin-4, -5, and -6 and tumor necrosis factor-alpha in normal and asthmatic airways: evidence for the human mast cell as a source of these cytokines. *Am. J Respir Cell Mol. Biol.* 10:471-480.

18. Carroll,N.G., S.Mutavdzic, and A.L.James. 2002. Increased mast cells and neutrophils in submucosal mucous glands and mucus plugging in patients with asthma. *Thorax* 57:677-682.

19. Brightling,C.E., P.Bradding, F.A.Symon, S.T.Holgate, A.J.Wardlaw, and I.D.Pavord. 2002. Mast-cell infiltration of airway smooth muscle in asthma. *N. Engl. J Med.* 346:1699-1705.

20. Begueret,H., P.Berger, J.M.Vernejoux, L.Dubuisson, R.Marthan, and J.M.Tunon-de-Lara. 2007. Inflammation of bronchial smooth muscle in allergic asthma. *Thorax* 62:8-15.

21. Bjorck,T. and S.E.Dahlen. 1993. Leukotrienes and histamine mediate IgE-dependent contractions of human bronchi: pharmacological evidence obtained with tissues from asthmatic and non-asthmatic subjects. *Pulm. Pharmacol.* 6:87-96.

22. Puxeddu,I., A.M.Piliponsky, I.Bachelet, and F.Levi-Schaffer. 2003. Mast cells in allergy and beyond. *Int. J Biochem. Cell Biol.* 35:1601-1607.

23. Casale,T.B., D.Wood, H.B.Richerson, B.Zehr, D.Zavala, and G.W.Hunninghake. 1987. Direct evidence of a role for mast cells in the pathogenesis of antigen-induced bronchoconstriction. *J Clin. Invest* 80:1507-1511.

24. Wenzel,S.E., J.Y.Westcott, and G.L.Larsen. 1991. Bronchoalveolar lavage fluid mediator levels 5 minutes after allergen challenge in atopic subjects with asthma: relationship to the development of late asthmatic responses. *J Allergy Clin. Immunol.* 87:540-548.

25. Fahy,J.V. 2002. Goblet cell and mucin gene abnormalities in asthma. *Chest* 122:320S-326S.

26. Bradding,P. and S.T.Holgate. 1999. Immunopathology and human mast cell cytokines. *Crit Rev. Oncol. Hematol.* 31:119-133.

27. Fabbri,L.M., P.Boschetto, E.Zocca, G.Milani, F.Pivirotto, M.Plebani, A.Burlina, B.Licata, and C.E.Mapp. 1987. Bronchoalveolar neutrophilia during late asthmatic reactions induced by toluene diisocyanate. *Am. Rev. Respir Dis.* 136:36-42.

28. Rossi,G.A., E.Crimi, S.Lantero, P.Gianiorio, S.Oddera, P.Crimi, and V.Brusasco. 1991. Late-phase asthmatic reaction to inhaled allergen is associated with early recruitment of eosinophils in the airways. *Am. Rev. Respir Dis.* 144:379-383.

29. Strohmeier,G.R., B.A.Brunkhorst, K.F.Seetoo, T.Meshulam, J.Bernardo, and E.R.Simons. 1995. Role of the Fc gamma R subclasses Fc gamma RII and Fc gamma RIII in the activation of human neutrophils by low and high valency immune complexes. *J Leukoc. Biol.* 58:415-422.

30. Kaneko,M., M.C.Swanson, G.J.Gleich, and H.Kita. 1995. Allergen-specific IgG1 and IgG3 through Fc gamma RII induce eosinophil degranulation. *J Clin. Invest* 95:2813-2821.

31. Samoszuk,M.K., A.Petersen, F.Gidanian, and C.Rietveld. 1988. Cytophilic and cytotoxic properties of human eosinophil peroxidase plus major basic protein. *Am. J Pathol.* 132:455-460.

32. Frigas,E., S.Motojima, and G.J.Gleich. 1991. The eosinophilic injury to the mucosa of the airways in the pathogenesis of bronchial asthma. *Eur Respir J Suppl* 13:123s-135s.

33. Filley,W.V., K.E.Holley, G.M.Kephart, and G.J.Gleich. 1982. Identification by immunofluorescence of eosinophil granule major basic protein in lung tissues of patients with bronchial asthma. *Lancet* 2:11-16.

34. Broide,D.H., M.M.Paine, and G.S.Firestein. 1992. Eosinophils express interleukin 5 and granulocyte macrophage-colony-stimulating factor mRNA at sites of allergic inflammation in asthmatics. *J Clin. Invest* 90:1414-1424.

35. Kita,H., T.Ohnishi, Y.Okubo, D.Weiler, J.S.Abrams, and G.J.Gleich. 1991. Granulocyte/macrophage colony-stimulating factor and interleukin 3 release from human peripheral blood eosinophils and neutrophils. *J Exp. Med.* 174:745-748.

36. Janeway,A., P.Travers, M.Walport, and M.Shlomchik. 2005. Immunobiology. Garland Publishing.

37. Werb,Z. and S.Gordon. 1975. Elastase secretion by stimulated macrophages. Characterization and regulation. *J Exp. Med.* 142:361-377.

38. Wahl,L.M., S.M.Wahl, S.E.Mergenhagen, and G.R.Martin. 1975. Collagenase production by lymphokine-activated macrophages. *Science* 187:261-263.

39. John,M., S.Lim, J.Seybold, P.Jose, A.Robichaud, B.O'Connor, P.J.Barnes, and K.F.Chung. 1998. Inhaled corticosteroids increase interleukin-10 but reduce macrophage inflammatory protein-1alpha, granulocyte-macrophage colony-stimulating factor, and interferon-gamma release from alveolar macrophages in asthma. *Am. J Respir Crit Care Med.* 157:256-262.

40. Hallsworth,M.P., C.P.Soh, S.J.Lane, J.P.Arm, and T.H.Lee. 1994. Selective enhancement of GM-CSF, TNF-alpha, IL-1 beta and IL-8 production by monocytes and macrophages of asthmatic subjects. *Eur Respir J* 7:1096-1102.

41. Ying,S., S.R.Durham, C.J.Corrigan, Q.Hamid, and A.B.Kay. 1995. Phenotype of cells expressing mRNA for TH2-type (interleukin 4 and interleukin 5) and TH1-type (interleukin 2 and interferon gamma) cytokines in bronchoalveolar lavage and bronchial biopsies from atopic asthmatic and normal control subjects. *Am. J Respir Cell Mol. Biol.* 12:477-487.

42. Robinson,D.S., Q.Hamid, S.Ying, A.Tsicopoulos, J.Barkans, A.M.Bentley, C.Corrigan, S.R.Durham, and A.B.Kay. 1992. Predominant TH2-like bronchoalveolar T-lymphocyte population in atopic asthma. *N. Engl. J Med.* 326:298-304.

43. Oettgen,H.C. 2000. Regulation of the IgE isotype switch: new insights on cytokine signals and the functions of epsilon germline transcripts. *Curr. Opin. Immunol.* 12:618-623.

44. Gail,D.B. and C.J.Lenfant. 1983. Cells of the lung: biology and clinical implications. *Am. Rev. Respir Dis.* 127:366-387.

45. Rhodin,J.A. 1966. The ciliated cell. Ultrastructure and function of the human tracheal mucosa. *Am. Rev. Respir Dis.* 93:Suppl-15.

46. Widdicombe,J.G. and R.J.Pack. 1982. The Clara cell. *Eur J Respir Dis.* 63:202-220.

47. Boers,J.E., A.W.Ambergen, and F.B.Thunnissen. 1998. Number and proliferation of basal and parabasal cells in normal human airway epithelium. *Am. J Respir Crit Care Med.* 157:2000-2006.

48. Godfrey,R.W., N.J.Severs, and P.K.Jeffery. 1992. Freeze-fracture morphology and quantification of human bronchial epithelial tight junctions. *Am. J Respir Cell Mol. Biol.* 6:453-458.

49. Hamid, Q., Martin, J., and Shannon, J. 2005. Physiological basis of respiratory disease. B.C. Decker Inc.

50. Evans,M.J., S.C.Guha, R.A.Cox, and P.C.Moller. 1993. Attenuated fibroblast sheath around the basement membrane zone in the trachea. *Am. J Respir Cell Mol. Biol.* 8:188-192.

51. Minoo,P. and R.J.King. 1994. Epithelial-mesenchymal interactions in lung development. *Annu. Rev. Physiol* 56:13-45.

52. Franklin Adkinson JR,N., J.Yunginger, W.Busse, B.Bochner, S.Holgate, F.Estelle, and R.Simons. 2003. Middleton's Allergy Principles & Practice. Mosby.

53. Shahana,S., E.Bjornsson, D.Ludviksdottir, C.Janson, O.Nettelbladt, P.Venge, and G.M.Roomans. 2005. Ultrastructure of bronchial biopsies from patients with allergic and non-allergic asthma. *Respir Med.* 99:429-443.

54. Shebani,E., S.Shahana, C.Janson, and G.M.Roomans. 2005. Attachment of columnar airway epithelial cells in asthma. *Tissue Cell* 37:145-152.

55. Bucchieri,F., S.M.Puddicombe, J.L.Lordan, A.Richter, D.Buchanan, S.J.Wilson, J.Ward, G.Zummo, P.H.Howarth, R.Djukanovic, S.T.Holgate, and D.E.Davies. 2002. Asthmatic bronchial epithelium is more susceptible to oxidant-induced apoptosis. *Am. J Respir Cell Mol. Biol.* 27:179-185.

56. Bayram,H., C.Rusznak, O.A.Khair, R.J.Sapsford, and M.M.Abdelaziz. 2002. Effect of ozone and nitrogen dioxide on the permeability of bronchial epithelial cell cultures of non-asthmatic and asthmatic subjects. *Clin. Exp. Allergy* 32:1285-1292.

57. Sidebotham,H.J. and W.R.Roche. 2003. Asthma deaths; persistent and preventable mortality. *Histopathology* 43:105-117.

58. Sheehan,J.K., P.S.Richardson, D.C.Fung, M.Howard, and D.J.Thornton. 1995. Analysis of respiratory mucus glycoproteins in asthma: a detailed study from a patient who died in status asthmaticus. *Am. J Respir Cell Mol. Biol.* 13:748-756.

59. Ordonez,C.L., R.Khashayar, H.H.Wong, R.Ferrando, R.Wu, D.M.Hyde, J.A.Hotchkiss, Y.Zhang, A.Novikov, G.Dolganov, and J.V.Fahy. 2001. Mild and moderate asthma is associated with airway goblet cell hyperplasia and abnormalities in mucin gene expression. *Am. J Respir Crit Care Med.* 163:517-523.

60. Bock,P. and L.Stockinger. 1984. Light and electron microscopic identification of elastic, elaunin and oxytalan fibers in human tracheal and bronchial mucosa. *Anat. Embryol. (Berl)* 170:145-153.

61. Evans,M.J., L.S.Van Winkle, M.V.Fanucchi, E.Toskala, E.C.Luck, P.L.Sannes, and C.G.Plopper. 2000. Three-dimensional organization of the lamina reticularis in the rat tracheal basement membrane zone. *Am. J Respir Cell Mol. Biol.* 22:393-397.

62. Merker,H.J. 1994. Morphology of the basement membrane. *Microsc. Res. Tech.* 28:95-124.

63. Bourdin,A., D.Neveu, I.Vachier, F.Paganin, P.Godard, and P.Chanez. 2007. Specificity of basement membrane thickening in severe asthma. *J Allergy Clin. Immunol.*

64. Payne,D.N., A.V.Rogers, E.Adelroth, V.Bandi, K.K.Guntupalli, A.Bush, and P.K.Jeffery. 2003. Early thickening of the reticular basement membrane in children with difficult asthma. *Am. J Respir Crit Care Med.* 167:78-82.

65. Kasahara,K., K.Shiba, T.Ozawa, K.Okuda, and M.Adachi. 2002. Correlation between the bronchial subepithelial layer and whole airway wall thickness in patients with asthma. *Thorax* 57:242-246.

66. Ward,C., D.P.Johns, R.Bish, M.Pais, D.W.Reid, C.Ingram, B.Feltis, and E.H.Walters. 2001. Reduced airway distensibility, fixed airflow limitation, and airway wall remodeling in asthma. *Am. J Respir Crit Care Med.* 164:1718-1721.

67. Minshall,E.M., D.Y.Leung, R.J.Martin, Y.L.Song, L.Cameron, P.Ernst, and Q.Hamid. 1997. Eosinophil-associated TGF-beta1 mRNA expression and airways fibrosis in bronchial asthma. *Am. J Respir Cell Mol. Biol.* 17:326-333.

68. Shiba,K., K.Kasahara, H.Nakajima, and M.Adachi. 2002. Structural changes of the airway wall impair respiratory function, even in mild asthma. *Chest* 122:1622-1626.

69. Hinz,B. 2007. Formation and function of the myofibroblast during tissue repair. *J Invest Dermatol.* 127:526-537.

70. Brewster,C.E., P.H.Howarth, R.Djukanovic, J.Wilson, S.T.Holgate, and W.R.Roche. 1990. Myofibroblasts and subepithelial fibrosis in bronchial asthma. *Am. J Respir Cell Mol. Biol.* 3:507-511.

71. Benayoun,L., A.Druilhe, M.C.Dombret, M.Aubier, and M.Pretolani. 2003. Airway structural alterations selectively associated with severe asthma. *Am. J Respir Crit Care Med.* 167:1360-1368.

72. Ebina,M., T.Takahashi, T.Chiba, and M.Motomiya. 1993. Cellular hypertrophy and hyperplasia of airway smooth muscles underlying bronchial asthma. A 3-D morphometric study. *Am. Rev. Respir Dis.* 148:720-726.

73. James,A. and N.Carroll. 2000. Airway smooth muscle in health and disease; methods of measurement and relation to function. *Eur Respir J* 15:782-789.

74. Matsumoto,H., L.M.Moir, B.G.Oliver, J.K.Burgess, M.Roth, J.L.Black, and B.E.McParland. 2007. Comparison of gel contraction mediated by asthmatic and non-asthmatic airway smooth muscle cells. *Thorax*.

75. Ma,X., Z.Cheng, H.Kong, Y.Wang, H.Unruh, N.L.Stephens, and M.Laviolette. 2002. Changes in biophysical and biochemical properties of single bronchial smooth muscle cells from asthmatic subjects. *Am. J Physiol Lung Cell Mol. Physiol* 283:L1181-L1189.

76. Saunders,W.B., B.L.Bohnsack, J.B.Faske, N.J.Anthis, K.J.Bayless, K.K.Hirschi, and G.E.Davis. 2006. Coregulation of vascular tube stabilization by endothelial cell TIMP-2 and pericyte TIMP-3. *J Cell Biol.* 175:179-191.

77. Kuwano,K., C.H.Bosken, P.D.Pare, T.R.Bai, B.R.Wiggs, and J.C.Hogg. 1993. Small airways dimensions in asthma and in chronic obstructive pulmonary disease. *Am. Rev. Respir Dis.* 148:1220-1225.

78. Carroll,N.G., C.Cooke, and A.L.James. 1997. Bronchial blood vessel dimensions in asthma. *Am. J Respir Crit Care Med.* 155:689-695.

79. Vrugt,B., S.Wilson, A.Bron, S.T.Holgate, R.Djukanovic, and R.Aalbers. 2000. Bronchial angiogenesis in severe glucocorticoid-dependent asthma. *Eur Respir J* 15:1014-1021.

80. Hoshino,M., M.Takahashi, and N.Aoike. 2001. Expression of vascular endothelial growth factor, basic fibroblast growth factor, and angiogenin immunoreactivity in asthmatic airways and its relationship to angiogenesis. *J Allergy Clin. Immunol.* 107:295-301.

81. Pohunek,P., W.Roche, J.Tarzikova, J.Kurdmann, and J.Warner. 2000. Eosinophilic inflammation in the bronchial mucosa in children with bronchial asthma. *Eur Respir J* (Abstr.)

82. Cokugras,H., N.Akcakaya, Seckin, Y.Camcioglu, N.Sarimurat, and F.Aksoy. 2001. Ultrastructural examination of bronchial biopsy specimens from children with moderate asthma. *Thorax* 56:25-29.

83. Puddicombe,S.M., R.Polosa, A.Richter, M.T.Krishna, P.H.Howarth, S.T.Holgate, and D.E.Davies. 2000. Involvement of the epidermal growth factor receptor in epithelial repair in asthma. *FASEB J* 14:1362-1374.

84. Puddicombe, S. M., Xiao, C., Haynes, R., Martin, S. A., Holgate, S. T, and Davies, D. E. Epithelial barrier is impaired in cultured asthmatic bronchial epithelial cells (BECs) differentiated *in vitro*. American thoracic society international conference 2006. 3;A424. 2006.

85. Hassim,Z., S.E.Maronese, and R.K.Kumar. 1998. Injury to murine airway epithelial cells by pollen enzymes. *Thorax* 53:368-371.

86. Wan,H., H.L.Winton, C.Soeller, D.C.Gruenert, P.J.Thompson, M.B.Cannell, G.A.Stewart, D.R.Garrod, and C.Robinson. 2000. Quantitative structural and biochemical analyses of tight junction dynamics following exposure of epithelial cells to house dust mite allergen Der p 1. *Clin. Exp. Allergy* 30:685-698.

87. Ring,P.C., H.Wan, C.Schou, K.A.Kroll, P.Roepstorff, and C.Robinson. 2000. The 18-kDa form of cat allergen Felis domesticus 1 (Fel d 1) is associated with gelatin- and fibronectin-degrading activity. *Clin. Exp. Allergy* 30:1085-1096.

88. Zhang,S., H.Smartt, S.T.Holgate, and W.R.Roche. 1999. Growth factors secreted by bronchial epithelial cells control myofibroblast proliferation: an in vitro co-culture model of airway remodeling in asthma. *Lab Invest* 79:395-405.

89. Redington,A.E., J.Madden, A.J.Frew, R.Djukanovic, W.R.Roche, S.T.Holgate, and P.H.Howarth. 1997. Transforming growth factor-beta 1 in asthma. Measurement in bronchoalveolar lavage fluid. *Am. J Respir Crit Care Med.* 156:642-647.

90. Richter,A., S.M.Puddicombe, J.L.Lordan, F.Bucchieri, S.J.Wilson, R.Djukanovic, G.Dent, S.T.Holgate, and D.E.Davies. 2001. The contribution of interleukin (IL)-4 and IL-13 to the epithelial-mesenchymal trophic unit in asthma. *Am. J Respir Cell Mol. Biol.* 25:385-391.

91. Wicks,J., H.M.Haitchi, S.T.Holgate, D.E.Davies, and R.M.Powell. 2006. Enhanced upregulation of smooth muscle related transcripts by TGF beta2 in asthmatic (myo) fibroblasts. *Thorax* 61:313-319.

92. Dube,J., J.Chakir, C.Dube, Y.Grimard, M.Laviolette, and L.P.Boulet. 2000. Synergistic action of endothelin (ET)-1 on the activation of bronchial fibroblast isolated from normal and asthmatic subjects. *Int. J Exp. Pathol.* 81:429-437.

93. Marini,M., S.Carpi, A.Bellini, F.Patalano, and S.Mattoli. 1996. Endothelin-1 induces increased fibronectin expression in human bronchial epithelial cells. *Biochem. Biophys. Res. Commun.* 220:896-899.

94. McWhinnie,R., D.V.Pechkovsky, D.Zhou, D.Lane, A.J.Halayko, D.A.Knight, and T.R.Bai. 2007. Endothelin-1 induces hypertrophy and inhibits apoptosis in human airway smooth muscle cells. *Am. J Physiol Lung Cell Mol. Physiol* 292:L278-L286.

95. Kondo,M., J.Tamaoki, K.Takeyama, J.Nakata, and A.Nagai. 2002. Interleukin-13 induces goblet cell differentiation in primary cell culture from Guinea pig tracheal epithelium. *Am. J Respir Cell Mol. Biol.* 27:536-541.

96. Kondo,M., J.Tamaoki, K.Takeyama, K.Isono, K.Kawatani, T.Izumo, and A.Nagai. 2006. Elimination of IL-13 reverses established goblet cell metaplasia into ciliated epithelia in airway epithelial cell culture. *Allergol Int.* 55:329-336.

97. Reader,J.R., D.M.Hyde, E.S.Schelegle, M.C.Aldrich, A.M.Stoddard, M.P.McLane, R.C.Levitt, and J.S.Tepper. 2003. Interleukin-9 induces mucous cell metaplasia independent of inflammation. *Am. J Respir Cell Mol. Biol.* 28:664-672.

98. Atherton,H.C., G.Jones, and H.Danahay. 2003. IL-13-induced changes in the goblet cell density of human bronchial epithelial cell cultures: MAP kinase and phosphatidylinositol 3-kinase regulation. *Am. J Physiol Lung Cell Mol. Physiol* 285:L730-L739.

99. Erpenbeck,V.J., J.M.Hohlfeld, B.Volkmann, A.Hagenberg, H.Geldmacher, A.Braun, and N.Krug. 2003. Segmental allergen challenge in patients with atopic asthma leads to increased IL-9 expression in bronchoalveolar lavage fluid lymphocytes. *J Allergy Clin. Immunol.* 111:1319-1327.

100. Liu,L., N.N.Jarjour, W.W.Busse, and E.A.Kelly. 2004. Enhanced generation of helper T type 1 and 2 chemokines in allergen-induced asthma. *Am. J Respir Crit Care Med.* 169:1118-1124.

101. Vermeer,P.D., R.Harson, L.A.Einwalter, T.Moninger, and J.Zabner. 2003. Interleukin-9 induces goblet cell hyperplasia during repair of human airway epithelia. *Am. J Respir Cell Mol. Biol.* 28:286-295.

102. Nakata,J., M.Kondo, J.Tamaoki, T.Takemiya, M.Nohara, K.Yamagata, and A.Nagai. 2005. Augmentation of allergic inflammation in the airways of cyclooxygenase-2-deficient mice. *Respirology.* 10:149-156.

103. Laoukili,J., E.Perret, T.Willems, A.Minty, E.Parthoens, O.Houcine, A.Coste, M.Jorissen, F.Marano, D.Caput, and F.Tournier. 2001. IL-13 alters mucociliary differentiation and ciliary beating of human respiratory epithelial cells. *J Clin. Invest* 108:1817-1824.

104. Virchow,J.C., Jr., P.Julius, H.Matthys, C.Kroegel, and W.Luttmann. 1998. CD14 expression and soluble CD14 after segmental allergen provocation in atopic asthma. *Eur Respir J* 11:317-323.

105. Lee,C.G., R.J.Homer, Z.Zhu, S.Lanone, X.Wang, V.Koteliansky, J.M.Shipley, P.Gotwals, P.Noble, Q.Chen, R.M.Senior, and J.A.Elias. 2001. Interleukin-13 induces tissue fibrosis by selectively stimulating and activating transforming growth factor beta(1). *J Exp. Med.* 194:809-821.

106. Wenzel,S.E., J.B.Trudeau, S.Barnes, X.Zhou, M.Cundall, J.Y.Westcott, K.McCord, and H.W.Chu. 2002. TGF-beta and IL-13 synergistically increase eotaxin-1 production in human airway fibroblasts. *J Immunol.* 169:4613-4619.

107. Teran,L.M., M.Mochizuki, J.Bartels, E.L.Valencia, T.Nakajima, K.Hirai, and J.M.Schroder. 1999. Th1- and Th2-type cytokines regulate the expression and production of eotaxin and RANTES by human lung fibroblasts. *Am. J Respir Cell Mol. Biol.* 20:777-786.

108. Moore,P.E., T.L.Church, D.D.Chism, R.A.Panettieri, Jr., and S.A.Shore. 2002. IL-13 and IL-4 cause eotaxin release in human airway smooth muscle cells: a role for ERK. *Am. J Physiol Lung Cell Mol. Physiol* 282:L847-L853.

109. Kay,A.B., S.Phipps, and D.S.Robinson. 2004. A role for eosinophils in airway remodelling in asthma. *Trends Immunol.* 25:477-482.

110. Flood-Page,P., A.Menzies-Gow, S.Phipps, S.Ying, A.Wangoo, M.S.Ludwig, N.Barnes, D.Robinson, and A.B.Kay. 2003. Anti-IL-5 treatment reduces deposition of ECM proteins in the bronchial subepithelial basement membrane of mild atopic asthmatics. *J Clin. Invest* 112:1029-1036.

111. Simcock,D.E., V.Kanabar, G.W.Clarke, B.J.O'connor, T.H.Lee, and S.J.Hirst. 2007. Pro-angiogenic Activity in Bronchoalveolar Lavage Fluid from Asthmatics. *Am. J Respir Crit Care Med.*

112. Alagappan,V.K., S.McKay, A.Widyastuti, I.M.Garrelds, A.J.Bogers, H.C.Hoogsteden, S.J.Hirst, and H.S.Sharma. 2005. Proinflammatory cytokines upregulate mRNA expression and secretion of vascular endothelial growth factor in cultured human airway smooth muscle cells. *Cell Biochem. Biophys.* 43:119-129.

113. Faffe,D.S., L.Flynt, K.Bourgeois, R.A.Panettieri, Jr., and S.A.Shore. 2006. Interleukin-13 and interleukin-4 induce vascular endothelial growth factor release from airway smooth muscle cells: role of vascular endothelial growth factor genotype. *Am. J Respir Cell Mol. Biol.* 34:213-218.

114. Calverley,P.M. 2004. Effect of corticosteroids on exacerbations of asthma and chronic obstructive pulmonary disease. *Proc. Am. Thorac. Soc.* 1:161-166.

115. Lim,S., A.Jatakanon, M.John, T.Gilbey, B.J.O'connor, K.F.Chung, and P.J.Barnes. 1999. Effect of inhaled budesonide on lung function and airway inflammation. Assessment by various inflammatory markers in mild asthma. *Am. J Respir Crit Care Med.* 159:22-30.

116. Chanez,P., A.Bourdin, I.Vachier, P.Godard, J.Bousquet, and A.M.Vignola. 2004. Effects of inhaled corticosteroids on pathology in asthma and chronic obstructive pulmonary disease. *Proc. Am. Thorac. Soc.* 1:184-190.

117. Gronemeyer,H. 1992. Control of transcription activation by steroid hormone receptors. *FASEB J* 6:2524-2529.

118. Beato,M., P.Herrlich, and G.Schutz. 1995. Steroid hormone receptors: many actors in search of a plot. *Cell* 83:851-857.

119. Truss,M. and M.Beato. 1993. Steroid hormone receptors: interaction with deoxyribonucleic acid and transcription factors. *Endocr. Rev.* 14:459-479.

120. Auphan,N., J.A.DiDonato, C.Rosette, A.Helmberg, and M.Karin. 1995. Immunosuppression by glucocorticoids: inhibition of NF-kappa B activity through induction of I kappa B synthesis. *Science* 270:286-290.

121. Scheinman,R.I., P.C.Cogswell, A.K.Lofquist, and A.S.Baldwin, Jr. 1995. Role of transcriptional activation of I kappa B alpha in mediation of immunosuppression by glucocorticoids. *Science* 270:283-286.

122. Rodrigo,G.J. 2006. Rapid effects of inhaled corticosteroids in acute asthma: an evidence-based evaluation. *Chest* 130:1301-1311.

123. Greening,A.P., P.W.Ind, M.Northfield, and G.Shaw. 1994. Added salmeterol versus higher-dose corticosteroid in asthma patients with symptoms on existing inhaled corticosteroid. Allen & Hanburys Limited UK Study Group. *Lancet* 344:219-224.

124. Shrewsbury,S., S.Pyke, and M.Britton. 2000. Meta-analysis of increased dose of inhaled steroid or addition of salmeterol in symptomatic asthma (MIASMA). *BMJ* 320:1368-1373.

125. Johnson,M. 1998. The beta-adrenoceptor. *Am. J Respir Crit Care Med.* 158:S146-S153.

126. O'connor,B.J., R.W.Fuller, and P.J.Barnes. 1994. Nonbronchodilator effects of inhaled beta 2 agonists. Greater protection against adenosine monophosphate- than methacholine-induced bronchoconstriction in asthma. *Am. J Respir Crit Care Med.* 150:381-387.

127. Cushley,M.J. and S.T.Holgate. 1985. Adenosine-induced bronchoconstriction in asthma: role of mast cell-mediator release. *J Allergy Clin. Immunol.* 75:272-278.

128. Barnes,P.J. 2002. Scientific rationale for inhaled combination therapy with long-acting beta2-agonists and corticosteroids. *Eur Respir J* 19:182-191.

129. British Guidline on the Management of Asthma. 2004. British Thoracic Society. Scottish Intercollegiate Guidelines Network.

130. Djukanovic,R., S.J.Wilson, M.Kraft, N.N.Jarjour, M.Steel, K.F.Chung, W.Bao, A.Fowler-Taylor, J.Matthews, W.W.Busse, S.T.Holgate, and J.V.Fahy. 2004. Effects of treatment with anti-immunoglobulin E antibody omalizumab on airway inflammation in allergic asthma. *Am. J Respir Crit Care Med.* 170:583-593.

131. Humbert,M., R.Beasley, J.Ayres, R.Slavin, J.Hebert, J.Bousquet, K.M.Beeh, S.Ramos, G.W.Canonica, S.Hedgecock, H.Fox, M.Blogg, and K.Surrey. 2005. Benefits of omalizumab as add-on therapy in patients with severe persistent asthma who are inadequately controlled despite best available therapy (GINA 2002 step 4 treatment): INNOVATE. *Allergy* 60:309-316.

132. Niebauer,K., S.Dewilde, J.Fox-Rushby, and D.A.Revicki. 2006. Impact of omalizumab on quality-of-life outcomes in patients with moderate-to-severe allergic asthma. *Ann. Allergy Asthma Immunol.* 96:316-326.

133. Corren,J., T.Casale, Y.Deniz, and M.Ashby. 2003. Omalizumab, a recombinant humanized anti-IgE antibody, reduces asthma-related emergency room visits and hospitalizations in patients with allergic asthma. *J Allergy Clin. Immunol.* 111:87-90.

134. Bousquet,J., S.Wenzel, S.Holgate, W.Lumry, P.Freeman, and H.Fox. 2004. Predicting response to omalizumab, an anti-IgE antibody, in patients with allergic asthma. *Chest* 125:1378-1386.

135. Wenzel,S.E., L.B.Schwartz, E.L.Langmack, J.L.Halliday, J.B.Trudeau, R.L.Gibbs, and H.W.Chu. 1999. Evidence that severe asthma can be divided pathologically into two inflammatory subtypes with distinct physiologic and clinical characteristics. *Am. J Respir Crit Care Med.* 160:1001-1008.

136. Jatakanon,A., C.Uasuf, W.Maziak, S.Lim, K.F.Chung, and P.J.Barnes. 1999. Neutrophilic inflammation in severe persistent asthma. *Am. J Respir Crit Care Med.* 160:1532-1539.

137. Green,R.H., C.E.Brightling, G.Woltmann, D.Parker, A.J.Wardlaw, and I.D.Pavord. 2002. Analysis of induced sputum in adults with asthma: identification of subgroup with isolated sputum neutrophilia and poor response to inhaled corticosteroids. *Thorax* 57:875-879.

138. Howarth,P.H., K.S.Babu, H.S.Arshad, L.Lau, M.Buckley, W.McConnell, P.Beckett, A.M.Al, A.Chauhan, S.J.Wilson, A.Reynolds, D.E.Davies, and S.T.Holgate. 2005. Tumour necrosis factor (TNFalpha) as a novel therapeutic target in symptomatic corticosteroid dependent asthma. *Thorax* 60:1012-1018.

139. Feldmann,M. and R.N.Maini. 2003. Lasker Clinical Medical Research Award. TNF defined as a therapeutic target for rheumatoid arthritis and other autoimmune diseases. *Nat. Med.* 9:1245-1250.

140. Berry,M.A., B.Hargadon, M.Shelley, D.Parker, D.E.Shaw, R.H.Green, P.Bradding, C.E.Brightling, A.J.Wardlaw, and I.D.Pavord. 2006. Evidence of a role of tumor necrosis factor alpha in refractory asthma. *N. Engl. J Med.* 354:697-708.

141. Hoshino,M., M.Takahashi, Y.Takai, and J.Sim. 1999. Inhaled corticosteroids decrease subepithelial collagen deposition by modulation of the balance between matrix metalloproteinase-9 and tissue inhibitor of metalloproteinase-1 expression in asthma. *J Allergy Clin. Immunol.* 104:356-363.

142. Trigg,C.J., N.D.Manolitsas, J.Wang, M.A.Calderon, A.McAulay, S.E.Jordan, M.J.Herdman, N.Jhalli, J.M.Duddle, S.A.Hamilton, and . 1994. Placebo-controlled immunopathologic study of four months of inhaled corticosteroids in asthma. *Am. J Respir Crit Care Med.* 150:17-22.

143. Hoshino,M., Y.Nakamura, J.J.Sim, Y.Yamashiro, K.Uchida, K.Hosaka, and S.Isogai. 1998. Inhaled corticosteroid reduced lamina reticularis of the basement membrane by modulation of insulin-like growth factor (IGF)-I expression in bronchial asthma. *Clin. Exp. Allergy* 28:568-577.

144. Jeffery,P.K., R.W.Godfrey, E.Adelroth, F.Nelson, A.Rogers, and S.A.Johansson. 1992. Effects of treatment on airway inflammation and thickening of basement membrane reticular collagen in asthma. A quantitative light and electron microscopic study. *Am. Rev. Respir Dis.* 145:890-899.

145. Boulet,L.P., H.Turcotte, M.Laviolette, F.Naud, M.C.Bernier, S.Martel, and J.Chakir. 2000. Airway hyperresponsiveness, inflammation, and subepithelial collagen deposition in recently diagnosed versus long-standing mild asthma.

Influence of inhaled corticosteroids. *Am. J Respir Crit Care Med.* 162:1308-1313.

146. Orsida,B.E., X.Li, B.Hickey, F.Thien, J.W.Wilson, and E.H.Walters. 1999. Vascularity in asthmatic airways: relation to inhaled steroid dose. *Thorax* 54:289-295.

147. Feltis,B.N., D.Wignarajah, D.W.Reid, C.Ward, R.Harding, and E.H.Walters. 2007. Effects of inhaled fluticasone on angiogenesis and vascular endothelial growth factor in asthma. *Thorax* 62:314-319.

148. Sont,J.K., L.N.Willems, E.H.Bel, J.H.van Krieken, J.P.Vandenbroucke, and P.J.Sterk. 1999. Clinical control and histopathologic outcome of asthma when using airway hyperresponsiveness as an additional guide to long-term treatment. The AMPUL Study Group. *Am. J Respir Crit Care Med.* 159:1043-1051.

149. Guilbert,T.W., W.J.Morgan, R.S.Zeiger, D.T.Mauger, S.J.Boehmer, S.J.Szefler, L.B.Bacharier, R.F.Lemanske, Jr., R.C.Strunk, D.B.Allen, G.R.Bloomberg, G.Heldt, M.Krawiec, G.Larsen, A.H.Liu, V.M.Chinchilli, C.A.Sorkness, L.M.Taussig, and F.D.Martinez. 2006. Long-term inhaled corticosteroids in preschool children at high risk for asthma. *N. Engl. J Med.* 354:1985-1997.

150. Nimmagadda,S.R., J.D.Spahn, D.Y.Leung, and S.J.Szefler. 1996. Steroid-resistant asthma: evaluation and management. *Ann. Allergy Asthma Immunol.* 77:345-355.

151. Kamada,A.K., D.Y.Leung, and S.J.Szefler. 1992. Steroid resistance in asthma: our current understanding. *Pediatr. Pulmonol.* 14:180-186.

152. Holberg,C.J., W.J.Morgan, A.L.Wright, and F.D.Martinez. 1998. Differences in familial segregation of FEV1 between asthmatic and nonasthmatic families. Role of a maternal component. *Am. J Respir Crit Care Med.* 158:162-169.

153. Litonjua,A.A., V.J.Carey, H.A.Burge, S.T.Weiss, and D.R.Gold. 1998. Parental history and the risk for childhood asthma. Does mother confer more risk than father? *Am. J Respir Crit Care Med.* 158:176-181.

154. Aberg,N. 1993. Familial occurrence of atopic disease: genetic versus environmental factors. *Clin. Exp. Allergy* 23:829-834.

155. Lander,E.S., L.M.Linton, B.Birren, C.Nusbaum, M.C.Zody, J.Baldwin, K.Devon, K.Dewar, M.Doyle, W.FitzHugh, R.Funke, D.Gage, K.Harris, A.Heaford, J.Howland, L.Kann, J.Lehoczky, R.LeVine, P.McEwan, K.McKernan, J.Meldrim, J.P.Mesirov, C.Miranda, W.Morris, J.Naylor, C.Raymond, M.Rosetti, R.Santos, A.Sheridan, C.Sougnez, N.Stange-Thomann, N.Stojanovic, A.Subramanian, D.Wyman, J.Rogers, J.Sulston, R.Ainscough, S.Beck, D.Bentley, J.Burton, C.Clee, N.Carter, A.Coulson, R.Deadman, P.Deloukas, A.Dunham, I.Dunham, R.Durbin, L.French, D.Grafham, S.Gregory, T.Hubbard, S.Humphray, A.Hunt, M.Jones, C.Lloyd, A.McMurray, L.Matthews, S.Mercer, S.Milne, J.C.Mullikin, A.Mungall,

R.Plumb, M.Ross, R.Shownkeen, S.Sims, R.H.Waterston, R.K.Wilson, L.W.Hillier, J.D.McPherson, M.A.Marra, E.R.Mardis, L.A.Fulton, A.T.Chinwalla, K.H.Pepin, W.R.Gish, S.L.Chissoe, M.C.Wendl, K.D.Delehaunty, T.L.Miner, A.Delehaunty, J.B.Kramer, L.L.Cook, R.S.Fulton, D.L.Johnson, P.J.Minx, S.W.Clifton, T.Hawkins, E.Branscomb, P.Predki, P.Richardson, S.Wenning, T.Slezak, N.Doggett, J.F.Cheng, A.Olsen, S.Lucas, C.Elkin, E.Uberbacher, M.Frazier, R.A.Gibbs, D.M.Muzny, S.E.Scherer, J.B.Bouck, E.J.Sodergren, K.C.Worley, C.M.Rives, J.H.Gorrell, M.L.Metzker, S.L.Naylor, R.S.Kucherlapati, D.L.Nelson, G.M.Weinstock, Y.Sakaki, A.Fujiyama, M.Hattori, T.Yada, A.Toyoda, T.Itoh, C.Kawagoe, H.Watanabe, Y.Totoki, T.Taylor, J.Weissenbach, R.Heilig, W.Saurin, F.Artiguenave, P.Brottier, T.Bruls, E.Pelletier, C.Robert, P.Wincker, D.R.Smith, L.Doucette-Stamm, M.Rubenfield, K.Weinstock, H.M.Lee, J.Dubois, A.Rosenthal, M.Platzer, G.Nyakatura, S.Taudien, A.Rump, H.Yang, J.Yu, J.Wang, G.Huang, J.Gu, L.Hood, L.Rowen, A.Madan, S.Qin, R.W.Davis, N.A.Federspiel, A.P.Abola, M.J.Proctor, R.M.Myers, J.Schmutz, M.Dickson, J.Grimwood, D.R.Cox, M.V.Olson, R.Kaul, C.Raymond, N.Shimizu, K.Kawasaki, S.Minoshima, G.A.Evans, M.Athanasiou, R.Schultz, B.A.Roe, F.Chen, H.Pan, J.Ramser, H.Lehrach, R.Reinhardt, W.R.McCombie, B.M.de la, N.Dedhia, H.Blocker, K.Hornischer, G.Nordsiek, R.Agarwala, L.Aravind, J.A.Bailey, A.Bateman, S.Batzoglou, E.Birney, P.Bork, D.G.Brown, C.B.Burge, L.Cerutti, H.C.Chen, D.Church, M.Clamp, R.R.Copley, T.Doerks, S.R.Eddy, E.E.Eichler, T.S.Furey, J.Galagan, J.G.Gilbert, C.Harmon, Y.Hayashizaki, D.Haussler, H.Hermjakob, K.Hokamp, W.Jang, L.S.Johnson, T.A.Jones, S.Kasif, A.Kaspryzk, S.Kennedy, W.J.Kent, P.Kitts, E.V.Koonin, I.Korf, D.Kulp, D.Lancet, T.M.Lowe, A.McLysaght, T.Mikkelsen, J.V.Moran, N.Mulder, V.J.Pollara, C.P.Ponting, G.Schuler, J.Schultz, G.Slater, A.F.Smit, E.Stupka, J.Szustakowski, D.Thierry-Mieg, J.Thierry-Mieg, L.Wagner, J.Wallis, R.Wheeler, A.Williams, Y.I.Wolf, K.H.Wolfe, S.P.Yang, R.F.Yeh, F.Collins, M.S.Guyer, J.Peterson, A.Felsenfeld, K.A.Wetterstrand, A.Patrinos, M.J.Morgan, J.P.de, J.J.Catanese, K.Osoegawa, H.Shizuya, S.Choi, and Y.J.Chen. 2001. Initial sequencing and analysis of the human genome. *Nature* 409:860-921.

156. 2004. Finishing the euchromatic sequence of the human genome. *Nature* 431:931-945.

157. Riley,J.H., C.J.Allan, E.Lai, and A.Roses. 2000. The use of single nucleotide polymorphisms in the isolation of common disease genes. *Pharmacogenomics.* 1:39-47.

158. Carroll,W. 2005. Asthma genetics: pitfalls and triumphs. *Paediatr. Respir Rev.* 6:68-74.

159. Chiang,C.H., Y.C.Tang, M.W.Lin, and M.Y.Chung. 2007. Association between the IL-4 promoter polymorphisms and asthma or severity of hyperresponsiveness in Taiwanese. *Respirology.* 12:42-48.

160. Basehore,M.J., T.D.Howard, L.A.Lange, W.C.Moore, G.A.Hawkins, P.L.Marshik, M.S.Harkins, D.A.Meyers, and E.R.Bleecker. 2004. A comprehensive evaluation of IL4 variants in ethnically diverse populations: association of total serum IgE levels and asthma in white subjects. *J Allergy Clin. Immunol.* 114:80-87.

161. Beghe,B., S.Barton, S.Rorke, Q.Peng, I.Sayers, T.Gaunt, T.P.Keith, J.B.Clough, S.T.Holgate, and J.W.Holloway. 2003. Polymorphisms in the interleukin-4 and interleukin-4 receptor alpha chain genes confer susceptibility to asthma and atopy in a Caucasian population. *Clin. Exp. Allergy* 33:1111-1117.

162. Howard,T.D., P.A.Whittaker, A.L.Zaiman, G.H.Koppelman, J.Xu, M.T.Hanley, D.A.Meyers, D.S.Postma, and E.R.Bleecker. 2001. Identification and association of polymorphisms in the interleukin-13 gene with asthma and atopy in a Dutch population. *Am. J Respir Cell Mol. Biol.* 25:377-384.

163. Heinzmann,A., X.Q.Mao, M.Akaiwa, R.T.Kreomer, P.S.Gao, K.Ohshima, R.Umeshita, Y.Abe, S.Braun, T.Yamashita, M.H.Roberts, R.Sugimoto, K.Arima, Y.Arinobu, B.Yu, S.Kruse, T.Enomoto, Y.Dake, M.Kawai, S.Shimazu, S.Sasaki, C.N.Adra, M.Kitaichi, H.Inoue, K.Yamauchi, N.Tomichi, F.Kurimoto, N.Hamasaki, J.M.Hopkin, K.Izuhara, T.Shirakawa, and K.A.Deichmann. 2000. Genetic variants of IL-13 signalling and human asthma and atopy. *Hum. Mol. Genet.* 9:549-559.

164. Nicolae,D., N.J.Cox, L.A.Lester, D.Schneider, Z.Tan, C.Billstrand, S.Kuldanek, J.Donfack, P.Kogut, N.M.Patel, J.Goodenbour, T.Howard, R.Wolf, G.H.Koppelman, S.R.White, R.Parry, D.S.Postma, D.Meyers, E.R.Bleecker, J.S.Hunt, J.Solway, and C.Ober. 2005. Fine mapping and positional candidate studies identify HLA-G as an asthma susceptibility gene on chromosome 6p21. *Am. J Hum. Genet.* 76:349-357.

165. Ober,C. 2005. HLA-G: an asthma gene on chromosome 6p. *Immunol. Allergy Clin. North Am.* 25:669-679.

166. Kormann,M.S., D.Carr, N.Klopp, T.Illig, W.Leupold, C.Fritzsch, S.K.Weiland, M.E.von, and M.Kabesch. 2005. G-Protein-coupled receptor polymorphisms are associated with asthma in a large German population. *Am. J Respir Crit Care Med.* 171:1358-1362.

167. Malerba,G., C.M.Lindgren, L.Xumerle, P.Kiviluoma, E.Trabetti, T.Laitinen, R.Galavotti, L.Pescollderungg, A.L.Boner, J.Kere, and P.F.Pignatti. 2007. Chromosome 7p linkage and GPR154 gene association in Italian families with allergic asthma. *Clin. Exp. Allergy* 37:83-89.

168. Laitinen,T., M.J.Daly, J.D.Rioux, P.Kauppi, C.Laprise, T.Petays, T.Green, M.Cargill, T.Haahtela, E.S.Lander, L.A.Laitinen, T.J.Hudson, and J.Kere. 2001. A susceptibility locus for asthma-related traits on chromosome 7 revealed by genome-wide scan in a founder population. *Nat. Genet.* 28:87-91.

169. Laitinen,T., A.Polvi, P.Rydman, J.Vendelin, V.Pulkkinen, P.Salmikangas, S.Makela, M.Rehn, A.Pirskanen, A.Rautanen, M.Zucchelli, H.Gullsten, M.Leino, H.Alenius, T.Petays, T.Haahtela, A.Laitinen, C.Laprise, T.J.Hudson, L.A.Laitinen, and J.Kere. 2004. Characterization of a common susceptibility locus for asthma-related traits. *Science* 304:300-304.

170. Vendelin,J., V.Pulkkinen, M.Rehn, A.Pirskanen, A.Raisanen-Sokolowski, A.Laitinen, L.A.Laitinen, J.Kere, and T.Laitinen. 2005. Characterization of

GPRA, a novel G protein-coupled receptor related to asthma. *Am. J Respir Cell Mol. Biol.* 33:262-270.

171. Kamada,F., Y.Suzuki, C.Shao, M.Tamari, K.Hasegawa, T.Hirota, M.Shimizu, N.Takahashi, X.Q.Mao, S.Doi, H.Fujiwara, A.Miyatake, K.Fujita, Y.Chiba, Y.Aoki, S.Kure, G.Tamura, T.Shirakawa, and Y.Matsubara. 2004. Association of the hCLCA1 gene with childhood and adult asthma. *Genes Immun.* 5:540-547.

172. Toda,M., M.K.Tulic, R.C.Levitt, and Q.Hamid. 2002. A calcium-activated chloride channel (HCLCA1) is strongly related to IL-9 expression and mucus production in bronchial epithelium of patients with asthma. *J Allergy Clin. Immunol.* 109:246-250.

173. Yasuo,M., K.Fujimoto, T.Tanabe, H.Yaegashi, K.Tsushima, K.Takasuna, T.Koike, M.Yamaya, and T.Nikaido. 2006. Relationship between calcium-activated chloride channel 1 and MUC5AC in goblet cell hyperplasia induced by interleukin-13 in human bronchial epithelial cells. *Respiration* 73:347-359.

174. Laing,I.A., J.Goldblatt, E.Eber, C.M.Hayden, P.J.Rye, N.A.Gibson, L.J.Palmer, P.R.Burton, and P.N.Le Souef. 1998. A polymorphism of the CC16 gene is associated with an increased risk of asthma. *J Med. Genet.* 35:463-467.

175. Candelaria,P.V., V.Backer, I.A.Laing, C.Porsbjerg, S.Nepper-Christensen, K.N.de, J.Goldblatt, and P.N.Le Souef. 2005. Association between asthma-related phenotypes and the CC16 A38G polymorphism in an unselected population of young adult Danes. *Immunogenetics* 57:25-32.

176. Gioldassi,X.M., H.Papadimitriou, V.Mikraki, and N.K.Karamanos. 2004. Clara cell secretory protein: determination of serum levels by an enzyme immunoassay and its importance as an indicator of bronchial asthma in children. *J Pharm. Biomed. Anal.* 34:823-826.

177. Wilkinson,J., N.S.Thomas, N.Morton, and S.T.Holgate. 1999. Candidate gene and mutational analysis in asthma and atopy. *Int. Arch. Allergy Immunol.* 118:265-267.

178. Laprise,C., L.P.Boulet, J.Morissette, E.Winstall, and V.Raymond. 2000. Evidence for association and linkage between atopy, airway hyper-responsiveness, and the beta subunit Glu237Gly variant of the high-affinity receptor for immunoglobulin E in the French-Canadian population. *Immunogenetics* 51:695-702.

179. Nickel,R., A.Haider, C.Sengler, S.Lau, B.Niggemann, K.A.Deichmann, U.Wahn, and A.Heinzmann. 2005. Association study of Glutathione S-transferase P1 (GSTP1) with asthma and bronchial hyper-responsiveness in two German pediatric populations. *Pediatr. Allergy Immunol.* 16:539-541.

180. Lee,Y.L., Y.C.Lin, Y.C.Lee, J.Y.Wang, T.R.Hsiue, and Y.L.Guo. 2004. Glutathione S-transferase P1 gene polymorphism and air pollution as interactive risk factors for childhood asthma. *Clin. Exp. Allergy* 34:1707-1713.

181. Van Eerdewegh P., R.D.Little, J.Dupuis, R.G.Del Mastro, K.Falls, J.Simon, D.Torrey, S.Pandit, J.McKenny, K.Braunschweiger, A.Walsh, Z.Liu, B.Hayward, C.Folz, S.P.Manning, A.Bawa, L.Saracino, M.Thackston, Y.Benchekroun, N.Capparell, M.Wang, R.Adair, Y.Feng, J.Dubois, M.G.FitzGerald, H.Huang, R.Gibson, K.M.Allen, A.Pedan, M.R.Danzig, S.P.Umland, R.W.Egan, F.M.Cuss, S.Rorke, J.B.Clough, J.W.Holloway, S.T.Holgate, and T.P.Keith. 2002. Association of the ADAM33 gene with asthma and bronchial hyperresponsiveness. *Nature* 418:426-430.

182. Kedda,M.A., D.L.Duffy, B.Bradley, R.E.O'Hehir, and P.J.Thompson. 2006. ADAM33 haplotypes are associated with asthma in a large Australian population. *Eur J Hum. Genet.* 14:1027-1036.

183. Hirota,T., K.Hasegawa, K.Obara, A.Matsuda, M.Akahoshi, K.Nakashima, T.Shirakawa, S.Doi, K.Fujita, Y.Suzuki, Y.Nakamura, and M.Tamari. 2006. Association between ADAM33 polymorphisms and adult asthma in the Japanese population. *Clin. Exp. Allergy* 36:884-891.

184. Howard,T.D., D.S.Postma, H.Jongepier, W.C.Moore, G.H.Koppelman, S.L.Zheng, J.Xu, E.R.Bleecker, and D.A.Meyers. 2003. Association of a disintegrin and metalloprotease 33 (ADAM33) gene with asthma in ethnically diverse populations. *J Allergy Clin. Immunol.* 112:717-722.

185. Lind,D.L., S.Choudhry, N.Ung, E.Ziv, P.C.Avila, K.Salari, C.Ha, E.G.Lovins, N.E.Coyle, S.Nazario, J.Casal, A.Torres, J.R.Rodriguez-Santana, H.Matallana, C.M.Lilly, J.Salas, M.Selman, H.A.Boushey, S.T.Weiss, R.Chapela, J.G.Ford, W.Rodriguez-Cintron, E.K.Silverman, D.Sheppard, P.Y.Kwok, and B.E.Gonzalez. 2003. ADAM33 is not associated with asthma in Puerto Rican or Mexican populations. *Am. J Respir Crit Care Med.* 168:1312-1316.

186. Wang,P., Q.J.Liu, J.S.Li, H.C.Li, C.H.Wei, C.H.Guo, and Y.Q.Gong. 2006. Lack of association between ADAM33 gene and asthma in a Chinese population. *Int. J Immunogenet.* 33:303-306.

187. Werner,M., N.Herbon, H.Gohlke, J.Altmuller, M.Knapp, J.Heinrich, and M.Wjst. 2004. Asthma is associated with single-nucleotide polymorphisms in ADAM33. *Clin. Exp. Allergy* 34:26-31.

188. Lee,J.H., H.S.Park, S.W.Park, A.S.Jang, S.T.Uh, T.Rhim, C.S.Park, S.J.Hong, S.T.Holgate, J.W.Holloway, and H.D.Shin. 2004. ADAM33 polymorphism: association with bronchial hyper-responsiveness in Korean asthmatics. *Clin. Exp. Allergy* 34:860-865.

189. Blakey,J., E.Halapi, U.S.Bjornsdottir, A.Wheatley, S.Kristinsson, R.Upmanyu, K.Stefansson, H.Hakonarson, and I.P.Hall. 2005. Contribution of ADAM33 polymorphisms to the population risk of asthma. *Thorax* 60:274-276.

190. Wjst,M. 2007. Public data mining shows extended linkage disequilibrium around ADAM33. *Allergy* 62:444-446.

191. Jongepier,H., H.M.Boezen, A.Dijkstra, T.D.Howard, J.M.Vonk, G.H.Koppelman, S.L.Zheng, D.A.Meyers, E.R.Bleecker, and D.S.Postma. 2004. Polymorphisms of the ADAM33 gene are associated with accelerated lung function decline in asthma. *Clin. Exp. Allergy* 34:757-760.

192. van Diemen,C.C., D.S.Postma, J.M.Vonk, M.Bruinenberg, J.P.Schouten, and H.M.Boezen. 2005. A disintegrin and metalloprotease 33 polymorphisms and lung function decline in the general population. *Am. J Respir Crit Care Med.* 172:329-333.

193. Simpson,A., N.Maniatis, F.Jury, J.A.Cakebread, L.A.Lowe, S.T.Holgate, A.Woodcock, W.E.Ollier, A.Collins, A.Custovic, J.W.Holloway, and S.L.John. 2005. Polymorphisms in a disintegrin and metalloprotease 33 (ADAM33) predict impaired early-life lung function. *Am. J Respir Crit Care Med.* 172:55-60.

194. Hamid,Q., M.Cosio, and S.Lim. 2004. Inflammation and remodeling in chronic obstructive pulmonary disease. *J Allergy Clin. Immunol.* 114:1479-1481.

195. Hogg,J.C., F.Chu, S.Utokaparch, R.Woods, W.M.Elliott, L.Buzatu, R.M.Cherniack, R.M.Rogers, F.C.Sciurba, H.O.Coxson, and P.D.Pare. 2004. The nature of small-airway obstruction in chronic obstructive pulmonary disease. *N. Engl. J Med.* 350:2645-2653.

196. Gosman,M.M., H.M.Boezen, C.C.van Diemen, J.B.Snoeck-Stroband, T.S.Lapperre, P.S.Hiemstra, N.H.Ten Hacken, J.Stolk, and D.S.Postma. 2007. A disintegrin and metalloprotease 33 and chronic obstructive pulmonary disease pathophysiology. *Thorax* 62:242-247.

197. White, J. M. and Wolfsberg, T. G. Table of ADAMs. 2005. White Lab. University of Virginia. School of Medicine.
Ref Type: Report

198. White,J.M. 2003. ADAMs: modulators of cell-cell and cell-matrix interactions. *Curr. Opin. Cell Biol.* 15:598-606.

199. Gilpin,B.J., F.Loechel, M.G.Mattei, E.Engvall, R.Albrechtsen, and U.M.Wewer. 1998. A novel, secreted form of human ADAM 12 (meltrin alpha) provokes myogenesis in vivo. *J Biol. Chem.* 273:157-166.

200. Van Wart,H.E. and H.Birkedal-Hansen. 1990. The cysteine switch: a principle of regulation of metalloproteinase activity with potential applicability to the entire matrix metalloproteinase gene family. *Proc. Natl. Acad. Sci. U. S. A* 87:5578-5582.

201. Loechel,F., M.T.Overgaard, C.Oxvig, R.Albrechtsen, and U.M.Wewer. 1999. Regulation of human ADAM 12 protease by the prodomain. Evidence for a functional cysteine switch. *J Biol. Chem.* 274:13427-13433.

202. Milla,M.E., M.A.Leesnitzer, M.L.Moss, W.C.Clay, H.L.Carter, A.B.Miller, J.L.Su, M.H.Lambert, D.H.Willard, D.M.Sheeley, T.A.Kost, W.Burkhart,

M.Moyer, R.K.Blackburn, G.L.Pahel, J.L.Mitchell, C.R.Hoffman, and J.D.Becherer. 1999. Specific sequence elements are required for the expression of functional tumor necrosis factor-alpha-converting enzyme (TACE). *J Biol. Chem.* 274:30563-30570.

203. Anders,A., S.Gilbert, W.Garten, R.Postina, and F.Fahrenholz. 2001. Regulation of the alpha-secretase ADAM10 by its prodomain and proprotein convertases. *FASEB J* 15:1837-1839.

204. Kang,T., H.Nagase, and D.Pei. 2002. Activation of membrane-type matrix metalloproteinase 3 zymogen by the proprotein convertase furin in the trans-Golgi network. *Cancer Res.* 62:675-681.

205. Zou,J., F.Zhu, J.Liu, W.Wang, R.Zhang, C.G.Garlisi, Y.H.Liu, S.Wang, H.Shah, Y.Wan, and S.P.Umland. 2004. Catalytic activity of human ADAM33. *J Biol. Chem.* 279:9818-9830.

206. Wewer,U.M., M.Morgelin, P.Holck, J.Jacobsen, M.C.Lydolph, A.H.Johnsen, M.Kveiborg, and R.Albrechtsen. 2006. ADAM12 is a four-leafed clover: the excised prodomain remains bound to the mature enzyme. *J Biol. Chem.* 281:9418-9422.

207. Bridges,L.C., D.Sheppard, and R.D.Bowditch. 2005. ADAM disintegrin-like domain recognition by the lymphocyte integrins alpha4beta1 and alpha4beta7. *Biochem. J* 387:101-108.

208. Huang,J., L.C.Bridges, and J.M.White. 2005. Selective modulation of integrin-mediated cell migration by distinct ADAM family members. *Mol. Biol. Cell* 16:4982-4991.

209. Kamiguti,A.S., F.S.Markland, Q.Zhou, G.D.Laing, R.D.Theakston, and M.Zuzel. 1997. Proteolytic cleavage of the beta1 subunit of platelet alpha2beta1 integrin by the metalloproteinase jararhagin compromises collagen-stimulated phosphorylation of pp72. *J Biol. Chem.* 272:32599-32605.

210. Alfandari,D., H.Cousin, A.Gaultier, K.Smith, J.M.White, T.Darribere, and D.W.DeSimone. 2001. Xenopus ADAM 13 is a metalloprotease required for cranial neural crest-cell migration. *Curr. Biol.* 11:918-930.

211. Mazzocca,A., R.Coppari, F.R.De, J.Y.Cho, T.A.Libermann, M.Pinzani, and A.Toker. 2005. A secreted form of ADAM9 promotes carcinoma invasion through tumor-stromal interactions. *Cancer Res.* 65:4728-4738.

212. Woods,A. 2001. Syndecans: transmembrane modulators of adhesion and matrix assembly. *J Clin. Invest* 107:935-941.

213. Iba,K., R.Albrechtsen, B.J.Gilpin, F.Loechel, and U.M.Wewer. 1999. Cysteine-rich domain of human ADAM 12 (meltrin alpha) supports tumor cell adhesion. *Am. J Pathol.* 154:1489-1501.

214. Iba,K., R.Albrechtsen, B.Gilpin, C.Frohlich, F.Loechel, A.Zolkiewska, K.Ishiguro, T.Kojima, W.Liu, J.K.Langford, R.D.Sanderson, C.Brakebusch, R.Fassler, and U.M.Wewer. 2000. The cysteine-rich domain of human ADAM 12 supports cell adhesion through syndecans and triggers signaling events that lead to beta1 integrin-dependent cell spreading. *J Cell Biol.* 149:1143-1156.

215. Blobel,C.P., T.G.Wolfsberg, C.W.Turck, D.G.Myles, P.Primakoff, and J.M.White. 1992. A potential fusion peptide and an integrin ligand domain in a protein active in sperm-egg fusion. *Nature* 356:248-252.

216. Black,R.A., C.T.Rauch, C.J.Kozlosky, J.J.Peschon, J.L.Slack, M.F.Wolfson, B.J.Castner, K.L.Stocking, P.Reddy, S.Srinivasan, N.Nelson, N.Boiani, K.A.Schooley, M.Gerhart, R.Davis, J.N.Fitzner, R.S.Johnson, R.J.Paxton, C.J.March, and D.P.Cerretti. 1997. A metalloproteinase disintegrin that releases tumour-necrosis factor-alpha from cells. *Nature* 385:729-733.

217. Salomon,D.S., R.Brandt, F.Ciardiello, and N.Normanno. 1995. Epidermal growth factor-related peptides and their receptors in human malignancies. *Crit Rev. Oncol. Hematol.* 19:183-232.

218. Sahin,U., G.Weskamp, K.Kelly, H.M.Zhou, S.Higashiyama, J.Peschon, D.Hartmann, P.Saftig, and C.P.Blobel. 2004. Distinct roles for ADAM10 and ADAM17 in ectodomain shedding of six EGFR ligands. *J Cell Biol.* 164:769-779.

219. Jackson,L.F., T.H.Qiu, S.W.Sunnarborg, A.Chang, C.Zhang, C.Patterson, and D.C.Lee. 2003. Defective valvulogenesis in HB-EGF and TACE-null mice is associated with aberrant BMP signaling. *EMBO J* 22:2704-2716.

220. Peschon,J.J., J.L.Slack, P.Reddy, K.L.Stocking, S.W.Sunnarborg, D.C.Lee, W.E.Russell, B.J.Castner, R.S.Johnson, J.N.Fitzner, R.W.Boyce, N.Nelson, C.J.Kozlosky, M.F.Wolfson, C.T.Rauch, D.P.Cerretti, R.J.Paxton, C.J.March, and R.A.Black. 1998. An essential role for ectodomain shedding in mammalian development. *Science* 282:1281-1284.

221. Mann,G.B., K.J.Fowler, A.Gabriel, E.C.Nice, R.L.Williams, and A.R.Dunn. 1993. Mice with a null mutation of the TGF alpha gene have abnormal skin architecture, wavy hair, and curly whiskers and often develop corneal inflammation. *Cell* 73:249-261.

222. Zhao,J., H.Chen, Y.L.Wang, and D.Warburton. 2001. Abrogation of tumor necrosis factor-alpha converting enzyme inhibits embryonic lung morphogenesis in culture. *Int. J Dev. Biol.* 45:623-631.

223. Asakura,M., M.Kitakaze, S.Takashima, Y.Liao, F.Ishikura, T.Yoshinaka, H.Ohmoto, K.Node, K.Yoshino, H.Ishiguro, H.Asanuma, S.Sanada, Y.Matsumura, H.Takeda, S.Beppu, M.Tada, M.Hori, and S.Higashiyama. 2002. Cardiac hypertrophy is inhibited by antagonism of ADAM12 processing of HB-EGF: metalloproteinase inhibitors as a new therapy. *Nat. Med.* 8:35-40.

224. Schafer,B., B.Marg, A.Gschwind, and A.Ullrich. 2004. Distinct ADAM metalloproteinases regulate G protein-coupled receptor-induced cell proliferation and survival. *J Biol. Chem.* 279:47929-47938.

225. Schafer,B., A.Gschwind, and A.Ullrich. 2004. Multiple G-protein-coupled receptor signals converge on the epidermal growth factor receptor to promote migration and invasion. *Oncogene* 23:991-999.

226. De Sanctis,G.T., M.Merchant, D.R.Beier, R.D.Dredge, J.K.Grobholz, T.R.Martin, E.S.Lander, and J.M.Drazen. 1995. Quantitative locus analysis of airway hyperresponsiveness in A/J and C57BL/6J mice. *Nat. Genet.* 11:150-154.

227. Umland,S.P., C.G.Garlisi, H.Shah, Y.Wan, J.Zou, K.E.Devito, W.M.Huang, E.L.Gustafson, and R.Ralston. 2003. Human ADAM33 messenger RNA expression profile and post-transcriptional regulation. *Am. J Respir Cell Mol. Biol.* 29:571-582.

228. Powell,R.M., J.Wicks, J.W.Holloway, S.T.Holgate, and D.E.Davies. 2004. The splicing and fate of ADAM33 transcripts in primary human airways fibroblasts. *Am. J Respir Cell Mol. Biol.* 31:13-21.

229. Haitchi,H.M., R.M.Powell, T.J.Shaw, P.H.Howarth, S.J.Wilson, D.I.Wilson, S.T.Holgate, and D.E.Davies. 2005. ADAM33 expression in asthmatic airways and human embryonic lungs. *Am. J Respir Crit Care Med.* 171:958-965.

230. Foley,S.C., A.K.Mogas, R.Olivenstein, P.O.Fiset, J.Chakir, J.Bourbeau, P.Ernst, C.Lemiere, J.G.Martin, and Q.Hamid. 2007. Increased expression of ADAM33 and ADAM8 with disease progression in asthma. *J Allergy Clin. Immunol.* 119:863-871.

231. Ito,I., J.D.Laporte, P.O.Fiset, K.Asai, Y.Yamauchi, J.G.Martin, and Q.Hamid. 2007. Downregulation of a disintegrin and metalloproteinase 33 by IFN-gamma in human airway smooth muscle cells. *J Allergy Clin. Immunol.* 119:89-97.

232. Lee,J.Y., S.W.Park, H.K.Chang, H.Y.Kim, T.Rhim, J.H.Lee, A.S.Jang, E.S.Koh, and C.S.Park. 2005. A Disintegrin and Metalloproteinase 33 Protein in Asthmatics : Relevance to Airflow Limitation. *Am. J Respir Crit Care Med.*

233. Chen,C., X.Huang, and D.Sheppard. 2006. ADAM33 is not essential for growth and development and does not modulate allergic asthma in mice. *Mol. Cell Biol.* 26:6950-6956.

234. Orth,P., P.Reichert, W.Wang, W.W.Prosise, T.Yarosh-Tomaine, G.Hammond, R.N.Ingram, L.Xiao, U.A.Mirza, J.Zou, C.Strickland, S.S.Taremi, H.V.Le, and V.Madison. 2004. Crystal structure of the catalytic domain of human ADAM33. *J Mol. Biol.* 335:129-137.

235. Zou,J., R.Zhang, F.Zhu, J.Liu, V.Madison, and S.P.Umland. 2005. ADAM33 enzyme properties and substrate specificity. *Biochemistry* 44:4247-4256.

236. Garlisi,C.G., J.Zou, K.E.Devito, F.Tian, F.X.Zhu, J.Liu, H.Shah, Y.Wan, B.M.Motasim, R.W.Egan, and S.P.Umland. 2003. Human ADAM33: protein maturation and localization. *Biochem. Biophys. Res. Commun.* 301:35-43.

237. Weskamp,G., J.W.Ford, J.Sturgill, S.Martin, A.J.Docherty, S.Swendeman, N.Broadway, D.Hartmann, P.Saftig, S.Umland, A.Sehara-Fujisawa, R.A.Black, A.Ludwig, J.D.Becherer, D.H.Conrad, and C.P.Blobel. 2006. ADAM10 is a principal 'sheddase' of the low-affinity immunoglobulin E receptor CD23. *Nat. Immunol.* 7:1293-1298.

238. Yoshisue,H., S.M.Puddicombe, S.J.Wilson, H.M.Haitchi, R.M.Powell, D.I.Wilson, A.Pandit, A.E.Berger, D.E.Davies, S.T.Holgate, and J.W.Holloway. 2004. Characterization of ciliated bronchial epithelium 1, a ciliated cell-associated gene induced during mucociliary differentiation. *Am. J Respir Cell Mol. Biol.* 31:491-500.

239. Starkey,P.M. and A.J.Barrett. 1973. Inhibition by alpha-macroglobulin and other serum proteins. *Biochem. J* 131:823-831.

240. Barrett,A.J. 1981. Alpha 2-macroglobulin. *Methods Enzymol.* 80 Pt C:737-754.

241. Diaz-Mochon,J.J., L.Bialy, L.Keinicke, and M.Bradley. 2005. Combinatorial libraries - from solution to 2D microarrays. *Chem. Commun. (Camb.)*1384-1386.

242. Diaz-Mochon,J.J., L.Bialy, and M.Bradley. 2006. Dual colour, microarray-based, analysis of 10,000 protease substrates. *Chem. Commun. (Camb.)*3984-3986.

243. Nath,D., P.M.Slocombe, P.E.Stephens, A.Warn, G.R.Hutchinson, K.M.Yamada, A.J.Docherty, and G.Murphy. 1999. Interaction of metargidin (ADAM-15) with alphavbeta3 and alpha5beta1 integrins on different haemopoietic cells. *J Cell Sci.* 112 (Pt 4):579-587.

244. Amour,A., C.G.Knight, A.Webster, P.M.Slocombe, P.E.Stephens, V.Knauper, A.J.Docherty, and G.Murphy. 2000. The in vitro activity of ADAM-10 is inhibited by TIMP-1 and TIMP-3. *FEBS Lett.* 473:275-279.

245. Prosise,W.W., T.Yarosh-Tomaine, Z.Lozewski, R.N.Ingram, J.Zou, J.J.Liu, F.Zhu, S.S.Taremi, H.V.Le, and W.Wang. 2004. Protease domain of human ADAM33 produced by Drosophila S2 cells. *Protein Expr. Purif.* 38:292-301.

246. Phan,T.C., K.J.Nowak, P.A.Akkari, M.H.Zheng, and J.Xu. 2003. Expression of caltrin in the baculovirus system and its purification in high yield and purity by cobalt (II) affinity chromatography. *Protein Expr. Purif.* 29:284-290.

247. Lehr,R.V., L.C.Elefante, K.K.Kikly, S.P.O'Brien, and R.B.Kirkpatrick. 2000. A modified metal-ion affinity chromatography procedure for the purification of histidine-tagged recombinant proteins expressed in Drosophila S2 cells. *Protein Expr. Purif.* 19:362-368.

248. Lum,L., M.S.Reid, and C.P.Blobel. 1998. Intracellular maturation of the mouse metalloprotease disintegrin MDC15. *J Biol. Chem.* 273:26236-26247.

249. Gonzales,P.E., A.Solomon, A.B.Miller, M.A.Leesnitzer, I.Sagi, and M.E.Milla. 2004. Inhibition of the tumor necrosis factor-alpha-converting enzyme by its pro domain. *J Biol. Chem.* 279:31638-31645.

250. Feinman,R.D. 1994. The proteinase-binding reaction of alpha 2M. *Ann. N. Y. Acad. Sci.* 737:245-266.

251. Kang,T., H.I.Park, Y.Suh, Y.G.Zhao, H.Tschesche, and Q.X.Sang. 2002. Autolytic processing at Glu586-Ser587 within the cysteine-rich domain of human adamalysin 19/disintegrin-metalloproteinase 19 is necessary for its proteolytic activity. *J Biol. Chem.* 277:48514-48522.

252. Yan,Y., K.Shirakabe, and Z.Werb. 2002. The metalloprotease Kuzbanian (ADAM10) mediates the transactivation of EGF receptor by G protein-coupled receptors. *J Cell Biol.* 158:221-226.

253. Gomis-Ruth,F.X. 2003. Structural aspects of the metzincin clan of metalloendopeptidases. *Mol. Biotechnol.* 24:157-202.

254. Yoshinaka,T., K.Nishii, K.Yamada, H.Sawada, E.Nishiwaki, K.Smith, K.Yoshino, H.Ishiguro, and S.Higashiyama. 2002. Identification and characterization of novel mouse and human ADAM33s with potential metalloprotease activity. *Gene* 282:227-236.

255. Browner,M.F., W.W.Smith, and A.L.Castelhano. 1995. Matrilysin-inhibitor complexes: common themes among metalloproteases. *Biochemistry* 34:6602-6610.

256. Galardy,R.E., M.E.Cassabonne, C.Giese, J.H.Gilbert, F.Lapierre, H.Lopez, M.E.Schaefer, R.Stack, M.Sullivan, B.Summers, and . 1994. Low molecular weight inhibitors in corneal ulceration. *Ann. N. Y. Acad. Sci.* 732:315-323.

257. Kang,T., H.Tschesche, and Q.X.my Sang. 2004. Evidence for disulfide involvement in the regulation of intramolecular autolytic processing by human adamalysin19/ADAM19. *Exp. Cell Res.* 298:285-295.

258. Contin,C., V.Pitard, T.Itai, S.Nagata, J.F.Moreau, and J.chanet-Merville. 2003. Membrane-anchored CD40 is processed by the tumor necrosis factor-alpha-converting enzyme. Implications for CD40 signaling. *J Biol. Chem.* 278:32801-32809.

259. Brew,K., D.Dinakarpandian, and H.Nagase. 2000. Tissue inhibitors of metalloproteinases: evolution, structure and function. *Biochim. Biophys. Acta* 1477:267-283.

260. Amour,A., P.M.Slocombe, A.Webster, M.Butler, C.G.Knight, B.J.Smith, P.E.Stephens, C.Shelley, M.Hutton, V.Knauper, A.J.Docherty, and G.Murphy. 1998. TNF-alpha converting enzyme (TACE) is inhibited by TIMP-3. *FEBS Lett.* 435:39-44.

261. Yu,W.H., S.Yu, Q.Meng, K.Brew, and J.F.Woessner, Jr. 2000. TIMP-3 binds to sulfated glycosaminoglycans of the extracellular matrix. *J Biol. Chem.* 275:31226-31232.

262. de Jong,P.M., M.A.van Sterkenburg, S.C.Hesseling, J.A.Kempenaar, A.A.Mulder, A.M.Mommaas, J.H.Dijkman, and M.Ponec. 1994. Ciliogenesis in human bronchial epithelial cells cultured at the air-liquid interface. *Am. J Respir Cell Mol. Biol.* 10:271-277.

263. Lawley,T.J. and Y.Kubota. 1989. Induction of morphologic differentiation of endothelial cells in culture. *J Invest Dermatol.* 93:59S-61S.

264. Staton,C.A., S.M.Stribbling, S.Tazzyman, R.Hughes, N.J.Brown, and C.E.Lewis. 2004. Current methods for assaying angiogenesis in vitro and in vivo. *Int. J Exp. Pathol.* 85:233-248.

265. Sanz,L., M.Pascual, A.Munoz, M.A.Gonzalez, C.H.Salvador, and L.varez-Vallina. 2002. Development of a computer-assisted high-throughput screening platform for anti-angiogenic testing. *Microvasc. Res.* 63:335-339.

266. Guidolin,D., A.Vacca, G.G.Nussdorfer, and D.Ribatti. 2004. A new image analysis method based on topological and fractal parameters to evaluate the angiostatic activity of docetaxel by using the Matrigel assay in vitro. *Microvasc. Res.* 67:117-124.

267. Muthuswamy,S.K., D.Li, S.Lelievre, M.J.Bissell, and J.S.Brugge. 2001. ErbB2, but not ErbB1, reinitiates proliferation and induces luminal repopulation in epithelial acini. *Nat. Cell Biol.* 3:785-792.

268. Schuger,L., K.S.O'Shea, B.B.Nelson, and J.Varani. 1990. Organotypic arrangement of mouse embryonic lung cells on a basement membrane extract: involvement of laminin. *Development* 110:1091-1099.

269. Gipson,I.K., S.Spurr-Michaud, P.Argueso, A.Tisdale, T.F.Ng, and C.L.Russo. 2003. Mucin gene expression in immortalized human corneal-limbal and conjunctival epithelial cell lines. *Invest Ophthalmol. Vis. Sci.* 44:2496-2506.

270. Hashimoto,M., H.Tanaka, and S.Abe. 2005. Quantitative analysis of bronchial wall vascularity in the medium and small airways of patients with asthma and COPD. *Chest* 127:965-972.

271. Davis,G.E. and D.R.Senger. 2005. Endothelial extracellular matrix: biosynthesis, remodeling, and functions during vascular morphogenesis and neovessel stabilization. *Circ. Res.* 97:1093-1107.

272. Handsley,M.M. and D.R.Edwards. 2005. Metalloproteinases and their inhibitors in tumor angiogenesis. *Int. J Cancer* 115:849-860.

273. Presta,M., P.Dell'Era, S.Mitola, E.Moroni, R.Ronca, and M.Rusnati. 2005. Fibroblast growth factor/fibroblast growth factor receptor system in angiogenesis. *Cytokine Growth Factor Rev.* 16:159-178.

274. Roy,H., S.Bhardwaj, and S.Yla-Herttuala. 2006. Biology of vascular endothelial growth factors. *FEBS Lett.* 580:2879-2887.

275. Horiuchi,K., G.Weskamp, L.Lum, H.P.Hammes, H.Cai, T.A.Brodie, T.Ludwig, R.Chiusaroli, R.Baron, K.T.Preissner, K.Manova, and C.P.Blobel. 2003. Potential role for ADAM15 in pathological neovascularization in mice. *Mol. Cell Biol.* 23:5614-5624.

276. Komiya,K., H.Enomoto, I.Inoki, S.Okazaki, Y.Fujita, E.Ikeda, E.Ohuchi, H.Matsumoto, Y.Toyama, and Y.Okada. 2005. Expression of ADAM15 in rheumatoid synovium: up-regulation by vascular endothelial growth factor and possible implications for angiogenesis. *Arthritis Res. Ther.* 7:R1158-R1173.

277. Matter,H., W.Schwab, D.Barbier, G.Billen, B.Haase, B.Neises, M.Schudok, W.Thorwart, H.Schreuder, V.Brachvogel, P.Lonze, and K.U.Weithmann. 1999. Quantitative structure-activity relationship of human neutrophil collagenase (MMP-8) inhibitors using comparative molecular field analysis and X-ray structure analysis. *J Med. Chem.* 42:1908-1920.

278. Hanemaaijer,R., T.Sorsa, Y.T.Konttinen, Y.Ding, M.Sutinen, H.Visser, H.van, V, T.Helaakoski, T.Kainulainen, H.Ronka, H.Tschesche, and T.Salo. 1997. Matrix metalloproteinase-8 is expressed in rheumatoid synovial fibroblasts and endothelial cells. Regulation by tumor necrosis factor-alpha and doxycycline. *J Biol. Chem.* 272:31504-31509.

279. Nguyen,M., J.Arkell, and C.J.Jackson. 2001. Human endothelial gelatinases and angiogenesis. *Int. J Biochem. Cell Biol.* 33:960-970.

280. Roy,R., U.M.Wewer, D.Zurakowski, S.E.Pories, and M.A.Moses. 2004. ADAM 12 cleaves extracellular matrix proteins and correlates with cancer status and stage. *J Biol. Chem.* 279:51323-51330.

281. Frohlich,C., R.Albrechtsen, L.Dyrskjot, L.Rudkjaer, T.F.Orntoft, and U.M.Wewer. 2006. Molecular profiling of ADAM12 in human bladder cancer. *Clin. Cancer Res.* 12:7359-7368.

282. Millichip,M.I., D.J.Dallas, E.Wu, S.Dale, and N.McKie. 1998. The metallo-disintegrin ADAM10 (MADM) from bovine kidney has type IV collagenase activity in vitro. *Biochem. Biophys. Res. Commun.* 245:594-598.

283. Martin,J., L.V.Eynstone, M.Davies, J.D.Williams, and R.Steadman. 2002. The role of ADAM 15 in glomerular mesangial cell migration. *J Biol. Chem.* 277:33683-33689.

284. Allen,M., A.Heinzmann, E.Noguchi, G.Abecasis, J.Broxholme, C.P.Ponting, S.Bhattacharyya, J.Tinsley, Y.Zhang, R.Holt, E.Y.Jones, N.Lench, A.Carey, H.Jones, N.J.Dickens, C.Dimon, R.Nicholls, C.Baker, L.Xue, E.Townsend, M.Kabesch, S.K.Weiland, D.Carr, M.E.von, I.M.Adcock, P.J.Barnes, G.M.Lathrop, M.Edwards, M.F.Moffatt, and W.O.Cookson. 2003. Positional cloning of a novel gene influencing asthma from chromosome 2q14. *Nat. Genet.* 35:258-263.

285. Zagha,E., A.Ozaita, S.Y.Chang, M.S.Nadal, U.Lin, M.J.Saganich, T.McCormack, K.O.Akinsanya, S.Y.Qi, and B.Rudy. 2005. DPP10 modulates Kv4-mediated A-type potassium channels. *J Biol. Chem.* 280:18853-18861.

286. Janes,P.W., N.Saha, W.A.Barton, M.V.Kolev, S.H.Wimmer-Kleikamp, E.Nievergall, C.P.Blobel, J.P.Himanen, M.Lackmann, and D.B.Nikolov. 2005. Adam meets Eph: an ADAM substrate recognition module acts as a molecular switch for ephrin cleavage in trans. *Cell* 123:291-304.

287. Gaultier,A., H.Cousin, T.Darribere, and D.Alfandari. 2002. ADAM13 disintegrin and cysteine-rich domains bind to the second heparin-binding domain of fibronectin. *J Biol. Chem.* 277:23336-23344.

288. Vlahakis,N.E., B.A.Young, A.Atakilit, and D.Sheppard. 2005. The lymphangiogenic vascular endothelial growth factors VEGF-C and -D are ligands for the integrin alpha9beta1. *J Biol. Chem.* 280:4544-4552.

289. Staniszewska,I., S.Zaveri, V.L.Del, I.Oliva, V.L.Rothman, S.E.Croul, D.D.Roberts, D.F.Mosher, G.P.Tuszynski, and C.Marcinkiewicz. 2007. Interaction of {alpha}9{beta}1 Integrin With Thrombospondin-1 Promotes Angiogenesis. *Circ. Res.*

290. Yokosaki,Y., N.Matsuura, S.Higashiyama, I.Murakami, M.Obara, M.Yamakido, N.Shigeto, J.Chen, and D.Sheppard. 1998. Identification of the ligand binding site for the integrin alpha9 beta1 in the third fibronectin type III repeat of tenascin-C. *J Biol. Chem.* 273:11423-11428.

291. Yokosaki,Y., N.Matsuura, T.Sasaki, I.Murakami, H.Schneider, S.Higashiyama, Y.Saitoh, M.Yamakido, Y.Taooka, and D.Sheppard. 1999. The integrin alpha(9)beta(1) binds to a novel recognition sequence (SVVYGLR) in the thrombin-cleaved amino-terminal fragment of osteopontin. *J Biol. Chem.* 274:36328-36334.

292. Taooka,Y., J.Chen, T.Yednock, and D.Sheppard. 1999. The integrin alpha9beta1 mediates adhesion to activated endothelial cells and transendothelial neutrophil migration through interaction with vascular cell adhesion molecule-1. *J Cell Biol.* 145:413-420.